Refined BPS Invariants, Chern-Simons Theory, and the Quantum Dilogarithm

Thesis by

Tudor Dan Dimofte

In partial fulfillment of the requirements
for the degree of Doctor of Philosophy

California Institute of Technology
Pasadena, California

2010

(Defended March 30, 2010)

There are many individuals without whom the present thesis would not have been possible. Among them, I especially wish to thank Dan Jafferis, Sergei Gukov, Jonatan Lenells, Andy Neitzke, Hirosi Ooguri, Carol Silberstein, Yan Soibelman, Ketan Vyas, Masahito Yamazaki, Don Zagier, and Christian Zickert for a multitude of discussions and collaborations over innumerable hours leading to the culmination of this work. I am extremely grateful to Hirosi Ooguri and to Sergei Gukov, who have both advised me during various periods of my studies. I also wish to thank my family and friends — in particular Mom, Dad, and David — for their constant, essential support.

Abstract

In this thesis, we consider two main subjects: the refined BPS invariants of Calabi-Yau threefolds, and three-dimensional Chern-Simons theory with complex gauge group. We study the wall-crossing behavior of refined BPS invariants using a variety of techniques, including a four-dimensional supergravity analysis, statistical-mechanical melting crystal models, and relations to new mathematical invariants. We conjecture an equivalence between refined invariants and the motivic Donaldson-Thomas invariants of Kontsevich and Soibelman. We then consider perturbative Chern-Simons theory with complex gauge group, combining traditional and novel approaches to the theory (including a new state integral model) to obtain exact results for perturbative partition functions. We thus obtain a new class of topological invariants, which are not of finite type, defined in the background of genuinely nonabelian flat connections. The two main topics, BPS invariants and Chern-Simons theory, are connected at both a formal and (we believe) deeper conceptual level by the striking central role that the quantum dilogarithm function plays in each.

This thesis is based on the publications [1, 2, 3], as well as [4] and [5], which are in preparation. Some aspects of Chern-Simons theory appear additionally in the conference proceedings [6]. The author's graduate work also included [7], which is not directly related to the present topics.

Contents

List of Figures

List of Tables

Chapter 1

Introduction and Overview

During the past thirty years, dualities have been a cornerstone of progress in theoretical physics, and have motivated some of the most interesting and nontrivial new relations between physics and mathematics. Almost all such dualities have proven to have some basis in string theory. Prominent examples include the AdS/CFT correspondence [8] and mirror symmetry. More related to the present thesis is the Gromov-Witten/Donaldson-Thomas correspondence [9, 10, 11, 12], which related (via M-theory) the spaces of holomorphic maps into a Calabi-Yau threefold to the spaces of holomorphic curves on the threefold itself. In a somewhat different context, Chern-Simons theory with compact gauge group provided the first intrinsically three-dimensional interpretation of knot polynomials [13]; different descriptions of the theory then related the finite-type Vassiliev invariants with the Kontsevich integral [14].

Along these lines, this thesis is about developing new connections: between physical theories, between mathematical theories, and most importantly between physics and mathematics. We will begin by studying so-called refined Bogomol'nyi-Prasad-Sommerfield (BPS) invariants of Calabi-Yau threefolds and their wall-crossing behavior. We show that they can be described and calculated in many ways, including via melting crystal models, and we will conjecture that they are related to the motivic Donaldson-Thomas invariants of Kontsevich and Soibelman [15]. We will then turn to Chern-Simons theory with *noncompact* gauge group, a theory intrinsically different from the compact Chern-Simons theory that computes Jones polynomials. We use a multitude of approaches to understand the relation between the compact and noncompact theories, to calculate exact partition functions

and new knot invariants, and to relate noncompact Chern-Simons theory to "quantum" hyperbolic geometry.

Refined BPS invariants

The BPS invariants of a Calabi-Yau threefold X can be thought of in several different ways. Physically, they describe the states of 1/2-BPS D-branes in type II string theory that is compactified on a product of X and four-dimensional Minkowski space, $X \times \mathbb{R}^{3,1}$. Equivalently, the same BPS invariants describe the bound states of supersymmetric point-like black holes in the low-energy supergravity theory on $\mathbb{R}^{3,1}$ [16]. Or, in a mathematical setting, BPS invariants describe objects in the derived category of coherent sheaves on X [17].

The actual Hilbert space of BPS states $\mathcal{H}_{BPS}$ in any of these descriptions depends on *stability conditions*, which in turn depend (say, in a type IIA duality frame) on the values of the Kähler moduli or "size parameters" of X [16, 17, 18]. In terms of D-branes, the stability conditions ensure roughly that a brane wraps a cycle of minimal volume, and that it cannot decay into a sum of noninteracting branes. Since $\mathcal{H}_{BPS}$ is a discrete object, it must be locally constant as a function of moduli. However, it can jump at special values of moduli where the stability conditions change. This happens at real codimension-1 wall in moduli space, and is a phenomenon known as wall crossing.

To study the properties of the space $\mathcal{H}_{BPS}$, it is useful to construct well-behaved supersymmetric indices that count its states. Often, such indices are sufficient for applications like approximating the entropy of black holes in string theory [19]. The simplest option for constructing an index is to observe that the Hilbert space $\mathcal{H}_{BPS}$ is graded by charge — in a string theory picture, this is the charge of the D-branes that make up various states. Then one can define an *unrefined index* $\Omega(\gamma)$ to be the signed count of charge-γ states in $\mathcal{H}_{BPS}$. For special values of Kähler moduli, the generating function of these unrefined indices is just the partition function of the well-known Gromov-Witten or Donaldson-Thomas invariants [20]. Indeed, as mentioned above, this is the context in which BPS invariants first became important in mathematics.

The *refined* BPS indices that play a main role in this thesis are defined by summing states in the Hilbert space $\mathcal{H}_{BPS}$ with an extra weight $(-y)^{2J_3}$ that keeps track of their spin

content. In terms of four-dimensional supergravity, this spin is just the physical $\widetilde{SO(3)} \simeq SU(2)$ spin of massive point-like particles. The resulting index $\Omega^{ref}(\gamma; y)$ retains much more of the information in $\mathcal{H}_{BPS}$ and reduces to the unrefined $\Omega(\gamma)$ when $y \to 1$. Alternatively, in situations where $\mathcal{H}_{BPS}$ has a description as the cohomology of a classical D-brane moduli space $\mathcal{M}$ (*cf.* [21]), the refined index is associated to the Poincaré polynomial of $\mathcal{M}$, while the unrefined index is its Euler characteristic.

Refined indices were first introduced in the special case of Gromov-Witten/Donaldson-Thomas theory. They allowed topological strings (*i.e.* Gromov-Witten theory) to compute equivariant instanton sums in four-dimensional gauge theory [22, 23]. For toric Calabi-Yau's, ordinary Gromov-Witten/Donaldson-Thomas generating functions could be calculated using the topological vertex of [24, 25], and a refined vertex was constructed to compute the corresponding refined generating functions [26]. Moreover, using large-N duality [27] and the relation between topological strings and compact Chern-Simons theory [28], it was realized that the refined partition functions should be related to homological invariants of knots (which categorify Jones, etc., polynomials) [29, 30].

All these previous applications of refined BPS invariants were restricted exclusively to the Gromov-Witten/Donaldson-Thomas chamber of Calabi-Yau moduli space (*i.e.* the special choice of moduli for which $\Omega^{ref}(\gamma)$ are refined Donaldson-Thomas invariants). In this thesis, we want to move beyond Gromov-Witten/Donaldson-Thomas theory and analyze refined BPS invariants in all chambers of Kähler moduli space, focusing in particular on their wall-crossing behavior.

In Chapter 2, we define refined indices more carefully, and generalize the wall-crossing formulas derived by Denef and Moore [20] from the unrefined to the refined case. There are some important differences between unrefined and refined invariants, such as a dependence of $\Omega^{ref}(\gamma)$ on complex structure (or hypermultiplet) moduli as well as the potential existence of new walls in Kähler moduli space where $\Omega^{ref}(\gamma)$ could jump. We give a (non)example of the latter in Section 2.4. In Chapter 3, we apply refined wall crossing to the resolved conifold geometry $\mathcal{O}(-1,-1) \to \mathbb{P}^1$, and derive a picture of refined generating functions in an infinite set of chambers, analogous to an unrefined description presented by [31]. Moreover, we relate the generating function in each chamber to a statistical melting crystal model of refined "pyramid partitions" with varying boundary conditions, which generalize the refined topological vertex. These models will suggested a new combinatorial interpretation of wall

crossing in [1], which has since been extended beyond the conifold [32, 33].

In Chapter 4, we arrive at our main mathematical conjecture: that refined invariants are equivalent to the motivic Donaldson-Thomas invariants of Kontsevich and Soibelman [15]. Kontsevich and Soibelman defined a version of Donaldson-Thomas invariants for Calabi-Yau categories that depend on a stability condition (just like physical BPS invariants), and obey a very general wall-crossing formula. It has previously been argued [34] that the "classical" or unrefined versions of motivic Donaldson-Thomas invariants are equivalent to physical unrefined BPS invariants. Motivic invariants, however, naturally depend on an extra parameter '$\mathbb{L}$' or 'q' (the motive of the affine line), which we argue is to be identified with the refined spin variable y. We substantiate our claim both theoretically, by matching refined and motivic wall-crossing formulas, and with direct examples from $SU(2)$ Seiberg-Witten theory.

The ultimate goal of the present program would be to study not the refined indices $\Omega^{ref}(\gamma)$ but the entire Hilbert space $\mathcal{H}_{BPS}$, its full dependence on *all* moduli, and its homological properties. We have by now come quite close to doing this, and hope it will be the subject of future interesting work.

Chern-Simons theory

In the second part of this thesis, we shift our focus to three-dimensional Chern-Simons gauge theory with complex, noncompact gauge group. Chern-Simons theory is a preeminent example of a topological quantum field theory (TQFT). By now, Chern-Simons theory with *compact* gauge group G is a mature subject with a history going back to the 1980's (see *e.g.* [35, 14] for excellent reviews), and has a wide range of applications, ranging from invariants of knots and 3-manifolds [13] on one hand, to condensed matter physics [36, 37] and to string theory [38] on the other.

We will specifically be interested in a version of Chern-Simons gauge theory with complex gauge group $G_{\mathbb{C}}$. Although at first it may appear merely as a variation on the subject, the physics of this theory is qualitatively different from that of Chern-Simons theory with compact gauge group. For example, one important difference is that to a compact Riemann surface Σ Chern-Simons theory with compact gauge group associates a finite-dimensional Hilbert space $\mathcal{H}_\Sigma$, whereas in a theory with non-compact (and, in particular, complex) gauge

group the Hilbert space is infinite-dimensional. Due to this and other important differences that will be explained in further detail below, Chern-Simons gauge theory with complex gauge group remains a rather mysterious subject. The first steps toward understanding this theory were made in [39] and, more recently, in [40, 41].

As in a theory with a compact gauge group, the classical action of Chern-Simons gauge theory with complex gauge group $G_{\mathbb{C}}$ is purely topological — that is, independent of the metric on the underlying 3-manifold M. However, since the gauge field $\mathcal{A}$ (a $\mathfrak{g}_{\mathbb{C}}$-valued 1-form on M) is now complex, one can write two topological terms in the action, involving $\mathcal{A}$ and $\bar{\mathcal{A}}$:

$$\begin{aligned} S &= \frac{t}{8\pi}\int_M \mathrm{Tr}\Big(\mathcal{A}\wedge d\mathcal{A}+\frac{2}{3}\,\mathcal{A}\wedge\mathcal{A}\wedge\mathcal{A}\Big) \\ &\quad+\frac{\bar{t}}{8\pi}\int_M \mathrm{Tr}\Big(\bar{\mathcal{A}}\wedge d\bar{\mathcal{A}}+\frac{2}{3}\bar{\mathcal{A}}\wedge\bar{\mathcal{A}}\wedge\bar{\mathcal{A}}\Big)\,. \end{aligned} \tag{1.0.1}$$

Although in general the complex coefficients ("coupling constants") t and $\bar{t}$ need not be complex conjugate to each other, they are not entirely arbitrary. Thus, if we write $t = k+\sigma$ and $\bar{t} = k-\sigma$, then consistency of the quantum theory requires the "level" k to be an integer, $k \in \mathbb{Z}$, whereas unitarity requires σ to be either real, $\sigma \in \mathbb{R}$, or purely imaginary, $\sigma \in i\mathbb{R}$ [39].

Given a 3-manifold M (possibly with boundary), Chern-Simons theory associates to M a "quantum $G_{\mathbb{C}}$ invariant" that we denote as $Z(M)$. Physically, $Z(M)$ is the partition function of the Chern-Simons gauge theory on M, defined as a Feynman path integral

$$Z(M) \;=\; \int \mathcal{D}\mathcal{A}\; e^{iS} \tag{1.0.2}$$

with the classical action (1.0.1). Since the action (1.0.1) is independent of the choice of metric on M, one might expect that the quantum $G_{\mathbb{C}}$ invariant $Z(M)$ is a topological invariant of M. This is essentially correct even though independence of metric is less obvious in the quantum theory, and $Z(M)$ does turn out to be an interesting invariant. How then does one compute $Z(M)$?

One approach is to use the topological invariance of the theory. In Chern-Simons theory with compact gauge group G, the partition function $Z(M)$ can be efficiently computed by cutting M into simple "pieces," on which the path integral (1.0.2) is easy to evaluate. Then, via "gluing rules," the answers for individual pieces are assembled together to produce

$Z(M)$. In practice, there may exist many different ways to decompose M into basic building blocks, resulting in different ways of computing $Z(M)$.

Although a similar set of gluing rules should exist in a theory with complex gauge group $G_{\mathbb{C}}$, they are expected to be more involved than in the compact case. The underlying reason for this was already mentioned: in Chern-Simons theory with complex gauge group the Hilbert space is infinite dimensional (as opposed to a finite-dimensional Hilbert space in the case of compact gauge group G). One consequence of this fact is that finite sums which appear in gluing rules for Chern-Simons theory with compact group G turn into integrals over continuous parameters in a theory with non-compact gauge group. This is one of the difficulties one needs to face in computing $Z(M)$ non-perturbatively, *i.e.* as a closed-form function of complex parameters t and $\bar{t}$.

A somewhat more modest goal is to compute $Z(M)$ perturbatively, by expanding the integral (1.0.2) in inverse powers of t and $\bar{t}$ around a saddle point (a classical solution). In Chern-Simons theory, classical solutions are flat gauge connections, that is gauge connections $\mathcal{A}$ which obey

$$d\mathcal{A} + \mathcal{A} \wedge \mathcal{A} \;=\; 0\,, \tag{1.0.3}$$

and similarly for $\bar{\mathcal{A}}$. A flat connection on M is determined by its holonomies, that is by a homomorphism

$$\rho : \pi_1(M) \to G_{\mathbb{C}}\,, \tag{1.0.4}$$

modulo gauge transformations, which act via conjugation by elements in $G_{\mathbb{C}}$.

Given a gauge equivalence class of the flat connection $\mathcal{A}$, or, equivalently, a conjugacy class of the homomorphism ρ, one can define a "perturbative partition function" $Z^{(\rho)}(M)$ by expanding the integral (1.0.2) in inverse powers of t and $\bar{t}$. Since the classical action (1.0.1) is a sum of two terms, the perturbation theory for the fields $\mathcal{A}$ and $\bar{\mathcal{A}}$ is independent. As a result, to all orders in perturbation theory, the partition function $Z^{(\rho)}(M)$ factorizes into a product of "holomorphic" and "antiholomorphic" terms:

$$Z^{(\rho)}(M) \;=\; Z^{(\rho)}(M;t) Z^{(\rho)}(M;\bar{t})\,. \tag{1.0.5}$$

This holomorphic factorization is only a property of the perturbative partition function. The exact, non-perturbative partition function $Z(M)$ depends in a non-trivial way on both

t and $\bar{t}$, and the best one can hope for is that it can be written in the form (*cf.* [40, 41])

$$Z(M) \;=\; \sum_{\rho} Z^{(\rho)}(M;t) Z^{(\rho)}(M;\bar{t})\,, \tag{1.0.6}$$

where the sum is over classical solutions (1.0.3) or, equivalently, conjugacy classes of homomorphisms (1.0.4).

In the greater part of this thesis, we study the perturbative partition function $Z^{(\rho)}(M)$. Due to the factorization (1.0.5), it suffices to consider only the holomorphic part $Z^{(\rho)}(M;t)$. Moreover, since the perturbative expansion is in the inverse powers of t, it is convenient to introduce a new expansion parameter $\hbar \;=\; 2\pi i/t$, which plays the role of Planck's constant (the semiclassical limit corresponds to $\hbar \to 0$). In general, the perturbative partition function $Z^{(\rho)}(M;\hbar)$ is an asymptotic power series in $\hbar$. To find its general form one applies the stationary phase approximation to the integral (1.0.2):

$$Z^{(\rho)}(M;\hbar) \;=\; \exp\left(\frac{1}{\hbar} S_0^{(\rho)} - \frac{1}{2}\delta^{(\rho)} \log\hbar \;+\; \sum_{n=0}^{\infty} S_{n+1}^{(\rho)} \hbar^n\right)\,. \tag{1.0.7}$$

This is the general form of the perturbative partition function in Chern-Simons gauge theory with any gauge group, compact or otherwise, computed with standard rules of perturbation theory [13, 42, 43, 44] that will be discussed in more detail below. Roughly speaking, $S_0^{(\rho)}$ is the value of the Chern-Simons functional evaluated on a flat gauge connection $\mathcal{A}^{(\rho)}$ associated with the homomorphism ρ, and each subleading coefficient $S_n^{(\rho)}$ is obtained by summing over Feynman diagrams with n loops.

In Chern-Simons theory with compact gauge group, perturbation theory is often developed in the background of a trivial (or reducible) flat connection $\mathcal{A}^{(\rho)}$. As a result, the perturbative coefficients $S_n^{(\rho)}$ have a fairly simple structure; they factorize into a product of topological invariants of M — the finite type (Vassiliev) invariants and variations thereof — and group-theory factors [14]. In particular, they are rational numbers. In contrast, Chern-Simons theory with complex gauge group naturally involves perturbation theory in the background of genuinely non-abelian (non-reducible) flat connections. Physically, this is a novelty that has not been properly addressed in previous literature. We shall see that the information about a non-abelian flat connection and the 3-manifold M is mixed within the $S_n^{(\rho)}(M)$ in a non-trivial way, and results in $S_n^{(\rho)}(M)$'s that are *not* finite type invariants and are typically not valued in $\mathbb{Q}$.

A primary example of non-abelian representations in the complex case comes from considering hyperbolic 3-manifolds, which, in a sense, constitute the richest and the most interesting class of 3-manifolds. A hyperbolic structure on a 3-manifold M corresponds to a discrete faithful representation of the fundamental group $\pi_1(M)$ into $\mathrm{Isom}^+(\mathbb{H}^3) \cong PSL(2,\mathbb{C})$, the group of orientation-preserving isometries of 3-dimensional hyperbolic space $\mathbb{H}^3$. Adding a choice of spin structure, this lifts to a representation $\rho : \pi_1(M) \to SL(2,\mathbb{C})$, which can then be composed with a morphism ϕ to any larger algebraic group $G_{\mathbb{C}}$ to obtain a representation $\rho : \pi_1(M) \to G_{\mathbb{C}}$. The flat connection associated to such a ρ is non-reducible (in fact, for a complete hyperbolic structure the holonomies of the connection are parabolic), and the corresponding perturbative coefficients $S_n^{(\rho)}$ are interesting new invariants of the hyperbolic 3-manifold M. See Table 6.3 on page 117 for the simplest example of this type.

A direct computation of the perturbative invariants $S_n^{(\rho)}$ via Feynman diagrams is straightforward in principle, but quickly becomes unwieldy as the number of loops n grows. Thus, it is useful to look for alternative methods of defining and computing these invariants. Altogether, different physical descriptions and quantizations of Chern-Simons theory lead us to the following four approaches:

1. **Feynman diagrams**, as already mentioned.

2. **Geometric quantization of** $\mathcal{M}_{\mathrm{flat}}(G_{\mathbb{C}};\Sigma)$, the moduli space of flat connections on the boundary Σ of a three-manifold M, which serves as the classical phase space of Chern-Simons theory.

3. **"Analytic continuation"** from Chern-Simons theory with compact gauge group G to its complexification $G_{\mathbb{C}}$.

4. **State sum model** obtained by decomposing M into tetrahedra, assigning a simple partition function to each tetrahedron, and integrating out boundary conditions as the tetrahedra are glued back together.

The first three have been previously employed to tackle Chern-Simons theory with complex gauge group, while the fourth is completely new. Used in conjunction, these methods lead to very powerful results, mathematically and physically.

We will begin by describing the "traditional" approach of Feynman diagrams in Chapter 5. They will lead us to define the concept of an Arithmetic TQFT, and conjecture that

Chern-Simons theory with complex gauge group belongs to this special class. For hyperbolic M, the arithmeticity of Chern-Simons theory will be very closely related to the arithmeticity of hyperbolic invariants.

In Chapter 6, we then consider the geometric quantization of Chern-Simons theory with complex gauge group on a three-manifold M with boundary Σ. One advantage of Chern-Simons theory with complex gauge group is that the classical phase space $\mathcal{M}_{\text{flat}}(G_{\mathbb{C}}, \Sigma)$ is a hyper-Kähler manifold, a fact that considerably simplifies the quantization problem in any of the existing frameworks (such as geometric quantization [45], deformation quantization [46, 47], or "brane quantization" [48]). We will see that the partition functions $Z^{(\rho)}(M; \hbar)$ obey a system of Schrödinger-like equations $\hat{A}_i Z^{(\rho)}(M; \hbar) = 0$, which, together with appropriate boundary conditions, uniquely determine $Z^{(\rho)}(M; \hbar)$.

Combining geometric quantization with "analytic continuation" will lead to a very efficient computation of the operators $\hat{A}_i$, since it will turn out that they also act on and annihilate partition functions of Chern-Simons theory with compact gauge group. Mathematically, perhaps the most interesting consequence of combining "analytic continuation" with geometric quantization is (almost) a physical proof of the volume conjecture. We will discuss this in Chapter 6 as well. Note that "analytic continuation" involves a very subtle limit of the compact Chern-Simons invariants, and, in particular, does not contradict the fact that the complex Chern-Simons invariants turn out to be qualitatively different from compact ones.

Our main examples throughout this work involve knot or link complements in closed three-manifolds. (In particular, all hyperbolic manifolds are of this type.) In Chern-Simons theory with compact gauge group, however, knot invariants are typically associated with the expectation values of Wilson loops in closed manifolds. In Chapter 7, we define Wilson loops also that carry infinite-dimensional irreducible representations of complex-gauge group, and explain how their expectation values are equivalent to partition functions on knot/link complements. The discussion will also clarify the limiting process involved in "analytic continuation."

In Chapter 8, we finally proceed to the fourth approach: the state sum model for Chern-Simons theory with complex gauge group. This involves cutting a manifold M into tetrahedra, assigning to each tetrahedron a partition function — specifically, an element of a Hilbert space $\mathcal{H}$ associated to the tetrahedron boundary — and taking inner products in

these boundary Hilbert spaces to glue the tetrahedra back together. Conceptually, such a cutting and gluing procedure should always be possible in TQFT; it was often employed to study Chern-Simons theory with compact gauge group, where boundary Hilbert spaces are finite-dimensional (*cf.*. [49, 50, 51]). In the complex case, boundary Hilbert spaces are infinite-dimensional, so that what one seeks is really a state *integral* model. We construct such a model for the case $G_{\mathbb{C}} = SL(2,\mathbb{C})$ and for M hyperbolic based on the work of K. Hikami [52, 53]. Extensions to completely general M and $G_{\mathbb{C}}$ should be possible, though they have not yet been fully developed.

Chapter 9 is then devoted to examples of computations in the state integral model. Schematically, the state integral model expresses $Z^{(\rho)}(M;\hbar)$ as a multi-dimensional integral of a product of *quantum dilogarithm* functions, on which classical saddle-point methods can be used to extract the invariants $S_n^{(\rho)}(M)$. We consider in detail the complements of the figure-eight knot $\mathbf{4_1}$ and the knot $\mathbf{5_2}$, computing $S_n^{(\rho)}(M)$ to high order. We also compare the integrals of the state integral model to similar expressions obtained by direct analytic continuation of compact G-invariants in some special cases, showing that the latter can also be used to find $S_n^{(\rho)}(M)$'s.

Future directions and the quantum dilogarithm

There are many directions in which to continue the studies of refined BPS invariants and complex Chern-Simons theory that have begun here. They are both still relatively unexplored fields. In the case of BPS invariants, it would be very exciting to find a proof of refined = motivic directly in physics, extending the proof of the classical Kontsevich-Soibelman formula in gauge theory given by [34]. Some progress along these lines was recently made in [54]. There is also much yet to be understood about the wall-crossing (or "locus-crossing") behavior of refined invariants in hypermultiplet moduli space, and about the existence of potential new walls in the vector multiplet moduli space. Ultimately, one would like to describe the full "categorical" dependence of the Hilbert space $\mathcal{H}_{BPS}$ itself on moduli.

In the case of Chern-Simons theory with complex gauge group, an immediate goal (and a subject of current research) is to generalize the state integral model to arbitrary manifolds and gauge groups. It is also not fully understood how to obtain the Schrödinger-

like operators $\hat{A}$ directly in geometric quantization. Perhaps more importantly, all the results that appear in this work describe Chern-Simons theory and knot invariants in the perturbative regime, and it would be exciting to move beyond this and understand Chern-Simons theory with complex gauge group nonperturbatively. The first steps in this direction were made in [41]. It is quite possible that a fully developed state integral model will be able to complete the program.

A final related direction concerns an intriguing connection between BPS invariants and the Chern-Simons state integral model. At the most rudimentary level, one find the same special function — a quantum dilogarithm — appearing in both. The simplest definition for the quantum dilogarithm is via the infinite product

$$\mathbf{E}_q(x) = \prod_{r=1}^{\infty} \left(1 + q^{r-1/2}x\right)^{-1}, \qquad |q| < 1\,. \tag{1.0.8}$$

It obeys a remarkable "pentagon" identity: if operators x_1 and x_2 are such that $x_1x_2 = qx_2x_2$, then

$$\mathbf{E}_q(x_1)\,\mathbf{E}_q(x_2) = \mathbf{E}_q(x_2)\,\mathbf{E}_q(q^{-\frac{1}{2}}x_1x_2)\,\mathbf{E}_q(x_1)\,. \tag{1.0.9}$$

The central role of the quantum dilogarithm and (1.0.9) throughout this thesis (see especially Chapters 2, 4, 8, and 9) has motivated its presence in the title.

Elsewhere in physics, the quantum dilogarithm appears as the generating function of a gas of free (charged) bosons. In a more specialized context, it also features as an ingredient in open topological string partition functions. In mathematics, the quantum dilogarithm is ubiquitous in representation theory of quantum groups and (noncompact) affine Lie algebras.

In the context of both BPS invariants and Chern-Simons theory, the quantum dilogarithm function really signals the presence of an entire structural apparatus involving quantizations of complex tori and cluster transformations [55] acting on triangulated surfaces. These triangulated surfaces were recently given physical meaning in terms of BPS wall crossing by [56]. In Chern-Simons theory, the quantization of triangulated surfaces is the quantization of boundary moduli spaces. It would be truly interesting to connect these two pictures via a physical duality — this will hopefully be the subject of future work.

Part I

Refined Wall-Crossing

Chapter 2

Multi-Centered Black Holes and Refined Microstate Counting

As explained in the Introduction, BPS indices for Calabi-Yau threefolds can be defined in several different ways. The most physically intuitive approach uses bound states of multi-centered black holes in four-dimensional $\mathcal{N} = 2$ supergravity. This approach was developed in a series of papers by F. Denef and others [16, 57, 20], and we will follow it here to give precise definitions of BPS indices (Section 2.1) and to obtain primitive and semi-primitive wall-crossing formulas in both unrefined and refined cases (Section 2.2).

The D-brane interpretation of BPS states, and its inevitable relation to the moduli spaces of quiver representations, is still of great importance in connecting the BPS invariants of supergravity to Gromov-Witten/Donaldson-Thomas invariants and more generally to the topological invariants of Kontsevich and Soibelman [15]. It forms the basic connection between physics and mathematics. We therefore describe this interpretation, at least on a conceptual level, in Section 2.3.

We finish in Section 2.4 by exploring one of the more interesting unanswered questions about refined invariants: can they see walls in moduli spaces that are invisible to unrefined indices? We give an explicit example using internal rearrangements of multi-center black hole systems, where the naive answer is "yes," but a number of factors conspire to eliminate the presence of such walls. We conjecture that in fact the answer is always "no."

The derivation of refined wall-crossing formulas is based on our work in [1] (though it is not a far jump from the careful descriptions of wall crossing in [20]). The work on invisible

walls was done in conjunction with S. Gukov and D. Jafferis and will appear in [4].

2.1 BPS states in $\mathcal{N} = 2$ supergravity

Type II compactifications and supergravity

Generally, $\mathcal{N} = 2$ supergravity in four dimensions contains some number n_V of vector multiplets and some number n_H of (ungauged) hypermultiplets. Each vector multiplet consists of a $U(1)$ vector boson, a complex scalar, and two gauginos; while each hypermultiplet consists of two complex scalars and their spin-1/2 superpartners. Of course, $\mathcal{N} = 2$ supergravity also has a supergravity multiplet, consisting of the graviton, the gravitinos, and the graviphoton — another $U(1)$ vector boson.

Such a supergravity theory can be obtained by compactifying 10-dimensional type II string theory on a Calabi-Yau 3-fold X. The $SU(3)$ holonomy group of the Calabi-Yau ensures that exactly two supersymmetries survive the compactification. Moreover, reducing the metric, the B-field, the dilaton, and the Ramond-Ramond form fields of 10-dimensional type II supergravity via the various harmonic forms of the Calabi-Yau produces the bosonic particle content of four-dimensional supergravity. Specifically,[1] the reduction of type IIA theory results in $n_V = h^{1,1}(X)$ vector multiplets whose scalar components describe Kähler structure deformations of X; and $n_H = h^{2,1}(X) + 1$ hypermultiplets describing complex structure deformations, including the "universal hypermultiplet" that contains the 10-dimensional dilaton. In a type IIB compactification, the situation is reversed: there are $n_V = h^{2,1}(X)$ vector multiplets and $n_H = h^{1,1}(X) + 1$ hypermultiplets, again including the universal hypermultiplet that contains the dilaton.

The complex scalars of the vector multiplets and hypermultiplets are moduli of the 4-dimensional theory. Indeed, due to $\mathcal{N} = 2$ supersymmetry, the full moduli space factors exactly into vector and hyper components,

$$\mathcal{M} = \mathcal{M}_V \times \mathcal{M}_H \,, \tag{2.1.1}$$

where

$$\dim_{\mathbb{C}} \mathcal{M}_V = n_V \,, \qquad \dim_{\mathbb{C}} \mathcal{M}_H = 2n_H \,. \tag{2.1.2}$$

[1] See *e.g.* [58] and Section 9.7 of [59] for a review of type II string compactifications.

The metrics on $\mathcal{M}_V$ and $\mathcal{M}_H$ multiply the kinetic terms in the 4-dimensional Lagrangian. The hypermultiplet moduli space $\mathcal{M}_H$ is a quaternionic Kähler manifold, while the vector multiplet moduli space $\mathcal{M}_V$, which we are primarily interested in here, has special Kähler geometry [60, 61]. Thus, the geometry of $\mathcal{M}_V$ can (locally) be described using $n_V + 1$ pairs of complex special coordinates $\{X^I, F_I\}_{I=1}^{n_V+1}$, in terms of which the Kähler potential is written as

$$K = -\log i(\bar{X}^I F_I - X^I \bar{F}_I)\,. \tag{2.1.3}$$

The X^I and F_I are implicitly functions of the n_V actual complex coordinates of $\mathcal{M}_V$; locally both $\{X^I\}$ and $\{F_I\}$ form complete sets of homogeneous projective coordinates.

In a type IIB compactification, the X^I and F_I are periods of the holomorphic 3-form $\Omega \in H^{3,0}(X;\mathbb{C})$,

$$X^I = \int_{\alpha^I} \Omega\,, \qquad F_I = \int_{\beta^I} \Omega\,, \tag{2.1.4}$$

where α^I and β_I are a symplectic basis for $H_3(X;\mathbb{R})$. In a type IIA compactification, relation (2.1.4) still holds if α^I and β_I are taken to be a symplectic basis for even homology $H_{even}(X,\mathbb{R})$, and Ω is interpreted as the even form

$$\Omega = e^{-(B+iJ)} \in H^{even}(X;\mathbb{C})\,, \tag{2.1.5}$$

where B is the B-field on X and J is the Kähler class of X.

It is often useful to consider the actual metrics on $\mathcal{M}_V$ and $\mathcal{M}_H$ as "corrected" forms of much simpler metrics that are obtained in the large volume (or $\alpha' \to 0$) and weak string coupling ($g_s \to 0$) limits.[2] Because the dilaton always belongs to a hypermultiplet, only $\mathcal{M}_H$ ever receives g_s corrections (*i.e.* quantum string corrections). Similarly, because the overall volume modulus of X is a Kähler modulus, only $\mathcal{M}_V$ receives α' corrections (or worldsheet instanton corrections) in a IIA compactification, and only $\mathcal{M}_H$ receives α' corrections in a IIB compactification. Therefore, the "tree-level" geometry of $\mathcal{M}_V$ is exact in IIB string theory. Moreover, mirror symmetry relates the geometry of $\mathcal{M}_V$ in a IIA compactification on X to the geometry of $\mathcal{M}_V$ in a IIB compactification on the mirror $\tilde{X}$, and can thus be used to obtain exact metrics in type IIA as well.

[2] In fact, (2.1.5) is only true at large volume, and otherwise receives α' corrections that can be computed via mirror symmetry.

BPS states

Now consider *states* in $\mathcal{N} = 2$ supergravity. Their quantum numbers include their charges under the n_V+1 $U(1)$ vector fields (*i.e.* from the vector multiplets plus the graviphoton) and their spin. For a massive state, the spin is a half-integer describing its weight as part of a representation of the 4-dimensional massive little group $Spin(3) = SU(2)$. The electric and magnetic $U(1)$ charges can be grouped into a $2(n_V + 1)$-dimensional vector γ of integers:

$$\begin{aligned} \gamma = (p^0,\ p^A,\ q_A,\ q_0) \qquad & A = 1, ..., n_V \\ mag. \quad elec. & \\ D6\ \ D4\ \ D2\ \ D0 \quad [IIA] \quad \text{or} \quad & \text{all } D3 \quad [IIB] \\ \in H^0\ \ H^2\ \ H^4\ \ H^6(X;\mathbb{Z})\ \ [IIA] \quad \text{or} \quad & H^3(X;\mathbb{Z})\ \ [IIB] \end{aligned} \tag{2.1.6}$$

We are particularly interested in *BPS states* that preserve half of the $\mathcal{N} = 2$ supersymmetry algebra. In 4-dimensional supergravity, such states are realized as "microstates" of charged and possibly multicentered (but bound) black holes. Alternatively, in a string theory picture, these states describe D-branes wrapped on various cycles in the three-fold X and extending only along the time direction in 4-dimensional spacetime $\mathbb{R}^{3,1}$. The charges are then interpreted as D-brane charges, associated to the cycles that the D-branes wrap, as indicated in (2.1.6). By dualizing cycles to forms, the charge vector γ can also be written as a cohomology class indicated on the last line of (2.1.6). We will say more about the D-brane interpretation of BPS states in Section 2.3.

There is a natural symplectic product on charges γ in the "charge lattice" $\Gamma \simeq H^{even}(X;\mathbb{Z})$ or $H^3(X;\mathbb{Z})$, simply given by multiplying magnetic charges times electric charges:

$$\langle \gamma, \gamma' \rangle = -p^0 q'_0 - p^A q'_A + q_0 p^{0\prime} + q_A p^{A\prime} \,. \tag{2.1.7}$$

Thinking of charges γ as differential forms, this can also be written as

$$\langle \gamma, \gamma' \rangle = \int_X \gamma \wedge (\gamma')^* \,, \tag{2.1.8}$$

where the '*' is trivial in a type IIB picture, and changes the signs of 2-form and 6-form components in a IIA picture.

Attractor equations and multicentered states

The Hilbert space of BPS states, $\mathcal{H}_{BPS}$, is a piecewise-constant "function" of the vector and hypermultiplet moduli. In the particular case of vector multiplet moduli — let us denote them generically as "t" — one is free to choose any value t_∞ of moduli at spatial infinity in $\mathbb{R}^{3,1}$. Given a collection of particles (*i.e.* black holes) in $\mathbb{R}^{3,1}$, the *attractor equations* then fix the values of t everywhere else [16]. Therefore, we should write

$$\mathcal{H}_{BPS} = \mathcal{H}_{BPS}(t_\infty)\,. \tag{2.1.9}$$

The *central charge* of a state of charge γ, defined as

$$Z(\gamma;t) = e^{\frac{1}{2}K}\langle\gamma,\Omega(t)\rangle = e^{\frac{1}{2}K}\langle\gamma,(X^I(t),F_I(t))\rangle\,, \tag{2.1.10}$$

also depends on vector multiplet moduli t. (The second equality of (2.1.10) expresses Z as the product of a vector of integer charges and the vector of periods of Ω, which implicitly depend on t.) A BPS state satisfies the condition that its mass is related to the absolute value of its central charge *evaluated at moduli* t_∞,[3]

$$M = \left(m_P^{(4d)}\right)|Z(\gamma,t_\infty)| = \frac{\sqrt{\mathrm{Vol}(X)/\ell_s^6}}{g_s\ell_s}\,|Z(\gamma;t_\infty)|\,. \tag{2.1.11}$$

The phase of this central charge describes which $\mathcal{N}=1$ subalgebra of the $\mathcal{N}=2$ supersymmetry algebra the BPS state preserves. For comparison, the leading contribution (at large charge) to the entropy of a single-centered black hole of charge γ is related to its central charge when evaluated at the values of moduli $t_*(\gamma)$ *at its horizon*,

$$S \sim \pi|Z(\gamma;t_*)|^2\,. \tag{2.1.12}$$

These "attractor values" $t_*(\gamma)$ depend only on γ and not on t_∞; by the attractor equations, they minimize the central charge as a function of t.

The Hilbert space $\mathcal{H}_{BPS}$ can jump across real codimension-1 walls in $\mathcal{M}_V$, so-called walls of *marginal stability*. (It can also jump at codimension-2 loci in $\mathcal{M}_H$; this will be discussed further in Sections 2.2-2.4.) In order to understand such a transition in supergravity, one needs to consider not only single-centered black holes, but also multi-centered bound states

[3]We will henceforth set the 4-dimensional Planck mass $m_P^{(4d)} \to 1$, but remind the reader of its value in (2.1.11).

of black holes. It was shown in [16] that such stationary but non-static bound states can form from two or more black holes with mutually nonlocal charges.

To be more specific, the spherically-symmetric, static metric ansatz

$$ds^2 = -e^{2U}dt^2 + e^{-2U}d\vec{x}^2 \qquad (U = U(\vec{x})) \tag{2.1.13}$$

in $\mathbb{R}^{3,1}$ leads to attractor equations (or BPS equations) for a single-centered black hole,

$$\begin{aligned} \partial_\tau U &= -e^U|Z|\,, \\ \partial_\tau t^a &= -2\,e^U g^{a\bar{b}}\bar{\partial}_{\bar{b}}|Z|\,, \end{aligned}$$

or more compactly

$$2\,\partial_\tau \mathrm{Im}(e^{-U}e^{-i\alpha}\hat{\Omega}) = -\gamma\,. \tag{2.1.14}$$

Here, $\tau = 1/r$ is the inverse of the radial coordinate in spatial $\mathbb{R}^3$, $\alpha = \arg Z(\gamma;t)$ is the argument of the central charge, $g_{a\bar{b}} = \partial_a\bar{\partial}_{\bar{b}}K$ is the metric on $\mathcal{M}_V$, and $\hat{\Omega}(t) = e^{K/2}\Omega(t)$. In (2.1.14), one thinks of both $\hat{\Omega}$ and γ as differential forms, or, taking period integrals, as vector-valued functions. The attractor equation (2.1.14) integrates to

$$2\,\mathrm{Im}(e^{-U}e^{-i\alpha}\hat{\Omega}) = -\frac{\gamma}{r} + 2\,\mathrm{Im}(e^{-U}e^{-i\alpha}\hat{\Omega})|_{t_\infty}\,. \tag{2.1.15}$$

The resulting solution flows to a minimum of $|Z|$ as $r \to 0$.

Being slightly more careful, (2.1.15) is really only valid and describes a massive BPS black hole if $|Z(\gamma;t)|$ attains a nonzero minimum in moduli space $\mathcal{M}_V$. If $|Z|$ vanishes at a singular point in $\mathcal{M}_V$, the minimum $|Z| = 0$ can be reached at a positive radius $r = r_0$ in $\mathbb{R}^3$, and for $r < r_0$ the moduli $t(\vec{x})$ are finite constants [62, 16]. This solution is called an "empty hole." If $|Z|$ vanishes at a regular point in $\mathcal{M}_V$, the attractor equations have no solution at all.

To generalize to the multi-centered case, following [16], one replaces the metric ansatz (2.1.13) with a more general stationary metric that contains angular momentum,

$$ds^2 = -e^{2U}(dt+\omega)^2 + e^{-2U}d\vec{x}^2 \qquad (U = U(\vec{x}),\ \omega = \omega(\vec{x}))\,. \tag{2.1.16}$$

The BPS equations for a multi-centered solution with n charges γ_i at centers $\vec{x}_i$ become

$$2\,e^{-U}\mathrm{Im}(e^{-i\alpha}\Omega) = H \tag{2.1.17}$$

$$*_0\mathbf{d}\omega = \langle \mathbf{d}H, H\rangle\,, \tag{2.1.18}$$

where $\mathbf{d}$ is the exterior derivative on $\mathbb{R}^3$, $*_0$ is the Hodge dual with respect to the flat metric on $\mathbb{R}^3$, α is the argument of the *total* central charge $Z(\gamma) = Z(\gamma_1) + Z(\gamma_2) + ... + Z(\gamma_n)$, and

$$H = -\sum_{i=1}^{n} \frac{\gamma_i}{|\vec{x} - \vec{x}_i|} + 2\,\mathrm{Im}(e^{-i\alpha}\hat{\Omega})|_{t_\infty}\,. \tag{2.1.19}$$

This is not so easy to integrate directly; however, (2.1.18) implies that $\langle \Delta H, H\rangle = 0$, which does lead to integrability conditions

$$\sum_{j=1}^{n} \frac{\langle \gamma_i, \gamma_j\rangle}{|\vec{x}_i - \vec{x}_j|} = 2\,\mathrm{Im}(e^{-i\alpha} Z(\gamma_i))|_{t_\infty} \qquad \forall\, i\,. \tag{2.1.20}$$

Conditions (2.1.20) fix $n-1$ independent center-to-center radii. In particular, in the 2-centered case, the distance between black holes is completely fixed:

$$r_{12} = \frac{1}{2}\langle \gamma_1, \gamma_2\rangle \frac{|Z_1 + Z_2|}{\mathrm{Im}(Z_1 \bar{Z}_2)}\bigg|_{t_\infty}\,, \qquad Z_i \equiv Z(\gamma_i)\,. \tag{2.1.21}$$

The resulting multi-centered black holes have an intrinsic electro-magnetic angular momentum that can simply be calculated by the Poynting vector[4]; in the 2-centered case, its magnitude is just

$$J_{12} = \frac{1}{2}|\langle \gamma_1, \gamma_2\rangle| - \frac{1}{2}\,. \tag{2.1.22}$$

Note that multi-centered bound states can *only* form if charges of constituents are mutually nonlocal, *i.e.* $\langle \gamma_i, \gamma_j\rangle \neq 0$. Otherwise, the attractive force between BPS centers will completely vanish.

The supergravity picture of wall crossing, *i.e.* jumps in $\mathcal{H}_{BPS}$, involves constituents of a multi-centered bound state coming unbound, causing the state to disappear from the single-particle spectrum. From (2.1.20) or (2.1.21), it is clear that this happens when the central charges of two constituents or groups of constituents align,[5] causing a center-to-center radius to diverge. Equivalently, conservation of energy during a split of BPS states $\gamma \to \gamma_1 + \gamma_2$ requires central charges to be aligned, so that

$$\begin{aligned} &|Z(\gamma_1 + \gamma_2)| = |Z(\gamma_1) + Z(\gamma_2)| = |Z(\gamma_1)| + |Z(\gamma_2)| \\ :\qquad &M = M_1 + M_2\,. \end{aligned} \tag{2.1.23}$$

[4]Up to a quantum correction that manifests itself as the shift by $-1/2$ in (2.1.22); see [16, 57] for details.

[5]From these equations alone, it looks like anti-aligned central charges will also correspond to splits, but anti-alignment is not compatible with mass conservation.

Also observe that the alignment of central charges implies that two BPS states preserve the same $\mathcal{N} = 1$ supersymmetry subalgebra, and from basic supersymmetry considerations it is then clear that the force between them must vanish.

Indices and refinement

A useful quantity to consider in supersymmetric theories is an *index* of BPS states. In the present situation, the *second helicity supertrace*

$$\Omega(t_\infty) = -2\,\mathrm{Tr}_{\mathcal{H}_{BPS}(t_\infty)}(-1)^{2J_3}{J_3}^2 \tag{2.1.24}$$

is a good index to use. The quantum number J_3 is the half-integer $SU(2)$ spin of a given state. $\Omega(t_\infty)$ counts short BPS multiplets, and evaluates to zero on long multiplets. In particular, $\Omega(t_\infty)$ is completely invariant under a transition where short BPS multiplets combine into long multiplets and leave the BPS spectrum. Such a transition is the only type expected to occur in the moduli space $\mathcal{M}_H$ (*cf.* [21]), so the index $\Omega(t_\infty)$ is independent of hypermultiplet moduli. Of course, $\Omega(t_\infty)$ *can* jump across walls of marginal stability in $\mathcal{M}_V$ as described on page 19, where states actually disappear from the (BPS *and* non-BPS) single-particle spectrum.

One can actually do somewhat better than (2.1.24). The BPS Hilbert space is graded by charge, so one can fix a charge γ and let

$$\Omega(\gamma; t_\infty) = -2\mathrm{Tr}_{\mathcal{H}(\gamma;t_\infty)}(-1)^{2J_3}{J_3}^2\,, \tag{2.1.25}$$

where $\mathcal{H}(\gamma; t_\infty)$ is the subspace of $\mathcal{H}_{BPS}$ containing states of charge γ. Moreover, due to quantization of center-of-mass degrees of freedom (and their superpartners), all states in $\mathcal{H}_{BPS}$ have a half-hypermultiplet contribution to their spin (*cf.* [57, 11, 12, 63]). Denoting the $(2j+1)$-dimensional $SU(2)$ representation as $[j]$, this means that there is a factorization

$$\mathcal{H}_{BPS} = \left(\left[\frac{1}{2}\right] + 2[0]\right) \otimes \mathcal{H}'\,. \tag{2.1.26}$$

In terms of the reduced Hilbert space $\mathcal{H}'$, the index can be written much more simply as

$$\Omega(\gamma; t_\infty) = \mathrm{Tr}_{\mathcal{H}'(\gamma;t_\infty)}(-1)^{2J_3}\,, \tag{2.1.27}$$

where J_3 is now the spin in $\mathcal{H}'$. Note, for example, that in the reduced Hilbert space a

(half)hypermultiplet is just written as [0] and a (half) vector multiplet as $\left[\frac{1}{2}\right]$, so

$$\Omega(\text{hyper}) = 1\,, \tag{2.1.28}$$

$$\Omega(\text{vector}) = -2\,. \tag{2.1.29}$$

The indices $\Omega(\gamma; t_\infty)$ have the same continuity (and discontinuity) properties as $\Omega(t_\infty)$.

The overarching goal of Part I of this thesis is to examine the implications of *refining* this index. In other words, instead of (2.1.27), we want to take spin into account and consider

$$\Omega^{ref}(\gamma; t_\infty; y) = \mathrm{Tr}_{\mathcal{H}'(\gamma;t_\infty)}(-y)^{2J_3}\,. \tag{2.1.30}$$

The resulting refined index is a Laurent polynomial in y; it is also convenient to define its (positive integer) coefficients Ω_n as

$$\Omega^{ref}(\gamma; t_\infty; y) = \sum_{n\in\mathbb{Z}} \Omega_n(\gamma; t_\infty)\,(-y)^n\,. \tag{2.1.31}$$

Note that $\Omega^{ref}(\gamma; t_\infty; y = 1) = \Omega(\gamma; t_\infty)$. The refined index encodes much of the information present in the Hilbert space $\mathcal{H}_{BPS}$. The integers $\Omega_n(\gamma; t_\infty)$ jump across walls of marginal stability in $\mathcal{M}_V$ just as $\Omega(\gamma; t_\infty)$ does. However, they *may* also jump whenever BPS states pair up into non-BPS multiplets. We call the locations of these discontinuities "invisible walls." In the hypermultiplet moduli space they only occur at codimension-2 loci,[6] and so are not terribly offensive. Nevertheless, to be absolutely sure that the Ω_n are constant on $\mathcal{M}_H$, we should restrict ourselves to rigid Calabi-Yau manifolds (in type IIA compactifications). We investigate the possibility of encountering codimension-1 invisible walls in $\mathcal{M}_V$ in Section 2.4.

To compare to the unrefined indices (2.1.28)-(2.1.29), note that

$$\Omega^{ref}(\text{hyper}; y) = 1\,, \tag{2.1.32}$$

$$\Omega^{ref}(\text{vector}; y) = -y - y^{-1}\,. \tag{2.1.33}$$

[6]The fact that jumps in $\mathcal{M}_H$ occur at (real) codimension-2 loci rather than codimension-1 walls is related to the fact that the superpotentials in supersymmetric quantum mechanics descriptions of low-energy D-brane dynamics (*cf.* Section 2.3) are *holomorphic* functions of the hypermultiplet moduli — thus the BPS spectrum can only jump in *complex* codimension ≥ 1. Physically, these arguments also arose in the study of enhanced gauge symmetries and geometric engineering, *cf.* [21].

Topological invariants

The refined and unrefined indices of BPS states are closely related to various topological invariants of the Calabi-Yau X. Let us assume that we are in a type IIA duality frame. For a distinguished choice of t_∞ corresponding roughly to the location of the wall near large volume where $D0$ states bind to a $D6$ state, the generating function of states with $D6$-$D2$-$D0$ charges,

$$\mathcal{Z}_{D6-D2-D0}(q,Q;t_\infty) = \sum_{m\in\mathbb{Z},\,\beta\in H_2(X;\mathbb{Z})} \Omega\big(\gamma=(1,0,\beta,m);t_\infty\big)(-q)^m Q^\beta\,, \tag{2.1.34}$$

is the Donaldson-Thomas/Gopakumar-Vafa partition function for X [20]. Or, more specifically, on one side of this $D6-D0$ wall (2.1.34) is the "reduced" Donaldson-Thomas partition function $\mathcal{Z}'_{DT}$, and on the other side it is the "unreduced" Donaldson-Thomas partition function

$$\mathcal{Z}_{DT} = M(q)^{\chi(X)}\,\mathcal{Z}'_{DT}\,, \tag{2.1.35}$$

which is multiplied by an extra factor of the MacMahon function.

Similarly, the refined generating function

$$\mathcal{Z}_{D6-D2-D0}(q,Q,y;t_\infty) = \sum_{m\in\mathbb{Z},\,\beta\in H_2(X;\mathbb{Z})} \Omega^{ref}\big(\gamma=(1,0,\beta,m);t_\infty;y\big)(-q)^m Q^\beta \tag{2.1.36}$$

turns out to be equivalent to the *refined* Donaldson-Thomas partition functions defined in [23, 26] — or to Nekrasov's partition function for $\mathcal{N}=2$ gauge theory in an Omega-background [22]. We shall see an explicit example of this in Section 3.1.

In another chamber of moduli space $\mathcal{M}_V$ with strong B-field, the partition functions (2.1.34) and (2.1.36), respectively, reproduce the "noncommutative Donaldson-Thomas" invariants of Szendröi [64] and a refined version thereof.

The relation between BPS indices and (*e.g.*) topological string invariants is based on the D-brane picture of BPS states that we describe further in Section 2.3 — combined with an argument relating D-brane states with Donaldson-Thomas/Gopakumar-Vafa theory as in [20, 65]. More generally, the unrefined indices $\Omega(\gamma;t_\infty)$ in *any* chamber of $\mathcal{M}_V$ should correspond to the "classical" version of Kontsevich and Soibelman's invariants for Calabi-Yau categories [15], where t_∞ parametrizes the choice of stability condition in the category. As we explain in Chapter 4, one of our main discoveries [1] is that the refined indices

$\Omega^{ref}(\gamma; t_\infty; y)$ in turn coincide to Kontsevich and Soibelman's *motivic* Donaldson-Thomas invariants [15].

Note that all the relations we describe here are of the form $\mathcal{Z}_{BH} \sim \mathcal{Z}_{top}$, in contrast with the famed OSV conjecture $\mathcal{Z}_{BH} \sim |\mathcal{Z}_{top}|^2$ [19]. This is not inconsistent. As described in [20], the OSV relation occurs in a very special limit corresponding to highly "polar" 2-center split attractor flows which causes the BPS generating functions to factorize.

2.2 Physical wall-crossing formulas

We now proceed to take a closer look at stability conditions for BPS states, largely in a supergravity context. Following [20] (and [1]), we use physical intuition from supergravity to derive "wall-crossing formulas" that describe how refined and unrefined indices jump across walls of marginal stability in $\mathcal{M}_V$.

Stability conditions and attractor flow trees

Let us begin by considering stability of black hole states more carefully. A minimal requirement for the multi-center attractor equations (2.1.17)-(2.1.18) to have a solution is that all the radii $r_{ij} = |\vec{x}_i - \vec{x}_j|$ appearing in the integrability condition (2.1.20) are positive. Indeed, for a bound state of two black holes (or two clusters of black holes) with charges γ_1 and γ_2, positivity of the center-to-center radius (2.1.21) shows that the (potentially) stable side of a wall of marginal stability must satisfy the *Denef stability condition*

$$\boxed{\langle \gamma_1, \gamma_2 \rangle \, \mathrm{Im}\big[Z(\gamma_1, t)\overline{Z(\gamma_2, t)}\big] > 0}\,. \tag{2.2.1}$$

The codimension-1 wall of marginal stability itself is defined by the equation

$$\begin{aligned} &\arg Z(\gamma_1, t_{ms}) = \arg Z(\gamma_2, t_{ms}) \\ &\quad : \quad \mathrm{Im}\big[Z(\gamma_1, t_{ms})\overline{Z(\gamma_2, t_{ms})}\big] = 0\,. \end{aligned} \tag{2.2.2}$$

On its "unstable" side, the quantity appearing in equation (2.2.1) is negative.

While condition (2.2.1) is necessary for the formation of a stable bound state, it is not sufficient. It was conjectured in [16] (see also [66, 20]) that the multi-center attractor equations have a physically reasonable solution if and only if it is possible to draw a *split*

attractor flow tree in moduli space $\mathcal{M}_V$ starting at t_∞ and ending on "good" attractor points, *i.e.* on minima of $|Z|$ that correspond to genuine single-center black holes or empty holes. Each segment of such a tree follows a single-center attractor flow trajectory, and the flows can split at walls of marginal stability that are crossed in the stable $\rightarrow$ unstable direction. For example, single-center, two-center, and three-center flows are shown in Figure 2.1.

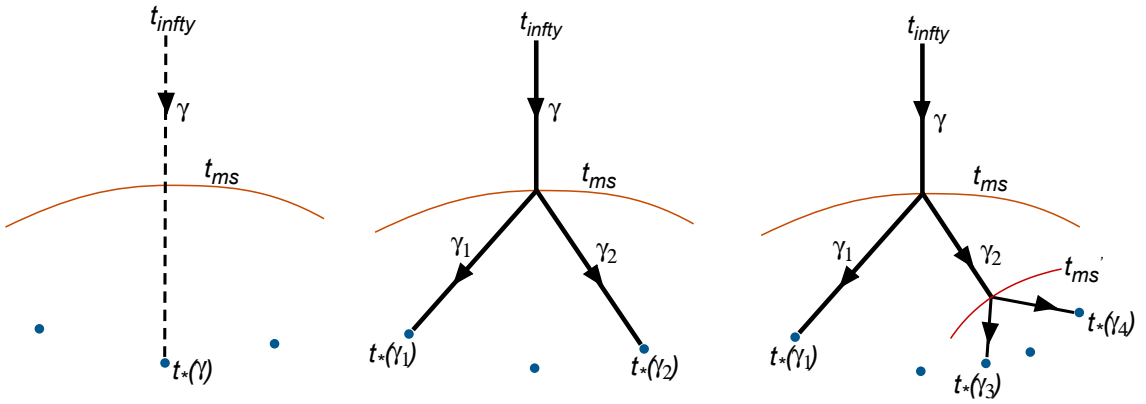

Figure 2.1: Split attractor flows in supergravity. The walls of marginal stability shown correspond to $\gamma \rightarrow \gamma_1 + \gamma + 2$ and $\gamma_2 \rightarrow \gamma_3 + \gamma_4$.

Note that flows do not *need* to split at walls of marginal stability. For example, suppose that regular positive minima (*i.e.* honest black hole solutions) exist for charges γ_1 and γ_2 on the "unstable" side of a $\gamma \rightarrow \gamma_1 + \gamma_2$ marginal stability wall, as in Figure 2.2. If a good attractor point for the total charge $\gamma = \gamma_1 + \gamma_2$ also exists on the same, unstable, side of the wall, then when t_∞ is on the stable side *both* single-center and 2-center bound states of total charge γ exist; whereas when t_∞ is on the unstable side only a single-center state of charge γ is in the spectrum. In contrast, in the case that the attractor point for $\gamma = \gamma_1 + \gamma_2$ is not a good minimum (*e.g.* if this is a regular point of moduli space with $Z(\gamma) = 0$ there), then the only possible state of total charge γ is a 2-center state that is in the spectrum on the stable side of the wall.

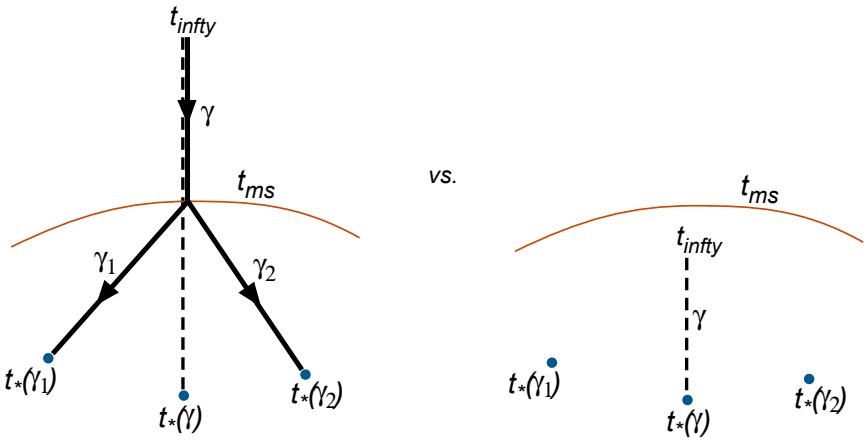

Figure 2.2: Possiblities when t_∞ is on the "stable" (LHS) and "unstable" (RHS) side of the wall.

Primitive wall crossing

We now return to the supergravity viewpoint and use physical intuition to derive *wall-crossing formulas*: formulas that describe the jumps in $\mathcal{H}_{BPS}$ and in the indices Ω and Ω^{ref} across walls of marginal stability. Many of these formulas were derived in [20]; the refined versions were also described in [67] and [1].

The simplest wall crossing scenario involves a bound state of total charge γ decomposing into two *primitive* states of charges γ_1 and γ_2 at a wall of marginal stability. Primitive means that γ_1 and γ_2 cannot be written as multiples of any smaller charge. Let the wall be at t_{ms}, and let t_+ and t_- be moduli on the stable and unstable sides of the wall, respectively. In a generic situation, $\mathcal{H}(\gamma_1)$ and $\mathcal{H}(\gamma_2)$ (and $\mathcal{H}$ for any charge that is not γ) will be continuous at t_{ms}; we may thus assume that

$$\mathcal{H}(\gamma_1; t_-) = \mathcal{H}(\gamma_1; t_+) = \mathcal{H}(\gamma_1; t_{ms})\,,$$
$$\mathcal{H}(\gamma_2; t_-) = \mathcal{H}(\gamma_2; t_+) = \mathcal{H}(\gamma_2; t_{ms})\,.$$

The separation of the bound state of charge γ into two infinitely separated black holes (or cluster of black holes) of charges γ_1 and γ_2 at t_{ms} then suggests that

$$\mathcal{H}'(\gamma; t_+) = [J_{12}] \otimes \mathcal{H}'(\gamma_1; t_{ms}) \otimes \mathcal{H}'(\gamma_2; t_{ms})\,. \tag{2.2.3}$$

This is the basis of the primitive wall-crossing formulas: the (reduced) Hilbert space on

the stable side of the wall is a product of Hilbert spaces for the components, times an electromagnetic angular momentum multiplet. Recall that the angular momentum is given by (2.1.22):

$$J_{12} = \frac{I_{12} - 1}{2}\,, \qquad I_{12} \equiv |\langle \gamma_1, \gamma_2 \rangle|\,. \tag{2.2.4}$$

Calculating the unrefined index using (2.1.27) is straightforward [20]:

$$\Omega(\gamma; t_+) = (-1)^{I_{12}-1} I_{12}\, \Omega(\gamma_1; t_{ms})\, \Omega(\gamma_2; t_{ms})\,. \tag{2.2.5}$$

Of course, there may be states of total charge γ in the BPS spectrum that do not split at the $\gamma \to \gamma_1 + \gamma_2$ wall; if so, then one should really write

$$\Delta\Omega(\gamma) \equiv \Omega(\gamma; t_+) - \Omega(\gamma; t_-) = (-1)^{I_{12}-1} I_{12}\, \Omega(\gamma_1; t_{ms})\, \Omega(\gamma_2; t_{ms})\,. \tag{2.2.6}$$

Similarly, one sees from the definition (2.1.30) that (*cf.* [67])

$$\boxed{\Delta\Omega^{ref}(\gamma; y) = [I_{12}]_{-y}\, \Omega^{ref}(\gamma_1; t_{ms}; y)\, \Omega^{ref}(\gamma_2; t_{ms}; y)}\,, \tag{2.2.7}$$

where $[I_{12}]_{-y}$ denotes the "quantum dimension"

$$[I_{12}]_{-y} = \frac{(-y)^{I_{12}} - (-y)^{I_{12}}}{(-y) - (-y)^{-1}} = (-y)^{-I_{12}+1} + (-y)^{-I_{12}+3} + ... + (-y)^{I_{12}-1}\,. \tag{2.2.8}$$

As expected, this reduces to (2.2.6) upon setting $y \to 1$.

Semi-primitive wall crossing

Now, let us view the above $\gamma \to \gamma_1 + \gamma_2$ split in reverse. As the wall of marginal stability is crossed, black holes or clusters of black holes with total charges γ_1 and γ_2 will bind to form states of total charge γ. However, the wall for $\gamma \to \gamma_1 + \gamma_2$ splits is *also* a wall for all $M\gamma_1 + N\gamma_2$ splits, with M, $N \geq 1$, and its stable and unstable sides are the same. Therefore, by the split attractor flow conjecture, bound states of any and all total charges

$$M\gamma_1 + N\gamma_2\,, \qquad M,\, N \geq 1 \tag{2.2.9}$$

should also form and be part of the BPS spectrum on the stable side of the wall. The case $M = 1$, $N \geq 1$ is called *semi-primitive* wall crossing, and can also be analyzed in the supergravity context. The general case M, $N \geq 1$ is harder to consider in supergravity, and

is most easily handled via the general Kontsevich-Soibelman wall-crossing formula that is described in Chapter 4.

During the semi-primitive splits $\gamma \to \gamma_1 + N\gamma_2$, the decomposition of the Hilbert spaces can be written as [20]

$$\bigoplus_{N=0}^{\infty} \mathcal{H}'(\gamma_1 + N\gamma_2; t_+)\, x^N = \mathcal{H}'(\gamma_1; t_{ms}) \otimes \bigotimes_{k=0}^{\infty} \mathcal{F}\left(x^k \left[J_{\gamma_1, k\gamma_2}\right] \otimes \mathcal{H}'(k\gamma_2; t_{ms})\right). \tag{2.2.10}$$

On the LHS, we have grouped all the Hilbert spaces $\mathcal{H}'(\gamma_1 + N\gamma_2; t_+)$ into a generating function. On the RHS, we consider all possible ways to bind arbitrary numbers of bound clusters of total charges γ_2, $2\gamma_2$, etc. to a γ_1 center at marginal stability (see the schematic in Figure 2.3). For each k, what is essentially a free gas of particles with charges $k\gamma_2$ are bound; $\mathcal{F}(\cdots)$ is a Fock space that describes the Hilbert space of this gas, taking into account the angular momentum contribution

$$J_{\gamma_1, k\gamma_2} = \frac{k\, I_{12} - 1}{2}, \qquad I_{12} = |\langle \gamma_1, \gamma_2 \rangle|, \tag{2.2.11}$$

and keeping track of total charge by weighing each particle with a variable x^k.

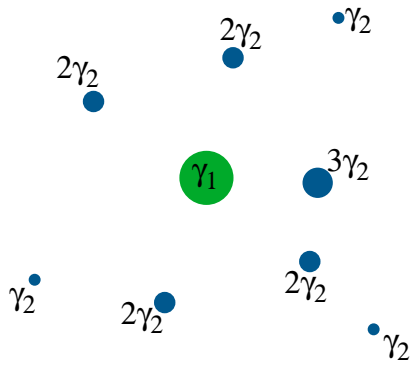

Figure 2.3: A "gas" of black holes with charges $k\gamma_2$ binding to a γ_1 center in physical space.

The resulting wall-crossing formula for unrefined indices is [20]

$$\Omega(\gamma_1; t_{ms}) + \sum_{N=1}^{\infty} \Omega(\gamma_1 + N\gamma_2; t_+)\, x^N = \Omega(\gamma_1; t_{ms}) \prod_{k=1}^{\infty} \left(1 - (-1)^{kI_{12}} x^k\right)^{kI_{12}\Omega(k\gamma_2; t_{ms})}. \tag{2.2.12}$$

The product on the RHS corresponds directly to the free gasses of particles mentioned above; the particles can be bosonic or fermionic, according to the sign of the exponent

$\Omega(k\gamma_2;t_{ms})$. In the refined case, the formula reads [1]

$$\Omega^{ref}(\gamma_1;y)+\sum_{N=1}^{\infty}\Omega^{ref}(\gamma_1+N\gamma_2;t_+;y)\,x^N \\ =\Omega^{ref}(\gamma_1;y)\prod_{k=1}^{\infty}\prod_{j=1}^{kI_{12}}\prod_{n\in\mathbb{Z}}\left(1+(-1)^n(-y)^{2j-kI_{12}-1+n}x^k\right)^{(-1)^n\Omega_n(k\gamma_2)}, \quad (2.2.13)$$

where the unambiguous moduli t_{ms} of $\Omega^{ref}(\gamma_1;t_{ms};y)$ and $\Omega^{ref}(k\gamma_2;t_{ms};y)$ have been suppressed. In the refined formula, the spin content has simply been distributed over the factors on the RHS.

Similarly to the unrefined case, formulas (2.2.12) and (2.2.13) are strictly only valid when $\mathcal{H}'(\gamma_1+N\gamma_2;t_-)$ is trivial for all $N\geq 1$ on the unstable side of the wall. If states with total charge $\gamma_1+N\gamma_2$ already exist on the unstable side of the wall, they will also bind gasses of $k\gamma_2$ particles. Then, for example, the unrefined formula reads

$$\Omega(\gamma_1)+\sum_{N=1}^{\infty}\Omega(\gamma_1+N\gamma_2;t_+)\,x^N \\ =\left[\Omega(\gamma_1)+\sum_{N=1}^{\infty}\Omega(\gamma_1+N\gamma_2;t_-)\,x^N\right]\times\prod_{k=1}^{\infty}\left(1-(-1)^{kI_{12}}x^k\right)^{kI_{12}\Omega(k\gamma_2)}, \quad (2.2.14)$$

and the refined formula generalized in an analogous fashion.

Derivation

For completeness, we finish this section by providing a derivation of the slightly non-trivial formula (2.2.13) (from which (2.2.12) also follows by setting $y\to 1$). The derivation utilizes standard techniques from statistical mechanics. It is easy to see that tracing over the LHS of (2.2.10) with weight $(-y)^{2J_3}$ gives

$$\Omega^{ref}(\gamma_1;y)+\sum_{N=1}^{\infty}\Omega^{ref}(\gamma_1+N\gamma_2;t_+;y)\,x^N\,, \quad (2.2.15)$$

and tracing over the RHS gives

$$\Omega^{ref}(\gamma_1;y)\prod_{k=1}^{\infty}\mathrm{Tr}_{\mathcal{F}^{(k)}}(-y)^{2J_3^{(k)}}x^{k\mathcal{N}}\,, \quad (2.2.16)$$

where each operator $J_3^{(k)}$ measures spin in the Fock space $\mathcal{F}^{(k)}\equiv\mathcal{F}\left(x^k[J_{\gamma_1,k\gamma_2}]\otimes\mathcal{H}'(k\gamma_2)\right)$ and $\mathcal{N}$ is the excitation number in this Fock space. We introduce quantum numbers $n_j=$

$-\frac{kI_{12}-1}{2}, ..., \frac{kI_{12}-1}{2}$ and $n \in \mathbb{Z}$, respectively, to keep track of the electromagnetic angular momentum and the internal spin of a state in the Hilbert space $[J_{\gamma_1,k\gamma_2}] \otimes \mathcal{H}'(k\gamma_2)$. For fixed n_j and n, the degeneracy of such a state is $\Omega_n(k\gamma_2)$, so we can introduce a third quantum number $m = 1, ..., \Omega_n(k\gamma_2)$ to keep track of this. The total spin is $J_3^{(k)}(n_j, n, m) = n_j + \frac{n}{2}$. Note that states with odd n are bosonic and states with even n are fermionic [20]. States in the *Fock* space $\mathcal{F}^{(k)}$ are described by entire sets of occupation numbers $\{d_{n_j,n,m}\}$, where $d_{n_j,n,m} \in \{0, 1\}$ if the state is fermionic and $d_{n_j,n,m} \in \{0, 1, ..., \infty\}$ if the state is bosonic. Thus, we have

$$\begin{aligned}
\mathrm{Tr}_{\mathcal{F}^{(k)}}(-y)^{2J_3^{(k)}} x^{k\mathcal{N}} &= \sum_{\text{sets } \{d_{n_j,n,m}\}} (-y)^{\sum_{n_j,n,m} d_{n_j,n,m}(2n_j+n)} x^{k\sum_{n_j,n,m} d_{n_j,n,m}} \\
&= \prod_{n_j,n,m} \sum_{d_{n_j,n,m}} (-y)^{d_{n_j,n,m}(2n_j+n)} x^{kd} \\
&= \Big(\prod_{n_j,n\,\text{even},m} \sum_{d=0}^{1} (-y)^{d(2n_j+n)} x^{kd} \Big) \times \Big(\prod_{n_j,n\,\text{odd},m} \sum_{d=0}^{\infty} (-y)^{d(2n_j+n)} x^{kd} \Big) \\
&= \Big(\prod_{n_j,n\,\text{even},m} \big(1 + (-y)^{2n_j+n} x^k\big) \Big) \times \Big(\prod_{n_j,n\,\text{odd},m} \big(1 - (-y)^{2n_j+n} x^k\big)^{-1} \Big) \\
&= \prod_{n_j,n,m} \big(1 + (-1)^n (-y)^{2n_j+n} x^k\big)^{(-1)^n} \\
&= \prod_{n_j,n} \big(1 + (-1)^n (-y)^{2n_j+n} x^k\big)^{(-1)^n \Omega_n(k\gamma_2)} \\
&= \prod_{j=1}^{kI_{12}} \prod_{n\in\mathbb{Z}} \big(1 + (-1)^n (-y)^{2j-kI_{12}-1+n} x^k\big)^{(-1)^n \Omega_n(k\gamma_2)} .
\end{aligned}$$

In the last step, we replaced n_j with the integral summation variable $j = 1 + \frac{kI_{12}-1}{2} + n_j$ to obtain the final answer.

2.3 BPS states of D-branes

The Hilbert space $\mathcal{H}'_{BPS}$ also has a description in terms of D-brane states, which is perhaps more common in the literature, and more intuitive in a string theory picture. Moreover, this description connects the supergravity picture that we have used heretofore with topological string invariants, melting crystals (Chapter 3), and the Kontsevich-Soibelman wall-crossing formulas (Chapter 4).

Roughly speaking, $\mathcal{H}'_{BPS}(\gamma)$ can be obtained in string theory compactified on a Calabi-Yau threefold X the following way. As explained in Section 2.1, charges $\gamma \in \Gamma$ can be naturally interpreted as charges of D-branes that wrap cycles of X and fill only the time direction of $\mathbb{R}^{3,1}$. In the case of type IIA theory, these are even-dimensional (holomorphic) cycles, while in type IIB theory they are odd dimensional (special Lagrangian) cycles. Fixing γ, one constructs the classical moduli space $\mathcal{M}(\gamma)$ of D-branes with this charge γ. $\mathcal{M}(\gamma)$ describes (*e.g.*) deformations of the D-branes and Wilson loop degrees of freedom on the branes. The quantum Hilbert space $\mathcal{H}'_{BPS}(\gamma)$, then, is just generated by the cohomology $H^*(\mathcal{M}(\gamma))$ as long as this cohomology makes sense[7] (*cf.* [21]). In particular, the unrefined index is an Euler characteristic and the refined index is a Poincaré polynomial:

$$\Omega(\gamma) = \chi(\mathcal{M}(\gamma))\,, \tag{2.3.1}$$

$$\Omega^{ref}(\gamma) = (-y)^{-\frac{\dim(\mathcal{M})}{2}} \text{Poincaré}(\mathcal{M}(\gamma); -y)\,. \tag{2.3.2}$$

Note that $\mathcal{M}(\gamma)$ is always Kähler, so $H^*(\mathcal{M}(\gamma))$ is organized into representations of an $SU(2)$ Lefschetz action. These coincide with the $SU(2)$ spin representations of states in $\mathbb{R}^{3,1}$, so that cohomological degree becomes identified with spin (see, for example, [57, 20, 65]). The middle cohomology (spin zero) actually corresponds to fermionic states in $\mathbb{R}^{3,1}$ once center-of-mass degrees of freedom are included; then $H^{\dim(\mathcal{M})/2+2n}(\mathcal{M})$, $n \in \mathbb{Z}$, is fermionic and $H^{\dim(\mathcal{M})/2+2n+1}(\mathcal{M})$ is bosonic. Of course, $\mathcal{M}(\gamma)$ and all related quantities depend on vector multiplet moduli, because these affect the *stability* condition for BPS branes.

We proceed to discuss some aspects of the D-brane $\leftrightarrow$ supergravity correspondence, including the inevitable realization of D-brane moduli spaces by quiver representations. We maintain the discussion at a conceptual level; for precise details we refer the reader to the references cited herein.

Quiver representations

The moduli space $\mathcal{M}(\gamma)$ of D-branes can often be described as a moduli space of quiver representations. Let us take a moment to explain what this means mathematically (see *e.g.*

[7] Generically, $\mathcal{M}(\gamma)$ is highly singular and $H^*\mathcal{M}(\gamma)$ is *not* well-defined. This is where motivic invariants become important, as described in Chapter 4. This "subtlety" is irrelevant for the present discussion, however.

[68] for a more thorough description).

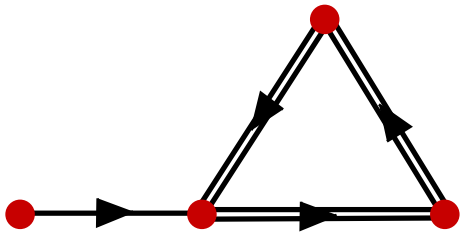

Figure 2.4: An example of a quiver with four nodes.

A quiver, as in Figure 2.4, is a collection of nodes labelled by $i \in I$ with a collection $\mathcal{A}$ of arrows connecting them. A *representation* of the quiver — or more precisely a representation of the path algebra generated by the arrows — is a collection of complex vector spaces $\{V_i\}_{i\in I}$ and a collection of homomorphisms from V_i to V_j for each arrow going from node i to node j. A quiver with closed loops can also have a superpotential W, which is a polynomial in the noncommutative arrow variables $a \in \mathcal{A}$. A representation must then obey the condition that the homomorphism corresponding to $\partial_a W$ vanishes for any $a \in \mathcal{A}$; in other words, it is a representation of the quotient of the path algebra $\mathcal{A}/dW$. There are fairly obvious notions of subrepresentations and isomorphism of representations for quivers. The latter is generated by a collection of automorphisms $g_i \in GL(V_i)$, one for each node V_i.

There is also a notion of stability for quivers called *θ-stability* [69]. For a given representation V of a quiver, let $\mathbf{n} = (n_i)_{i\in I}$ be its dimension vector, such that $n_i = \dim V_i$. Let $\boldsymbol{\theta} = (\theta_i)_{i\in I}$ be a collection of real numbers. Then a representation is θ-stable if every nontrivial proper subrepresentation $\tilde{V}$ with dimension vector $\tilde{\mathbf{n}}$ satisfies

$$\boldsymbol{\theta} \cdot \tilde{\mathbf{n}} < \boldsymbol{\theta} \cdot \mathbf{n}\,. \tag{2.3.3}$$

For a given choice of $\boldsymbol{\theta}$, we let $\mathcal{M}_s(\mathbf{n};\boldsymbol{\theta})$ be the moduli space of stable representations with dimension vector $\mathbf{n}$, modulo isomorphism — *i.e.* a quotient of all possible representations by the isomorphism group $\prod_i GL(V_i)$.

Quivers, D-branes, and supergravity

The relation between quivers, D-branes, and BPS states in supergravity is nicely described by Denef in [57]. The transition between a D-brane description and a supergravity

description is a smooth one, induced by varying the string coupling g_s. At large $g_s|\gamma|$, a BPS state of charge γ is best described as a backreacting, multi-center, solitonic black hole in supergravity, whereas at small $g_s|\gamma|$ this state is best described as a bound state of D-branes living at a *single* point in $\mathbb{R}^3$. There is no contradiction between the multi-center supergravity state and the single-center D-brane bound state: the 4-dimensional Planck length

$$\ell_P^{(4)} = \frac{\ell_s g_s}{\sqrt{\mathrm{Vol}(X)/\ell_s^6}}\,, \tag{2.3.4}$$

which sets the separation between black hole centers, becomes smaller than the string length at small g_s, so that the centers effectively fuse together.

The resulting single-center collection of bound D-branes is held together by open strings stretched between the branes. Suppose that each distinct D-brane (say D_i) supports a rank-n_i vector bundle. The low-energy dynamics of this collection can be described in nice cases by a (0+1)-dimensional supersymmetric $\prod_i U(n_i)$ gauge theory (reduced to the common noncompact worldvolume of the branes), whose matrix-valued fields describe the open string excitations between pairs of branes. The classical moduli space of this gauge theory, $\mathcal{M}_{QM}$, is equivalent to the classical moduli space of the D-branes. $\mathcal{M}_{QM}$ is obtained by solving the F-term equations $dW = 0$ as well as one D-term equation for every distinct D-brane involved in the bound state. Each D-term equation depends on a FI parameter θ_i, and the values of these parameters are a reflection in the gauge theory of the stability condition in supergravity.

It was shown by [69] that the moduli space of such a supersymmetric gauge theory is equivalent (for generic choices of $\boldsymbol{\theta}$) to the moduli space of θ-stable quiver representations with $\boldsymbol{\theta}$ set equal to the FI parameters. The relevant quiver is simply constructed by associating a node i to every $U(n_i)$ gauge field, and arrows from node i to node j to every bifundamental field representing string states from brane D_i to brane D_j. The net number of arrows between i and j is the same as the intersection number between the corresponding D-brane charges, $\langle\gamma_i, \gamma_j\rangle$.[8] The superpotential for the quiver is the same as the superpotential in the gauge theory. One then looks for θ-stable representations of the quiver with

[8]It is easy to see that this should be the case in a IIB compactification, where all branes are special Lagrangian, and open strings live at the intersections between pairs of branes. At least if all intersections have the same sign, there are $\langle\gamma_i, \gamma_j\rangle$ of them, and this must also be the number of $U(n_i) - U(n_j)$ bifundamental fields in the gauge theory.

dimension vector $\mathbf{n} = (n_i)$ to describe the D-brane state. An isomorphism of representations is just a gauge transformation.

Such quiver descriptions of D-brane moduli spaces are known to be accurate for fractional D-branes on orbifolds [70]. They also exist for some non-compact Calabi-Yau models (like the conifold) in which D-brane central charges can have almost equal arguments [71, 68]. For a compact Calabi-Yau, however, a quiver gives at best a local description of the moduli space of D-branes near a wall of marginal stability.

As $g_s \to 0$, a bound collection of D-branes can undergo tachyon condensation due to tachyonic modes acquired by open string states between pairs of branes. Indeed, if the bound collection of D-branes is to be stable, it *must* undergo tachyon condensation, "decaying" to a *single*, potentially complicated, D-brane state at very small g_s. It was argued in [57] that near a wall of marginal stability, the Denef stability condition (2.2.1) is equivalent to θ-stability for a quiver or gauge theory, and equivalent to the physical requirement of having tachyonic open string states present.

Categories of branes

Mathematically, D-branes are described by objects in the Fukaya category (in type IIB compactification) or the derived category of coherent sheaves $D^b coh(X)$ (in type IIA compactification).[9] In each case, BPS branes must satisfy a stability condition — respectively, Joyce stability [73] and Π-stability [18] — to ensure that they are stable objects that cannot decay (in a physical type II theory) into independent constituent branes. These stability conditions depend on the vector multiplet moduli t_∞ of the Calabi-Yau compactification, and are equivalent to Denef stability near walls of marginal stability. Moreover, for quiver quantum mechanics, they should be equivalent to θ-stability. To summarize, there is a (still conjectural!) equivalence of stable moduli spaces

$$\begin{aligned}\mathcal{M}_{Fuk}\big(\tilde{\gamma}; \text{Joyce}(t_\infty)\big) \overset{\text{mirror}}{=} \mathcal{M}_{D^b coh}\big(\gamma; \Pi(t_\infty)\big) &= \mathcal{M}_s\big(\gamma = \sum n_i\gamma_i; \boldsymbol{\theta}(t_\infty)\big) \\ &= \mathcal{M}(\text{D-brane bound state of charge } \gamma \text{ at } t_\infty)\,,\end{aligned} \tag{2.3.5}$$

and a corresponding equivalence of Hilbert spaces

$$\mathcal{H}'^{brane}_{BPS}(\gamma; t_\infty) = \mathcal{H}'^{sugra}_{BPS}(\gamma; t_\infty)\,. \tag{2.3.6}$$

[9] There is a large body of literature on this topic; see [72] for an excellent review.

As a final comment, note that there exists a general construction of quivers directly from the categorical description of branes. Suppose that we are in a IIA compactification, so the relevant category is $D^b coh(X)$. Given a collection of branes that form a basis for the associated K-theory on X — *i.e.* branes whose charges γ_i generate the charge lattice Γ — one can form a quiver by associating a node to each such brane, arrows to each Ext^1 group between pairs of branes, and a superpotential computed from the Ext^2 groups. Then quiver representations of dimension vector $\mathbf{n}$ such that $\sum_i n_i\gamma_i = \gamma$ (such a dimension vector can be found for any γ) should describe D-brane states of total charge γ. Unfortunately, if some of the branes in the chosen K-theory basis are not rigid, the resulting quiver can have closed loops (from a node to itself) that are not "obstructed" by the superpotential. In this case, the moduli space of quiver representations is noncompact, and only describes the D-brane moduli space $\mathcal{M}(\gamma)$ locally. As it is not known how to compactify $\mathcal{M}(\gamma)$, it is not clear how to compute the respective $\mathcal{H}'_{BPS}(\gamma)$. A rigid, complete basis for the quiver *can* be found in the situations mentioned above: orbifolds and some non-compact Calabi-Yau's. In some cases, it is possible to consider a sublattice of $\Gamma' \subset \Gamma$ that has a rigid basis of branes, and to obtain compact moduli spaces for $\gamma \in \Gamma'$.

2.4 Invisible walls

In this final section, we examine the "invisible walls" introduced in Section 2.1. We defined these to be walls in moduli space across which the unrefined index $\Omega(\gamma)$ is continuous, but the refined index $\Omega^{ref}(\gamma; y)$ jumps. The basic mechanism for how this happens can be understood in a simple situation where $\mathcal{H}_{BPS}(\gamma)$ admits a description as the cohomology of a brane moduli space $\mathcal{M}(\gamma)$. As t_∞ (say) crosses an invisible wall, $\mathcal{M}(\gamma)$ can develop a singularity and undergo a topology-changing transition, so that the Poincaré polynomial of $\mathcal{M}$ changes while the Euler characteristic does not.

In the vector multiplet moduli space $\mathcal{M}_V$, one tempting place to look for such invisible walls is in internal rearrangements of multi-center black holes that were first considered in [20] (Section 5.2.3 therein). The basic idea is that as t_∞ varies the components of a multi-center state can change their binding structure, and presumably change the spin structure of the overall configuration, without ever undergoing a marginal stability transition. We focus here on this example — and find, amazingly, that multiple factors conspire to assure

that the refined index remains unchanged.

Multi-center rearrangements

The simplest scenario, involving a 3-center bound state of total charge $\gamma = \gamma_1 + \gamma_2 + \gamma_3$ with all component charges primitive, is depicted in Figure 2.5. For one value of moduli $t_\infty = t_0$, an attractor flow first encounters a $\arg Z(\gamma_2) = \arg Z(\gamma_1 + \gamma_3)$ wall. If the flow splits, it eventually forms attractor flow tree (A). If it crosses this wall without splitting, it forms attractor flow tree (B). However, for a slightly different value of moduli $t_\infty = t_1$, the flow hits a $\arg Z(\gamma_3) = \arg Z(\gamma_1 + \gamma_2)$ wall first and must split there to form attractor flow tree (C). *Note that there is no marginal stability wall between t_0 and t_1.*

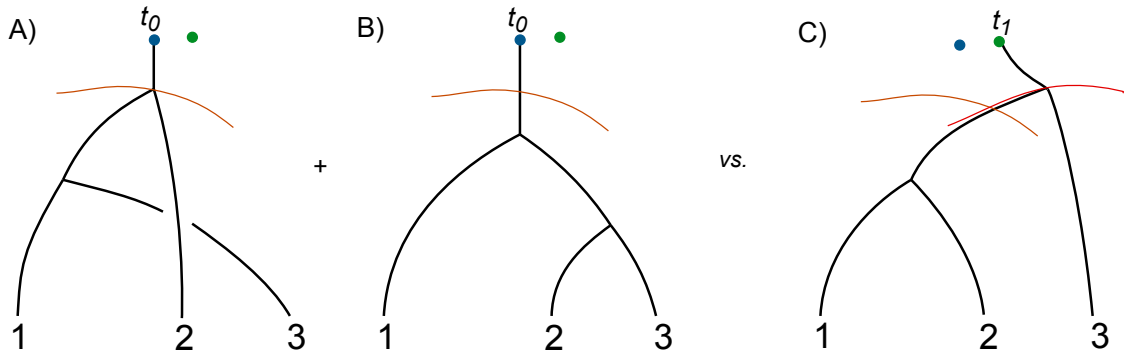

Figure 2.5: A three-center rearrangement.

This scenario may seem somewhat contrived, but it can actually happen in a physical context: the example given in [20] involves a 3-centered $D6 - D6 - \overline{D6}$ bound state (where the two $D6$'s have nontrivial worldvolume flux). Generally, a necessary condition for this transition is that the three quantities

$$a = \langle \gamma_2, \gamma_3 \rangle \qquad b = \langle \gamma_3, \gamma_1 \rangle \qquad c = \langle \gamma_1, \gamma_2 \rangle \tag{2.4.1}$$

all have the same sign. Assuming (WLOG) they are all positive, it is also necessary that

$$a > b > c\,. \tag{2.4.2}$$

Since the transition does not involve crossing a wall of marginal stability, the unrefined index $\Omega(\gamma)$ should not change. To see that this is indeed the case, one can use repeated

applications of the primitive wall-crossing formula (2.2.6). Since $\mathcal{H}(\gamma;t_0) = \mathcal{H}^{(A)}(\gamma;t_0) \oplus \mathcal{H}^{(B)}(\gamma;t_0)$, the index at t_0 is

$$\begin{aligned}\Omega(\gamma;t_0) &= (-1)^{a-c+b}(a-c)b\,\Omega(\gamma_1)\Omega(\gamma_2)\Omega(\gamma_3) + (-1)^{c-b+a}(c-b)a\,\Omega(\gamma_1)\Omega(\gamma_2)\Omega(\gamma_3) \\ &= (-1)^{a+b+c}\big[(a-c)b + (c-b)a\big]\,\Omega(\gamma_1)\Omega(\gamma_2)\Omega(\gamma_3)\,. \end{aligned} \tag{2.4.3}$$

The index at t_1 is similarly given by

$$\Omega(\gamma;t_1) = (-1)^{a-b+c}(a-b)c\,\Omega(\gamma_1)\Omega(\gamma_2)\Omega(\gamma_3)\,, \tag{2.4.4}$$

and $\Omega(\gamma;t_0) = \Omega(\gamma;t_1)$ results from the simple fact that $(a-c)b + (c-b)a = (a-b)c$.

In the refined case, we can similarly iterate the refined primitive wall-crossing formula (2.2.7) to find that

$$\begin{aligned}&\Omega^{ref}(\gamma;t_0;y) - \Omega^{ref}(\gamma;t_1;y) \\ &\quad = \big([a-c]_{-y}[b]_{-y} + [c-b]_{-y}[a]_{-y} - [a-b]_{-y}[c]_{-y}\big)\,\Omega^{ref}(\gamma_1;y)\Omega^{ref}(\gamma_2;y)\Omega^{ref}(\gamma_3;y)\,. \end{aligned} \tag{2.4.5}$$

It is a surprising fact that the quantity in parentheses actually vanishes, due to an algebraic identity of quantum dimensions. Therefore, in this case, there is no change in the refined index either: although the internal configuration of the bound state is rearranged, the total structure of the spin is unmodified!

Although the scenario just described is a rather simple example, it forms the basis for an argument that no invisible walls exist for rearrangements of *any* multi-center states, at least when the component black holes have primitive charges. Observe first that if there *had* existed an invisible wall in the 3-center rearrangement, it would correspond to all moduli t_{inv} such that the attractor flow for charge γ from t_{inv} would hit the codimension-2 locus Y where

$$\arg Z(\gamma_1) = \arg Z(\gamma_2) = \arg Z(\gamma_3)\,. \tag{2.4.6}$$

This is shown schematically in Figure 2.6. The (non-generic!) attractor flow tree from moduli t_∞ on this putative wall undergoes a triple split, serving as a transition between trees (A) and (B) and tree (C).

Now imagine a general (primitive) multi-center rearrangement, where for some value of starting moduli $t_\infty = t_0$ a certain set $\mathcal{T}_0$ of tree topologies are possible; and for some other value $t_\infty = t_1$ some other set $\mathcal{T}_1$ of topologies are achieved. A path in moduli space from t_0 to t_1 encounters putative invisible walls at some set of moduli $t^{(1)}, t^{(2)}, t^{(3)}, ...$ whose

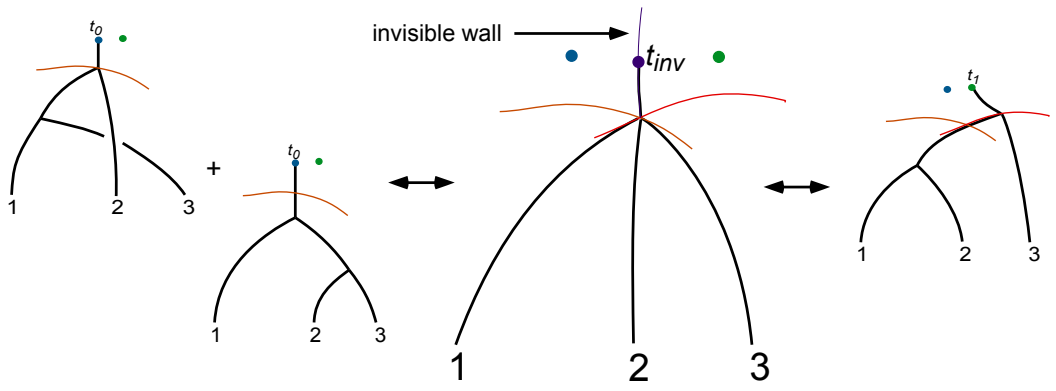

Figure 2.6: An invisible wall located at a three-way split.

attractor flows hit points where the arguments of three or more central charges align — at these points topologies in the set $\mathcal{T}_0$ can merge and split, so they eventually transition to the topologies of $\mathcal{T}_1$. However, since a locus where n central charges align is generically of real codimension $(n-1)$ in $\mathcal{M}_V$, it should be possible to adjust the path from t_0 to t_1 such that all the putative invisible walls it encounters correspond to the arguments of just three central charges aligning. Then the transition between sets $\mathcal{T}_0$ and $\mathcal{T}_1$ factors completely into a sequence of 3-center transitions that locally look just like the one in Figure 2.6. Since the refined index does not change in the 3-center case, it cannot change in the multi-center case either.

Non-primitive rearrangements

The above analysis can be extended to non-primitive rearrangements, though the relevant scenarios quickly increase in complexity. For example, consider the formation of a bound state with total charge

$$\gamma = \gamma_1 + \gamma_2 + 2\gamma_3 \,. \tag{2.4.7}$$

In addition to the three basic tree topologies corresponding to Figure 2.5, there are three additional options as shown below in Figure 2.7. In a physical scenario like the $D6$–$D6$–$\overline{D6}$ bound states of [20], only a subset of the potential tree topologies will be realized. Exactly which ones appear depends on the relative magnitudes of $a = \langle\gamma_2, \gamma_3\rangle$, $b = \langle\gamma_3, \gamma_1\rangle$, and $c = \langle\gamma_1, \gamma_2\rangle$. Unlike the primitive case, where (2.4.2) was the only nontrivial possibility, there are *multiple* parameter regimes for which topology transitions can take place.

All these regimes, and even more complicated non-primitive examples, are analyzed in [4]. The astonishing result is that the refined index *never* changes from one side of a putative invisible wall to the other. This suggests a

Conjecture: In the vector multiplet moduli space, the refined index can only jump at true walls of marginal stability.

In other words, we expect that continuity of the unrefined index implies continuity of the refined index. This conjecture is pleasingly consistent with the general quantum/motivic wall-crossing formula that will be discussed in Chapter 4. Indeed, if motivic Donaldson-Thomas invariants are a completely accurate mathematical realization of refined physical BPS invariants — and so far we have no reason to think otherwise — then motivic wall crossing *predicts* the absence of invisible walls.

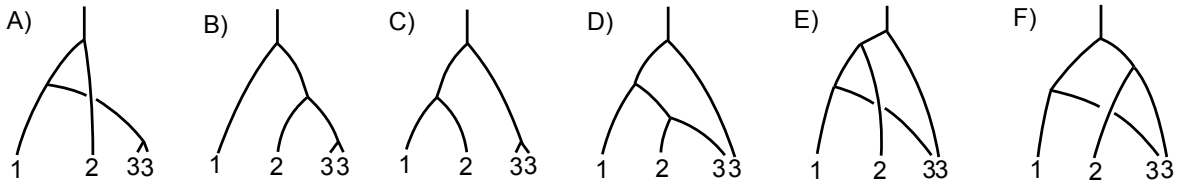

Figure 2.7: Possible multi-center tree topologies in the simplest non-primitive case. Here we draw two separate γ_3 attractor points just to distinguish flows of charge γ_3 and $2\gamma_3$; physically, they are the same point in moduli space.

As an explicit illustration of a non-primitive rearrangement, let us take $a > b > c > 0$, as in (2.4.2). Then physical considerations predict that (A) and (D) will be realized on one side of the putative invisible wall, while (B) and (C) will be realized on the other. The refined semi-primitive wall-crossing formula (2.2.13) predicts in general that

$$\Omega^{ref}(\gamma+2\eta;y) = \Omega^{ref}(\gamma;y)\left(\frac{1}{2}[I]_y^2\Omega^{ref}(\eta;y)^2 - \frac{1}{2}[I]_{y^2}\Omega^{ref}(\eta;y^2) - [2I]_y\Omega^{ref}(2\eta;y)\right), \tag{2.4.8}$$

where $I = |\langle\gamma,\eta\rangle|$, and we have suppressed the dependence on moduli $t_\pm$ in Ω^{ref}. Using this formula to work out the total degeneracy $\Omega^{ref}(\gamma_1+\gamma_2+2\gamma_3)$ for each tree topology, we find that $\Omega_A^{ref} + \Omega_D^{ref} = \Omega_B^{ref} + \Omega_C^{ref}$ can only hold in general if each of the following three

relations is satisfied:

$$[2a-c]_y[2b]_y = [c]_y[2a-2b]_y + [2b-c]_y[2a]_y \tag{2.4.9a}$$

$$[2a-c]_y[b]_{y^2} = [c]_y[a-b]_{y^2} + [2b-c]_y[a]_{y^2} \tag{2.4.9b}$$

$$[2a-c]_y[b]_y^2 + 2[a-b]_y[a-c]_y[b]_y = [c]_y[a-b]_y^2 + [2b-c]_y[a]_y^2\,. \tag{2.4.9c}$$

These are all identities for the quantum dimension.

Chapter 3

Refined Wall Crossing via Melting Crystals

In this chapter, we specialize to type IIA "compactifications" on the resolved conifold $X = \mathcal{O}(-1) \oplus \mathcal{O}(-1) \to \mathbb{P}^1$. This is a noncompact Calabi-Yau, but can be thought of as the local (or decompactification) limit of a compact Calabi-Yau into which the conifold is embedded. In this decompactification limit, all Kähler classes except the class of a distinguished $\mathbb{P}^1$ become large. The resolved conifold is a *rigid* Calabi-Yau, in the sense that it has no complex structure deformations. Thus $\mathcal{M}_H$ is trivial and the refined BPS index (2.1.30) is a well-defined function on the Kähler moduli space $\mathcal{M}_V$. (Noncompact toric Calabi-Yau's generally have this property.)

The conifold provides an excellent example of the wall-crossing formulas of Section 2.2, and the relation between BPS indices and standard topological string invariants. In Section 3.1, following [31], we describe the picture of walls, chambers, and unrefined generating functions for the conifold. We then generalize this picture to our refined invariants, and use refined wall crossing to produce refined generating functions in all chambers (following our work in [1]).

The latter part of this chapter is devoted to the study of melting crystal models for conifold invariants and their connection to refined and unrefined wall crossing. The idea that melting crystals can encode topological invariants of Calabi-Yau threefolds (and describe topological strings in such backgrounds) goes back to [25] and [74]. There, the topological vertex, the building block of Gromov-Witten/Gopakumar-Vafa/Donaldson-Thomas parti-

tion functions for noncompact toric Calabi-Yau's, is reinterpreted as the generating function of *plane partitions* — or cubic crystals melting in the corner of a room. However, another set of crystal models, based more closely on the toric web of a noncompact Calabi-Yau,is also discussed in this literature. For a conifold, this "other model" consists of *pyramid partitions*.

More recently, B. Szendröi [64] used pyramid partitions to describe the representations of the noncommutative path algebra generated by the conifold quiver (or by a noncommutative resolution of the conifold). This path algebra defined "noncommutative Donaldson-Thomas theory." The generating function for pyramid partitions computes the noncommutative Donaldson-Thomas partition function. Jafferis and Chaung [75] then generalized this approach to the generating function of D6-D2-D0 bound states in all chambers for the resolved conifold: in each chamber, the meltings of a pyramid crystal with different boundary conditions determine the corresponding generating function.

In Section 3.3, we very briefly describe the approach used by [75] to identify crystal boundary conditions with stability conditions. It requires the study of quiver representations at different choices of θ-stability. In Section 3.3, we then review a mathematical proof by B. Young [76] that crystals with differing boundary conditions actually reproduce the generating functions for the resolved conifold, and argue that an algorithm called *dimer shuffling* provides a combinatorial realization of wall crossing. Moreover, we use dimer shuffling/wall crossing to relate a limit of pyramid partitions to the topological vertex. Finally, in Section 3.4, we show that the everything can be refined. By splitting pyramid partitions on diagonals and thereby modifying the weights assigned to their atoms, we obtain refined partition functions in all chambers; and we related refined pyramid partitions to the refined topological vertex. Sections 3.3 and 3.4 are based on our work in [1].

Although we focus mainly on the example of the conifold here, many results *should* generalize to more complicated noncompact Calabi-Yau manifolds. Indeed, since [1] was published, some partial generalizations have appeared in [32, 33].

3.1 Wall crossing for the conifold

The picture of walls and chambers for the resolved conifold $X = \mathcal{O}(-1) \oplus \mathcal{O}(-1) \to \mathbb{P}^1$ was developed in [31]. In order to analyze wall crossing this non-compact Calabi-Yau properly, one must embed it in a compact global geometry and then look at the subset of walls and BPS states that survive in the local limit — the limit where all Kähler classes except that of the $\mathbb{P}^1$ become large.

To be more specific, let β be the generator of $H^4(X;\mathbb{Z})$, dual to the rigid cycle on $\mathbb{P}^1 \in X$. Then, the Kähler parameter in the compact geometry is taken to be

$$t = z\,\mathcal{P} + \Lambda e^{i\varphi}\,\mathcal{P}' \ \in H^2(X,\mathbb{C})\,, \tag{3.1.1}$$

where $\mathcal{P}\cdot\beta = 1$, $\mathcal{P}'\cdot\beta = 0$, and $(\mathcal{P}')^3 > 0$. Here, z is a complex number parametrizing $B + iJ$ on $\mathbb{P}^1$, and $\Lambda e^{i\varphi}$ is a complex number parametrizing all the other Kähler classes, whose magnitude Λ one takes to be very large. In the limit $\Lambda \to \infty$, the phase φ still survives as a finite parameter, and effectively enlarges the Kähler parameter space of the resolved conifold to have real dimension *three*.

In the notation of [31], charge of a bound state of a D6 brane, M D2 branes, and N D0 branes can be written as a cohomology class

$$\gamma_{1,M,N} = 1 - M\beta + N dV \ \in H^{even}(X;\mathbb{Z}), \tag{3.1.2}$$

where dV is the volume element on X, normalized so that $\int_X dV = 1$ (in any compact approximation). In the local limit $\Lambda \to \infty$, the central charge of a D6 brane with any number of bound $D2$ and $D0$ branes becomes

$$Z(1 - \ldots) \sim \Lambda^3 e^{3i\varphi}\,, \tag{3.1.3}$$

while the central charge of a D2-D0 bound state (with no D6) is

$$Z(-M\beta + N dV) = -Mz - N\,. \tag{3.1.4}$$

Thus the parameter φ can also be interpreted as the phase of the central charge of the D6 brane. It is fairly easy to see that in the local limit

- The only single-center (single attractor flow) state is a pure D6.

- The only possible walls of marginal stability correspond to primitive or semi-primitive splits

$$1 - M\beta + NdV \to (1 - M'\beta + N'dV) + (M''\beta + N''dV)\,. \tag{3.1.5}$$

  In particular, no D6-$\overline{\text{D6}}$ bound states ever form.

As φ is varied while keeping z constant, what effectively happens is that the central charge of a D6 brane sweeps across moduli space, binding MD2+ND0 fragments whenever walls of marginal stability

$$\arg e^{3i\varphi} = \arg(-Mz - N) \tag{3.1.6}$$

are encountered.

Since the fragments $-M\beta + nDV$ undergo no wall crossings throughout the local-limit moduli space, one can obtain their unrefined indices from the Gopakumar-Vafa invariants for the conifold [11, 12]:

$$\begin{aligned} \Omega(\pm\beta + NdV) &= 1\,, \\ \Omega(NdV) &= -2\,, \\ \Omega(-M\beta + NdV) &= 0 \quad \text{otherwise}\,. \end{aligned} \tag{3.1.7}$$

This results in the picture of walls and chambers shown in Figure 3.1, covering a large section of moduli space. There is a core region $\tilde{C}_0$, corresponding to Kähler moduli near the attractor point for the D6 brane, where only the pure D6 brane is stable. Varying φ away from this region, one encounters first a D2+D0 wall, then a D2+2D0 wall, then a D2+3D0 wall, etc.; at each transition, the D6 brane binds with an arbitrary number of D2+ND0 particles, *à la* semi-primitive wall crossing. After crossing all D2+ND0 walls, at finite distance in moduli space, one encounters the D0 wall, where any number of D0 particles bind to the D6. Then $\overline{\text{D2}} + ND0$ particles begin to bind until, after crossing a $\overline{\text{D2}} + D0$ wall, one ends up in the Szendröi region of moduli space.

Generating functions

In the core region of moduli space, the partition function of D6-D2-D0 bound states

$$\mathcal{Z}(q, Q; t_\infty) = \sum_{M,N\in\mathbb{Z}} \Omega(1 - M\beta + NdV; t_\infty)(-q)^N Q^M \tag{3.1.8}$$

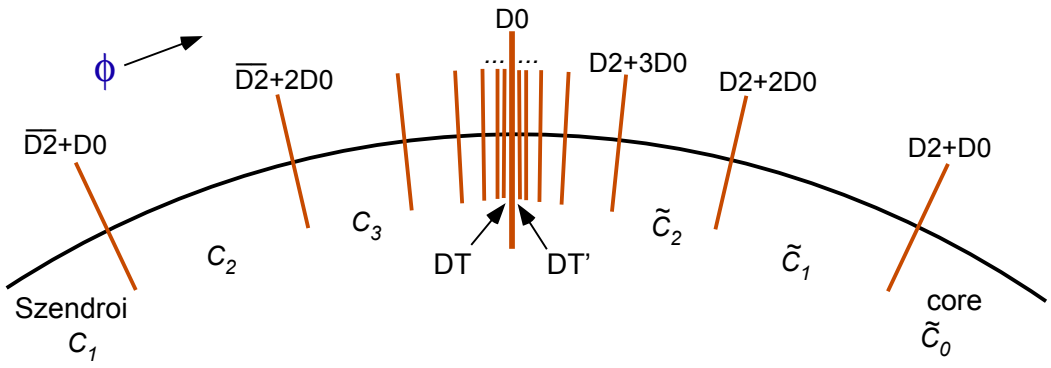

Figure 3.1: Walls and chambers for the refined conifold.

simply takes the value $\mathcal{Z}(q,Q;\tilde{C}_0)=1$. By the semi-primitive wall-crossing formula (2.2.14),[1] the partition function in chamber $\tilde{C}_n$ is then

$$\mathcal{Z}(q,Q;\tilde{C}_n)=\prod_{j=1}^{N}(1-q^jQ)^j\,, \tag{3.1.9}$$

which converges to the reduced Donaldson-Thomas partition function immediately before the D0 wall,

$$\mathcal{Z}(q,Q;\tilde{C}_\infty)=\mathcal{Z}'_{DT}(q,Q)=\prod_{j=1}^{\infty}(1-q^jQ)^j\,. \tag{3.1.10}$$

On the other side of the wall, the binding of a gas of D0's (and 2D0's, 3D0's, etc.) multiplies the partition function by the MacMahon function, resulting in the unreduced Donaldson-Thomas partition function

$$\mathcal{Z}(q,Q;C_\infty)=\mathcal{Z}_{DT}(q,Q)=M(q)^2\prod_{j=1}^{\infty}(1-q^jQ)^j\,. \tag{3.1.11}$$

This is a general phenomenon: when crossing the D6-D0 wall, which exists generically in the large-volume moduli space of Calabi-Yau's, the D6-D2-D0 partition function acquires a factor of $M(q)^{\chi(X)}$.

As one progresses to the Szendöi region, the partition function becomes

$$\mathcal{Z}(q,Q;C_n)=M(q)^2\prod_{j=1}^{\infty}(1-q^jQ)^j\prod_{k=N}^{\infty}(1-q^kQ^{-1})^k\,. \tag{3.1.12}$$

[1]Note that the D2-D0 states are fermionic, whereas the D0 states are bosonic. Thus, the wall-crossing formula at D2-D0 walls tends to be much simpler than at the D0 wall.

In the Szendröi region itself, this finally becomes Szendröi's "noncommutative Donaldson-Thomas" partition function [64]

$$\mathcal{Z}(q,Q;C_1) = \mathcal{Z}_{Sz}(q,Q) = M(q)^2 \prod_{j=1}^{\infty}(1-q^jQ)^j \prod_{k=1}^{\infty}(1-q^kQ^{-1})^k \,. \tag{3.1.13}$$

Refined generating functions

It is not too difficult to generalize the above story, summarized from [31], to our unrefined invariants. There do not seem to be any invisible walls in the region of moduli space depicted in Figure 3.1, so we only need worry about marginal stability transitions. Furthermore, it is clear from an analysis of the moduli space of D0 and D2-D0 branes on the conifold (or from refined Gopakumar-Vafa invariants [23, 26]) that D2+ND0 states belong to fermionic hypermultiplets and ND0 states belong to bosonic vector multiplets — "bosonic" and "fermionic" referring to their statistics in the internal Hilbert space $\mathcal{H}'$, with center-of-mass degrees of freedom factored out. Therefore (*cf.* (2.1.32)-(2.1.33)),

$$\begin{aligned} \Omega^{ref}(\pm\beta + NdV; y) &= 1\,, \\ \Omega^{ref}(NdV; y) &= -y - y^{-1}\,, \\ \Omega^{ref}(-M\beta + NdV; y) &= 0 \quad \text{otherwise}\,. \end{aligned} \tag{3.1.14}$$

As in Section 2.1, let us define the refined generating function of D6-D2-D0 states as

$$\mathcal{Z}(q,Q,y;t_\infty) = \sum_{M,N\in\mathbb{Z}} \Omega^{ref}(1-M\beta+NdV;t_\infty;y)(-q)^N Q^M \,. \tag{3.1.15}$$

It is also convenient to change variables from y and q to q_1 and q_2, which are more standard in the literature on topological string invariants, *cf.* [22, 23, 26, 29]:

$$q_1 = qy\,, \qquad q_2 = \frac{q}{y}\,. \tag{3.1.16}$$

Then we have

$$\mathcal{Z}(q_1,q_2,Q;\tilde{C}_0) = 1\,, \tag{3.1.17}$$

$$\mathcal{Z}(q_1,q_2,Q;\tilde{C}_n) = \prod_{\substack{i,j\geq 1\\ i+j\leq N+1}} \left(1+q_1^{i-\frac{1}{2}}q_2^{j-\frac{1}{2}}Q\right), \tag{3.1.18}$$

$$\mathcal{Z}(q_1,q_2,Q;\tilde{C}_\infty) = \prod_{i,j\geq 1} \left(1+q_1^{i-\frac{1}{2}}q_2^{j-\frac{1}{2}}Q\right) = \mathcal{Z}_{DT}^{ref\,\prime}(q_1,q_2,Q)\,, \tag{3.1.19}$$

$$\mathcal{Z}(q_1,q_2,Q;C_\infty) = M(q_1,q_2)^2 \prod_{i,j\geq 1} \left(1+q_1^{i-\frac{1}{2}}q_2^{j-\frac{1}{2}}Q\right) = \mathcal{Z}_{DT}^{ref}(q_1,q_2,Q)\,, \tag{3.1.20}$$

$$\mathcal{Z}(q_1,q_2,Q;C_N) = M(q_1,q_2)^2 \prod_{i,j\geq 1} \left(1+q_1^{i-\frac{1}{2}}q_2^{j-\frac{1}{2}}Q\right) \prod_{\substack{k,l\geq 1\\ k+l\geq N}} \left(1+q_1^{k-\frac{1}{2}}q_2^{l-\frac{1}{2}}Q^{-1}\right), \tag{3.1.21}$$

$$\mathcal{Z}(q_1,q_2,Q;C_1) = M(q_1,q_2)^2 \prod_{i,j\geq 1} \left(1+q_1^{i-\frac{1}{2}}q_2^{j-\frac{1}{2}}Q\right)\left(1+q_1^{i-\frac{1}{2}}q_2^{j-\frac{1}{2}}Q^{-1}\right) = \mathcal{Z}_{Sz}^{ref}(q_1,q_2,Q)\,. \tag{3.1.22}$$

These generating functions all follow by applying the semi-primitive wall-crossing formula (2.2.13) at each D2-D0, D0, and $\overline{\text{D2}}$-D0 wall, starting from the core region $\tilde{C}_0$. Of course, in the core region both refined and unrefined generating functions are trivial, since the only state in the spectrum is the pure D6.

Observe that on either side of the D0 wall the refined generating function reproduces the refined Donaldson-Thomas/Gopakumar-Vafa partition function for the resolved conifold, as calculated with the refined topological vertex [26]. This should be no great surprise: the stability conditions near the D0 wall are such that all D2-D0 fragments can bind to the D6, but no $\overline{\text{D2}} - D0$ fragments can bind, which appropriately describes the ideal sheaves in Donaldson-Thomas theory [65]. The extra spin content of the present BPS invariants is equivalent to the extra $SU(2)$ Lefschetz action used in defining refined Donaldson-Thomas invariants.

The two sides of the D0 wall are related by a *refined MacMahon function*, which we have normalized symmetrically here to be $M(q_1,q_2) = \prod_{i,j\geq 1}\left(1-q_1^{i-\frac{1}{2}}q_2^{j-\frac{1}{2}}\right)$. In general, when studying BPS invariants one encounters a family of refinements

$$M_\delta(q_1,q_2) = \prod_{i,j\geq 1}\left(1-q_1^{i-\frac{1}{2}+\frac{\delta}{2}}q_2^{j-\frac{1}{2}-\frac{\delta}{2}}\right), \tag{3.1.23}$$

which all reduce to the ordinary MacMahon function $M(q)$ in the limit $y\to 1$. (In the "opposite" opposite $y\to -1$, the functions (3.1.23) specialize to $M(-q)$, which describes the contribution of the 0-dimensional subschemes to the $\widehat{\text{DT}}$-invariants of [77].)

In the Szendröi chamber C_1, the generating function (3.1.22) refines Szendröi's partition function for noncommutative Donaldson-Thomas theory on the conifold. The answer here, derived via wall-crossing, agrees with a more rigorous mathematical calculation for an appropriately refined noncommutative Donaldson-Thomas partition function.[2]

3.2 Crystals and quivers

In the final two sections of this chapter, we will discuss refined and unrefined crystal-melting models and "combinatorial wall crossing" for the D6-D2-D0 BPS generating functions of the refined conifold. In order to maintain continuity of ideas, we presently take a moment to very briefly review the general connection between crystal models, quivers, and BPS states.

Crystal-melting models were first used to describe BPS states in the Gromov-Witten/ Donaldson-Thomas chamber of noncompact toric Calabi-Yau's in [25], where it was realized that the topological vertex [24] was a generating function of three-dimensional plane partitions (or boxes stacked in the corner of a room). In terms of Donaldson-Thomas theory, plane partitions describe fixed points under a torus action in the moduli space of ideal sheaves on $\mathbb{C}^3$ [9, 10]. In the topological vertex formalism, the full toric Calabi-Yau X is glued together from copies of $\mathbb{C}^3$, and the moduli space $\mathcal{M}$ of ideal sheaves on X is glued together from moduli spaces on $\mathbb{C}^3$. The Euler characteristic or cohomology of $\mathcal{M}$ (hence Donaldson-Thomas invariants) can then be related to the plane partitions that describe local fixed points, by standard localization theorems (*cf.* [78]). The topological vertex was generalized to a *refined* vertex (with refined plane partitions) in [26], to describe refined Gromov-Witten/Donaldson-Thomas invariants.

Szendröi [64] recently described a very different melting crystal model for the noncommutative Donaldson-Thomas chamber C_1 of the conifold. In this special, extreme chamber of $\mathcal{M}_V$, the classical moduli spaces $\mathcal{M}(\gamma)$ of BPS states (*i.e.* the moduli spaces whose "quantization" give $\mathcal{H}_{BPS}(\gamma)$) correspond to *cyclic* representations of the conifold quiver algebra. All the vector spaces V_i (*cf.* Section 2.3) of a cyclic representation of a quiver are

[2]We thank B. Szendröi for discussions on this topic.

generated by a single basis element $\mathbf{e}$ in the vector space $V_{i'}$ of some distinguished vertex i'. The resulting moduli spaces $\mathcal{M}\gamma$ have a toric action, whose fixed points again describe partitions, or molten crystal configurations. However, the relevant pyramid crystal, shown on the left-hand side of Figure 3.4 on page 50, looks very different from the plane partitions of the topological vertex. Such Szendröi-chamber melting crystal models were generalized to other noncompact toric Calabi-Yau's in [79] (see also [80]), but they have not yet been refined. (We will present a refinement in Section 3.4.)

Of course, there are many more chambers of moduli space, and one would like to have a crystal model in each one. Jafferis and Chuang [75] realized how to accomplish this by relating cyclic quiver representations — which lead directly to crystals — with θ-stable representations. In the case of noncompact toric Calabi-Yau's with a good quiver description, the moduli spaces $\mathcal{M}(\gamma; t)$ at different moduli $t \in \mathcal{M}_V$ correspond to stable quiver representations with different $\boldsymbol{\theta}$ parameters. Jafferis and Chaung showed that by appropriately choosing a different basis of coherent sheaves to generate the quiver in each chamber $\mathcal{M}_V$, θ-stability could always reduce to cyclicity.

As an example of this construction, consider the conifold in the Szendröi chamber C_1. The appropriate representation of the conifold quiver in this chamber is shown in Figure 3.2. The basis of coherent sheaves consists of the D6-brane $\mathcal{O}_X[1]$, the $\overline{\text{D2}}$+D0 brane $\mathcal{O}_{\mathbb{P}^1}(-2)[1]$, and the D2 brane $\mathcal{O}_{\mathbb{P}^1}(-1)$. In the Szendröi chamber, the θ-parameters for the three corresponding vertices satisfy $\theta_1 > 0$, $\theta_2 < 0$, and $\theta_3 < 0$, respectively. The stable representations with dimension vector $\mathbf{n} = (1, N, M+N)$, corresponding to bound states of D6+MD2+ND0 branes, then become completely equivalent to the cyclic representations generated by the D6 vertex.

It is also fairly easy to see in this simple example how pyramid partitions (meltings of the C_1 crystal in Figure 3.4) are identified with representations corresponding to fixed points of the full moduli space of stable/cyclic representations. Consider a set of atoms that have been removed in a melting configuration, such as in Figure 3.3. Suppose there are N white atoms and $M + N$ black atoms. This corresponds to a quiver representation of dimension $\mathbf{n} = (\dim V_1, \dim V_2, \dim V_3) = (1, N, M + N)$, where each white atom is associated to a basis element of V_2 and each black atom to a basis element of V_3. To determine the homomorphisms represented by the arrows A_1, A_2, B_1, B_2, draw four arrows from each white atom to the layer of black atoms below it (and vice verse) as shown on the

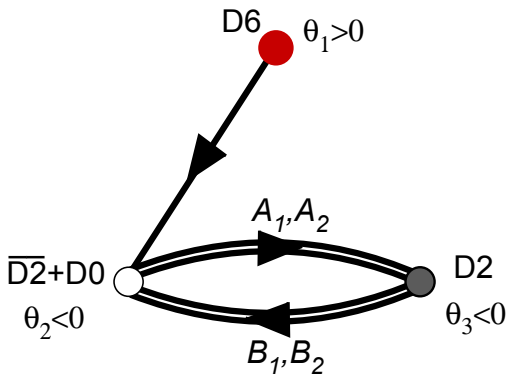

Figure 3.2: The conifold quiver for the C_1 chamber, with charges of nodes and θ-parameters as indicated. The superpotential is $W = \mathrm{Tr}(A_1B_1A_2B_2 - A_1B_2A_2B_1)$.

right side of Figure 3.3. Each A_1 arrow connecting two atoms in the finite removed/melted set corresponds to a '1' entry in the homomorphism matrix representing A_1, a mapping between the basis elements associated to the atoms. All other entries in the matrix A_1 are set to zero. Likewise, A_2, B_1, and B_2 are constructed, completing the representation. It is argued in [64] that *every fixed point* in the moduli space of cyclic representations is identified uniquely with a melting configuration like this. Note that the "distinguished" vector that generates these cyclic representations is basis of the one-dimensional space V_1, which maps to the basis element of V_2 corresponding to the single white atom at the top of the crystal (present in every crystal melting), and maps subsequently to the rest of the melted atoms. The superpotential conditions $dW = 0$ for a good quiver representation simply state that different paths connecting a black or white atom to any atom three layers under it are equivalent.

3.3 Pyramid crystals and wall crossing

We now consider the (unrefined) melting crystal descriptions of the conifold partition functions in chambers $\tilde{C}_n$ and $\tilde{C}_n$ more carefully. After summarizing the basic result from [75] in all chambers, we review Young's mathematical proof that the infinite crystals corresponding to chambers C_n actually give the right answers. Moreover, we argue that *dimer shuffling*, to be defined below, provides a combinatorial realization of wall crossing that, in the limit $n \to \infty$ (the DT chamber), causes pyramid partitions to reduce to the usual

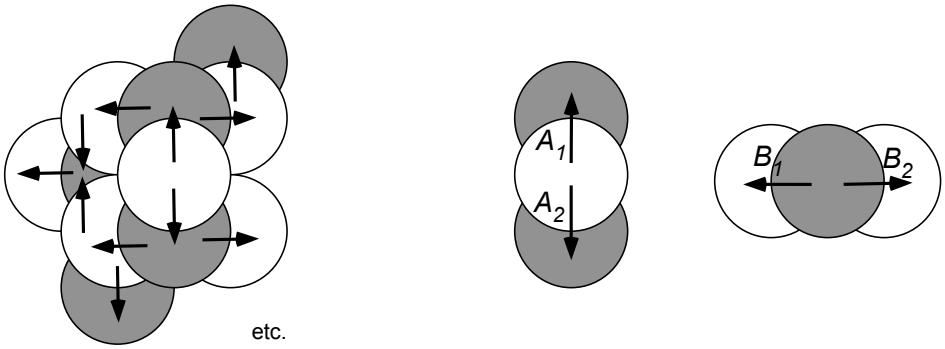

Figure 3.3: A set of atoms melted from the C_1 crystal (right); and assignment of arrows A_1, A_2, B_1, B_2 to atoms (left).

topological vertex model for the conifold.

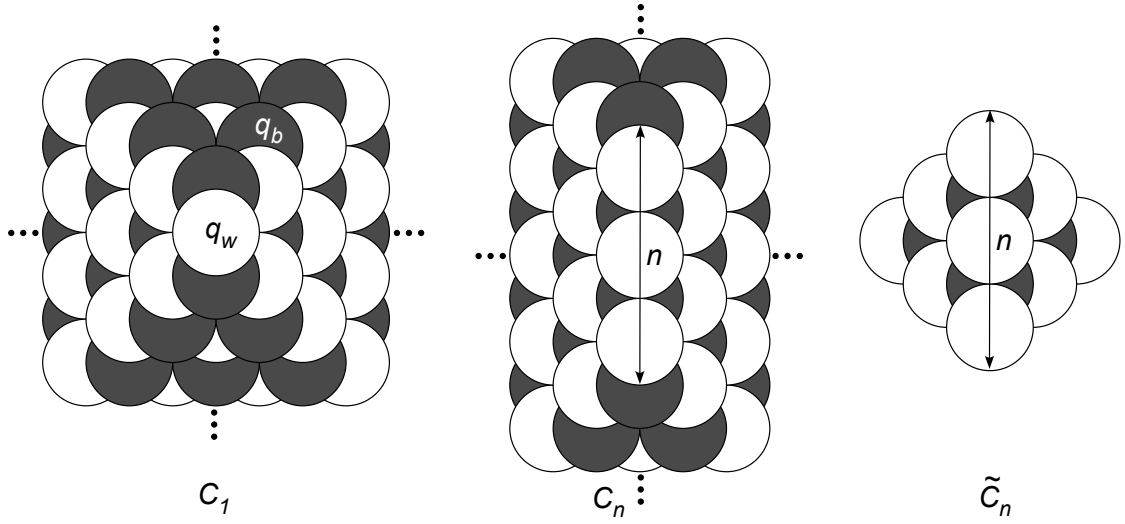

Figure 3.4: The "empty room configurations" for the crystals that count BPS states in chambers C_n and $\tilde{C}_n$.

In the chamber C_n, the unrefined generating function of BPS states is obtained by counting the melting configurations of an infinite pyramid-shaped crystal whose top row of atoms has length n (sometimes also called an empty room configuration, or ERC, of length n) [64, 75]. As shown in Figure 3.4, this crystal has two different types of atoms, corresponding to the two vertices of the Klebanov-Witten quiver. The top edge of the pyramid always consists of n white atoms. The remainder of the pyramid is then constructed by placing two black atoms underneath each white atom, oriented vertically, and two white

atoms underneath each black one, oriented horizontally.[3] In order for an atom to be removed during crystal melting, all atoms lying above it must be removed as well. The partition function is defined as a sum over all melting configurations (*i.e.* pyramid partitions) π,

$$Z(q_w, q_b; C_n) = \sum_{\pi} q_w^{w_w(\pi)} q_b^{w_b(\pi)} \,, \tag{3.3.1}$$

where $w_w(\pi)$ and $w_b(\pi)$, respectively, are the numbers of white and black atoms removed. It was proven in [76] that this agrees with the partition function (3.1.12),

$$Z(q_w, q_b; C_n) = Z(q, Q; C_n) = M(q)^2 \prod_{j=1}^{\infty} (1 - q^j Q)^j \prod_{k=n}^{\infty} (1 - q^k Q^{-1})^k \,, \tag{3.3.2}$$

provided that one makes an n-dependent identification as in [75],

$$C_n : \qquad q_w = -q^n Q^{-1} \,, \qquad q_b = -q^{-(n-1)} Q \,. \tag{3.3.3}$$

Similarly, it was argued in [75] that to obtain the unrefined partition function in the chamber $\tilde{C}_n$ one must sum over the melting configurations of a *finite* crystal configuration of length n, also shown in Figure 3.4. Then

$$Z(q, Q; \tilde{C}_n) = \prod_{j=1}^{n} (1 - q^j Q)^j = \sum_{\pi} q_w^{w_w(\pi)} q_b^{w_b(\pi)} \tag{3.3.4}$$

if one identifies

$$\tilde{C}_n : \qquad q_w = -q^n Q \,, \qquad q_b = -q^{-(n+1)} Q^{-1} \,. \tag{3.3.5}$$

To proceed further, let us translate the above partition functions into the language of dimers. The partitions of a length-n pyramid correspond bijectively to the states of a dimer model on a square lattice with prescribed asymptotic boundary conditions. (We will refer to these states as partitions as well.) An intuitive way to visualize the correspondence (see also [76]) is to actually draw dimers on the black and white atoms, as in Figure 3.5. Then the dimer state corresponding to a given crystal automatically appears when viewing the crystal from above.

As in [76], we have included an extra decoration on the lattices in these figures: lattice points are colored with alternating black and white dots. This canonical decoration carries no extra information, but is very useful in describing weights and wall crossing. We will

[3] In nature, such a crystal structure, very similar to that of diamond, occurs in moissanite (silicon carbide) and the semiconductor gallium arsenide.

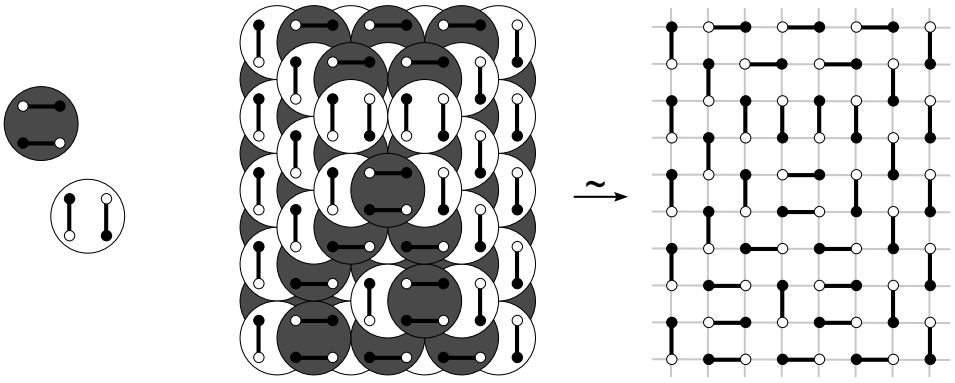

Figure 3.5: The relation between pyramid partitions and dimer states, illustrated for $n = 2$.

Figure 3.6: Even and odd boxes of dimers.

also call squares in the dimer lattice *even* or *odd* depending on their vertex decorations. As shown in Figure 3.6, we call two dimers lying on the edges of an even (resp. odd) square an even (resp. odd) *box*; an even (resp. odd) box with two horizontal (resp. vertial) dimers corresponds to a fully uncovered black (resp. white) atom in the crystal.

One can assign weights to each edge in the dimer lattice so that the total weight of a dimer partition π, defined as[4]

$$w(\pi) = \frac{\text{product of weights of dimerized edges in } \pi}{\text{product of weights of dimerized edges in the ground state of the lattice}}\,, \qquad (3.3.6)$$

agrees with the pyramid partition weight $q_w^{w_w(\pi)} q_b^{w_b(\pi)}$. To implement such a weighting, it is sufficient to ensure that the ratio of horizontal to vertical edges in every odd and even square, respectively, equals q_w and q_b^{-1} — corresponding to white atoms being removed and black atoms being replaced.

Here, it is most convenient to use a weighting that is n-dependent. Vertical edges are always assigned weight 1. For the horizontal edges, we draw two diagonals on the dimer lattice, which pass through the lowermost and uppermost odd blocks in the ground

[4]Technically, both the numerator and denominator in this definition must be "regularized." For a given state π, one fixes a large box in the dimer lattice so that all dimers outside the box match the ground state (corresponding to an unmelted pyramid of length n); then one only multiplies together the weights of dimers inside this box.

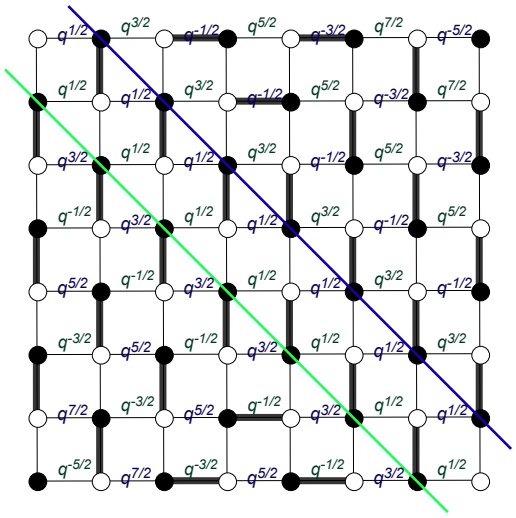

Figure 3.7: The weights assigned to edges of the dimer lattice of "length n," for $n = 2$. (The $n = 2$ ground state has been shaded in.) All vertical edges have weight 1 and all horizontal edges have an additional factor of $(-Q)^{-1/2}$.

state dimer (*i.e.* the lowermost and uppermost uncovered white atoms in the unmelted pyramid). For positive integers a, the horizontal edges $2a-1$ units above and $2a$ units below the lower diagonal are assigned weights $q^{(2a-1)/2}(-Q)^{-1/2}$ and $q^{-(2a-1)/2}(-Q)^{-1/2}$, respectively, where $a = 0$ means that an edge is touching the diagonal. Likewise the horizontal edges $2a-1$ units below and $2a$ units above the upper diagonal are assigned weights $q^{(2a-1)/2}(-Q)^{-1/2}$ and $q^{-(2a-1)/2}(-Q)^{-1/2}$, respectively. An example is shown in Figure 3.7. For a dimer model corresponding to a length-n crystal, one can check that the ratios of horizontal to vertical edges in every odd block is indeed $-q^n Q^{-1} = q_w$, and in every even block the ratio is $-q^{n-1}Q^{-1} = q_b^{-1}$. Since the resulting weight function itself is n-dependent in terms of variables q and Q, let us call it w_n rather than w.

We let the weight w_n be a function acting linearly on formal sums of partitions, and define $\Theta^{(n)}$ to be the formal sum of all possible partitions of a dimer lattice with asymptotic boundary conditions corresponding to the length-n crystal. Then

$$Z(q_a, q_b; C_n) = \sum_{\pi} q_w^{w_w(\pi)} q_b^{w_b(\pi)} = w_n(\Theta^{(n)})\,. \tag{3.3.7}$$

The operation that we claim is the combinatorial equivalent of wall crossing is described in [76] as *dimer shuffling*. It maps partitions of length n to partitions of length $n+1$. To define it, first consider an operation $\tilde{S}$, which maps a dimer state $\tilde{\pi}^{(n)}$, all of whose odd

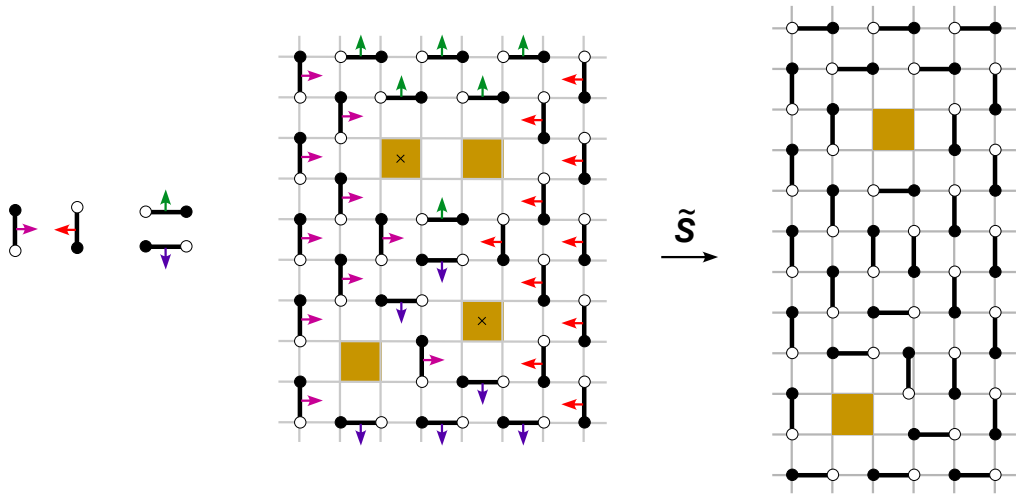

Figure 3.8: The directions in which dimers move under the shuffle $\tilde{S}$, and an example of shuffling a partition of length $n = 2$ with odd boxes deleted.

blocks have been deleted, to a dimer state $\tilde{\pi}^{(n+1)}$, all of whose even blocks are deleted. By "deleted" we mean that any dimers forming odd (resp. even) blocks are removed. The operation $\tilde{S}$ simply moves every non-deleted dimer one unit to the left, right, up, or down, according to the rules on the left side of Figure 3.8. We show an example of such a shuffling in Figure 3.8 as well; note that dimers carry their vertex decorations with them when they move. As a function from the set of {dimer partitions with odd blocks deleted} to the set of {dimer partitions with even blocks deleted}, $\tilde{S}$ is bijective [76, 81]. The actual dimer shuffling operation S can then be defined to act on finite "subsums" in $\Theta^{(n)}$. It maps each formal sum[5] of 2^m dimer states with a fixed set of m odd blocks (for any m) to the finite formal sum of all dimer states with a fixed set of even blocks in the obvious way: by deleting odd blocks, applying $\tilde{S}$, and filling in the missing even blocks in all possible combinations. Letting S act linearly on all such formal sub-sums of $\Theta^{(n)}$, it must, because $\tilde{S}$ is bijective, send $\Theta^{(n)}$ precisely to $\Theta^{(n+1)}$.

What happens to weights under dimer shuffling? We defined our weight function above so that the dimers in a partition $\tilde{\pi}$ of a length-n model with odd boxes deleted do not change weight at all under the action of $\tilde{S}$. In other words, $w_n(\tilde{\pi}) = w_{n+1}(\tilde{S}(\tilde{\pi}))$. The only change in weights of a genuine dimer state π under the action of S arises from the deletion of odd blocks and the subsequent creation of new even blocks after shuffling. An important

[5]We could also define shuffling, as in [76], to act on individual π's, but this is unnecessary.

lemma in [76] (which we will refine later in this section) is that the difference between the number of deleted odd blocks in $\tilde{\pi}$ and the missing even blocks in $\tilde{S}(\tilde{\pi})$ is always exactly n. Then a quick exercise shows that for a fixed $\tilde{\pi}$ with m deleted odd blocks,

$$w_n(\text{sum of } \pi \text{ s.t. } \pi \text{ agrees with } \tilde{\pi}) = (1 - q^n Q^{-1})^m \cdot w_n(\tilde{\pi})\,, \tag{3.3.8}$$

$$w_{n+1}(\text{sum of } \pi \text{ s.t. } \pi \text{ agrees with } \tilde{S}(\tilde{\pi})) = (1 - q^n Q^{-1})^{m-n} \cdot w_{n+1}(\tilde{S}(\tilde{\pi}))\,. \tag{3.3.9}$$

(By "agrees with," we mean aside from deleted blocks.) The ratio of these quantities is independent of m, immediately proving that

$$w_n(\Theta^{(n)}) = (1 - q^n Q^{-1})^n w_{n+1}(\Theta^{(n+1)})\,. \tag{3.3.10}$$

This is precisely the wall-crossing formula between chambers C_n for the conifold.

Formula (3.3.10) suggests (correctly) that we can write the crystal or dimer partition function for a model of length n as

$$w_n(\Theta^{(n)}) = \prod_{j=n}^{\infty} (1 - q^j Q^{-1})^j \cdot w_\infty(\Theta^{(\infty)})\,. \tag{3.3.11}$$

Of course, the quantity $w_\infty(\Theta^{(\infty)})$ must be the Donaldson-Thomas partition function of the conifold, and this relation holds because pyramid partitions of length $n \to \infty$ effectively reduce to the topological vertex formalism of [24, 25] (see also [74, 9, 10]).

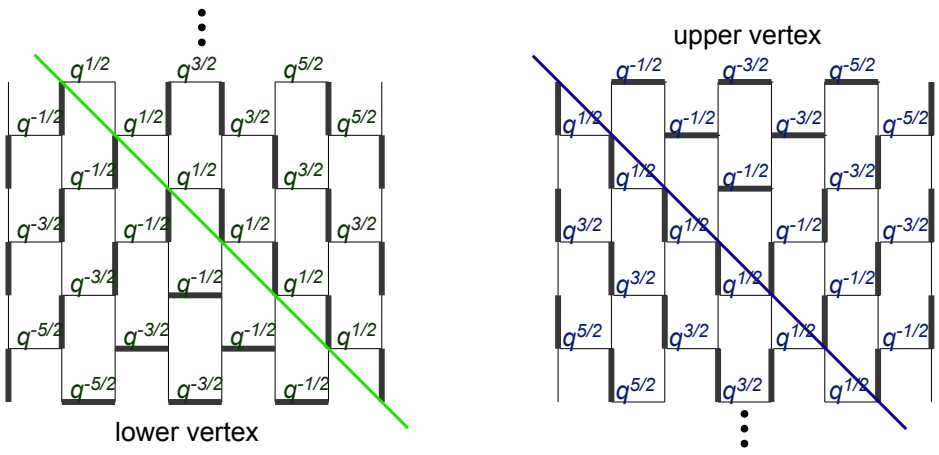

Figure 3.9: The brick-like lattices around the upper and lower vertices as $n \to \infty$. The ground state state of the dimer is shaded in. As before, each horizontal edge also carries a weight of $(-Q)^{-1/2}$

To understand this relation, consider the n-dependent weighting system of Figure 3.7. In the limit $n \to \infty$, the weights of half the edges around the lower vertex (of the pyramid,

or of the dimer model) acquire infinitely large, positive powers of q and cease to contribute to the partition function. Likewise for half the edges around the upper vertex. Therefore, the only dimer partitions around these vertices that can contribute to the length-infinity partition function involve dimers on edges of the brick-like lattices of Figure 3.9. These brick-like lattices, however, are equivalent to hexagonal dimer lattices, which correspond to the three-dimensional cubic partitions that arise in the topological vertex.

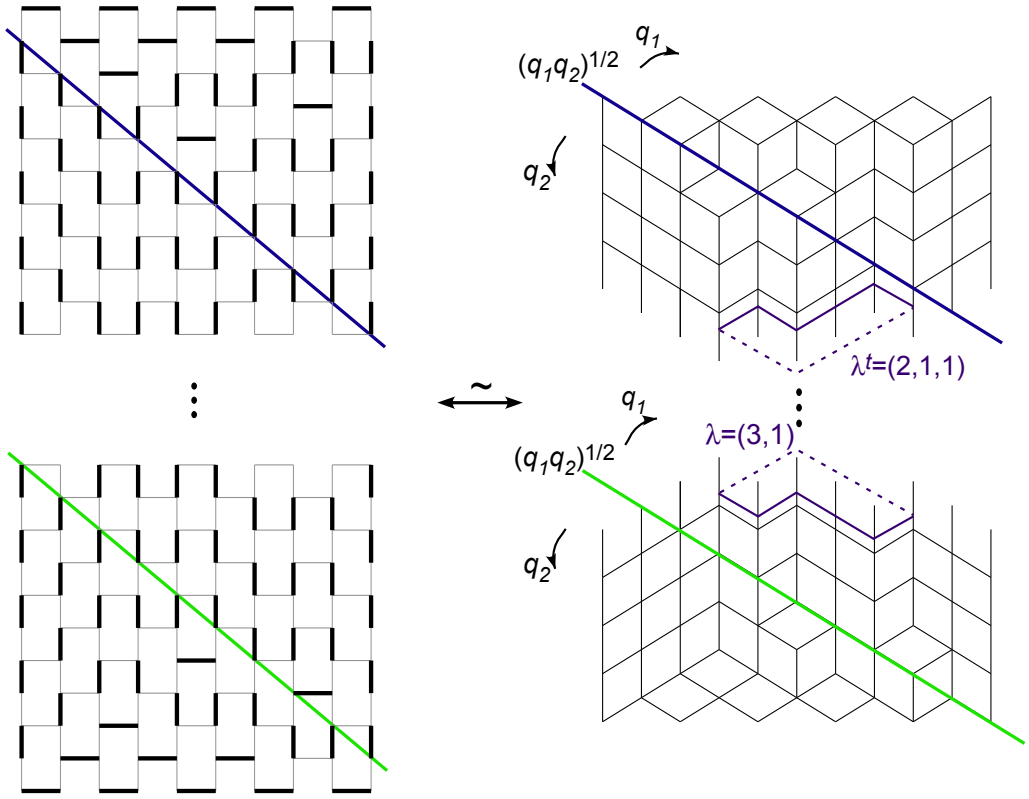

Figure 3.10: The map between the length-infinity dimer model and a pair of topological vertices. (The extra q_1 and q_2 notations are for the refined case in Section 3.4.)

As argued more carefully in [76], any (nontrivial) configuration of the length-infinity dimer model can be constructed via a series of moves that amount to 1) cutting out a Young diagram λ simultaneously from the upper and lower vertices, 2) stacking up individual boxes to form a cubic partition π_λ^- around the lower vertex, and 3) stacking up boxes to form a partition π_λ^+ around the upper vertex. An example of such a dimer configuration and its corresponding topological vertex partitions is shown in Figure 3.10. By observing how dimers shift in these three steps and using our $n \to \infty$ weighting, it is not too hard to

see that the contributions to the partition function are $(-Q)^{|\lambda|}q^{\frac{1}{2}||\lambda||^2}q^{\frac{1}{2}||\lambda^t||^2}$ from step (1), $q^{|\pi^-_\lambda|}$ from step (2), and $q^{|\pi^+_{\lambda^t}|}$ from step (3).[6] Therefore, the total partition function is

$$w_\infty(\Theta^{(\infty)}) = \sum_\lambda \sum_{\pi^+_{\lambda^t},\,\pi^-_\lambda} (-Q)^{|\lambda|} q^{\frac{1}{2}||\lambda||^2+\frac{1}{2}||\lambda^t||^2} q^{|\pi^+_{\lambda^t}|+|\pi^-_\lambda|}\,, \tag{3.3.12}$$

which is *precisely* the topological vertex expression for the (unreduced) partition function of the conifold [24, 25]. In terms of Schur functions, the generating function for three-dimensional cubic partitions with a single nontrivial asymptotic boundary condition λ is $\sum_{\pi_\lambda} q^{|\pi_\lambda|} = M(q)\, q^{-\frac{1}{2}||\lambda||^2} s_{\lambda^t}(q^{-\rho}) = M(q)\, q^{-\frac{1}{2}||\lambda||^2} s_{\lambda^t}(q^{1/2}, q^{3/2}, q^{5/2}, ...)$. Thus, as expected,

$$\begin{aligned} w_\infty(\Theta^{(\infty)}) &= Z(q, Q; C_\infty) \\ &= M(q)^2 \sum_\lambda (-Q)^\lambda s_\lambda(q^{-\rho}) s_{\lambda^t}(q^{-\rho}) \qquad (3.3.13) \\ &= M(q)^2 \prod_{j,k=1}^{\infty} (1 - q^{j-1/2} q^{k-1/2} Q) \qquad (3.3.14) \\ &= M(q)^2 \prod_{j=1}^{\infty} (1 - q^j Q)^j\,. \end{aligned}$$

3.4 Refined crystals

We finally come to the crystal-melting models for refined invariants. We will first describe the models that compute the refined partition functions in all chambers C_n and $\tilde{C}_n$ for the conifold. Then, generalizing Section 3.3, we will prove the formulas in chambers C_n by showing that a refined version of dimer shuffling leads to refined wall crossing. We also show that as $n \to \infty$ refined pyramid partitions reduce to a pair of refined topological vertices.

At the level of crystal models, one must draw a series of diagonals on the pyramid partition, and interpolate weights between the variable q_1 on one side of the diagonals and q_2 on the other. To be more specific, consider the pyramid of length $n = 1$, corresponding to the Szendröi chamber C_1. On this crystal model, we draw a single diagonal as shown in

[6] We use conventional notation for Young diagrams and three-dimensional cubic partitions; λ^t is the transpose of the diagram λ, the rows of λ have lengths λ_i, $|\lambda| = \sum \lambda_i$ is the number of boxes in λ, $||\lambda||^2 = \sum \lambda_i^2$, and $|\pi|$ is the number of boxes in a three-dimensional partition.

Figure 3.11; we assign white atoms above the diagonal a weight q_w^+, white atoms below the diagonal a weight q_w^-, and white atoms on the diagonal itself a weight $(q_w^+ q_w^-)^{1/2}$. All black atoms are assigned weight q_b. Letting $w_w^+(\pi)$, $w_w^-(\pi)$, and $w_w^0(\pi)$ be the numbers of white atoms above, below, and on the diagonal, respectively, in the partition π, and identifying $q_w^+ = -q_1 Q^{-1}$, $q_w^- = -q_2 Q^{-1}$, and $q_b = -Q$, we find

$$\begin{aligned} Z(q_w^+, q_w^-, q^b; C_1) &= \sum_\pi (q_w^+)^{w_w^+(\pi)} (q_w^-)^{w_w^-(\pi)} (q_w^+ q_w^-)^{\frac{1}{2} w_w^0(\pi)} q_b^{w_b(\pi)} \\ &= Z^{ref}(q_1, q_2, Q; C_1) \\ &= M(q_1, q_2)^2 \prod_{i,j=1}^{\infty} (1 - q_1^{i-\frac{1}{2}} q_2^{j-\frac{1}{2}} Q)(1 - q_1^{i-\frac{1}{2}} q_2^{j-\frac{1}{2}} Q^{-1}) \,. \end{aligned} \tag{3.4.1}$$

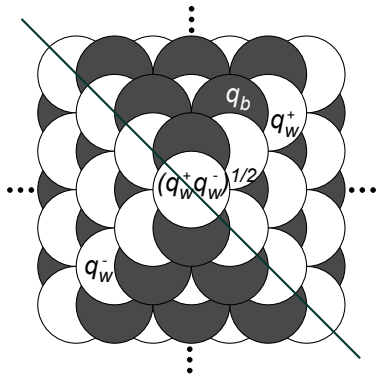

Figure 3.11: Weights of atoms for the refined partition function in chamber C_1.

To generalize to the length-n pyramid, we draw n diagonals, as in the left half of Figure 3.12. It is more natural to work directly in terms of the variables q_1, q_2, and Q. We assign weights $-q_1^n Q^{-1}$ (resp. $-q_1^{-(n-1)} Q$) to the white (resp. black) atoms above all the diagonals and weights $-q_2^n Q^{-1}$ (resp. $-q_2^{-(n-1)} Q$) to the white (resp. black) atoms below all the diagonals. The diagonals themselves intersect white atoms; we assign the same weight to all the white atoms on a single diagonal, interpolating between $-q_1^{n-\frac{1}{2}} q_2^{\frac{1}{2}} Q^{-1}$ on the uppermost diagonal and $-q_1^{\frac{1}{2}} q_2^{n-\frac{1}{2}} Q^{-1}$ on the lowermost (multiplying by $q_1^1 q_2^{-1}$ in each intermediate step). Similarly, black atoms lie between diagonals, and we assign them weights ranging from $-q_1^{-n+\frac{3}{2}} q_2^{-\frac{1}{2}} Q$ directly below the upper diagonal to $-q_1^{-\frac{1}{2}} q_2^{-n+\frac{3}{2}} Q$ directly above the lower diagonal. Multiplying together the weights of all atoms removed in

a given partition π and summing these quantities over partitions, we obtain the expected

$$Z^{ref}(q_1, q_2, Q; C_n) = M(q_1, q_2)^2 \prod_{i,j=1}^{\infty} (1 - q_1^{i-\frac{1}{2}} q_2^{j-\frac{1}{2}} Q) \prod_{\substack{i\geq 1,\, j\geq 1 \\ i+j>n}} (1 - q_1^{i-\frac{1}{2}} q_2^{j-\frac{1}{2}} Q^{-1}) \,. \quad (3.4.2)$$

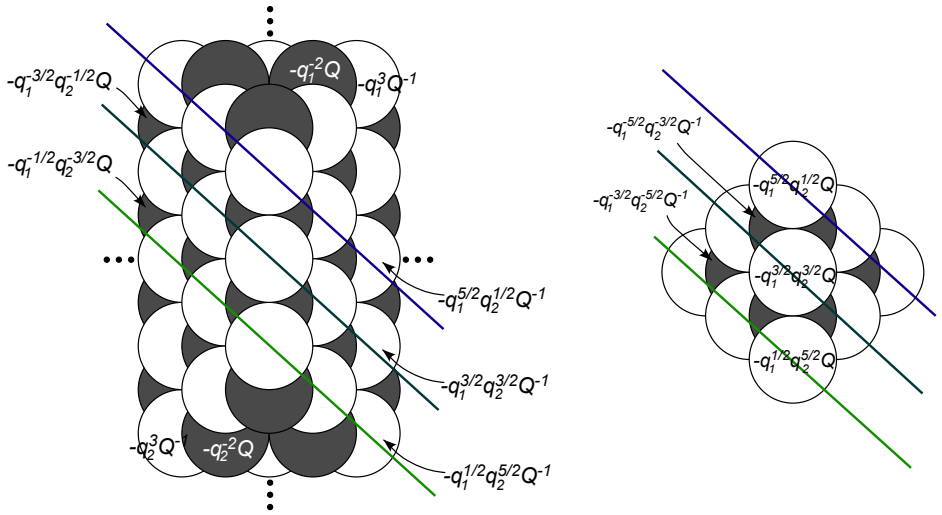

Figure 3.12: Refined weights of atoms for chambers C_n and $\tilde{C}_n$, with $n = 3$.

For chambers $\tilde{C}_n$, the finite pyramid of length n can also be split by n diagonals, as shown in the right half of Figure 3.12. If one assigns weights such that (1) when $q_1 \to q$ and $q_2 \to q$ white atoms have weight $-q^n Q$ and black atoms have weight $-q^{-(n+1)}Q^{-1}$; (2) when moving up one step, either on or inbetween diagonals, the absolute value of the power of q_2 (resp. q_1) decreases (resp. increases) by 1; and (3) the assignment is symmetric about the middle diagonal(s) of the crystal, the resulting partition function is precisely

$$Z^{ref}(q_1, q_2, Q; \tilde{C}_n) = M(q_1, q_2)^2 \prod_{\substack{i\geq 1,\, j\geq 1 \\ i+j\leq n+1}} (1 - q_1^{i-\frac{1}{2}} q_2^{j-\frac{1}{2}} Q) \,.$$

For the remainder of the section we return to the infinite pyramid of length n, generalizing the previous unrefined discussion to refine the connection between shuffling, wall crossing, and the refined topological vertex (and to prove formula (3.4.2)). We first observe that in order to equate refined pyramid partitions and their weights with states (configurations) of a dimer lattice, we can use almost the same n-dependent weighting described in Figure 3.7. Now, for positive integers a, the horizontal edges $2a-1$ units above and $2a$ units below the lower diagonal are assigned weights $q_1^{(2a-1)/2}(-Q)^{-1/2}$ and $q_2^{-(2a-1)/2}(-Q)^{-1/2}$,

respectively. Likewise the horizontal edges $2a-1$ units below and $2a$ units above the upper diagonal are assigned weights $q_2^{(2a-1)/2}(-Q)^{-1/2}$ and $q_1^{-(2a-1)/2}(-Q)^{-1/2}$. See the example in Figure 3.13.

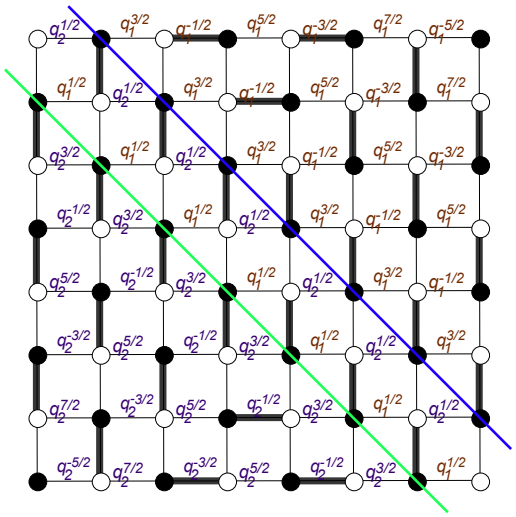

Figure 3.13: Refined weighting of the length-n dimer, for $n = 2$.

As in the unrefined case, the weights of dimers which are not part of deleted odd or even blocks do not change during dimer shuffling $\tilde{S}$, due to our n-dependent weighting. In order to understand the behavior of the deleted blocks, we observe that the shuffling $\tilde{S}$ removes *exactly* one (deleted) odd block from each of the n diagonals of a dimer configuration of length n. Moreover, the remaining (deleted) odd blocks are mapped to deleted even blocks with exactly the same weights — if (for instance) they were above all the diagonals, then they remain above all the diagonals. These statements can be proved with careful counting arguments, considering the number of dimers on and around each diagonal in an arbitrary configuration before and after shuffling. The result is that when the actual shuffling S maps a formal sum of states π agreeing with a fixed odd-deleted state $\tilde{\pi}$ on all but their odd blocks to a formal sum of states agreeing on all but their even blocks, the weight of this formal sum changes by exactly $\prod_{i+j=n+1}(1 - q_1^{i-\frac{1}{2}} q_2^{j-\frac{1}{2}} Q^{-1})$; therefore,

$$w_n(\Theta^{(n)}) = \prod_{\substack{i\geq 1,\, j\geq 1 \\ i+j=n+1}} (1 - q_1^{i-\frac{1}{2}} q_2^{j-\frac{1}{2}} Q^{-1}) \cdot w_{n+1}(\Theta^{(n+1)}) \,. \tag{3.4.3}$$

This, of course, is the refined wall-crossing formula for chambers C_n.

The crystal-melting or dimer partition function of length n can now be written as

$$w_n(\Theta^{(n)}) = \prod_{i,j=1}^{\infty} (1 - q_1^{i-\frac{1}{2}} q_2^{j-\frac{1}{2}} Q^{-1}) \cdot w_\infty(\Theta^{(\infty)}) \,. \tag{3.4.4}$$

The last term, $w_\infty(\Theta^{(\infty)})$, is obtained from a slightly modified version of the refined topological vertex of [26]. To see this, observe that as $n \to \infty$ the neighborhoods of the upper and lower vertices of the dimer lattice still reduce to effective brick-like lattices, now shown in Figure 3.14. In terms of three-dimensional cubic partitions, states of the length-infinity dimer are again created by 1) cutting out a Young diagram λ simultaneously from the upper and lower vertices, 2) stacking up individual boxes to form a cubic partition π_λ^- around the lower vertex, and 3) stacking up boxes to form a partition π_λ^+ around the upper vertex. The creation of the Young diagram λ comes with a fairly simple weight $(-Q)^{|\lambda|} q_1^{\frac{1}{2}||\lambda||^2} q_2^{\frac{1}{2}||\lambda^t||^2}$. However, both the upper and lower "room corners" are now split along a diagonal, as shown in Figure 3.10. In the case of the lower corner, boxes stacked below the diagonal come with

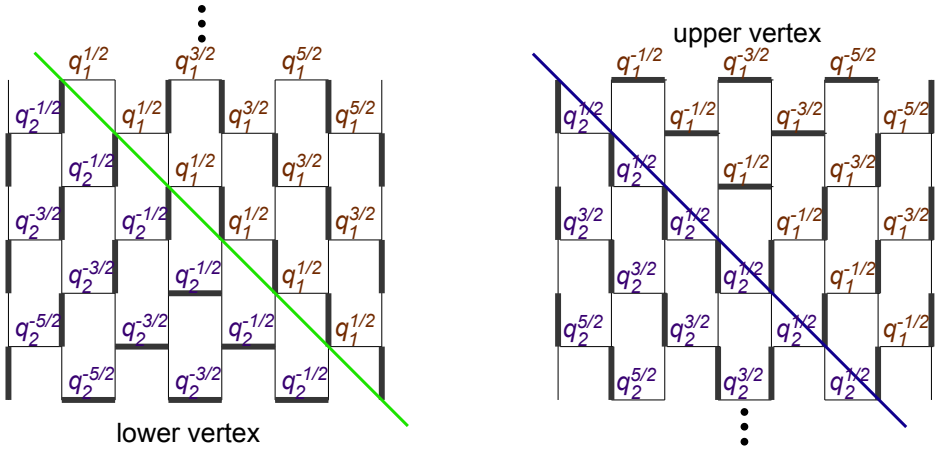

Figure 3.14: Neighborhoods of the refined upper and lower vertices as $n \to \infty$.

weight q_2, those above the diagonal with weight q_1, and those that the diagonal intersects have weight $(q_1 q_2)^{\frac{1}{2}}$. The situation is reversed for the upper vertex. The generating function for such three-dimensional cubic partitions with one asymptotic boundary condition λ is (for example, at the lower vertex)

$$\sum_{\pi_\lambda} q_1^{|\pi_\lambda|^{(q_1)}} q_2^{|\pi_\lambda|^{(q_2)}} (q_1 q_2)^{\frac{1}{2}|\pi_\lambda|^{(0)}} = M(q_1, q_2)\, q_2^{-\frac{1}{2}||\lambda^t||^2} s_\lambda(q_2^{-\rho}) \,, \tag{3.4.5}$$

with $M(q_1, q_2) = \prod_{i,j=1}^{\infty} (1 - q_1^{i-\frac{1}{2}} q_2^{j-\frac{1}{2}})^{-1}$. Therefore, the length-infinity pyramid partition

function is

$$
\begin{aligned}
w_\infty(\Theta^{(\infty)}) &= \sum_\lambda \sum_{\pi^+_{\lambda^t},\pi^-_\lambda} (-Q)^{|\lambda|}\, q_1^{\frac{1}{2}||\lambda||^2} q_2^{\frac{1}{2}||\lambda^t||^2} \\
&\qquad \times q_1^{|\pi^-_\lambda|^{(q_1)}} q_2^{|\pi^-_\lambda|^{(q_2)}} (q_1q_2)^{\frac{1}{2}|\pi^-_\lambda|^{(0)}}\, q_2^{|\pi^+_{\lambda^t}|^{(q_2)}} q_1^{|\pi^+_{\lambda^t}|^{(q_1)}} (q_1q_2)^{\frac{1}{2}|\pi^+_{\lambda^t}|^{(0)}} \\
&= M(q_1,q_2)^2 \sum_\lambda (-Q)^{|\lambda|} s_\lambda(q_2^{-\rho}) s_{\lambda^t}(q_1^{-\rho}) \\
&= M(q_1,q_2)^2 \prod_{i,j=1}^\infty (1 - q_1^{i-\frac{1}{2}} q_2^{j-\frac{1}{2}} Q)\,. \qquad (3.4.6)
\end{aligned}
$$

Note that expression (3.4.5) differs very slightly from the refined topological vertex used in [26] (with the boundary condition λ placed along an "unpreferred" direction). The difference comes from our symmetric choice of normalization, as discussed in Section 3.1. In [26] the diagonal is assigned to q_2 rather than $(q_1q_2)^{\frac{1}{2}}$, resulting in the fact that the refined MacMahon function appearing in the analogue of (3.4.5) is not $M(q_1,q_2) = \prod_{i,j=1}^\infty (1 - q_1^{i-\frac{1}{2}} q_2^{j-\frac{1}{2}})^{-1}$, but rather $M_{-1}(q_1,q_2) = \prod i,j = 1^\infty (1 - q_1^{i-1} q_2^j)^{-1}$ (*cf.* (3.1.23)). The refined A-model (Gromov-Witten/Gopakumar-Vafa) partition functions calculated with the refined vertex are always normalized by the prefactor $M(q_1,q_2)^{\chi}(X)$, so in many previous calculations this has made no difference.

Chapter 4

Refined = Motivic

Despite its obvious conceptual advantages, the direct interpretation of $\mathcal{H}_{BPS}$ as the cohomology of a moduli space of D-branes or representations of a quiver discussed in Section 2.3 does *not* generally work. Thinking in terms of quiver representations, and even putting aside the issue of noncompact moduli spaces (working, for example, with nice rigid noncompact toric Calabi-Yau's), the general problem is that the moduli spaces $\mathcal{M}(\gamma)$ are highly singular. In particular, $\mathcal{M}(\gamma)$ is defined as the quotient of an algebraic variety by a "gauge group" $\prod_i GL(n_i)$, so it is mathematically a moduli stack (*not* a variety). It is often not clear how to compute its cohomology, or even its Euler characteristic.

Kontsevich and Soibelman address this problem in both unrefined and (we argue) refined cases in [15]. They work with quiver descriptions of Calabi-Yau's and D-branes, using a stability condition very similar to II-stability[1] to define generalized Donaldson-Thomas invariants. These invariants should reproduce physical BPS indices $\Omega(\gamma; t_\infty)$ in all chambers of Kähler moduli space $\mathcal{M}_V$, in a type IIA duality frame. In [34], it was proven that this is indeed the case in a rigid limit of 4-dimensional supergravity.

Kontsevich and Soibelman also define a "q-deformed" version of the generalized Donaldson-Thomas invariants: the motivic Donaldson-Thomas invariants. They essentially use motivic integration as a well-defined alternative to calculating the cohomology of moduli spaces. Note, however, that motivic integration can be thought of (from one point of view) as cutting up a space into copies of the noncompact affine line $\mathbb{L}$, the affine plane $\mathbb{L}^2$, the

[1] *I.e.* a stability condition based on comparing arguments of central charges of states, also similar to Denef stability (2.2.1).

affine space $\mathbb{L}^3$, etc. The motivic DT invariants are functions of $\mathbb{L}^{1/2}$, the square root of the motive of the affine line. One can also use the Schur functor to pass from motivic to "quantum" invariants, replacing $\mathbb{L}^{1/2}$ with the quantum variable $-q^{1/2}$. As $q^{1/2} \to -1$, the motivic invariants reduce to the classical generalized Donaldson-Thomas invariants. Our main conjecture is that motivic DT invariants are equivalent to refined invariants in any chamber of moduli space, with

$$\boxed{\mathbb{L}^{1/2} \quad \longleftrightarrow \quad -q^{1/2} \quad \longleftrightarrow \quad y}\,. \tag{4.0.1}$$

Why should this be true? Besides the potentially naive fact that both motivic and refined invariants are fairly natural deformations of the classical BPS indices/invariants, we will argue in this chapter that motivic and refined invariants have identical wall crossing behavior. In Section 4.1, we will review the classical and motivic wall-crossing formulas from [15], and then show in Section 4.2 that motivic wall crossing implies primitive and semi-primitive refined wall crossing. In Section 4.3, we will provide several very explicit examples of the equivalence between refined and motivic invariants in the context of $SU(2)$ Seiberg-Witten theory with $N_f = 0, 1, 2, 3$ flavors — using geometric engineering [82] to view Seiberg-Witten theory as a rigid limit of string theory compactified on a local Calabi-Yau. The results of this chapter are based on work in [1, 2].

There also exists direct evidence for the equivalence of refined and motivic invariants coming from knot theory and the interpretation of knot homologies via BPS invariants of Calabi-Yau threefolds, as in [29, 30]. In [83], motivic invariants were related to knot Floer homology. We hope to investigate the motivic nature of knot homologies further in the future.

4.1 Classical and motivic KS wall crossing

We begin by reviewing the classical (or unrefined) and motivic wall-crossing formulas of Kontsevich and Soibelman [15]. In the classical case, we borrow some of the notation and formalism of [34].

Classical

The classical wall-crossing formula generalizes both the primitive (2.2.6) and semiprimitive (2.2.12) cases derived physically in Section 2.2. It encodes the degeneracies of BPS states in a given chamber of moduli space $\mathcal{M}_V$ in terms of a non-commuting product of symplectomorphisms acting on a complexified charge lattice.

Specifically, let Γ be the lattice of D-brane charges (as above), let $\Gamma^\vee$ be its dual, and let

$$\mathbf{T}_\Gamma = \Gamma^\vee \otimes \mathbb{C}^* \tag{4.1.1}$$

be an r-dimensional complex torus, where r is the rank of Γ. One can define functions X_γ on this complex torus corresponding to any $\gamma \in \Gamma$, acting as $X_\gamma : \sum C_a \gamma_a^\vee \mapsto \exp \sum C_a \gamma_a^\vee(\gamma)$. These satisfy $X_\gamma X_{\gamma'} = X_{\gamma+\gamma'}$, and if $\{\gamma_i\}$ is any basis of Γ, the corresponding $X_i = X_{\gamma_i}$ will be coordinates on $\mathbf{T}_\Gamma$. The complex torus can moreover be endowed with a natural symplectic structure

$$\omega = \frac{1}{2}\langle \gamma_i, \gamma_j \rangle^{-1} \frac{dX_i}{X_i} \wedge \frac{dX_j}{X_j}\,, \tag{4.1.2}$$

where $\langle \gamma_i, \gamma_j \rangle^{-1}$ is the inverse of the intersection form on Γ (in any chosen basis).

Under this symplectic structure, the family of maps $\{U_\gamma\}_{\gamma\in\Gamma}$,

$$\begin{aligned} \mathbf{T}_\Gamma &\to \mathbf{T}_\Gamma \\ U_\gamma : X_{\gamma'} &\mapsto X_{\gamma'}(1-\sigma(\gamma)X_\gamma)^{\langle \gamma', \gamma\rangle}\,. \end{aligned} \tag{4.1.3}$$

are classical symplectomorphisms. The coefficient $\sigma(\gamma)$ is just a sign ± 1; choosing an electric-magnetic duality frame (or symplectic splitting)[2] for Γ and writing $\gamma = \gamma_e + \gamma_m$, this coefficient equals $(-1)^{\langle \gamma_e, \gamma_m\rangle}$. If one defines vector fields e_γ to be the infinitesimal symplectomorphisms generated by the Hamiltonians $\sigma(\gamma)X_\gamma$, then the e_γ's generate a Lie algebra with relations

$$[e_{\gamma_1}, e_{\gamma_2}] = (-1)^{\langle \gamma_1, \gamma_2\rangle}\langle \gamma_1, \gamma_2\rangle e_{\gamma_1+\gamma_2}\,, \tag{4.1.4}$$

and the symplectomorphism U_γ can be expressed as

$$U_\gamma = \exp \mathrm{Li}_2(e_\gamma)\,. \tag{4.1.5}$$

[2]Technically, one needs to take the charge lattice Γ and the corresponding torus $\mathbf{T}_\Gamma$ to be fibered over the moduli space $\mathcal{M}_V$, and an electric-magnetic split only works locally. However, this issue is relatively unimportant for the present discussion — it would only be relevant if one were interested in crossing walls all the way around a singularity in $\mathcal{M}_V$. See [15] and [34] for further discussion.

Here, $\mathrm{Li}_2(x) = \sum_{n=1}^{\infty} \frac{x^n}{n^2}$ is the classical Euler dilogarithm function.

Now, for a given Calabi-Yau, a point t (*i.e.* t_∞) in Kähler moduli space $\mathcal{M}_V$, and a ray in the charge lattice generated by a primitive charge γ, one forms the composite symplectomorphism

$$A_\gamma(t) = \prod_{\gamma' \in \mathrm{ray}} U_{\gamma'}^{\Omega(\gamma';t)} = \prod_{k \geq 1} U_{k\gamma}^{\Omega(k\gamma;t)} \,. \tag{4.1.6}$$

The BPS indices $\Omega(\gamma;t)$ are exactly as in (2.1.27), and this product is over all stable BPS states in the ray (otherwise $\Omega(\gamma;t)$ obviously vanishes). Notice that $U_{d\gamma}$ and $U_{d'\gamma}$ commute for any d, d'. The statement of wall crossing is that the product over all rays of states whose central charges become aligned at a wall of marginal stability,

$$A(t) = \overset{\curvearrowright}{\prod_{\mathrm{rays}\,\gamma}} A_\gamma(t) = \overset{\curvearrowright}{\prod_{\mathrm{states}\,\gamma'}} U_{\gamma'}^{\Omega(\gamma';t)} \,, \tag{4.1.7}$$

taken in order of *increasing phase of the central charge* $Z(\gamma,t)$, is the same on both sides of the wall.[3] In other words, going from $t = t_+$ on one side of the wall to $t = t_-$ on the other, both the BPS indices and the ordering will change but the overall product will remain the same:

$$\boxed{\overset{\curvearrowright}{\prod_{\gamma}} U_{\gamma'}^{\Omega(\gamma',t_+)} = \overset{\curvearrowright}{\prod_{\gamma'}} U_{\gamma'}^{\Omega(\gamma,t_-)}} \,. \tag{4.1.8}$$

Motivic

To simplify the description of motivic invariants, we use the Serre functor to pass from the motive $\mathbb{L}^{1/2}$ to the quantum variable $-q^{1/2}$, as explained in [15]. The motivic DT invariants can then be defined as automorphisms of a quantum torus.

The quantum torus $\widehat{\mathbf{T}}_\Gamma$ in question is simply the quantization of (4.1.1), using the symplectic structure (4.1.2). The Lie algebra (4.1.4) is q-deformed to an associative algebra generated by operators $\{\hat{e}_\gamma\}_{\gamma \in \Gamma}$, such that

$$\hat{e}_{\gamma_1} \hat{e}_{\gamma_2} = q^{\frac{1}{2}\langle \gamma_1, \gamma_2 \rangle} \; \hat{e}_{\gamma_1 + \gamma_2} \tag{4.1.9}$$

and $\hat{e}_0 = 1$. In particular, these generators obey the commutation relations

$$[\hat{e}_{\gamma_1}, \hat{e}_{\gamma_2}] = \left(q^{\frac{1}{2}\langle \gamma_1, \gamma_2 \rangle} - q^{-\frac{1}{2}\langle \gamma_1, \gamma_2 \rangle} \right) \hat{e}_{\gamma_1 + \gamma_2} \,. \tag{4.1.10}$$

[3] Being more careful, one must make a choice of "particles" vs. "antiparticles" and only include the former in this product; so exactly half the rays that align really contribute. This will become clear in the examples of Sections 4.2 and 4.3.

In the "classical limit" $q^{1/2} \to -1$, one finds that

$$\lim_{q^{1/2}\to -1} (q-1)^{-1} \left(q^{\frac{1}{2}\langle \gamma_1,\gamma_2\rangle} - q^{-\frac{1}{2}\langle \gamma_1,\gamma_2\rangle} \right) = (-1)^{\langle \gamma_1,\gamma_2\rangle} \langle \gamma_1,\gamma_2\rangle \,, \tag{4.1.11}$$

so that the elements

$$e_\gamma := \lim_{q^{1/2}\to -1} \frac{\hat{e}_\gamma}{q-1} \,. \tag{4.1.12}$$

satisfy (4.1.4).

In the original work of Kontsevich and Soibelman, the motivic DT invariants were composite operators $\mathbf{A}_\gamma(t)$ associated to entire rays. These operators had Taylor expansions

$$\mathbf{A}_\gamma(t) = 1 + \frac{\Omega^{mot}(\gamma;t;q)}{q^{1/2}-q^{-1/2}}\, \hat{e}_\gamma + (\ )\, \hat{e}_\gamma^2 + \dots, \tag{4.1.13}$$

with coefficients given by motivic integrals. It has since become clear, however, that these operators have a factorization property just as in the classical case, *cf.* [84, 2]. We shall see that physically, this factorization is both necessary and natural. As in [15], let us introduce the quantum dilogarithm function

$$\mathbf{E}(x) = \sum_{n=0}^{\infty} \frac{\left(-q^{\frac{1}{2}}x\right)^n}{(1-q)\dots(1-q^n)} \,, \tag{4.1.14}$$

and define operators

$$\mathbf{U}_\gamma(\hat{e}_\gamma) = \mathbf{E}(\hat{e}_\gamma) \,. \tag{4.1.15}$$

Then, for a ray of BPS states in Γ generated by a charge γ, we have

$$\mathbf{A}_\gamma(t) = \prod_{\gamma' \in \text{ray}} \prod_{n\in\mathbb{Z}} \mathbf{U}_{\gamma'}\big((-q^{1/2})^n \hat{e}_{\gamma'}\big)^{(-1)^n \Omega_n^{mot}(\gamma';t)} \,. \tag{4.1.16}$$

$$= \prod_{k\geq 1} \prod_{n\in\mathbb{Z}} \mathbf{U}_{k\gamma}\big((-q^{1/2})^n \hat{e}_\gamma^{\,k}\big)^{(-1)^n \Omega_n^{mot}(k\gamma;t)} \,. \tag{4.1.17}$$

for (positive) integral motivic invariants $\Omega_n^{mot}(\gamma;t)$. Of course, we want to claim that $\Omega_n^{mot}(\gamma;t) = \Omega_n(\gamma;t)$ as defined in (2.1.31).

The statement of motivic wall crossing is that the product over all rays of states whose central charges become aligned at a wall of marginal stability,

$$\mathbf{A}(t) = \overset{\curvearrowright}{\prod_{\text{rays }\gamma}} \mathbf{A}_\gamma(t) = \overset{\curvearrowright}{\prod_{\text{states }\gamma'}} \prod_{n\in\mathbb{Z}} \mathbf{U}_{\gamma'}\big((-q^{1/2})^n \hat{e}_{\gamma'}\big)^{(-1)^n \Omega_n^{mot}(\gamma';t)} \,, \tag{4.1.18}$$

taking the product in order of increasing phase of central charges, is constant as the wall is crossed. Or, as in (4.1.8),

$$\boxed{\overset{\curvearrowright}{\prod_{\text{states }\gamma'}} \prod_{n\in\mathbb{Z}} \mathbf{U}_{\gamma'}\big((-q^{1/2})^n \hat{e}_{\gamma'}\big)^{(-1)^n \Omega_n^{mot}(\gamma';t_+)} = \overset{\curvearrowright}{\prod_{\text{states }\gamma'}} \prod_{n\in\mathbb{Z}} \mathbf{U}_{\gamma'}\big((-q^{1/2})^n \hat{e}_{\gamma'}\big)^{(-1)^n \Omega_n^{mot}(\gamma';t_-)}} \,. \tag{4.1.19}$$

Note that the operators $\mathbf{U}_\gamma$ and their products generate q-deformed symplectomorphisms on the quantum torus with coordinates $\{\hat{e}_\gamma\}$ via the *conjugation* action $\mathrm{Ad}_{\mathbf{U}_\gamma}$.

The quantum dilogarithm will be of central importance in Part II of this thesis, and we will examine many of its properties further in Section 8.3. For now, however, let us note that in the classical limit $q^{1/2} \to -1$ it has the asymptotic expansion

$$\mathbf{E}(x) = \exp\left(-\frac{1}{2\hbar}\mathrm{Li}_2(x) + \frac{x\hbar}{12(1-x)} + \dots\right) \tag{4.1.20}$$

where $q^{1/2} = -e^{\hbar}$, thereby relating (conjugation by) $\mathbf{U}_\gamma$ with the classical U_γ. Moreover, the function obeys a fundamental "pentagon" identity

$$\mathbf{E}(x_1)\mathbf{E}(x_2) = \mathbf{E}(x_2)\mathbf{E}(x_{12})\mathbf{E}(x_1) \tag{4.1.21}$$

when $x_1 x_2 = q x_2 x_1$ and $x_{12} = q^{-1/2} x_1 x_2 = q^{1/2} x_2 x_1$. This will provide the simplest example of motivic/refined wall crossing in Section 4.2. Finally, it will be useful to note that there exists an infinite product expansion

$$\mathbf{E}(x) = \prod_{r=0}^{\infty} (1 + q^{r+\frac{1}{2}} x)^{-1}\,, \tag{4.1.22}$$

equivalent to the sum (4.1.14).

4.2 Refined = Motivic

We now show that the motivic wall-crossing formula (4.1.19) is equivalent to the refined physical formulas (2.2.7)-(2.2.13) in primitive and semi-primitive cases, with $\boxed{-q^{1/2} = y}$. Since the motivic formula reduces to the classical formula (4.1.8) in the limit $q^{1/2} \to -1$, this also constitutes an alternative proof that the classical KS formula agrees with unrefined physical wall crossing. The primitive and semi-primitive arguments given here appear in our work [1, 2].

Warmup

We begin with the pentagon identity (4.1.21). This can be interpreted as crossing a wall where two primitive hypermultiplets with charges γ_1 and γ_2, satisfying

$$\langle \gamma_1, \gamma_2 \rangle = 1 \tag{4.2.1}$$

form a bound state. The corresponding local quiver for this wall is shown in Figure 4.1. Since $\hat{e}_{\gamma_1}\hat{e}_{\gamma_2} = q\,\hat{e}_{\gamma_1}\hat{e}_{\gamma_2}$, the pentagon identity implies a wall-crossing formula

$$\mathbf{U}_{\gamma_1}(\hat{e}_{\gamma_1})\,\mathbf{U}_{\gamma_2}(\hat{e}_{\gamma_2}) = \mathbf{U}_{\gamma_2}(\hat{e}_{\gamma_2})\,\mathbf{U}_{\gamma_1+\gamma_2}(\hat{e}_{\gamma_1+\gamma_2})\,\mathbf{U}_{\gamma_1}(\hat{e}_{\gamma_1})\,. \tag{4.2.2}$$

Since these two products are taken in order of increasing argument of the central charge, this predicts that the bound state of charge $\gamma_1+\gamma_2$ is stable on the side of the wall where $\arg Z(\gamma_2) < \arg Z(\gamma_1)$, which is equivalent to the Denef stability condition (2.2.1). Moreover, this formula predicts that the bound state will also be a hypermultiplet, since the refined index for a hypermultiplet is $\Omega^{ref}(\gamma;t;y) = \sum_n \Omega_n y^n = 1$ (and all exponents here are 1); this is in agreement with primitive wall crossing (2.2.7).

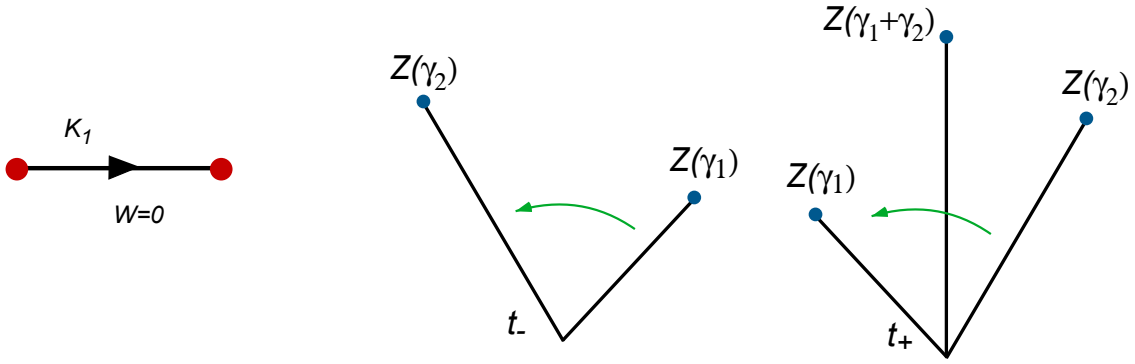

Figure 4.1: Left: the K_1 quiver. Right: the BPS rays of states γ_1, γ_2, and $\gamma_1+\gamma_2$ in the *central charge plane* for stable (t_+) and unstable (t_-) values of moduli.

Note that only states whose central charges actually align at a wall enter the KS wall-crossing formulas.[4] Generically, the charges of these states lie on a 2-dimensional sublattice of Γ. In the present simple example, this sublattice is generated by charges γ_1 and γ_2.

Primitive wall crossing

The pentagon-identity example can easily be generalized to an arbitrary primitive wall crossing. Again, we want to consider two states of charges γ_1 and γ_2 forming a bound state

[4]One could consider other states too, but their corresponding operators would just appear at one side or the other of the product $\prod \mathbf{U}_\gamma$ and their order would not change.

as a wall is crossed, but now $\langle\gamma_1,\gamma_2\rangle$ can be an arbitrary integer. WLOG, we assume

$$\langle\gamma_1,\gamma_2\rangle = I_{12} > 0\,. \tag{4.2.3}$$

Then the motivic wall-crossing formula looks like

$$\mathbf{A}_{\gamma_1}(t_-)\,\mathbf{A}_{\gamma_1+\gamma_2}(t_-)\,\mathbf{A}_{\gamma_2}(t_-) = \mathbf{A}_{\gamma_2}(t_+)\,\mathbf{A}_{\gamma_1+\gamma_2}(t_+)\,\mathbf{A}_{\gamma_1}(t_+)\,. \tag{4.2.4}$$

We expect that $\arg Z(\gamma_1) < \arg Z(\gamma_2)$ on the unstable side of the wall, and so label the LHS of the above formula with the parameter t_-. Let us also assume that the primitive states of charges γ_1 and γ_2 are stable across the wall, so that

$$\mathbf{A}_{\gamma_1}(t_-) = \mathbf{A}_{\gamma_1}(t_+) = \mathbf{A}_{\gamma_1}(t_{ms})\,,$$
$$\mathbf{A}_{\gamma_2}(t_-) = \mathbf{A}_{\gamma_2}(t_+) = \mathbf{A}_{\gamma_2}(t_{ms})\,.$$

The key to understanding this wall-crossing formula (and, indeed, any motivic wall-crossing formula) is to observe that the associative algebra $\mathcal{A}$ generated by $\hat{e}_{\gamma_1}$ and $\hat{e}_{\gamma_2}$ with

$$\hat{e}_{\gamma_1}\hat{e}_{\gamma_2} = q^{I_{12}/2}\hat{e}_{\gamma_1+\gamma_2} = q^{I_{12}}\hat{e}_{\gamma_2}\hat{e}_{\gamma_1} \tag{4.2.5}$$

has filtrations of the form

$$\{1\} \subset \mathcal{A}_{1,0} \subset \mathcal{A}_{1,1} \subset \mathcal{A}_{2,1} \subset \ldots \subset \mathcal{A}_{\infty,\infty} = \mathcal{A}\,, \tag{4.2.6}$$

where at level $\mathcal{A}_{m,n}$ one includes q-polynomials in $\hat{e}_{\gamma_1}$ and $\hat{e}_{\gamma_2}$ of degrees no more than m and n, respectively. For practical purposes, this means that we can consistently expand a formula like (4.2.4) as a series in $\hat{e}_{\gamma_1}$ and $\hat{e}_{\gamma_2}$, keeping any degree we want in these two generators. After commuting all products $\hat{e}_{\gamma_1}^{m'}\hat{e}_{\gamma_2}^{n'}$ in a uniform manner, we can relate the indices $\Omega_n^{mot}(\gamma;t)$ on both sides by simply equating coefficients of like powers.

In this case, let us define

$$\Omega^{mot}(\gamma;t;q) = \sum_{n\in Z}(-q^{1/2})^n\Omega_n^{mot}(\gamma;t)\,, \tag{4.2.7}$$

in analogy to (2.1.31) in the refined case. It is then fairly clear from (4.1.14)-(4.1.17) that for a primitive ray, such that only $k=1$ contributes to (4.1.17), we have

$$\mathbf{A}_\gamma(t) = 1 + \frac{\Omega^{mot}(\gamma;t;q)}{q^{1/2}-q^{-1/2}}\,\hat{e}_\gamma + \ldots. \tag{4.2.8}$$

Substituting this for $\gamma = \gamma_1, \gamma_2, \gamma_1+\gamma_2$ on the two sides of (4.2.4) and keeping only terms of first order in $\hat{e}_{\gamma_1}$ and $\hat{e}_{\gamma_2}$, we find that the coefficients of 1, $\hat{e}_{\gamma_1}$, and $\hat{e}_{\gamma_2}$ agree trivially, whereas the terms of order $\hat{e}_{\gamma_1}\hat{e}_{\gamma_2}$ are

$$\frac{\Omega^{mot}(\gamma_1;t_{ms};q)\Omega^{mot}(\gamma_2;t_{ms};q)}{(q^{1/2}-q^{-1/2})^2}\,\hat{e}_{\gamma_1}\hat{e}_{\gamma_2} + \frac{\Omega^{mot}(\gamma_1+\gamma_2;t_-;q)}{q^{1/2}-q^{-1/2}}\,\hat{e}_{\gamma_1+\gamma_2} = \frac{\Omega^{mot}(\gamma_1;t_{ms};q)\Omega^{mot}(\gamma_2;t_{ms};q)}{(q^{1/2}-q^{-1/2})^2}\,\hat{e}_{\gamma_2}\hat{e}_{\gamma_1} + \frac{\Omega^{mot}(\gamma_1+\gamma_2;t_+;q)}{q^{1/2}-q^{-1/2}}\,\hat{e}_{\gamma_1+\gamma_2} \quad (4.2.9)$$

Using the commutation relations (4.2.5) to (say) push $\hat{e}_{\gamma_2}$ all the way to the left in each term, this immediately implies that

$$\Delta\Omega^{mot}(\gamma_1+\gamma_2;t_-\to t_+;q) = -\frac{q^{I_{12}/2}-q^{-I_{12}/2}}{q^{1/2}-q^{-1/2}}\,\Omega^{mot}(\gamma_1;t_{ms};q)\,\Omega^{mot}(\gamma_2;t_{ms};q)\,, \quad (4.2.10)$$

which is equivalent to the refined primitive formula (2.2.7) upon identifying $\Omega^{mot}(\gamma;t;q) = \Omega^{ref}(\gamma;t;y)$. We can write the prefactor in (4.2.10) as the quantum dimension $[I_{12}]_{q^{1/2}}$.

Semi-primitive wall crossing

To obtain the refined semi-primitive formula (2.2.13), suppose again that states with primitive charges γ_1 and γ_2, satisfying $\langle\gamma_1,\gamma_2\rangle = I_{12} \geq 0$, bind as a wall is crossed at $t = t_{ms}$. This time, however, consider bound states of all charges $\gamma_1 + N\gamma_2$ with $N \geq 1$.[5] Also assume, for simplicity, that no states of charge $\gamma_1 + N\gamma_2$ exist in the spectrum on the unstable side of the wall. Adding in such states is possible, and results in a derivation of the refined version of (2.2.14) rather than (2.2.13), but it demonstrates no new features.

The resulting motivic wall-crossing formula must take the form

$$\mathbf{A}_{\gamma_1}(t_-)\,\mathbf{A}_{\gamma_2}(t_-) = \mathbf{A}_{\gamma_2}(t_+)\times\cdots\mathbf{A}_{\gamma_1+3\gamma_2}(t_+)\,\mathbf{A}_{\gamma_1+2\gamma_2}(t_+)\,\mathbf{A}_{\gamma_1+\gamma_2}(t_+)\,\mathbf{A}_{\gamma_1}(t_+)\,. \quad (4.2.11)$$

As in the primitive case, we assume that

$$\mathbf{A}_{\gamma_1}(t_-) = \mathbf{A}_{\gamma_1}(t_+) = \mathbf{A}_{\gamma_1}(t_{ms})\,,$$
$$\mathbf{A}_{\gamma_2}(t_-) = \mathbf{A}_{\gamma_2}(t_+) = \mathbf{A}_{\gamma_2}(t_{ms})\,,$$

[5]Note that it is not physically possible to have both $\gamma_1 + N\gamma_2$ and $\gamma_1 - N\gamma_2$ bound states. We choose one or the other, and for KS formulas the choices are related by the particle-antiparticle split of the charge lattice.

and will suppress the parameter t in these operators. We want to expand each operator, keeping first-order terms in $\hat{e}_{\gamma_1}$ and all orders in $\hat{e}_{\gamma_2}$. In fact, $\hat{e}_{\gamma_2}$ shall become the generating function variable x. We have:

$$\mathbf{A}_{\gamma_1} = 1 + \frac{\Omega^{mot}(\gamma_1; q)}{q^{1/2} - q^{-1/2}}\, \hat{e}_{\gamma_1} + \dots, \tag{4.2.12}$$

and

$$\begin{aligned}\prod_{N\geq 0}^{\leftarrow} \mathbf{A}_{\gamma_1+N\gamma_2}(t_+) &= 1 + \sum_{N=0}^{\infty} \frac{\Omega^{mot}(\gamma_1 + N\gamma_2; t_+; q)}{q^{1/2} - q^{-1/2}}\, \hat{e}_{\gamma_1+N\gamma_2} + \dots \\ &= 1 + \sum_{N=0}^{\infty} \frac{\Omega^{mot}(\gamma_1 + N\gamma_2; t_+; q)}{q^{1/2} - q^{-1/2}}\, q^{\frac{NI_{12}}{2}} \hat{e}_{\gamma_2}^N \hat{e}_{\gamma_1} + \dots . \end{aligned} \tag{4.2.13}$$

For $\mathbf{A}_{\gamma_2}$, we keep all k terms in (4.1.17) and use the infinite product formula (4.1.22) to write

$$\mathbf{A}_{\gamma_2} = \prod_{k=1}^{\infty} \prod_{n\in\mathbb{Z}} \mathbf{E}\big((-q^{1/2})^n \hat{e}_{\gamma_2}^{\,k}\big)^{\Omega_n^{mot}(k\gamma_2)}. \tag{4.2.14}$$

Now, observe that for any two charges γ, η with $I = \langle \gamma, \eta \rangle > 0$, the quantum dilogarithm satisfies the commutation relation

$$\hat{e}_\gamma\, \mathbf{E}(\hat{e}_\eta) = \hat{e}_\gamma \prod_{r=0}^{\infty} (1 + q^{r+\frac{1}{2}} \hat{e}_\eta)^{-1} = \prod_{r=0}^{\infty} (1 + q^{r+\frac{1}{2}+I} \hat{e}_\eta)^{-1} \hat{e}_\gamma = \left[\prod_{r=0}^{I-1} (1 + q^{r+\frac{1}{2}} \hat{e}_\eta)\right] \mathbf{E}(\hat{e}_\eta)\, \hat{e}_\gamma\,,$$

and similarly for any q-shifted versions of its argument $\hat{e}_\eta$. Therefore, the LHS of (4.2.11) can be written as

$$\begin{aligned} LHS:\ &\left(1 + \frac{\Omega^{mot}(\gamma_1; q)}{q^{\frac{1}{2}} - q^{-\frac{1}{2}}} \hat{e}_{\gamma_1} + \dots\right) \mathbf{A}_{\gamma_2} \\ &= \mathbf{A}_{\gamma_2} \left(1 + \frac{\Omega^{mot}(\gamma_1; q)}{q^{\frac{1}{2}} - q^{-\frac{1}{2}}} \left(\prod_{k=1}^{\infty} \prod_{n\in\mathbb{Z}} \prod_{r=0}^{kI_{12}-1} \big(1 + (-q^{\frac{1}{2}})^n q^{r+\frac{1}{2}} \hat{e}_{\gamma_2}^k\big)^{\Omega_n^{mot}(k\gamma_2)} \right) \hat{e}_{\gamma_1} + \dots \right), \end{aligned}$$

and the RHS as

$$RHS:\ \ \mathbf{A}_{\gamma_2} \left(1 + \frac{1}{q^{\frac{1}{2}} - q^{-\frac{1}{2}}} \sum_{N=0}^{\infty} \Omega^{mot}(\gamma_1 + N\gamma_2; t_+; q) q^{\frac{NI_{12}}{2}} \hat{e}_{\gamma_2}^N \hat{e}_{\gamma_1} + \dots \right).$$

Setting these two sides equal and matching the coefficients of $\hat{e}_{\gamma_1}$ leads to

$$\sum_{N=0}^{\infty} \Omega^{mot}(\gamma_1 + N\gamma_2; t_+; q)\, x^N = \Omega^{mot}(\gamma_1; q) \prod_{k=1}^{\infty} \prod_{n\in\mathbb{Z}} \prod_{r=0}^{kI_{12}-1} \big(1 + (-q^{\frac{1}{2}})^n q^{r+\frac{1}{2}-\frac{I_{12}}{2}} x^k\big)^{\Omega_n^{mot}(k\gamma_2)}, \tag{4.2.15}$$

where

$$x = q^{\frac{I_{12}}{2}} \hat{e}_{\gamma_2}\,. \tag{4.2.16}$$

After a shift in the product in r and the identifications $-q^{1/2} = y$ and $\Omega^{mot} = \Omega^{ref}$, formula (4.2.15) becomes identical to the refined semi-primitive wall-crossing formula (2.2.13).

The careful reader may have wondered why it was consistent to simply declare that there were no $\gamma_1 + N\gamma_2$ states (with $N \geq 2$) when deriving the primitive wall-crossing formula earlier in this section. The answer should now be clear: the primitive formula (4.2.4) can simply be though of as the part of the semi-primitive formula (4.2.11) that is at most first-order in $\hat{e}_{\gamma_2}$. (Or, more properly, this would be true had we added $\gamma_1 + N\gamma_2$ states to the unstable side of the semi-primitive formula.) So there *could* have been higher $\gamma_1 + N\gamma_2$ states in the primitive formula, but we would not have seen them at first order. Likewise, the semi-primitive formula is best thought of as a consistent truncation of the full wall-crossing formula, in a theory with all possible combinations of bound BPS states.

4.3 Examples: $SU(2)$ Seiberg-Witten theory

In this final section, we provide several examples of semi-primitive and non-semi-primitive(!) refined/motivic wall crossing using 4-dimensional $\mathcal{N} = 2$ gauge theory with gauge group $SU(2)$ and $N_f < 4$ flavors of fundamental matter [85, 86]. We first begin with a review of geometric engineering of these theories and their physical moduli spaces and spectra. A much more thorough analysis of physical and motivic wall crossing in $\mathcal{N} = 2$ gauge theory is found in [2].

Gauge theory via string compactification

The construction of 4-dimensional $\mathcal{N} = 2$ gauge theories in the context of string theory compactifications has come to be known as geometric engineering [82]. To obtain $SU(N)$ gauge theory in a type IIA compactification, one begins with a non-compact Calabi-Yau threefold X_N that is a fibration of a 2-complex-dimensional A_{N-1} ADE singularity over $\mathbb{P}^1$. This geometry can arise from a compact $K3$ fibration over $\mathbb{P}^1$ — dual to heterotic string theory on $K3 \times T^2$ [87] — in the limit of $K3$ moduli space where the $K3$ fibers develop an A_{N-1} singularity and all Kähler moduli not associated with the singularity become large. This results in an $SU(N)$ supergravity theory. As the ADE singularity is blown up it

turns into a string of $N-1$ $\mathbb{P}^1$'s fibered over the base $\mathbb{P}^1$, whose sizes correspond to the eigenvalues of the scalar Higgs field of the $SU(N)$ vector multiplet, and break the gauge group generically to $U(1)^{N-1}$. To decouple gravity while keeping the W-boson masses and the four-dimensional gauge coupling constant, one takes the size of the base $\mathbb{P}^1$ to infinity and the overall size of the fiber $\mathbb{P}^1$'s to zero [82]. This finally produces $\mathcal{N}=2$ $SU(N)$ super-Yang-Mills theory on the Coulomb branch.

The resolved local Calabi-Yau X_N has $2N$ compact even-dimensional cycles. Of these, $2N-2$ survive the rigid limit and generate the lattice of electric and magnetic charges in the gauge theory. For example, for $SU(2)$ theory, X_2 can simply be taken as the total space of the canonical line bundle over $\mathbb{P}^1_{(fiber)} \times \mathbb{P}^1_{(base)}$. The dimensions of its compact homology are $(b_0, b_2, b_4, b_6) = (1, 2, 1, 0)$. Electric charges, such as the charge of the W-boson, correspond to $D2$ branes wrapped on the fiber $\mathbb{P}^1$, while magnetic charges of solitons correspond to $D4$ branes wrapped on the entire $\mathbb{P}_1 \times \mathbb{P}_1$, *cf.* [71]. The low-energy theory of the D-branes and the resulting BPS states in the gauge theory can be described by representations of a "subquiver" of the quiver of the Calabi-Yau. In the case of pure $SU(2)$ theory, it is the K_2 Krönecker quiver of Figure 4.2 [71, 88].

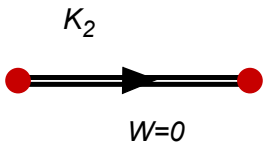

Figure 4.2: The K_2 Krönecker quiver.

To add matter to the $SU(N)$ theories, similar local Calabi-Yau's with extra base $\mathbb{P}^1$'s can be used [89, 90]. The states of the gauge theory are still described by a $2N-2$ sublattice of independent D-brane charges, but the relevant quivers are somewhat more complicated.

Note that there exist type IIB mirrors of these IIA compactifications that encode the Seiberg-Witten curves and the electric-magnetic duality of the gauge theories in a much more explicit manner — though we are less interested in them here because we seek a direct connection with the IIA formalism of Kontsevich-Soibelman. The mirrors of the noncompact Calabi-Yau's X_N's are given by equations of the form

$$xy = H(z, w)\,, \tag{4.3.1}$$

where $H(z,w)=0$ is a Riemann surface whose complex structure corresponds to the Kähler parameters of X_N. In a certain limit of the complex structure (corresponding to decoupling supergravity from the gauge theory) this becomes the Seiberg-Witten curve [82] (see also [63]). BPS states are given by compact $D3$-branes, which descend to non-critical strings on the Riemann surface [91, 92]. It is then easy to identify which branes generate electric and magnetic charges from the corresponding electric and magnetic cycles on the Seiberg-Witten curve.

Moduli spaces and spectra

The moduli space of the Coulomb branch of $SU(2)$ Seiberg-Witten theory is a limit, or slice, of the Kähler moduli space $\mathcal{M}_V$ for the Calabi-Yau X_2 (or the corresponding Calabi-Yau's that include fundamental matter). This moduli space is parametrized by the complex-valued Casimir u of the Higgs field [85, 86]. We draw its structure for theories with $N_f=0,1,2$, and 3 flavors of matter in Figure 4.3, following [93]. When $N_f<4$, the gauge theory is asymptotically free. The large-$|u|$ region corresponds to weak coupling, while the small-u region corresponds to strong coupling, and the two regions are separated by a wall of marginal stability $\mathcal{W}$. The central charge of a state with electric charge q and magnetic charge p is given by

$$Z(p,q;u)=a(u)q+a_D(u)p\,, \tag{4.3.2}$$

where $a(u)$ and $a_D(u)$ can be identified as period integrals on the Seiberg-Witten curve or, more relevantly for us, central charges of $D2$ and $D4$ branes in X_2. The wall of marginal stability is then defined by the condition

$$\arg a(u)=\arg a_D(u)\,,\qquad \text{or}\qquad \frac{a(u)}{a_D(u)}\in\mathbb{R}\,. \tag{4.3.3}$$

Since the charge lattice is two-dimensional, the central charges of *all* states align on $\mathcal{W}$.

In each case $N_f=0,1,2,3$, there are magnetically-charged states that become massless at singular points on $\mathcal{W}$. The BPS spectrum at any point in the weak coupling region can be represented in terms of single-center attractor flows that end on one of these singular points, as well as multi-center attractor flows that split on $\mathcal{W}$ into sums of flows to the singular points [16]. This leads to an infinite spectrum. In contrast, the strong-coupling

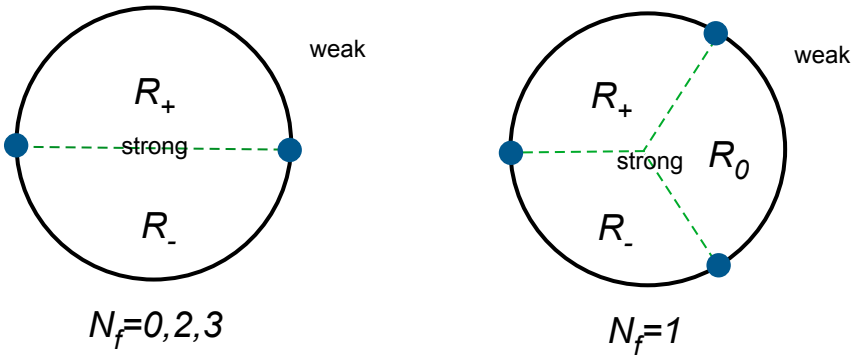

Figure 4.3: The approximate structure of the wall of marginal stability separating weak and strong coupling in the u-plane of Seiberg-Witten theories. We also indicate different local regions within the strong-coupling chamber. For $N_f = 0, 2, 3$, there are BPS states of two different charges that become massless at singularities in the moduli space (the dots here), and for $N_f = 1$ there are three.

spectrum at points inside the wall of marginal stability is simply represented by the finite number of single-center flows to the singularities. Note that the Coulomb branch of an $\mathcal{N} = 2$ gauge theory only possesses a global version of special geometry, as opposed to the local special geometry of supergravity that was described in Section 2.1; nevertheless, a simplified version of the attractor mechanism still functions and BPS states can still be described in terms of attractor flow trees [94].

The spectra of $N_f = 0, 1, 2, 3$ $SU(2)$ theories was carefully derived in [93] using field-theory methods and global properties of the moduli space (see also [91] for an alternative approach). The fundamental electric charge $q = 1$ is *half* the charge of the W-boson. The weak-coupling spectra include the $W^{\pm}$-bosons with $(q, p) = \pm(2, 0)$ and the fundamental quarks with $(q, p) = \pm(1, 0)$. They also contain the monopole and dyons that become massless at singularities on the Coulomb branch and all their conjugates under the monodromy around $u = \infty$ (which must be a symmetry of the weakly-coupled theory). This monodromy acts as

$$M_\infty \,:\, (q, p) \to (q + N_f\, p, p) \tag{4.3.4}$$

on the charge lattice. Altogether, one finds weak-coupling spectra

$$N_f = 0: \quad (2,0)\,,\ (2n,1)\ \ n \in \mathbb{Z}\,, \tag{4.3.5}$$

$$N_f = 1: \quad (2,0)\,,\ (1,0)_2\,,\ (n,1)\ \ n \in \mathbb{Z}\,, \tag{4.3.6}$$

$$N_f = 2: \quad (2,0)\,,\ (1,0)_4\,,\ (n,1)_2\ \ n \in \mathbb{Z}\,, \tag{4.3.7}$$

$$N_f = 3: \quad (2,0)\,,\ (1,0)_6\,,\ (n,1)_4\ \ (2n+1,2)\,,\ n \in \mathbb{Z}\,. \tag{4.3.8}$$

We have suppressed $\pm$ signs for antiparticles, and the subscripts here denote nontrivial multiplicities. At strong-coupling, inside the wall of marginal stability, the spectrum has no single canonical description, due to the nontrivial fibration of the charge lattice over the moduli space. In some of the regions indicated in Figure 4.3, the spectra can be described as

$$N_f = 0: \quad [\mathcal{R}_+]\ \ (2,1)\,,\ (0,1) \qquad [\mathcal{R}_-]\ \ (-2,1)\,,\ (0,1) \tag{4.3.9}$$

$$N_f = 1: \quad [\mathcal{R}_0]\ \ (0,1)\,,\ (-1,1)\,,\ (1,0) \qquad [\mathcal{R}_+]\ \ (2,-1)\,,\ (-1,1)\,,\ (1,0)$$
$$[\mathcal{R}_-]\ \ (0,1)\,,\ (1,1)\,,\ (1,0) \tag{4.3.10}$$

$$N_f = 2: \quad [\mathcal{R}_+]\ \ (1,-1)_2\,,\ (0,1)_2 \qquad [\mathcal{R}_-]\ \ (1,1)_2\,,\ (0,1)_2 \tag{4.3.11}$$

$$N_f = 3: \quad [\mathcal{R}_+]\ \ (-1,2)\,,\ (1,-1)_4 \qquad [\mathcal{R}_-]\ \ (-1,2)\,,\ (0,1)_4\,. \tag{4.3.12}$$

It is also possible to generate the spectra from stable quiver representations. For example, the $N_f = 0$ case is derived from the K_2 quiver of Figure 4.2 in [71] (see also [95]). The $N_f = 1$ case appears in [2].

Refined/motivic wall crossing

We now show that the above physically-determined spectra agree perfectly with motivic wall crossing.

Consider the case $N_f = 0$. Let us choose a basis $\{\gamma_1, \gamma_2\}$ of the charge lattice related to electric and magnetic charges (q, p) by

$$\gamma_1 = (1,-1)\,, \qquad \gamma_2 = (0,1) \tag{4.3.13}$$

with $\langle \gamma_1, \gamma_2 \rangle = 1$ (this is not necessary but will be convenient later). We also choose "particles" (as opposed to antiparticles) to have $q > 0$ for any p, or $q = 0$ and $q > 0$. All

states except the W boson come in hypermultiplets, and should be represented by operators

$$\mathbf{U}_{m,n} := \mathbf{E}_{m\gamma_1+n\gamma_2}(\hat{e}_{\gamma_1+\gamma_2}) \qquad \sim \text{charge } (m, n-m) \tag{4.3.14}$$

in the motivic wall-crossing formula. The W-boson comes in a vector multiplet and should be represented by an operator

$$\mathbf{U}_{2,2}^{\text{vect}} := \mathbf{E}_{2\gamma_1+2\gamma_2}(-q^{1/2}\hat{e}_{2\gamma_1+2\gamma_2})^{-1}\,\mathbf{E}_{2\gamma_1+2\gamma_2}(-q^{-1/2}\hat{e}_{2\gamma_1+2\gamma_2})^{-1}\,. \tag{4.3.15}$$

Near the wall of marginal stability, the central charges of γ_1 and γ_2 coincide. Slightly away from this wall, we either have $\arg Z(2\gamma_1+\gamma_2) < \arg Z(\gamma_2)$ or $\arg Z(2\gamma_1+\gamma_2) > \arg Z(\gamma_2)$. Identifying the former with strong coupling and the latter with weak coupling, the BPS spectra (4.3.5) and (4.3.9) (in region $\mathcal{R}_-$) lead to a predicted motivic wall-crossing formula

$$\mathbf{U}_{2,1}\,\mathbf{U}_{0,1} \stackrel{?}{=} \mathbf{U}_{0,1}\,\mathbf{U}_{2,3}\,\mathbf{U}_{4,5}\,\mathbf{U}_{6,7}\cdots\mathbf{U}_{2,2}^{\text{vect}}\cdots\mathbf{U}_{6,5}\,\mathbf{U}_{4,3}\,\mathbf{U}_{2,1}\,. \tag{4.3.16}$$

This formula is in fact true. It can be checked algebraically, order by order in $\hat{e}_{\gamma_1}$ and $\hat{e}_{\gamma_2}$. (This is in fact one reason for our choice of basis (4.3.13) — so no negative powers of $\hat{e}$'s appear, making it possible to easily truncate series at any degree.) It is also possible to prove (4.3.16) directly by deriving motivic invariants from the K_2 quiver [2]. After the arguments in Section 4.2, it may not be too surprising that this formula works; however, in our research it preceded the proof of refined wall crossing from motivic wall crossing, and provided the first hint that the factorization property (4.1.16) should hold.

Using the same basis (4.3.13) and choice of particles vs. antiparticles, the BPS spectra for $N_f = 1$ and $N_f = 2$ theories predict motivic wall-crossing formulas

$$N_f = 1: \quad \mathbf{U}_{1,0}\,\mathbf{U}_{1,1}\,\mathbf{U}_{0,1} = \mathbf{U}_{0,1}\,\mathbf{U}_{1,2}\,\mathbf{U}_{2,3}\,\mathbf{U}_{3,4}\cdots\mathbf{U}_{1,1}^{2}\,\mathbf{U}_{2,2}^{\text{vect}}\cdots\mathbf{U}_{3,2}\,\mathbf{U}_{2,1}\,\mathbf{U}_{1,0} \tag{4.3.17}$$

$$N_f = 2: \quad \mathbf{U}_{1,0}^{2}\,\mathbf{U}_{0,1}^{2} = \mathbf{U}_{0,1}^{2}\,\mathbf{U}_{1,2}^{2}\,\mathbf{U}_{2,3}^{2}\,\mathbf{U}_{3,4}^{2}\cdots\mathbf{U}_{1,1}^{4}\,\mathbf{U}_{2,2}^{\text{vect}}\cdots\mathbf{U}_{3,2}^{2}\,\mathbf{U}_{2,1}^{2}\,\mathbf{U}_{1,0}^{2}\,. \tag{4.3.18}$$

With a slightly different choice of particles vs. antiparticles, the following is obtained,

$$N_f = 3: \quad \mathbf{U}_{1,-1}\,\mathbf{U}_{0,1}^{4} = \mathbf{U}_{0,1}^{4}\,\mathbf{U}_{1,3}\,\mathbf{U}_{1,2}^{4}\,\mathbf{U}_{3,5}\,\mathbf{U}_{2,3}^{4}\cdots\mathbf{U}_{1,1}^{6}\,\mathbf{U}_{2,2}^{\text{vect}}\cdots\mathbf{U}_{2,1}^{4}\,\mathbf{U}_{3,1}\,\mathbf{U}_{1,0}^{4}\,\mathbf{U}_{1,-1}\,. \tag{4.3.19}$$

Algebraically, the validity of all these formulas follows directly from the validity of (4.3.16). They can be derived by commuting operators $\mathbf{U}_{1,1}$ through the infinite products on the RHS using the pentagon relation; a sample proof for $N_f = 1$ appears at the end of this section.

Formulas (4.3.17), (4.3.18), and (4.3.19) correspond to the strong-coupling spectra in regions $\mathcal{R}_0$, $\mathcal{R}_+$, and $\mathcal{R}_-$, respectively. This choice of regions is correlated to the choice of split between particles and antiparticles. For example, for $N_f = 1$ the following formulas also hold:

$$N_f = 1\,[\mathcal{R}_+]: \quad \mathbf{U}_{2,1}\,\mathbf{U}_{1,1}\,\mathbf{U}_{-1,0} = \mathbf{U}_{-1,0}\,\mathbf{U}_{0,1}\,\mathbf{U}_{1,2}\,\mathbf{U}_{2,3}\,\mathbf{U}_{3,4}\cdots\mathbf{U}_{1,1}^2\,\mathbf{U}_{2,2}^{\text{vect}}\cdots\mathbf{U}_{3,2}\,\mathbf{U}_{2,1}$$
$$N_f = 1\,[\mathcal{R}_-]: \quad \mathbf{U}_{0,-1}\,\mathbf{U}_{1,1}\,\mathbf{U}_{1,2} = \mathbf{U}_{1,2}\,\mathbf{U}_{2,3}\,\mathbf{U}_{3,4}\cdots\mathbf{U}_{1,1}^2\,\mathbf{U}_{2,2}^{\text{vect}}\cdots\mathbf{U}_{3,2}\,\mathbf{U}_{2,1}\,\mathbf{U}_{1,0}\,\mathbf{U}_{0,-1}\,.$$

Altogether, we find that the physical derivations of refined BPS spectra agree perfectly with mathematical motivic formulas.

Proving $N_f = 0 : N_f = 1, 2, 3$

The key to deriving (4.3.17), (4.3.18), (4.3.19) from (4.3.16) is to observe that all terms on the RHS are of the form $\mathbf{U}_{k,k+1}$ or $\mathbf{U}_{k+1,k}$, and that, due to the pentagon identity (4.1.21),

$$\mathbf{U}_{1,1}\,\mathbf{U}_{k,k+1} = \mathbf{U}_{k,k+1}\,\mathbf{U}_{k+1,k+2}\,\mathbf{U}_{1,1}\,, \qquad \mathbf{U}_{k+1,k}\,\mathbf{U}_{1,1} = \mathbf{U}_{1,1}\,\mathbf{U}_{k+2,k+1}\,\mathbf{U}_{k+1,k}\,. \quad (4.3.20)$$

Therefore, fundamental quark operators $\mathbf{U}_{1,1}$ can be commuted through the semi-infinite products on the RHS of (4.3.16) in pairs to obtain the other formulas. For example, for $N_f = 1$ we have

$$\begin{aligned}
&\mathbf{U}_{0,1}\,\mathbf{U}_{1,2}\,\mathbf{U}_{2,3}\,\mathbf{U}_{3,4}\,\mathbf{U}_{4,5}\cdots\mathbf{U}_{1,1}^2\,\mathbf{U}_{2,2}^{\text{vect}}\cdots\mathbf{U}_{5,4}\,\mathbf{U}_{4,3}\,\mathbf{U}_{3,2}\,\mathbf{U}_{2,1}\,\mathbf{U}_{1,0} \\
&\qquad = \mathbf{U}_{1,1}\left[\,\mathbf{U}_{0,1}\,\mathbf{U}_{2,3}\,\mathbf{U}_{4,5}\cdots\mathbf{U}_{2,2}^{\text{vect}}\cdots\mathbf{U}_{6,5}\,\mathbf{U}_{4,3}\,\mathbf{U}_{2,1}\,\right]\mathbf{U}_{1,1}\,\mathbf{U}_{1,0} \\
&\qquad \overset{N_f=0}{=} \mathbf{U}_{1,1}\left[\,\mathbf{U}_{2,1}\,\mathbf{U}_{0,1}\,\right]\mathbf{U}_{1,1}\,\mathbf{U}_{1,0} \\
&\qquad = \mathbf{U}_{1,1}\,\mathbf{U}_{2,1}\,\mathbf{U}_{1,0}\,\mathbf{U}_{0,1} \\
&\qquad = \mathbf{U}_{1,0}\,\mathbf{U}_{1,1}\,\mathbf{U}_{0,1}\,.
\end{aligned}$$

The last two lines follow by further applications of the pentagon identity (4.1.21).

Part II

Chern-Simons Theory with Complex Gauge Group

Chapter 5

Perturbation theory around a nontrivial flat connection

We now change focus to consider Chern-Simons theory with noncompact, complex gauge group, and in particular the various approaches to computing its perturbative partition functions that were outlined in the Introduction.

We begin here by reviewing some basic features of Chern-Simons theory with complex gauge group and its perturbative expansion, following mainly [39] and [40]. The notations we introduce will be used throughout Part II. We then pursue the most traditional approach to Chern-Simons theory, based on the evaluation of Feynman diagrams. This analysis will show that the perturbative coefficients in the Chern-Simons partition functions have a very special structure, motivating the definition of "arithmetic TQFT." We define a "geometric" flat $SL(2,\mathbb{C})$ Chern-Simons connection that is related to the hyperbolic structure on a hyperbolic three-manifold M, and conjecture that in the background of this connection $SL(2,\mathbb{C})$ Chern-Simons theory *is* such an arithmetic TQFT. In the last section of the chapter, we substantiate this claim with explicit computations for the knots $\mathbf{4_1}$ and $\mathbf{5_2}$. The discussions of Feynman diagrams and arithmeticity follow [3].

Starting in Section 5.2, some understanding of hyperbolic geometry will be helpful. We will introduce several basic concepts as needed, but also refer the reader to Section 8.1 for a more thorough treatment of hyperbolic three-manifolds. Similarly, the computations in Section 5.4 will require some familiarity with the Volume Conjecture, which is described much more fully in Sections 6.2 and 7.4.

5.1 Basics

Let us denote a compact gauge group by G, its noncompact complexification by $G_{\mathbb{C}}$, and the respective Lie algebras of these groups as $\mathfrak{g}$ and $\mathfrak{g}_{\mathbb{C}}$. We can assume that G, $G_{\mathbb{C}}$ are reductive. As noted in the Introduction, the Chern-Simons action for a complex gauge field $\mathcal{A}$ can be written as a sum of two (classically) topological terms, one for $\mathcal{A}$ and one for $\bar{\mathcal{A}}$:

$$\begin{aligned} S &= \frac{t}{8\pi}\int_M \mathrm{Tr}\Big(\mathcal{A}\wedge d\mathcal{A}+\frac{2}{3}\,\mathcal{A}\wedge\mathcal{A}\wedge\mathcal{A}\Big) \\ &\quad + \frac{\bar{t}}{8\pi}\int_M \mathrm{Tr}\Big(\bar{\mathcal{A}}\wedge d\bar{\mathcal{A}}+\frac{2}{3}\bar{\mathcal{A}}\wedge\bar{\mathcal{A}}\wedge\bar{\mathcal{A}}\Big)\,. \end{aligned} \tag{5.1.1}$$

The field $\mathcal{A}$ here is a locally-defined $\mathfrak{g}_{\mathbb{C}}$-valued one-form on the euclidean three-manifold M. The two coupling constant t and $\bar{t}$ can be written as

$$t = k+\sigma\,, \qquad t = k-\sigma\,, \tag{5.1.2}$$

and different physical unitarity structures force the "level" k to be an integer and σ to be either real or imaginary [39]. For example, in the case $G_{\mathbb{C}} = SL(2,\mathbb{C})$, the above action can be recast as the action for euclidean gravity with negative cosmological constant by writing $\mathcal{A}$ as a vielbein and a spin connection, $\mathcal{A} = -(w+ie)$ [96], and under the resulting unitarity structure the coupling σ must be real. Unlike in the case of compact gauge group, the level k does *not* undergo a shift in the quantum theory [44].

It is explained in [39] that introducing a noncompact gauge group is a perfectly acceptable option in Chern-Simons theory. In Yang-Mills theories, a noncompact gauge group would lead to a kinetic term that is not positive definite, and hence to unbounded energy (or an ill-defined path integral). In Chern-Simons theory with complex gauge group the kinetic term *is* indefinite, but this is no problem: the Hamiltonian of the theory vanishes due to topological invariance, so the "energy" is always exactly zero.

The classical solutions, or extrema of the action (5.1.1), are flat connections, *i.e.* connections that obey

$$\mathcal{A}+\mathcal{A}\wedge\mathcal{A}=0\,, \qquad \bar{\mathcal{A}}+\bar{\mathcal{A}}\wedge\bar{\mathcal{A}}=0\,. \tag{5.1.3}$$

Flat $G_{\mathbb{C}}$-connections on a three-manifold M are completely determined by their holonomies, *i.e.* by a homomorphism

$$\rho\,:\,\pi_1(M)\to G_{\mathbb{C}}\,, \tag{5.1.4}$$

up to conjugacy (*i.e.* up to gauge transformations). Thus the moduli space of classical solutions can be written as

$$\mathcal{M}_{\text{flat}}(G_{\mathbb{C}}; M) = \text{Hom}(\pi_1(M),\, G_{\mathbb{C}})/\!\!/G_{\mathbb{C}}\,. \tag{5.1.5}$$

As discussed in the introduction, one can then consider perturbation theory around a given flat connection $\mathcal{A}^{(\rho)} \in \mathcal{M}_{\text{flat}}(G_{\mathbb{C}}; M)$ corresponding to the homomorphism ρ. Since the classical action is a sum of terms for $\mathcal{A}$ and $\bar{\mathcal{A}}$, the *perturbative* expansion of the partition function around $\mathcal{A}^{(\rho)}$ will factorize as (*cf.* [40, 41])

$$Z^{(\rho)}(M) = Z^{(\rho)}(M; t)\, Z^{(\rho)}(M; \bar{t})\,. \tag{5.1.6}$$

One may *hope* that the full non-perturbative path integral obeys a relation of the form

$$Z(M) = \int \mathcal{D}\mathcal{A}\, e^{iS} = \sum_{\rho} Z^{(\rho)}(M; t)\, Z^{(\rho)}(M; \bar{t})\,, \tag{5.1.7}$$

summing over all flat connections. Here, however, we merely focus on the perturbative pieces $Z^{(\rho)}(M; t)$.

By standard methods of quantum field theory — essentially a stationary phase approximation to the path integral — each component $Z^{(\rho)}(M; t)$ can be expanded in inverse powers of t. Explicitly, let us define Planck's constant

$$\boxed{\hbar = \frac{2\pi i}{t}} \tag{5.1.8}$$

and expand

$$Z^{(\rho)}(M; \hbar) \;=\; \exp\left(\frac{1}{\hbar} S_0^{(\rho)} - \frac{1}{2}\delta^{(\rho)} \log \hbar \,+\, \sum_{n=0}^{\infty} S_{n+1}^{(\rho)} \hbar^n\right)\,. \tag{5.1.9}$$

The coefficients $S_n^{(\rho)}$ (and $\delta^{(\rho)}$) completely characterize $Z^{(\rho)}(M; t)$ to all orders in perturbation theory.

5.2 Coefficients and Feynman diagrams

Let us examine each term in the expansion (5.1.9) more carefully. As already mentioned in the introduction, the leading term $S_0^{(\rho)}$ is the value of the classical holomorphic Chern-Simons functional

$$\frac{1}{4}\int_M \text{Tr}\left(\mathcal{A}\wedge d\mathcal{A} + \frac{2}{3}\mathcal{A}\wedge\mathcal{A}\wedge\mathcal{A}\right) \tag{5.2.1}$$

evaluated on a flat gauge connection $\mathcal{A}^{(\rho)}$ that corresponds to a homomorphism ρ. It is also easy to understand the integer coefficient $\delta^{(\rho)}$ in (5.1.9). The homomorphism ρ defines a flat $G_{\mathbb{C}}$ bundle over M, which we denote as E_ρ. Letting $H^i(M; E_\rho)$ be the i-th cohomology group of M with coefficients in the flat bundle E_ρ, the coefficient $\delta^{(\rho)}$ is given by

$$\delta^{(\rho)} \;=\; h^1 - h^0\,, \tag{5.2.2}$$

where $h^i := \dim H^i(M; E_\rho)$. Both this term and $S_1^{(\rho)}$ come from the "one-loop" contribution to the path integral (1.0.2); $S_1^{(\rho)}$ can be expressed in terms of the Ray-Singer torsion [97] of M with respect to the flat bundle E_ρ (*cf.* [13, 44, 98]),

$$S_1^{(\rho)} \;=\; \frac{1}{2}\log\left(\frac{T(M; E_\rho)}{2}\right). \tag{5.2.3}$$

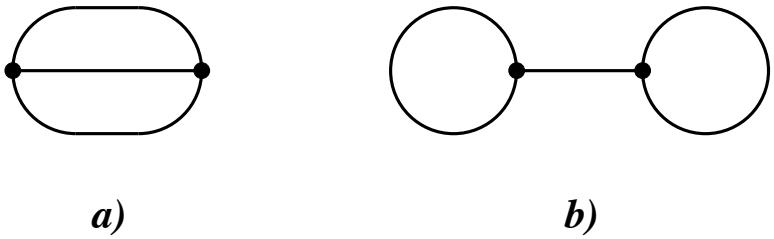

Figure 5.1: Two kinds of 2-loop Feynman diagrams that contribute to $S_2^{(\rho)}$.

The geometric interpretation of the higher-order terms $S_n^{(\rho)}$ with $n > 1$ is more interesting, yet less obvious. To understand it better, we note that the saddle-point approximation to the path integral (1.0.2) gives an expression for $S_n^{(\rho)}$ as a sum of Feynman diagrams with n loops. For example, the relevant diagrams for $n = 2$ are shown schematically in Figure 5.1. Since the Chern-Simons action (5.1.1) is cubic, all vacuum diagrams (that is, Feynman diagrams with no external lines) are closed trivalent graphs; lines in such graphs have no open end-points. Therefore, a Feynman diagram with n loops ($n > 1$) has $3(n-1)$ line segments with end-points meeting at $2(n-1)$ trivalent vertices. Each such diagram contributes an integral of the form (*cf.* [42])

$$\int_{M^{2n-2}} L^{3n-3}\,, \tag{5.2.4}$$

where M^{2n-2} denotes a product of $2n-2$ copies of M and L^{3n-3} denotes a wedge product of a 2-form $L(x,y) \in \Omega^2(M_x \times M_y; \mathfrak{g}_{\mathbb{C}} \otimes \mathfrak{g}_{\mathbb{C}})$. The 2-form $L(x,y)$, called the "propagator,"

is a solution to the first-order PDE,

$$d_{\mathcal{A}^{(\rho)}} L(x,y) \;=\; \delta^3(x,y)\,, \tag{5.2.5}$$

where $\delta^3(x,y)$ is a δ-function 3-form supported on the diagonal in $M_x \times M_y$ and $d_{\mathcal{A}^{(\rho)}}$ is the exterior derivative twisted by a flat connection $\mathcal{A}^{(\rho)}$ on the $G_{\mathbb{C}}$ bundle E_ρ.

For example, suppose that M is a geodesically complete hyperbolic 3-manifold of finite volume. As we pointed out in the Introduction, such 3-manifolds provide some of the most interesting examples for Chern-Simons theory with complex gauge group. Every such M can be represented as a quotient

$$M \;=\; \mathbb{H}^3/\Gamma \tag{5.2.6}$$

of the hyperbolic space $\mathbb{H}^3$ by a discrete, torsion-free subgroup $\Gamma \subset PSL(2,\mathbb{C})$, which is a holonomy representation of the fundamental group $\pi_1(M)$ into $\mathrm{Isom}^+(\mathbb{H}^3) = PSL(2,\mathbb{C})$. Furthermore, one can always choose a spin structure on M such that this holonomy representation lifts to a map from $\pi_1(M)$ to $SL(2,\mathbb{C})$. In what follows, we call this representation "geometric" and denote the corresponding flat $SL(2,\mathbb{C})$ connection as $\mathcal{A}^{(\mathrm{geom})}$.

In order to explicitly describe the flat connection $\mathcal{A}^{(\mathrm{geom})}$, recall that $\mathbb{H}^3$ can be defined as the upper half-space with the standard hyperbolic metric

$$ds^2 \;=\; \frac{1}{x_3^2}(dx_1^2 + dx_2^2 + dx_3^2)\,, \qquad x_3 > 0\,. \tag{5.2.7}$$

The components of the vielbein and spin connection corresponding to this metric can be written as

$$\begin{aligned} e^1 &= \frac{dx_1}{x_3} & w^1 &= \frac{dx_2}{x_3} \\ e^2 &= \frac{dx_2}{x_3} & w^2 &= -\frac{dx_1}{x_3} \\ e^3 &= \frac{dx_3}{x_3} & w^3 &= 0\,. \end{aligned}$$

These satisfy $de^a + \epsilon^{abc} w_b \wedge e_c = 0$. It is easy to check that the corresponding $(P)SL(2,\mathbb{C})$ connection

$$\mathcal{A}^{(\mathrm{geom})} \;=\; -(w + ie) \;=\; \frac{1}{2x_3}\begin{pmatrix} dx_3 & 2dx_1 - 2idx_2 \\ 0 & -dx_3 \end{pmatrix} \tag{5.2.8}$$

is flat, *i.e.* obeys (1.0.3) on page 6. In Chern-Simons theory with gauge group $G_{\mathbb{C}} = (P)SL(2,\mathbb{C})$, this gives an explicit expression for the flat gauge connection that corresponds

to the hyperbolic structure on M. In a theory with a larger gauge group, one can also define a geometric connection $\mathcal{A}^{(\mathrm{geom})}$ by embedding (5.2.8) into a larger matrix. We note, however, that $\mathcal{A}^{(\mathrm{geom})}$ constructed in this way is not unique and depends on the choice of embedding. Nevertheless, we will continue to use the notation $\mathcal{A}^{(\mathrm{geom})}$ even in the higher-rank case whenever the choice of embedding introduces no confusion.

The action of Γ on $\mathbb{H}^3$ can be conveniently expressed by identifying a point $(x_1, x_2, x_3) \in \mathbb{H}^3$ with a quaternion $q = x_1 + x_2 i + x_3 j$ and defining

$$\gamma : q \mapsto (aq + b)/(cq + d)\,, \qquad \gamma = \begin{pmatrix} a & b \\ c & d \end{pmatrix} \in PSL(2, \mathbb{C})\,. \tag{5.2.9}$$

Explicitly, setting $z = x_1 + i x_2$, we find

$$\gamma(z + x_3 j) \;=\; z' + x_3' j\,, \tag{5.2.10}$$

where

$$z' \;=\; \frac{(az + b)(\bar{c}\bar{z} + \bar{d}) + a\bar{c}x_3^2}{|cz + d|^2 + |c|^2 x_3^2}\,, \qquad x_3' \;=\; \frac{x_3}{|cz + d|^2 + |c|^2 x_3^2}\,. \tag{5.2.11}$$

Let $L_0(x, y)$ be the propagator for $\mathbb{H}^3$, *i.e.* a solution to equation (5.2.5) on $\mathbb{H}^3 \times \mathbb{H}^3$ with the non-trivial flat connection $\mathcal{A}^{(\mathrm{geom})}$. Then, for a hyperbolic quotient space (5.2.6), the propagator $L(x, y)$ can simply be obtained by summing over images:

$$L(x, y) \;=\; \sum_{\gamma \in \Gamma} L_0(x, \gamma y)\,. \tag{5.2.12}$$

5.3 Arithmeticity

Now, we would like to consider what kind of values the perturbative invariants $S_n^{(\rho)}$ can take. For $n \geq 1$, the $S_n^{(\rho)}$'s are given by sums over Feynman diagrams, each of which contributes an integral of the form (5.2.4). *A priori* the value of every such integral can be an arbitrary complex number (complex because we are studying Chern-Simons theory with complex gauge group) that depends on the 3-manifold M, the gauge group $G_{\mathbb{C}}$, and the classical solution ρ. However, for a hyperbolic 3-manifold $M = \mathbb{H}^3/\Gamma$ and for the flat connection $\mathcal{A}^{(\mathrm{geom})}$ associated with the hyperbolic structure on M, we find that the $S_n^{(\mathrm{geom})}$'s are significantly more restricted.

Most basically, one might expect that the values of $S_n^{(\mathrm{geom})}$'s are *periods* [99]

$$S_n^{(\mathrm{geom})} \in \mathcal{P}. \tag{5.3.1}$$

Here $\mathcal{P}$ is the set of all periods, satisfying

$$\mathbb{Q} \subset \overline{\mathbb{Q}} \subset \mathcal{P} \subset \mathbb{C}. \tag{5.3.2}$$

By definition, a period is a complex number whose real and imaginary parts are (absolutely convergent) integrals of rational functions with rational coefficients, over domains in $\mathbb{R}^n$ defined by polynomial inequalities with rational coefficients [99]. Examples of periods are powers of π, special values of L-functions, and logarithmic Mahler measures of polynomials with integer coefficients. Thus, periods can be transcendental numbers, but they form a countable set, $\mathcal{P}$. Moreover, $\mathcal{P}$ is an algebra; a sum or a product of two periods is also a period.

Although the formulation of the perturbative invariants $S_{n\geq 1}^{(\mathrm{geom})}$ in terms of Feynman diagrams naturally leads to integrals of the form (5.2.4), which have the set of periods, $\mathcal{P}$, as their natural home, here we make a stronger claim and conjecture that for $n > 1$ the $S_n^{(\mathrm{geom})}$'s are algebraic numbers, *i.e.* they take values in $\overline{\mathbb{Q}}$. As we indicated in (5.3.2), the field $\overline{\mathbb{Q}}$ is contained in $\mathcal{P}$, but leads to a much stronger condition on the arithmetic nature of the perturbative invariants $S_n^{(\mathrm{geom})}$. In order to formulate a more precise conjecture, we introduce the following definition:

Definition: A perturbative quantum field theory is called *arithmetic* if, for all $n > 1$, the perturbative coefficients $S_n^{(\rho)}$ take values in some algebraic number field $\mathbb{K}$,

$$S_n^{(\rho)} \ \in \ \mathbb{K}\,, \tag{5.3.3}$$

and $S_1^{(\rho)} \in \mathbb{Q} \cdot \log \mathbb{K}\,.$

Therefore, to a manifold M and a classical solution ρ an arithmetic topological quantum field theory (arithmetic TQFT for short) associates an algebraic number field $\mathbb{K}$,

$$(M, \rho) \rightsquigarrow \mathbb{K}\,. \tag{5.3.4}$$

This is very reminiscent of arithmetic topology, a program proposed in the sixties by D. Mumford, B. Mazur, and Yu. Manin, based on striking analogies between number theory and low-dimensional topology. For instance, in arithmetic topology, 3-manifolds correspond to algebraic number fields and knots correspond to primes.

Usually, in perturbative quantum field theory the normalization of the expansion parameter is a matter of choice. Thus, in the notations of the present paper, a rescaling of the coupling constant $\hbar \to \lambda\hbar$ by a numerical factor λ is equivalent to a redefnition $S_n^{(\rho)} \to \lambda^{1-n} S_n^{(\rho)}$. While this transformation does not affect the physics of the perturbative expansion, it certainly is important for the arithmetic aspects discussed here. In particular, the above definition of arithmetic QFT is preserved by such a transformation only if $\lambda \in \mathbb{Q}$. In a theory with no canonical scale of $\hbar$, it is natural to choose it in such a way that makes the arithmetic nature of the perturbative coefficients $S_n^{(\rho)}$ as simple as possible. However, in some cases (which include Chern-Simons gauge theory), the coupling constant must obey certain quantization conditions, which, therefore, can lead to a "preferred" normalization of $\hbar$ up to irrelevant $\mathbb{Q}$-valued factors.

We emphasize that our definition of arithmetic QFT is perturbative. In particular, it depends on the choice of the classical solution ρ. In the present context of Chern-Simons gauge theory with complex gauge group $G_{\mathbb{C}}$, there is a natural choice of ρ when M is a geodesically complete hyperbolic 3-manifold, namely the geometric representation that corresponds to $\mathcal{A}^{(\mathrm{geom})}$. In this case, we conjecture:

Arithmeticity conjecture: *As in* (5.2.6)*, let M be a geodesically complete hyperbolic 3-manifold of finite volume, and let $\rho = \mathrm{geom}$ be the corresponding discrete faithful representation of $\pi_1(M)$ into $PSL(2,\mathbb{C})$. Then the perturbative Chern-Simons theory with complex gauge group $G_{\mathbb{C}} = PSL(2,\mathbb{C})$ (or its double cover, $SL(2,\mathbb{C})$) in the background of a non-trivial flat connection $\mathcal{A}^{(\mathrm{geom})}$ is arithmetic on M.*

In fact, we can be a little bit more specific. In all the examples that we studied, we find that, for M as in (5.2.6) and for all values of $n > 1$, the perturbative invariants $S_n^{(\mathrm{geom})}$ take values in the trace field of Γ,

$$S_n^{(\mathrm{geom})} \ \in \ \mathbb{Q}(\mathrm{tr}\Gamma)\,, \tag{5.3.5}$$

where, by definition, $\mathbb{Q}(\mathrm{tr}\Gamma)$ is the minimal extension of $\mathbb{Q}$ containing $\mathrm{tr}\gamma$ for all $\gamma \in \Gamma$. We conjecture that this is the case in general, namely that the $SL(2,\mathbb{C})$ Chern-Simons theory on a hyperbolic 3-manifold $M = \mathbb{H}^3/\Gamma$ is arithmetic with $\mathbb{K} = \mathbb{Q}(\mathrm{tr}\Gamma)$. This should be contrasted with the case of a compact gauge group, where one usually develops perturbation theory in the background of a trivial flat connection, and the perturbative invariants $S_n^{(\rho)}$

turn out to be rational numbers.

Of course, in this conjecture it is important that the representation ρ is fixed, *e.g.* by the hyperbolic geometry of M as in the case at hand. As we shall see below, in many cases the representation ρ admits continuous deformations or, put differently, comes in a family. For geometric representations, this does not contradict the famous rigidity of hyperbolic structures because the deformations correspond to incomplete hyperbolic structures on M. In a sense, the second part of this section is devoted to studying such deformations. As we shall see, the perturbative $G_{\mathbb{C}}$ invariant $Z^{(\rho)}(M;\hbar)$ is a function of the deformation parameters, which on the *geometric branch*[1] can be interpreted as shape parameters of the associated hyperbolic structure.

In general, one might expect the perturbative coefficients $S^{(\rho)}_{n>1}$ to be rational functions of these shape parameters. Note that, if true, this statement would imply the above conjecture, since at the point corresponding to the complete hyperbolic structure the shape parameters take values in the trace field $\mathbb{Q}(\mathrm{tr}\Gamma)$. This indeed appears to be the case, at least for several simple examples of hyperbolic 3-manifolds that we have studied.

For the arithmeticity conjecture to hold, it is important that $\hbar$ is defined (up to $\mathbb{Q}$-valued factors) as in (5.1.8) on page 83, so that the leading term $S_0^{(\rho)}$ is a rational multiple of the classical Chern-Simons functional. This normalization is natural for a number of reasons. For example, it makes the arithmetic nature of the perturbative coefficients $S_n^{(\rho)}$ as clear as possible. Namely, according to the above arithmeticity conjecture, in this normalization $S_1^{(\mathrm{geom})}$ is a period, whereas $S^{(\mathrm{geom})}_{n>1}$ take values in $\overline{\mathbb{Q}}$. However, although we are not going to use it here, we note that another natural normalization of $\hbar$ could be obtained by a redefinition $\hbar \to \lambda\hbar$ with $\lambda \in (2\pi i)^{-1}\cdot\mathbb{Q}$. As we shall see below, this normalization is especially natural from the viewpoint of the analytic continuation approach. In this normalization, the arithmeticity conjecture says that all $S^{(\mathrm{geom})}_{n>1}$ are expected to be periods. More specifically, it says that $S_n^{(\rho)} \in (2\pi i)^{n-1}\cdot\overline{\mathbb{Q}}$, suggesting that the n-loop perturbative invariants $S_n^{(\mathrm{geom})}$ are periods of (framed) mixed Tate motives $\mathbb{Q}(n-1)$. In this form, the arithmeticity of perturbative Chern-Simons invariants discussed here is very similar to the motivic interpretation of Feynman integrals in [100].

Finally, we note that, for some applications, it may be convenient to normalize the path integral (1.0.2) by dividing the right-hand side by $Z(\mathbf{S}^3;\hbar)$. (Since $\pi_1(\mathbf{S}^3)$ is trivial, we have

[1] *i.e.* on the branch containing the discrete faithful representation.

$Z(\mathbf{S}^3;\hbar) = Z^{(0)}(\mathbf{S^3};\hbar)$.) This normalization does not affect the arithmetic nature of the perturbative coefficients $S_n^{(\mathrm{geom})}$ because, for $M = \mathbf{S}^3$, all the $S_n^{(0)}$'s are rational numbers. Specifically,

$$Z(\mathbf{S}^3;\hbar) \;=\; \left(\frac{\hbar}{i\pi}\right)^{r/2} \left(\frac{\mathrm{Vol}\Lambda_{\mathrm{wt}}}{\mathrm{Vol}\Lambda_{\mathrm{rt}}}\right)^{1/2} \prod_{\alpha\in\Lambda_{\mathrm{rt}}^+} 2\sinh\left(\hbar(\alpha\cdot\varrho)\right), \tag{5.3.6}$$

where the product is over positive roots $\alpha \in \Lambda_{\mathrm{rt}}^+$, r is the rank of the gauge group, and ϱ is half the sum of the positive roots, familiar from the Weyl character formula. Therefore, in the above conjecture and in eq. (5.3.5) we can use the perturbative invariants of M with either normalization.

The arithmeticity conjecture discussed here is a part of a richer structure: the quantum $G_{\mathbb{C}}$ invariants are only the special case $x = 0$ of a collection of functions indexed by rational numbers x which each have asymptotic expansions in $\hbar$ satisfying the arithmeticity conjecture and which have a certain kind of modularity behavior under the action of $SL(2,\mathbb{Z})$ on $\mathbb{Q}$ [101]. A better understanding of this phenomenon and its interpretation is a subject of ongoing research.

5.4 Examples

In this section, we explicitly calculate the perturbative $SL(2,\mathbb{C})$ invariants $S_n^{(\mathrm{geom})}$ for the simplest hyperbolic knot complements in S^3, *i.e.* for $M = S^3\backslash K$. It was conjectured in [40] that such invariants can be extracted from the asymptotic expansion of knot invariants computed by Chern-Simons theory with compact gauge group $G = SU(2)$ in a double-scaling limit

$$k\to\infty\,, \qquad \hbar = \frac{i\pi}{N}\to 0\,, \qquad \frac{N}{k+2}\equiv 1\,. \tag{5.4.1}$$

Here, k is the (unnormalized) level of the $SU(2)$ theory, and N is the dimension of an $SU(2)$ representation associated to a Wilson loop in S^3 supported on the given knot K. (This will be explained in much greater detail in Sections 6.2 and 7.4.) The relevant $SU(2)$ knot invariant is

$$\mathcal{J}(K;N) = \frac{J_N\big(K;\,q\big)}{J_N\big(\mathrm{unknot};\,q\big)}\,, \qquad q = e^{2\hbar} = e^{\frac{2\pi i}{N}}\,, \tag{5.4.2}$$

where $J_N(K;q)$ is the "N-colored Jones polynomial" of K, normalized such that

$$J_N(\mathrm{unknot};q) = \frac{q^{N/2}-q^{-N/2}}{q^{1/2}-q^{-1/2}} \tag{5.4.3}$$

is the "quantum dimension" of the N-dimensional representation of $SU(2)$.

According to the Generalized Volume Conjecture [40], the invariant $\mathcal{J}(K;N)$ should have the asymptotics

$$\mathcal{J}(K;N) \;\sim\; \frac{Z^{(\mathrm{geom})}(M;\, i\pi/N)}{Z(\mathbf{S}^1 \times \mathbf{D}^2;\, i\pi/N)} \;\sim\; N^{3/2} \exp\left(\sum_{n=0}^{\infty} s_n \left(\frac{2\pi i}{N}\right)^{n-1}\right) \tag{5.4.4}$$

as $N \to \infty$, where

$$\begin{aligned} S_n^{(\mathrm{geom})} &= s_n \cdot 2^{n-1} \qquad (n \neq 1) \\ S_1^{(\mathrm{geom})} &= s_1 + \frac{1}{2}\log 2 \qquad (n = 1) \end{aligned} \tag{5.4.5}$$

are the perturbative $SL(2,\mathbb{C})$ invariants of $M = \mathbf{S}^3 \smallsetminus K$. (Here, we view the solid torus, $\mathbf{S}^1 \times \mathbf{D}^2$, as the complement of the unknot in the 3-sphere.) Specifically, one has

$$s_0 \;=\; i\,\big(\mathrm{Vol}(M) \,+\, i\,\mathrm{CS}(M)\big) \tag{5.4.6}$$

(Volume Conjecture) and s_1 is the Ray-Singer torsion of M twisted by a flat connection, *cf.* eq. (5.2.3). The Arithmeticity Conjecture of Section 5.3 predicts that

$$s_1 \;\in\; \mathbb{Q}\cdot\log\mathbb{K}\,, \qquad\qquad s_n \;\in\; \mathbb{K} \qquad (n \geq 2), \tag{5.4.7}$$

where $\mathbb{K}$ is the trace field of the knot. We will present numerical computations supporting this conjecture for the two simplest hyperbolic knots $\mathbf{4_1}$ and $\mathbf{5_2}$, following our work in [3].

The formulas for $\mathcal{J}(K;N)$ in both cases are known explicitly, see *e.g.* [102]. One has

$$\mathcal{J}(\mathbf{4_1};N) = \sum_{m=0}^{N-1} (q)_m (q^{-1})_m\,, \tag{5.4.8}$$

$$\mathcal{J}(\mathbf{5_2};N) = \sum_{m=0}^{N-1} \sum_{k=0}^{m} q^{-(m+1)k} (q)_m^2/(q^{-1})_k\,, \tag{5.4.9}$$

where $(q)_m = (1-q)\cdots(1-q^m)$ is the q-Pochhammer symbol as in Section 8.3. The first

few values of these invariants are

N	$\mathcal{J}(\mathbf{4_1};N)$	$\mathcal{J}(\mathbf{5_2};N)$
1	1	1
2	5	7
3	13	$18-5q$
4	27	$40-23q$
5	$44-4q^2-4q^3$	$46-55q-31q^2+q^3$
6	89	$120-187q$
7	$100-14q^2-25q^3-25q^4-14q^5$	$-154q-88q^2+47q^3+58q^4+77q^5$
8	$187-45q-45q^3$	$-84-407q-150q^2+96q^3$

Using formula (5.4.8) for N of the order of 5000 and the numerical interpolation method explained in [103] and [104], the values of s_n for $0 \le n \le 27$ were computed to very high precision, resulting in

$$s_0 = \frac{1}{2\pi^2 i}\, D\big(e^{\pi i/3}\big), \qquad s_1 = -\frac{1}{4}\log 3\,, \tag{5.4.10}$$

the first in accordance with the volume conjecture and the second in accordance with the first statement of (5.4.7), since $\mathbb{K} = \mathbb{Q}\big(\sqrt{-3}\big)$ in this case. Moreover the numbers

$$s'_n = s_n \cdot \big(6\sqrt{-3}\big)^{n-1} \qquad (n \ge 2) \tag{5.4.11}$$

are very close to rational numbers with relatively small and highly factored denominators:

n	2	3	4	5	6	7	8	9
s'_n	$\frac{11}{12}$	2	$\frac{1081}{90}$	98	$\frac{110011}{105}$	$\frac{207892}{15}$	$\frac{32729683}{150}$	$\frac{139418294}{35}$

n	10	...	27
s'_n	$\frac{860118209659}{10395}$	...	$\frac{2406050609802903695294787102911727632617819860985 52}{814172781296875}$

confirming the second prediction in (5.4.7). Here $D(z)$ is the Bloch-Wigner dilogarithm (8.1.3), *cf.* Section 8.1. (That s_n is a rational multiple of $(\sqrt{-3})^{n-1}$, and not merely an element of $\mathbb{Q}(\sqrt{-3})$ is a consequence of (5.4.4) and the fact that $\mathcal{J}(\mathbf{4_1};N)$ is real.)

Actually, in this case one can prove the correctness of the expansion rigorously: the two formulas in (5.4.10) were proved in [105] and the rationality of the numbers s'_n defined by (5.4.11) in [106, 107] and [108], and can therefore check that the numerically determined values are the true ones (see also [101] for a generalization of this analysis). In the case of $\mathbf{5_2}$, such an analysis has not been done, and the numerical interpolation method is therefore needed. If one tries to do this directly using eq. (5.4.9), the process is very time-consuming because, unlike the figure-8 case, there are now $\mathrm{O}(N^2)$ terms. To get around this difficulty, we use the formula

$$\sum_{k=0}^{m} \frac{q^{(m+1)k}}{(q)_k} = (q)_m \sum_{k=0}^{m} \frac{q^{k^2}}{(q)_k^2}\,, \tag{5.4.12}$$

which is proved by observing that both sides vanish for $m = -1$ and satisfy the recursion $t_m = (1-q^m)t_{m-1} + q^{m^2}/(q)_m$. This proof gives a way to successively compute each t_m in $\mathrm{O}(1)$ steps (compute $y = q^m$ as q times the previous y, $(q)_m$ as $1-y$ times its previous value, and then t_m by the recursion) and hence to compute the whole sum in (5.4.9) in only $\mathrm{O}(N)$ steps. The interpolation method can therefore be carried out to just as high precision as in the figure-eight ($\mathbf{4_1}$) case.

The results are as follows. The first coefficient is given to high precision by

$$s_0 = -\frac{3}{2\pi}\left(\mathrm{Li}_2(\alpha) + \frac{1}{2}\log(\alpha)\log(1-\alpha)\right) + \frac{\pi}{3}\,, \tag{5.4.13}$$

in accordance with the prediction (5.4.6), where $\alpha = 0.87743\cdots - 0.74486\ldots i$ is the root of

$$\alpha^3 - \alpha^2 + 1 = 0 \tag{5.4.14}$$

with negative imaginary part. The next four values are (again numerically to very high precision)

$$s_1 = \frac{1}{4}\log\frac{1+3\alpha}{23}\,, \qquad s_2 = \frac{198\alpha^2 + 1452\alpha - 1999}{24\cdot 23^2},$$
$$s_3 = \frac{465\alpha^2 - 465\alpha + 54}{2\cdot 23^3}\,, \qquad s_4 = \frac{-2103302\alpha^2 + 55115\alpha + 5481271}{240\cdot 23^5}\,,$$

in accordance with the arithmeticity conjecture since $\mathbb{K} = \mathbb{Q}(\alpha)$ in this case.

These coefficients are already quite complicated, and the next values even more so. We can simplify them by making the rescaling

$$s'_n = s_n\,\lambda^{n-1} \tag{5.4.15}$$

(*i.e.*, by expanding in powers of $2\pi i/\lambda N$ instead of $2\pi i/N$), where

$$\lambda = \alpha^5(3\alpha-2)^3 = \alpha^{-1}(\alpha^2-3)^3\,. \tag{5.4.16}$$

(This number is a generator of $\mathfrak{p}^3$, where $\mathfrak{p} = (3\alpha-2) = (\alpha^2-3)$ is the unique ramified prime ideal of $\mathbb{K}$, of norm 23.) We then find

$$\begin{aligned}
s'_2 &= -\tfrac{1}{24}\left(12\,\alpha^2 - 19\,\alpha + 86\right),\\
s'_3 &= -\tfrac{3}{2}\left(2\,\alpha^2 + 5\,\alpha - 4\right),\\
s'_4 &= \tfrac{1}{240}\left(494\,\alpha^2 + 12431\,\alpha + 1926\right),\\
s'_5 &= -\tfrac{1}{8}\left(577\,\alpha^2 - 842\,\alpha + 1497\right),\\
s'_6 &= \tfrac{1}{10080}\left(176530333\,\alpha^2 - 80229954\,\alpha - 18058879\right),\\
s'_7 &= -\tfrac{1}{240}\left(99281740\,\alpha^2 + 40494555\,\alpha + 63284429\right),\\
s'_8 &= -\tfrac{1}{403200}\left(3270153377244\,\alpha^2 - 4926985303821\,\alpha - 8792961648103\right),\\
s'_9 &= \tfrac{1}{13440}\left(9875382391800\,\alpha^2 - 939631794912\,\alpha - 7973863388897\right),\\
s'_{10} &= -\tfrac{1}{15966720}\left(188477928956464660\,\alpha^2 + 213430022592301436\,\alpha + 61086306651454303\right),\\
s'_{11} &= -\tfrac{1}{1209600}\left(517421716298434577\,\alpha^2 - 286061854126193276\,\alpha - 701171308042539352\right),
\end{aligned}$$

with much simpler coefficients than before, and with each denominator dividing $(n+2)!$. These highly nontrivial numbers give a strong experimental confirmation of the conjecture.

We observe that in both of the examples treated here the first statement of the conjecture (5.4.7) can be strengthened to

$$\exp(4s_1) \;\in\; \mathbb{K}\,. \tag{5.4.17}$$

It would be interesting to know if the same statement holds for all hyperbolic knot complements (or even all hyperbolic 3-manifolds). Another comment in this vein is that (5.4.6) also has an arithmetic content: one knows that the right-hand side of this equation is in the image under the extended regulator map of an element in the Bloch group (or, equivalently, the third algebraic K-group) of the number field $\mathbb{K}$.

Chapter 6

Geometric quantization

In Chapter 5, we introduced Chern-Simons perturbation theory and described the traditional approach to computing perturbative partition functions via Feynman diagrams. Now we want to consider another approach, based on the quantization of moduli space spaces of flat connections. Combined with the existence of a perturbative expansions (5.1.9), it will yield a powerful method for calculating perturbative invariants (Section 6.3). We will also find that quantization of Chern-Simons theory with complex gauge group $G_{\mathbb{C}}$ is closely related to quantization for compact group G, justifying a third approach to computing $G_{\mathbb{C}}$ invariants: "analytic continuation" (Section 6.2). Here, we mainly use analytic continuation to find the operators $\hat{A}_i$ that annihilate $G_{\mathbb{C}}$ partition functions, as explained in the introduction. In Chapter 9, we will revisit analytic continuation, employing it more directly to find classical integral expressions for partition functions.

Most of the results in this section follow [3]. We also include a short discussion of "brane quantization" for Chern-Simons theory with complex gauge group from [3], as it is closely related to geometric quantization.

6.1 Quantization of $\mathcal{M}_{\text{flat}}(G_{\mathbb{C}}, \Sigma)$

As a TQFT, Chern-Simons gauge theory (with any gauge group) associates a Hilbert space $\mathcal{H}_\Sigma$ to a closed Riemann surface Σ and a vector in $\mathcal{H}_\Sigma$ to every 3-manifold M with boundary Σ. We denote this vector as $|M\rangle \in \mathcal{H}_\Sigma$. If there are two such manifolds, M_+ and M_-, glued along a common boundary Σ (with matching orientation), then the quantum

invariant $Z(M)$ that Chern-Simons theory associates to the closed 3-manifold $M = M_+ \cup_\Sigma M_-$ is given by the inner product of two vectors $|M_+\rangle$ and $|M_-\rangle$ in $\mathcal{H}_\Sigma$

$$Z(M) \;=\; \langle M_+|M_-\rangle\,. \tag{6.1.1}$$

Therefore, in what follows, our goal will be to understand Chern-Simons gauge theory on manifolds with boundary, from which invariants of closed manifolds without boundary can be obtained via (6.1.1).

Since the Chern-Simons action (5.1.1) is first order in derivatives, the Hilbert space $\mathcal{H}_\Sigma$ is obtained by quantizing the classical phase space, which is the space of classical solutions on the 3-manifold $\mathbb{R}\times\Sigma$. Such classical solutions are given precisely by the flat connections on the Riemann surface Σ. Therefore, in a theory with complex gauge group $G_\mathbb{C}$, the classical phase space is the moduli space of flat $G_\mathbb{C}$ connections on Σ, modulo gauge equivalence,

$$\mathcal{M}_{\rm flat}(G_\mathbb{C},\Sigma) \;=\; {\rm Hom}(\pi_1(\Sigma),G_\mathbb{C})/{\rm conj.} \tag{6.1.2}$$

As a classical phase space, $\mathcal{M}_{\rm flat}(G_\mathbb{C},\Sigma)$ comes equipped with a symplectic structure ω, which can also be deduced from the classical Chern-Simons action (5.1.1). Since we are interested only in the "holomorphic" sector of the theory, we shall look only at the kinetic term for the field $\mathcal{A}$ (and not $\bar{\mathcal{A}}$); it leads to a holomorphic symplectic 2-form on $\mathcal{M}_{\rm flat}(G_\mathbb{C},\Sigma)$:

$$\omega \;=\; \frac{i}{4\hbar}\int_\Sigma {\rm Tr}\;\delta\mathcal{A}\wedge\delta\mathcal{A}\,. \tag{6.1.3}$$

We note that this symplectic structure does not depend on the complex structure of Σ, in accord with the topological nature of the theory. Then, in Chern-Simons theory with complex gauge group $G_\mathbb{C}$, the Hilbert space $\mathcal{H}_\Sigma$ is obtained by quantizing the moduli space of flat $G_\mathbb{C}$ connections on Σ with symplectic structure (6.1.3):

$$\text{quantization of } (\mathcal{M}_{\rm flat}(G_\mathbb{C},\Sigma),\omega) \quad\rightsquigarrow\quad \mathcal{H}_\Sigma\,. \tag{6.1.4}$$

Now, let us consider a closed 3-manifold M with boundary $\Sigma=\partial M$, and its associated state $|M\rangle\in\mathcal{H}_\Sigma$. In a (semi-)classical theory, quantum states correspond to Lagrangian submanifolds of the classical phase space. Recall that, by definition, a Lagrangian submanifold $\mathcal{L}$ is a middle-dimensional submanifold such that the restriction of ω to $\mathcal{L}$ vanishes,

$$\omega|_\mathcal{L} \;=\; 0\,. \tag{6.1.5}$$

For the problem at hand, the phase space is $\mathcal{M}_{\text{flat}}(G_{\mathbb{C}}, \Sigma)$ and the Lagrangian submanifold $\mathcal{L}$ associated to a 3-manifold M with boundary $\Sigma = \partial M$ consists of flat connections on Σ that can be extended to classical solutions on all of M [40]. Since the space of classical solutions on M is the moduli space of flat $G_{\mathbb{C}}$ connections on M,

$$\mathcal{M}_{\text{flat}}(G_{\mathbb{C}}, M) = \text{Hom}(\pi_1(M), G_{\mathbb{C}})/\text{conj.}\,, \tag{6.1.6}$$

it follows that

$$\mathcal{L} \;=\; \iota\big(\mathcal{M}_{\text{flat}}(G_{\mathbb{C}}, M)\big) \tag{6.1.7}$$

is the image of $\mathcal{M}_{\text{flat}}(G_{\mathbb{C}}, M)$ under the map

$$\iota : \mathcal{M}_{\text{flat}}(G_{\mathbb{C}}, M) \to \mathcal{M}_{\text{flat}}(G_{\mathbb{C}}, \Sigma) \tag{6.1.8}$$

induced by the natural inclusion $\pi_1(\Sigma) \to \pi_1(M)$. One can show that $\mathcal{L} \subset \mathcal{M}_{\text{flat}}(G_{\mathbb{C}}, \Sigma)$ is indeed Lagrangian with respect to the symplectic structure (6.1.3).

Much of what we described so far is very general and has an obvious analogue in Chern-Simons theory with arbitrary gauge group. However, quantization of Chern-Simons theory with complex gauge group has a number of good properties. In this case the classical phase space $\mathcal{M}_{\text{flat}}(G_{\mathbb{C}}, \Sigma)$ is an algebraic variety; it admits a complete hyper-Kähler metric [109], and the Lagrangian submanifold $\mathcal{L}$ is a holomorphic subvariety of $\mathcal{M}_{\text{flat}}(G_{\mathbb{C}}, \Sigma)$. The hyper-Kähler structure on $\mathcal{M}_{\text{flat}}(G_{\mathbb{C}}, \Sigma)$ can be obtained by interpreting it as the moduli space $\mathcal{M}_H(G, \Sigma)$ of solutions to Hitchin's equations on Σ. Note that this requires a choice of complex structure on Σ, whereas $\mathcal{M}_{\text{flat}}(G_{\mathbb{C}}, \Sigma) \cong \mathcal{M}_H(G, \Sigma)$ as a complex symplectic manifold does not. Existence of a hyper-Kähler structure on $\mathcal{M}_{\text{flat}}(G_{\mathbb{C}}, \Sigma)$ considerably simplifies the quantization problem in any of the existing frameworks, such as geometric quantization [45], deformation quantization [46, 47], or "brane quantization" [48].

The hyper-Kähler moduli space $\mathcal{M}_H(G, \Sigma)$ has three complex structures that we denote as I, J, and $K = IJ$, and three corresponding Kähler forms, ω_I, ω_J, and ω_K (*cf.* [110]). In the complex structure usually denoted by J, $\mathcal{M}_H(G, \Sigma)$ can be identified with $\mathcal{M}_{\text{flat}}(G_{\mathbb{C}}, \Sigma)$ as a complex symplectic manifold with the holomorphic symplectic form (6.1.3),

$$\omega \;=\; \frac{1}{\hbar}(\omega_K + i\omega_I)\,. \tag{6.1.9}$$

Moreover, in this complex structure, $\mathcal{L}$ is an algebraic subvariety of $\mathcal{M}_{\text{flat}}(G_{\mathbb{C}}, \Sigma)$. To be more precise, it is a (finite) union of algebraic subvarieties, each of which is defined by

polynomial equations $A_i = 0$. In the quantum theory, these equations are replaced by corresponding operators $\widehat{A}_i$ acting on $\mathcal{H}_\Sigma$ that annihilate the state $|M\rangle$.

Now, let us consider in more detail the simple but important case when Σ is of genus 1, that is $\Sigma = T^2$. In this case, $\pi_1(\Sigma) \cong \mathbb{Z} \times \mathbb{Z}$ is abelian, and

$$\mathcal{M}_{\rm flat}(G_{\mathbb{C}}, T^2) \;=\; (\mathbb{T}_{\mathbb{C}} \times \mathbb{T}_{\mathbb{C}})/\mathcal{W}\,, \tag{6.1.10}$$

where $\mathbb{T}_{\mathbb{C}}$ is the maximal torus of $G_{\mathbb{C}}$ and $\mathcal{W}$ is the Weyl group. We parametrize each copy of $\mathbb{T}_{\mathbb{C}}$ by complex variables $l = (l_1, \ldots, l_r)$ and $m = (m_1, \ldots, m_r)$, respectively. Here, r is the rank of the gauge group $G_{\mathbb{C}}$. The values of l and m are eigenvalues of the holonomies of the flat $G_{\mathbb{C}}$ connection over the two basic 1-cycles of $\Sigma = T^2$. They are defined up to Weyl transformations, which act diagonally on $\mathbb{T}_{\mathbb{C}} \times \mathbb{T}_{\mathbb{C}}$.

The moduli space of flat $G_{\mathbb{C}}$ connections on a 3-manifold M with a single toral boundary, $\partial M = T^2$, defines a complex Lagrangian submanifold

$$\mathcal{L} \subset (\mathbb{T}_{\mathbb{C}} \times \mathbb{T}_{\mathbb{C}})/\mathcal{W}\,. \tag{6.1.11}$$

(More precisely, this Lagrangian submanifold comprises the top-dimensional (stable) components of the moduli space of flat $G_{\mathbb{C}}$ connections on Σ.) In particular, a generic irreducible component of $\mathcal{L}$ is defined by r polynomial equations

$$A_i(l, m) \;=\; 0\,, \qquad i = 1, \ldots, r\,, \tag{6.1.12}$$

which must be invariant under the action of the Weyl group $\mathcal{W}$ (which simultaneously acts on the eigenvalues $l_1, \ldots, l_r$ and $m_1, \ldots, m_r$).

In the quantum theory, the equations (6.1.12) are replaced by the operator equations,

$$\widehat{A}_i(\hat{l}, \hat{m})\; Z(M) \;=\; 0\,, \qquad i = 1, \ldots, r\,. \tag{6.1.13}$$

For $\Sigma = T^2$ the complex symplectic structure (6.1.3) takes a very simple form

$$\omega \;=\; \frac{i}{\hbar} \sum_{i=1}^{r} du_i \wedge dv_i\,, \tag{6.1.14}$$

where we introduce new variables u and v (defined modulo elements of the cocharacter lattice $\Lambda_{\rm cochar} \;=\; {\rm Hom}(U(1), \mathbb{T})$), such that $l = -e^v$ and $m = e^u$. In the quantum theory, u and v are replaced by operators $\hat{u}$ and $\hat{v}$ that obey the canonical commutation relations

$$[\hat{u}_i, \hat{v}_j] \;=\; -\hbar\, \delta_{ij}\,. \tag{6.1.15}$$

As one usually does in quantum mechanics, we can introduce a complete set of states $|u\rangle$ on which $\hat{u}$ acts by multiplication, $\hat{u}_i|u\rangle = u_i|u\rangle$. Similarly, we let $|v\rangle$ be a complete basis, such that $\hat{v}_i|v\rangle = v_i|v\rangle$. Then, we can define the wave function associated to a 3-manifold M either in the u-space or v-space representation, respectively, as $\langle u|M\rangle$ or $\langle v|M\rangle$. We will mostly work with the former and let $Z(M;u) := \langle u|M\rangle$.

We note that a generic value of u does not uniquely specify a flat $G_{\mathbb{C}}$ connection on M or, equivalently, a unique point on the representation variety (6.1.7). Indeed, for a generic value of u, equations (6.1.12) may have several solutions that we label by a discrete parameter α. Therefore, in the u-space representation, flat $G_{\mathbb{C}}$ connections on M (previously labeled by the homomorphism $\rho \in \mathcal{L}$) are now labeled by a set of continuous parameters $u = (u_1, \ldots, u_r)$ and a discrete parameter α:

$$\rho \quad \longleftrightarrow \quad (u, \alpha)\,. \tag{6.1.16}$$

The perturbative $G_{\mathbb{C}}$ invariant $Z^{(\rho)}(M;\hbar)$ can then be written in this notation as $Z^{(\alpha)}(M;\hbar,u) = \langle u, \alpha|M\rangle$. Similarly, the coefficients $S_n^{(\rho)}$ in the $\hbar$-expansion can be written as $S_n^{(\alpha)}(u)$.

To summarize, in the approach based on quantization of $\mathcal{M}_{\rm flat}(G_{\mathbb{C}}, \Sigma)$ the calculation of $Z^{(\rho)}(M;\hbar)$ reduces to two main steps: *i*) the construction of quantum operators $\widehat{A}_i(\hat{l}, \hat{m})$, and *ii*) the solution of Schrödinger-like equations (6.1.13). Below we explain how to implement each of these steps.

6.2 Analytic continuation and the Volume Conjecture

For a generic 3-manifold M with boundary $\Sigma = T^2$, constructing the quantum operators $\widehat{A}_i(\hat{l}, \hat{m})$ may be a difficult task. However, when M is the complement of a knot K in the 3-sphere,

$$M = \mathbf{S}^3 \setminus K\,, \tag{6.2.1}$$

there is a simple way to find the $\widehat{A}_i$'s. Indeed, as anticipated in the introduction, these operators also annihilate the polynomial knot invariants $P_{G,R}(K;q)$, which are defined in terms of Chern-Simons theory with compact gauge group G,

$$\widehat{A}_i(\hat{l}, \hat{m})\; P_{G,R}(K;q) = 0\,. \tag{6.2.2}$$

The operator $\hat{l}_i$ acts on the set of polynomial invariants $\{P_{G,R}(K;q)\}$ by shifting the highest weight $\lambda = (\lambda_1, \ldots, \lambda_r)$ of the representation R by the i-th basis elements of the weight lattice $\Lambda_{\rm wt}$, while the operator $\hat{m}_j$ acts simply as multiplication by $q^{\lambda_j/2}$. Let us briefly explain how this comes about.

In general, the moduli space $\mathcal{M}_{\rm flat}(G_{\mathbb{C}}, \Sigma)$ is a complexification of $\mathcal{M}_{\rm flat}(G, \Sigma)$. The latter is the classical phase space in Chern-Simons theory with compact gauge group G and can be obtained from $\mathcal{M}_{\rm flat}(G_{\mathbb{C}}, \Sigma)$ by requiring all the holonomies to be "real," *i.e.* in G. Similarly, restricting to real holonomies in the definition of $\mathcal{L}$ produces a Lagrangian submanifold in $\mathcal{M}_{\rm flat}(G, \Sigma)$ that corresponds to a quantum state $|M\rangle$ in Chern-Simons theory with compact gauge group G. In the present example of knot complements, restricting to such "real" holonomies means replacing $\mathbb{T}_{\mathbb{C}}$ by $\mathbb{T}$ in (6.1.10) and taking purely imaginary values of u_i and v_i in equations (6.1.12). Apart from this, the quantization problem is essentially the same for gauge groups G and $G_{\mathbb{C}}$. In particular, the symplectic structure (6.1.14) has the same form (with imaginary u_i and v_i in the theory with gauge group G) and the quantum operators $\widehat{A}_i(\hat{l}, \hat{m})$ annihilate both $P_{G,R}(K;q)$ and $Z^{(\alpha)}(M;\hbar,u)$ computed, respectively, by Chern-Simons theories with gauge groups G and $G_{\mathbb{C}}$.

In order to understand the precise relation between the parameters in these theories, let us consider a Wilson loop operator, $W_R(K)$, supported on $K \subset \mathbf{S}^3$ in Chern-Simons theory with compact gauge group G. It is labeled by a representation $R = R_\lambda$ of the gauge group G, which we assume to be an irreducible representation with highest weight $\lambda \in \mathfrak{t}^\vee$. The path integral in Chern-Simons theory on $\mathbf{S}^3$ with a Wilson loop operator $W_R(K)$ computes the polynomial knot invariant $P_{G,R}(K;q)$, with $q = e^{2\hbar}$. Using (6.1.1), we can represent this path integral as $\langle R|M\rangle$, where $|R\rangle$ is the result of the path integral on a solid torus containing a Wilson loop $W_R(K)$, and $|M\rangle$ is the path integral on its complement, M.

In the semi-classical limit, the state $|R\rangle$ corresponds to a Lagrangian submanifold of $\mathcal{M}_{\rm flat}(G, T^2) = (\mathbb{T}\times\mathbb{T})/\mathcal{W}$ defined by the fixed value of the holonomy $m = e^u$ on a small loop around the knot. The relation between $m = e^u$, which is an element of the maximal torus $\mathbb{T}$ of G, and the representation R_λ is given by the invariant quadratic form $-\mathrm{Tr}$ (restricted to $\mathfrak{t}$). Specifically,

$$m \;=\; \exp \hbar(\lambda^* + \rho^*) \in \mathbb{T}\,, \tag{6.2.3}$$

where λ^* is the unique element of $\mathfrak{t}$ such that $\lambda^*(x) = -\mathrm{Tr}\,\lambda x$ for all $x \in \mathfrak{t}$, and ρ^* is the

analogous dual of the Weyl vector (half the sum of positive weights of G). For example, for the N-colored Jones polynomial, corresponding to the N-dimensional representation of $SU(2)$, (6.2.3) looks like $m = \exp \hbar N$. In "analytic continuation," we analytically continue this relation to $m \in \mathbb{T}_{\mathbb{C}}$. A perturbative partition function arises as

$$\hbar \to 0\,, \qquad \lambda^* \to \infty \qquad \text{for } \; u = \hbar(\lambda^* + \rho^*) \text{ fixed}\,. \tag{6.2.4}$$

A more detailed explanation of the limit (6.2.3), will appear in Chapter 7, where we discuss Wilson loops for complex as well as compact groups.

For a given value of $m = e^u$, equations (6.1.12) have a finite set of solutions l_α, labeled by α. Only for one particular value of α is the perturbative $G_{\mathbb{C}}$ invariant $Z^{(\alpha)}(M;\hbar,u)$ related to the asymptotic behavior of $P_{G,R}(K;q)$. This is the value of α which maximizes $\mathrm{Re}\big(S_0^{(\alpha)}(M;u)\big)$. For this α, we have:

$$\frac{Z^{(\alpha)}(M;\hbar,u)}{Z(\mathbf{S}^3;\hbar)} \;=\; \text{asymptotic expansion of } P_{G,R}(K;q)\,. \tag{6.2.5}$$

For hyperbolic knots and u sufficiently close to 0, this "maximal" value of α is always $\alpha = \mathrm{geom}$.

It should nevertheless be noted that the analytic continuation described here is not as "analytic" as it sounds. In particular, the limit (6.2.4) is very subtle and requires much care. As explained in [40], in taking this limit it is important that values of $q = e^{2\hbar}$ avoid roots of unity. If one takes the limit with $\hbar^{-1} \in \frac{1}{i\pi}\mathbb{Z}$, which corresponds to the allowed values of the coupling constant in Chern-Simons theory with compact gauge group G, then one can never see the exponential asymptotics (5.1.9) with $\mathrm{Im}(S_0^{(\rho)}) > 0$. The exponential growth characteristic to Chern-Simons theory with complex gauge group emerges only in the limit with $\hbar = u/(\lambda^* + \rho^*)$ and u generic.[1]

6.3 Hierarchy of differential equations

The system of Schrödinger-like equations (6.1.13) determines the perturbative $G_{\mathbb{C}}$ invariant $Z^{(\alpha)}(M;\hbar,u)$ up to multiplication by an overall function of $\hbar$, which can be fixed by suitable boundary conditions.

[1]The subtle behavior of the compact Chern-Simons partition function as the level $k = i\pi/\hbar$ and the representation λ^* are continued away from integers has recently been analyzed carefully in [41]. In particular, the transition from polynomial to exponential growth is explained there.

In order to see in detail how the perturbative coefficients $S_n^{(\alpha)}(u)$ may be calculated and to avoid cluttering, let us assume that the rank $r = 1$. (A generalization to arbitrary values of r is straightforward.) In this case, $A(l, m)$ is the so-called A-polynomial of M, originally introduced in [111], and the system (6.1.13) consists of a single equation

$$\widehat{A}(\hat{l}, \hat{m})\, Z^{(\alpha)}(M; \hbar, u) \;=\; 0\,. \tag{6.3.1}$$

In the u-space representation the operator $\hat{m} = \exp(\hat{u})$ acts on functions of u simply via multiplication by e^u, whereas $\hat{l} = \exp(\hat{v} + i\pi) = \exp(\hbar\, \frac{d}{du})$ acts as a "shift operator":

$$\hat{m} f(u) \;=\; e^u f(u)\,, \qquad \hat{l} f(u) \;=\; f(u + \hbar)\,. \tag{6.3.2}$$

In particular, the operators $\hat{l}$ and $\hat{m}$ obey the relation

$$\hat{l}\hat{m} \;=\; q^{\frac{1}{2}} \hat{m}\hat{l}\,, \tag{6.3.3}$$

which follows directly from the commutation relation (6.1.15) for $\hat{u}$ and $\hat{v}$, with

$$q \;=\; e^{2\hbar}\,. \tag{6.3.4}$$

We would like to recast eq. (6.3.1) as an infinite hierarchy of differential equations that can be solved recursively for the perturbative coefficients $S_n^{(\alpha)}(u)$. Just like its classical limit $A(l, m)$, the operator $\widehat{A}(\hat{l}, \hat{m})$ is a polynomial in $\hat{l}$. Therefore, pushing all operators $\hat{l}$ to the right, we can write it as

$$\widehat{A}(\hat{l}, \hat{m}) \;=\; \sum_{j=0}^{d} a_j(\hat{m}, \hbar)\, \hat{l}^j \tag{6.3.5}$$

for some functions $a_j(m, \hbar)$ and some integer d. Using (6.3.2), we can write eq. (6.3.1) as

$$\sum_{j=0}^{d} a_j(m, \hbar) Z^{(\alpha)}(M; \hbar, u + j\hbar) \;=\; 0\,. \tag{6.3.6}$$

Then, substituting the general form (5.1.9) of $Z^{(\alpha)}(M; \hbar, u)$, we obtain the equation

$$\sum_{j=0}^{d} a_j(m, \hbar) \exp\left[\frac{1}{\hbar} S_0^{(\alpha)}(u + j\hbar) - \frac{1}{2}\delta^{(\alpha)} \log\hbar + \sum_{n=0}^{\infty} \hbar^n S_{n+1}^{(\alpha)}(u + j\hbar)\right] \;=\; 0\,. \tag{6.3.7}$$

Since $\delta^{(\alpha)}$ is independent of u, we can just factor out the $-\frac{1}{2}\delta^{(\alpha)} \log\hbar$ term and remove it from the exponent. Now we expand everything in $\hbar$. Let

$$a_j(m, \hbar) \;=\; \sum_{p=0}^{\infty} a_{j,p}(m) \hbar^p \tag{6.3.8}$$

and

$$\sum_{n=-1}^{\infty} \hbar^n S_{n+1}(u+j\hbar) \;=\; \sum_{r=-1}^{\infty}\sum_{m=-1}^{r} \frac{j^{r-m}}{(r-m)!}\hbar^r S_{m+1}^{(r-m)}(u)\,, \tag{6.3.9}$$

suppressing the index α to simplify notation. We can substitute (6.3.8) and (6.3.9) into (6.3.7) and divide the entire expression by $\exp(\sum_n \hbar^n S_{n+1}(u))$. The hierarchy of equations then follows by expanding the exponential in the resulting expression as a series in $\hbar$ and requiring that the coefficient of every term in this series vanishes (see also [112]). The first four equations are shown in Table 6.1.

$$\sum_{j=0}^{d} e^{jS_0'} a_{j,0} = 0$$

$$\sum_{j=0}^{d} e^{jS_0'}\left(a_{j,1} + a_{j,0}\big(\frac{1}{2}j^2 S_0'' + jS_1'\big)\right) = 0$$

$$\sum_{j=0}^{d} e^{jS_0'}\left(a_{j,2} + a_{j,1}\big(\frac{1}{2}j^2 S_0'' + jS_1'\big) + a_{j,0}\left(\frac{1}{2}\big(\frac{1}{2}j^2 S_0'' + jS_1'\big)^2 + \frac{j^3}{6}S_0''' + \frac{j^2}{2}S_1'' + jS_2'\right)\right) = 0$$

$$\begin{aligned}\sum_{j=0}^{d} e^{jS_0'}\Bigg(&a_{j,3} + a_{j,2}\big(\frac{1}{2}j^2 S_0'' + jS_1'\big) + a_{j,1}\left(\frac{1}{2}\big(\frac{1}{2}j^2 S_0'' + jS_1'\big)^2 + \frac{j^3}{6}S_0''' + \frac{j^2}{2}S_1'' + jS_2'\right)\\ &+ a_{j,0}\Bigg(\frac{1}{6}\big(\frac{1}{2}j^2 S_0'' + jS_1'\big)^3 + \big(\frac{1}{2}j^2 S_0'' + jS_1'\big)\big(\frac{j^3}{6}S_0''' + \frac{j^2}{2}S_1'' + jS_2'\big)\\ &+ \frac{j^4}{24}S_0^{(4)} + \frac{j^3}{6}S_1''' + \frac{j^2}{2}S_2'' + jS_3'\Bigg)\Bigg) = 0\end{aligned}$$

$\ldots$

Table 6.1: Hierarchy of differential equations derived from $\widehat{A}(\hat{l},\hat{m})\; Z^{(\alpha)}(M;\hbar,u) = 0$.

The equations in Table 6.1 can be solved recursively for the $S_n(u)$'s, since each S_n first appears in the $(n+1)^{\text{st}}$ equation, differentiated only once. Indeed, after S_0 is obtained, the remaining equations feature the $S_{n\geq 1}$ linearly the first time they occur, and so determine these coefficients uniquely up to an additive constant of integration.

The first equation, however, is somewhat special. Since $a_{j,0}(m)$ is precisely the coefficient of l^j in the classical A-polynomial $A(l,m)$, we can rewrite this equation as

$$A(e^{S_0'(u)}, e^u) = 0\,. \tag{6.3.10}$$

This is exactly the classical constraint $A(e^{v+i\pi}, e^u) = 0$ that defines the complex Lagrangian submanifold $\mathcal{L}$, with $S_0'(u) = v + i\pi$. Therefore, we can integrate along a branch ($l_\alpha =$

$e^{v_\alpha+i\pi}, m = e^u$) of $\mathcal{L}$ to get the value of the classical Chern-Simons action (5.2.1) [40]

$$S_0^{(\alpha)}(u) = \text{const} + \int^u \theta|_{\mathcal{L}}\,, \tag{6.3.11}$$

where $\theta|_{\mathcal{L}}$ denotes a restriction to $\mathcal{L}$ of the Liouville 1-form on $\mathcal{M}_{\rm flat}(G_{\mathbb{C}}, \Sigma)$,

$$\theta = v du + i\pi du\,. \tag{6.3.12}$$

The expression (6.3.11) is precisely the semi-classical approximation to the wave function $Z^{(\alpha)}(M;\hbar,u)$ supported on the Lagrangian submanifold $\mathcal{L}$, obtained in the WKB quantization of the classical phase space $\mathcal{M}_{\rm flat}(G_{\mathbb{C}}, \Sigma)$. By definition, the Liouville form θ (associated with a symplectic structure ω) obeys $d\theta = i\hbar\omega$, and it is easy to check that this is indeed the case for the forms ω and θ on $\mathcal{M}_{\rm flat}(G_{\mathbb{C}}, \Sigma)$ given by eqs. (6.1.14) and (6.3.12), respectively.

The semi-classical expression (6.3.11) gives the value of the classical Chern-Simons functional (5.1.1) evaluated on a flat gauge connection $\mathcal{A}^{(\rho)}$, labeled by a homomorphism ρ. As we explained in (6.1.16), the dependence on ρ is encoded in the dependence on a continuous holonomy parameter u, as well as a discrete parameter α that labels different solutions $v_\alpha(u)$ to $A(e^{v+i\pi}, e^u) = 0$, at a fixed value of u. In other words, α labels different branches of the Riemann surface $A(l,m) = 0$, regarded as a cover of the complex plane $\mathbb{C}$ parametrized by $m = e^u$,

$$A(l_\alpha, m) = 0\,. \tag{6.3.13}$$

Since $A(l,m)$ is a polynomial in both l and m, the set of values of α is finite (in fact, its cardinality is equal to the degree of $A(l,m)$ in l). Note, however, that for a given choice of α there are infinitely many ways to lift a solution $l_\alpha(u)$ to $v_\alpha(u)$; namely, one can add to $v_\alpha(u)$ any integer multiple of $2\pi i$. This ambiguity implies that the integral (6.3.11) is defined only up to integer multiples of $2\pi i u$,

$$S_0^{(\alpha)}(u) - \text{const} = \int^u \log l_\alpha(u')\, du' = \int^u v_\alpha(u')\, du' \;+\; i\pi u \qquad (\text{mod } 2\pi i u)\,. \tag{6.3.14}$$

In practice, this ambiguity can always be fixed by imposing suitable boundary conditions on $S_0^{(\alpha)}(u)$, and it never affects the higher-order terms $S_n^{(\alpha)}(u)$. Therefore, since our main goal is to solve the *quantum* theory (to all orders in perturbation theory) we shall not worry about this ambiguity in the classical term. As we illustrate later (see Section 6.6), it will always be easy to fix this ambiguity in concrete examples.

Before we proceed, let us remark that if M is a hyperbolic 3-manifold with a single torus boundary $\Sigma = \partial M$ and $\mathcal{A}^{(\rm geom)}$ is the "geometric" flat $SL(2,\mathbb{C})$ connection associated with

a hyperbolic metric on M (not necessarily geodesically complete), then the integral (6.3.14) is essentially the complexified volume function, $i(\mathrm{Vol}(M;u) + i\mathrm{CS}(M;u))$, which combines the (real) hyperbolic volume and Chern-Simons invariants[2] of M. Specifically, the relation is [40, 114]:

$$S_0^{(\mathrm{geom})}(u) = \frac{i}{2}\Big[\mathrm{Vol}(M;u) + i\mathrm{CS}(M;u)\Big] + v_{\mathrm{geom}}(u)\,\mathrm{Re}(u) + i\pi u\,, \tag{6.3.15}$$

modulo the integration constant and multiples of $2\pi i u$.

6.4 Classical and quantum symmetries

A vast supply of 3-manifolds with a single toral boundary can be obtained by considering knot complements as in (6.2.1); our main examples throughout this thesis are of this type. As discussed above, the Lagrangian subvariety $\mathcal{L} \in \mathcal{M}_{\mathrm{flat}}(G_{\mathbb{C}}, \Sigma)$ for any knot complement M is defined by polynomial equations (6.1.12). Such an $\mathcal{L}$ contains multiple branches, indexed by α, corresponding to the different solutions to $\{A_i(l,m) = 0\}$ for fixed m. In this section, we describe relationships among these branches and the corresponding perturbative invariants $Z^{(\alpha)}(M;\hbar,u)$ by using the symmetries of Chern-Simons theory with complex gauge group $G_{\mathbb{C}}$.

Before we begin, it is useful to summarize what we already know about the branches of $\mathcal{L}$. As mentioned in the previous discussion, there always exists a geometric branch — or in the case of rank $r > 1$ several geometric branches — when M is a hyperbolic knot complement. Like the geometric branch, most other branches of $\mathcal{L}$ correspond to genuinely nonabelian representations $\rho : \pi_1(\Sigma) \to G_{\mathbb{C}}$. However, for any knot complement M there also exists an "abelian" component of $\mathcal{L}$, described by the equations

$$l_1 = \ldots = l_r = 1\,. \tag{6.4.1}$$

Indeed, since $H_1(M)$ is the abelianization of $\pi_1(M)$, the representation variety (6.1.6) always

[2]Here u describes the cusp of a hyperbolic metric on M. For example, imaginary u parametrizes a conical singularity. See, *e.g.* [113, 114, 115] and our discussion in Section 8.1 for more detailed descriptions of $\mathrm{Vol}(M;u)$ and $\mathrm{CS}(M;u)$. In part of the literature (*e.g.* in [114]), the parameters (u,v) are related to those used here by $2u_{\mathrm{here}} = u_{\mathrm{there}}$ and $2(v_{\mathrm{here}} + i\pi) = v_{\mathrm{there}}$. We include a shift of $i\pi$ in our definition of v so that the complete hyperbolic structure arises at $(u,v) = (0,0)$.

has a component corresponding to abelian representations that factor through $H_1(M) \cong \mathbb{Z}$,

$$\pi_1(M) \to H_1(M) \to G_{\mathbb{C}}\,. \tag{6.4.2}$$

The corresponding flat connection, $\mathcal{A}^{(\mathrm{abel})}$, is characterized by the trivial holonomy around a 1-cycle of $\Sigma = T^2$ which is trivial in homology $H_1(M)$; choosing it to be the 1-cycle whose holonomy was denoted by $l = (l_1, \ldots, l_r)$ we obtain (6.4.1). Note that, under projection to the u-space, the abelian component of $\mathcal{L}$ corresponds to a single branch that we denote by $\alpha = \mathrm{abel}$.

The first relevant symmetry of Chern-Simons theory with complex gauge group $G_{\mathbb{C}}$ is conjugation. We observe that for every flat connection $\mathcal{A}^{(\rho)}$ on M, with $\rho = (u, \alpha)$, there is a conjugate flat connection $\mathcal{A}^{(\bar\rho)} := \overline{\mathcal{A}^{(\rho)}}$ corresponding to a homomorphism $\bar\rho = (\bar u, \bar\alpha)$. We use $\bar\alpha$ to denote the branch of $\mathcal{L}$ "conjugate" to branch α; the fact that branches of $\mathcal{L}$ come in conjugate pairs is reflected in the fact that eqs. (6.1.12) have real (in fact, integer) coefficients. The perturbative expansions around $\mathcal{A}^{\rho}$ and $\mathcal{A}^{\bar\rho}$ are very simply related. Namely, by directly conjugating the perturbative path integral and noting that the Chern-Simons action has real coefficients, we find[3] $\overline{Z^{\alpha}(M;\hbar,u)} = Z^{(\bar\alpha)}(M;\bar\hbar,\bar u)$. The latter partition function is actually in the antiholomorphic sector of the Chern-Simons theory, but we can just rename $(\bar\hbar,\bar u) \mapsto (\hbar, u)$ (and use analyticity) to obtain a perturbative partition function for the conjugate branch in the holomorphic sector,

$$Z^{(\bar\alpha)}(M;\hbar,u) = \overline{Z^{(\alpha)}}(M;\hbar,u)\,. \tag{6.4.3}$$

Here, for any function $f(z)$ we define $\bar f(z) := \overline{f(\bar z)}$. In particular, if f is analytic, $f(z) = \sum f_n z^n$, then $\bar f$ denotes a similar function with conjugate coefficients, $\bar f(z) = \sum \bar f_n z^n$.

In the case $r = 1$, the symmetry (6.4.3) implies that branches of the classical $SL(2,\mathbb{C})$ A-polynomial come in conjugate pairs v_α and $v_{\bar\alpha}(u) = \overline{v_\alpha}(u)$. Again, these pairs arise algebraically because the A-polynomial has integer coefficients. (See *e.g.* [111, 116] for a detailed discussion of properties of $A(l,m)$.) Some branches, like the abelian branch, may be self-conjugate. For the abelian branch, this is consistent with $S_0^{(abel)} = 0$. The geometric

[3] More explicitly, letting $I_{CS}(\hbar,\mathcal{A}) = -\frac{1}{4\hbar}\int_M \mathrm{Tr}\big(\mathcal{A}\wedge\mathcal{A} + \frac{2}{3}\mathcal{A}\wedge\mathcal{A}\wedge\mathcal{A}\big)$, we have

$$\overline{Z^{\alpha}(M;\hbar,u)} = \left(\int_{(u,\alpha)} \mathcal{D}\mathcal{A}\, e^{I_{CS}(\hbar,\mathcal{A})}\right)^{*} = \int_{(\bar u,\bar\alpha)} \mathcal{D}\bar{\mathcal{A}}\, e^{I_{CS}(\bar\hbar,\bar{\mathcal{A}})} = Z^{(\bar\alpha)}(M;\bar\hbar,\bar u)\,.$$

branch, on the other hand, has a distinct conjugate because $\mathrm{Vol}(M;0) > 0$; from (6.3.15) we see that its leading perturbative coefficient obeys

$$S_0^{(\mathrm{conj})}(u) = \frac{i}{2}\Big[- \mathrm{Vol}(M;\bar{u}) + i\mathrm{CS}(M;\bar{u})\Big] + \overline{v_{\mathrm{geom}}}(u)\mathrm{Re}(u) - i\pi u\,. \tag{6.4.4}$$

In general, we have

$$S_0^{(\bar{\alpha})}(u) = \overline{S_0^{(\alpha)}}(u) \qquad (\mathrm{mod}\ 2\pi u)\,. \tag{6.4.5}$$

Now, let us consider symmetries that originate from geometry, *i.e.* symmetries that involve involutions of M,

$$\tau : \quad M \to M\,. \tag{6.4.6}$$

Every such involution restricts to a self-map of $\Sigma = \partial M$,

$$\tau|_\Sigma : \quad \Sigma \to \Sigma\,, \tag{6.4.7}$$

which, in turn, induces an endomorphism on homology, $H_i(\Sigma)$. Specifically, let us consider an orientation-preserving involution τ which induces an endomorphism $(-1,-1)$ on $H_1(\Sigma) \cong \mathbb{Z}\times\mathbb{Z}$. This involution is a homeomorphism of M; it changes our definition of the holonomies,

$$m_i \to \frac{1}{m_i} \qquad \text{and} \qquad l_i \to \frac{1}{l_i}\,, \tag{6.4.8}$$

leaving the symplectic form (6.1.14) invariant. Therefore, it preserves both the symplectic phase space $\mathcal{M}_{\mathrm{flat}}(G_{\mathbb{C}},\Sigma)$ and the Lagrangian submanifold $\mathcal{L}$ (possibly permuting some of its branches).

In the basic case of rank $r = 1$, the symmetry (6.4.8) corresponds to the simple, well-known relation $A(l^{-1},m^{-1}) = A(l,m)$, up to overall powers of l and m. Similarly, at the quantum level, $\widehat{A}(\hat{l}^{-1},\hat{m}^{-1}) = \widehat{A}(\hat{l},\hat{m})$ when $\widehat{A}(\hat{l},\hat{m})$ is properly normalized. Branches of the A-polynomial are individually preserved, implying that the perturbative partition functions (and the coefficients $S_n^{(\alpha)}$) are all *even*:

$$Z^{(\alpha)}(M;\hbar,-u) = Z^{(\alpha)}(M;\hbar,u)\,, \tag{6.4.9}$$

modulo factors of $e^{2\pi u/\hbar}$ that are related to the ambiguity in $S_0^{(\alpha)}(u)$. Note that in the $r = 1$ case one can also think of the symmetry (6.4.8) as the Weyl reflection. Since, by definition, holonomies that differ by an element of the Weyl group define the same point in the moduli space (6.1.10), it is clear that both $\mathcal{M}_{\mathrm{flat}}(G_{\mathbb{C}},\Sigma)$ and $\mathcal{L}$ are manifestly invariant

under this symmetry. (For $r > 1$, Weyl transformations on the variables l and m lead to new, independent relations among the branches of $\mathcal{L}$.)

Finally, let us consider a more interesting "parity" symmetry, an orientation-reversing involution

$$P: \quad M \to \overline{M} \tag{6.4.10}$$

$$P|_\Sigma: \quad \Sigma \to \overline{\Sigma} \tag{6.4.11}$$

that induces a map $(1,-1)$ on $H_1(\Sigma) \cong \mathbb{Z}\times\mathbb{Z}$. This operation by itself cannot be a symmetry of the theory because it does not preserve the symplectic form (6.1.14). We can try, however, to combine it with the transformation $\hbar \to -\hbar$ to get a symmetry of the symplectic phase space $(\mathcal{M}_{\rm flat}(G_{\mathbb{C}}, \Sigma), \omega)$. We are still not done because this combined operation changes the orientation of both Σ and M, and unless $\overline{M} \cong M$ the state $|M\rangle$ assigned to M will be mapped to a different state $|\overline{M}\rangle$. But if M is an amphicheiral[4] manifold, then both $m_i \to \frac{1}{m_i}$ and $l_i \to \frac{1}{l_i}$ (independently) become symmetries of the theory, once combined with $\hbar \to -\hbar$. This now implies that solutions come in signed pairs, $v_\alpha(u)$ and $v_{\hat\alpha}(u) = -v_\alpha(u)$, such that the corresponding perturbative $G_{\mathbb{C}}$ invariants satisfy

$$Z^{(\hat\alpha)}(M;\hbar,u) = Z^{(\alpha)}(M;-\hbar,u)\,. \tag{6.4.12}$$

For the perturbative coefficients, this leads to the relations

$$S_0^{(\hat\alpha)}(u) = -S_0^{(\alpha)}(u) \qquad (\mathrm{mod}\ 2\pi u)\,, \tag{6.4.13}$$

$$S_n^{(\hat\alpha)}(u) = (-1)^{n+1} S_n^{(\alpha)}(u) \qquad n \geq 1\,. \tag{6.4.14}$$

Assuming that the $\sim \pm\frac{i}{2}\mathrm{Vol}(M;u)$ behavior of the geometric and conjugate branches is unique, their signed and conjugate pairs must coincide for amphicheiral 3-manifolds. $S_0^{(\rm geom)}$, then, is an even analytic function of u with strictly real series coefficients; at $u \in i\mathbb{R}$, the Chern-Simons invariant $\mathrm{CS}(M;u)$ will vanish.

6.5 Brane quantization

Now, let us briefly describe how a new approach to quantization based on D-branes in the topological A-model [48] can be applied to the problem of quantizing the moduli space

[4] A manifold is called chiral or amphicheiral according to whether the orientation cannot or can be reversed by a self-map.

of flat connections, $\mathcal{M}_{\rm flat}(G_{\mathbb{C}}, \Sigma)$. This discussion is not crucial for the rest of the chapter — although it can be useful for obtaining a better understanding of Chern-Simons theory with complex gauge group — and the reader not interested in this approach may skip directly to Section 6.6.

In the approach of [48], the problem of quantizing a symplectic manifold N with symplectic structure ω is solved by complexifying (N, ω) into a new space (Y, Ω) and studying the A-model of Y with symplectic structure $\omega_Y = {\rm Im}\Omega$. Here, Y is a complexification of N, *i.e.* a complex manifold with complex structure $\mathcal{I}$ and an antiholomorphic involution

$$\tau : Y \to Y\,, \tag{6.5.1}$$

such that N is contained in the fixed point set of τ and $\tau^*\mathcal{I} = -\mathcal{I}$. The 2-form Ω on Y is holomorphic in complex structure $\mathcal{I}$ and obeys

$$\tau^*\Omega = \overline{\Omega} \tag{6.5.2}$$

and

$$\Omega|_N = \omega\,. \tag{6.5.3}$$

In addition, one needs to pick a unitary line bundle $\mathfrak{L} \to Y$ (extending the "prequantum line bundle" $\mathfrak{L} \to N$) with a connection of curvature ${\rm Re}\Omega$. This choice needs to be consistent with the action of the involution τ, meaning that $\tau : Y \to Y$ lifts to an action on $\mathfrak{L}$, such that $\tau|_N = {\rm id}$. To summarize, in brane quantization the starting point involves the choice of Y, Ω, $\mathfrak{L}$, and τ.

In our problem, the space $N = \mathcal{M}_{\rm flat}(G_{\mathbb{C}}, \Sigma)$ that we wish to quantize is already a complex manifold. Indeed, as we noted earlier, it comes equipped with the complex structure J (that does not depend on the complex structure on Σ). Therefore, its complexification[5] is $Y = N \times \overline{N}$ with the complex structure on $\overline{N}$ being prescribed by $-J$ and the complex structure on Y being $\mathcal{I} = (J, -J)$. The tangent bundle $TY = TN \oplus T\overline{N}$ is identified with the complexified tangent bundle of N, which has the usual decomposition $\mathbb{C}TN = T^{1,0}N \oplus T^{0,1}N$. Then, the "real slice" N is embedded in Y as the diagonal

$$N \ni x \mapsto (x, x) \in N \times \overline{N}\,. \tag{6.5.4}$$

[5]Note that, since in our problem we start with a hyper-Kähler manifold $\mathcal{M}_{\rm flat}(G_{\mathbb{C}}, \Sigma)$, its complexification Y admits many complex structures. In fact, Y has holonomy group $Sp(n) \times Sp(n)$, where n is the quaternionic dimension of $\mathcal{M}_{\rm flat}(G_{\mathbb{C}}, \Sigma)$.

In particular, N is the fixed point set of the antiholomorphic involution $\tau : Y \to Y$ which acts on $(x, y) \in Y$ as $\tau : (x, y) \mapsto (y, x)$.

Our next goal is to describe the holomorphic 2-form Ω that obeys (6.5.2) and (6.5.3) with[6]

$$\omega = \frac{t}{2\pi i}(\omega_K + i\omega_I) - \frac{\bar{t}}{2\pi i}(\omega_K - i\omega_I) \tag{6.5.5}$$

Note, that $(\omega_K + i\omega_I)$ is holomorphic on $N = \mathcal{M}_{\rm flat}(G_{\mathbb{C}}, \Sigma)$ and $(\omega_K - i\omega_I)$ is holomorphic on $\overline{N}$. Moreover, if we take $\bar{t}$ to be a complex conjugate of t, the antiholomorphic involution τ maps $t(\omega_K + i\omega_I)$ to $\bar{t}(\omega_K - i\omega_I)$, so that $\tau^*\omega = \omega$. Therefore, we can simply take

$$\Omega = \frac{t}{2\pi i}(\omega_K^{(1)} + i\omega_I^{(1)}) - \frac{\bar{t}}{2\pi i}(\omega_K^{(2)} - i\omega_I^{(2)}) \tag{6.5.6}$$

where the superscript $i = 1, 2$ refers to the first (resp. second) factor in $Y = N \times \overline{N}$. It is easy to verify that the 2-form Ω defined in this way indeed obeys $({\rm Im}\Omega)^{-1}{\rm Re}\Omega = \mathcal{I}$. Moreover, one can also check that if $\bar{t}$ is a complex conjugate of t then the restriction of $\omega_Y = {\rm Im}\Omega$ to the diagonal (6.5.4) vanishes, so that the "real slice" $N \subset Y$, as expected, is a Lagrangian submanifold in (Y, ω_Y).

Now, the quantization problem can be realized in the A-model of Y with symplectic structure $\omega_Y = {\rm Im}\Omega$. In particular, the Hilbert space $\mathcal{H}_\Sigma$ is obtained as the space of $(\mathcal{B}_{cc}, \mathcal{B}')$ strings,

$$\mathcal{H}_\Sigma = \text{ space of } (\mathcal{B}_{cc}, \mathcal{B}') \text{ strings} \tag{6.5.7}$$

where $\mathcal{B}_{cc}$ and $\mathcal{B}'$ are A-branes on Y (with respect to the symplectic structure ω_Y). The brane $\mathcal{B}'$ is the ordinary Lagrangian brane supported on the "real slice" $N \subset Y$. The other A-brane, $\mathcal{B}_{cc}$, is the so-called canonical coisotropic brane supported on all of Y. It carries a Chan-Paton line bundle of curvature $F = {\rm Re}\Omega$. Note that for $[F]$ to be an integral cohomology class we need ${\rm Re}(t) \in \mathbb{Z}$. Since in the present case the involution τ fixes the "real slice" pointwise, it defines a hermitian inner product on $\mathcal{H}_\Sigma$ which is positive definite.

[6]Notice that while elsewhere we consider only the "holomorphic" sector of the theory (which is sufficient in the perturbative approach), here we write the complete symplectic form on $\mathcal{M}_{\rm flat}(G_{\mathbb{C}}, \Sigma)$ that follows from the classical Chern-Simons action (5.1.1), including the contributions of both fields $\mathcal{A}$ and $\bar{\mathcal{A}}$.

6.6 Examples

To conclude this chapter, we give several examples of explicit computations using the hierarchy of differential equations described in Section 6.3. We focus on the gauge group $SL(2,\mathbb{C})$. We will begin with the trefoil, whose higher-order perturbative invariants on the non-abelian branch of flat connections actually vanish. This behavior was also noticed by direct analytic continuation of the colored Jones polynomial in [117]. We then consider figure-eight knot $\mathbf{4_1}$, the simplest hyperbolic knot, which has new, interesting, non-trivial perturbative invariants to all orders. It is quite possible to apply the hierarchy of differential equations to other knots as well (for example, explicit operators $\hat{A}$ for twist knots appear in [118]), but computations start to become somewhat inefficient. In Chapter 9, we will employ a different method (the state integral model) to find perturbative invariants for knots like $\mathbf{4_1}$ and $\mathbf{5_2}$ and to verify that they satisfy $\hat{A} \cdot Z = 0$.

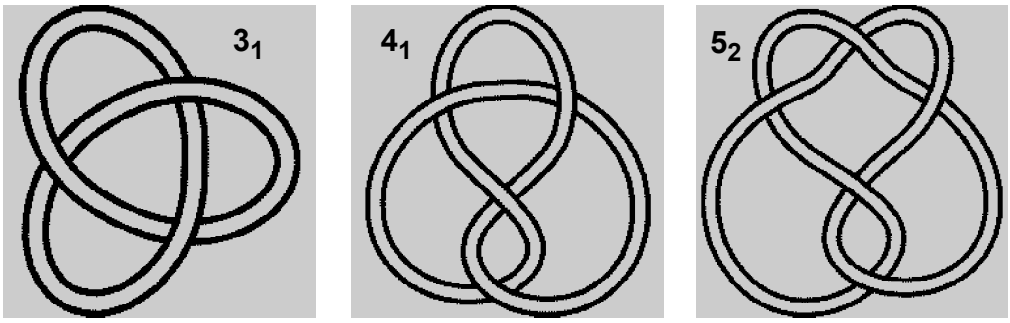

Figure 6.1: Recurrent examples: the trefoil knot $\mathbf{3_1}$, figure-eight knot $\mathbf{4_1}$, and "three-twist" knot $\mathbf{5_2}$, courtesy of `KnotPlot`.

6.6.1 Trefoil

The classical $SL(2,\mathbb{C})$ A-polynomial for the trefoil knot is

$$A(l,m) = (l-1)(l+m^6)\,. \tag{6.6.1}$$

It is a special case of the A-polynomial for (p,q) torus knots, which takes the form $(l-1)(lm^{pq}+1)$. This A-polynomial has two branches of solutions, an

$$\text{abelian branch}: \qquad l_{abel} = 1\,, \tag{6.6.2}$$

and a

$$\text{non-abelian branch}: \qquad l_{na} = -m^6\,. \tag{6.6.3}$$

Since the trefoil is a chiral knot, the A-polynomial is not invariant under the transformation $m \to m^{-1}$, which takes the right-handed trefoil to the left-handed trefoil. (It was explained in Section 6.4 how the quantum partition function must change under this mirror action.)

As explained earlier, *cf.* (6.2.2), a simple way to find the operator $\widehat{A}(\hat{l},\hat{m})$ is to note that it also annihilates the polynomial invariants of the knot K computed by Chern-Simons theory with compact gauge group G. In the present case, $G = SU(2)$ and the equation (6.2.2) takes the form of a recursion relation on the set of colored Jones polynomials, $\{J_n(K;q)\}$. Specifically, using the fact that $\hat{l}$ acts by shifting the value of the highest weight of the representation and writing $\widehat{A}(\hat{l},\hat{m}) = \sum_{j=0}^{d} a_j(\hat{m},q)\hat{l}^j$ as in (6.3.5), we obtain

$$\sum_{j=0}^{d} a_j(q^{n/2},q)J_{n+j}(K;q) = 0\,. \tag{6.6.4}$$

It is easy to verify that the colored Jones polynomials of the trefoil knot indeed satisfy such a recursion relation, with the coefficients (see also[7] [119, 120]):

$$a_0(\hat{m},q) = q^2m^6(q^3m^4-1)\,, \tag{6.6.5a}$$

$$a_1(\hat{m},q) = \sqrt{q}(-q^5m^{10}+q^4m^6+q^3m^4-1)\,, \tag{6.6.5b}$$

$$a_2(\hat{m},q) = 1-qm^4\,. \tag{6.6.5c}$$

Note that in the classical limit $q = e^{2\hbar} \to 1$, we have

$$\widehat{A}(\hat{l},\hat{m}) \underset{\hbar\to 0}{\longrightarrow} (1-m^4)A(l,m)\,. \tag{6.6.6}$$

We could divide all the a_j's by the extra factor $(1-m^4)$ in(6.6.6) (or a q-deformation thereof) to obtain a more direct correspondence between $\widehat{A}(\hat{l},\hat{m})$ and $A(l,m)$, but this does not affect any of the following calculations.

To find the exact perturbative invariant $Z^{(\alpha)}(M;\hbar,u)$ for each α, we reduce $\hat{m}$ to a classical variable m (since in the u-space representation the operator $\hat{m}$ just acts via ordinary

[7] Note that [119, 120] look at asymptotics of the colored Jones polynomial normalized by its value at the unknot, while the $SL(2,\mathbb{C})$ Chern-Simons partition function should agree with the unnormalized colored Jones polynomial. Hence, we must divide the expressions for a_j given there by $(m^2q^{j/2}-q^{-j/2})$ to account for the difference, introducing a few factors of $q^{1/2}$ in our formulas.

multiplication), expand each of the above a_j's as $a_j(m,q) = \sum_{p=0}^{\infty} a_{j,p}(m)\hbar^p$, and substitute the $a_{j,p}$ into the hierarchy of differential equations derived in Section 6.1 and displayed in Table 6.1. The equations are then solved recursively on each branch α of the A-polynomial to determine the coefficients $S_n^{(\alpha)}(u)$.

Non-abelian branch

For the non-abelian branch, which one would naively expect to be the more non-trivial one, all higher-order perturbative invariants actually vanish. It is easy to check directly that

$$Z^{(na)}(\mathbf{3_1};\hbar;u) = \exp\left(\frac{3u^2 + i\pi u}{\hbar}\right) \tag{6.6.7}$$

is an exact solution to $\hat{A}(\hat{l},\hat{m})\cdot Z = 0$. This implies that

$$S_0^{(na)}(u) = 3u^2 + i\pi u \qquad (\text{mod } 2\pi i u)\,, \tag{6.6.8}$$

and agrees with the fact that the volume of the (non-hyperbolic) trefoil knot complement is zero.

Moreover, all higher-order invariants $S_n^{(na)}(u)$ must be constants. In [117, 121], it is independently argued (via direct analytic continuation of the colored Jones polynomial) that this is indeed the correct behavior, and that $S_1^{(na)}$ is a nonzero constant, while all other $S_n^{(na)}$ vanish.

Abelian branch

The abelian branch, surprisingly, is non-trivial. It senses the fact that the operator $\hat{A}$ does contain more information than the classical A-polynomial. Setting $S_0(u) = 0$ to single out the abelian branch, we find that

$$\begin{aligned}
S_1(u) &= \log\frac{m\left(m^2-1\right)}{m^4-m^2+1}\,,\\
S_2(u) &= \frac{2m^4}{\left(m^4-m^2+1\right)^2}\,,\\
S_3(u) &= -\frac{2\left(m^{12}-4m^8+m^4\right)}{\left(m^4-m^2+1\right)^4}\,,
\end{aligned}$$

$$S_4(u) = \frac{4m^4\left(m^{16}+2m^{14}-23m^{12}-4m^{10}+60m^8-4m^6-23m^4+2m^2+1\right)}{3\left(m^4-m^2+1\right)^6},$$

$$S_5(u) = -\frac{2m^4}{3\left(m^4-m^2+1\right)^8}\left(m^{24}+8m^{22}-84m^{20}-144m^{18}+868m^{16}+200m^{14}-1832m^{12}\right.$$
$$\left.+200m^{10}+868m^8-144m^6-84m^4+8m^2+1\right),$$

$$\ldots.$$

Since the abelian branch is self-conjugate (in the language of Section 6.4), the powers of m appearing here are all balanced; for $u \in i\mathbb{R}$ or $u \in \mathbb{R}$ the coefficients are real. Unfortunately, since this *is* an abelian branch, all the perturbative invariants at $u = 0$ are uninteresting rational numbers.

6.6.2 Figure-eight knot

The classical A-polynomial of the figure-eight knot is

$$A(l,m) = (l-1)(m^4 - (1-m^2-2m^4-m^6+m^8)l + m^4l^2)\,. \tag{6.6.9}$$

Observe that $A(l^{-1},m^{-1}) \sim A(l,m)$ and that $A(l^{-1},m) \sim A(l,m)$, the latter reflecting the fact that the figure-eight knot is amphicheiral. The zero locus of this A-polynomial has three branches: the abelian branch $l_{\text{abel}} = 1$ (or $v_{\text{abel}} = -i\pi$) from the first factor, and two other branches from the second, given explicitly by

$$l_{\text{geom,conj}}(m) = \frac{1-m^2-2m^4-m^6+m^8}{2m^4} \pm \frac{1-m^4}{2m^2}\Delta(m) \tag{6.6.10}$$

or

$$v_{\text{geom,conj}}(u) = \log(-l_{\text{geom,conj}}(e^u))\,, \tag{6.6.11}$$

where we have defined

$$\Delta(m) = i\sqrt{-m^{-4}+2m^{-2}+1+2m^2-m^4}\,. \tag{6.6.12}$$

Note that $\Delta(m)$ is an analytic function of $m = e^u$ around $u = 0$, as are $l(m)$ and $v(u)$. In particular, $\Delta(1) = \sqrt{-3}$ is the generator of the trace field $\mathbb{K} = \mathbb{Q}(\text{tr}\Gamma)$ for the figure-eight knot.

Since there are only two non-abelian branches, they must (as indicated in Section 6.4) be the geometric and conjugate ones. By looking at the behavior of these two branches in

the neighborhood of the point $(l,m)=(-1,1)$ that corresponds to the complete hyperbolic structure, where the geometric branch must have maximal volume, and using (6.3.15), one can check that the identification in (6.6.10) is the correct one. (It is also possible to check this directly once the hyperbolic structure of the figure-eight knot complement is understood, *cf.* Section 8.1.1.)

The quantum A-polynomial $\hat{A}(\hat{l},\hat{m}) = \sum_{j=0}^{3} a_j(\hat{m},q)\hat{l}^j$ for the figure-eight knot has coefficients

$$a_0(\hat{m},q) = \frac{q\hat{m}^2}{(1+q\hat{m}^2)(-1+q\hat{m}^4)}\,, \tag{6.6.13a}$$

$$a_1(\hat{m},q) = \frac{1+(q^2-2q)\hat{m}^2-(q^3-q^2+q)\hat{m}^4-(2q^3-q^2)\hat{m}^6+q^4\hat{m}^8}{q^{1/2}\hat{m}^2(1+q^2\hat{m}^2-q\hat{m}^4-q^3\hat{m}^6)}\,, \tag{6.6.13b}$$

$$a_2(\hat{m},q) = -\frac{1-(2q^2-q)\hat{m}^2-(q^5-q^4+q^3)\hat{m}^4+(q^7-2q^6)\hat{m}^6+q^8\hat{m}^8}{q\hat{m}^2(1+q\hat{m}^2-q^5\hat{m}^4-q^6\hat{m}^6)}\,, \tag{6.6.13c}$$

$$a_3(\hat{m},q) = -\frac{q^4\hat{m}^2}{q^{1/2}(1+q^2\hat{m}^2)(-1+q^5\hat{m}^4)}\,. \tag{6.6.13d}$$

In the classical limit $q=e^{2\hbar}\to 1$, we have

$$\widehat{A}(\hat{l},\hat{m}) \quad \xrightarrow[\hbar\to 0]{} \quad \frac{A(l,m)}{m^2(m^2-1)(m^2+1)^2}\,. \tag{6.6.14}$$

Again, we could multiply all the a_j's by the denominator of (6.6.14) (or a q-deformation thereof) to obtain a more direct correspondence between $\widehat{A}(\hat{l},\hat{m})$ and $A(l,m)$.

Geometric branch

For the geometric branch, the solution to the first equation in Table 6.1 is chosen to be

$$S_0^{(\mathrm{geom})}(u) = \frac{i}{2}\mathrm{Vol}(\mathbf{4_1};0) + \int_0^u du\, v_{\mathrm{geom}}(u) + i\pi u\,, \tag{6.6.15}$$

with $v_{\mathrm{geom}}(u)$ as in (6.6.11). The integration constant $i(\mathrm{Vol}(0)+i\mathrm{CS}(0))$ is not important for determining the remaining coefficients (since only derivatives of S_0 appear in the equations), but we have fixed it by requiring that $S_0^{(\mathrm{geom})}(0) = \frac{i}{2}(\mathrm{Vol}(\mathbf{4_1};0)+i\mathrm{CS}(\mathbf{4_1};0)) = \frac{i}{2}\mathrm{Vol}(\mathbf{4_1};0) = (1.01494\ldots)i$, as expected for the classical action of Chern-Simons theory.

Substituting the above $S_0^{(\mathrm{geom})}(u)$ into the hierarchy of equations, the rest are readily solved[8] for the subleading coefficients. The first eight functions $S_n^{(\mathrm{geom})}(u)$ appear below:

[8]It is computationally advantageous to express everything in terms of $m=e^u$ and $m\frac{d}{dm} = \frac{d}{du}$, *etc.*, when implementing this on a computer.

$$
\begin{aligned}
S_1(u) &= -\frac{1}{2}\log\left(\frac{-i\Delta(m)}{2}\right),\\
S_2(u) &= \frac{-1}{12\Delta(m)^3m^6}\left(1-m^2-2m^4+15m^6-2m^8-m^{10}+m^{12}\right),\\
S_3(u) &= \frac{2}{\Delta(m)^6m^6}\left(1-m^2-2m^4+5m^6-2m^8-m^{10}+m^{12}\right),\\
S_4(u) &= \frac{1}{90\Delta(m)^9m^{16}}\big(1-4m^2-128m^4+36m^6\\
&\quad +1074m^8-5630m^{10}+5782m^{12}+7484m^{14}-18311m^{16}+7484m^{18}\\
&\quad +5782m^{20}-5630m^{22}+1074m^{24}+36m^{26}-128m^{28}-4m^{30}+m^{32}\big),\\
S_5(u) &= \frac{2}{3\Delta(m)^{12}m^{18}}\big(1+5m^2-35m^4+240m^6-282m^8-978m^{10}\\
&\quad +3914m^{12}-3496m^{14}-4205m^{16}+9819m^{18}-4205m^{20}-3496m^{22}\\
&\quad +3914m^{24}-978m^{26}-282m^{28}+240m^{30}-35m^{32}+5m^{34}+m^{36}\big),\\
S_6(u) &= \frac{-1}{945\Delta(m)^{15}m^{28}}\big(1+2m^2+169m^4+4834m^6\\
&\quad -24460m^8+241472m^{10}-65355m^{12}-3040056m^{14}+13729993m^{16}\\
&\quad -15693080m^{18}-36091774m^{20}+129092600m^{22}-103336363m^{24}\\
&\quad -119715716m^{26}+270785565m^{28}-119715716m^{30}-103336363m^{32}\\
&\quad +129092600m^{34}-36091774m^{36}-15693080m^{38}+13729993m^{40}-3040056m^{42}\\
&\quad -65355m^{44}+241472m^{46}-24460m^{48}+4834m^{50}+169m^{52}+2m^{54}+m^{56}\big),\\
S_7(u) &= \frac{4}{45\Delta(m)^{18}m^{30}}\big(1+47m^2-176m^4+3373m^6+9683m^8\\
&\quad -116636m^{10}+562249m^{12}-515145m^{14}-3761442m^{16}+14939871m^{18}\\
&\quad -15523117m^{20}-29061458m^{22}+96455335m^{24}-71522261m^{26}\\
&\quad -80929522m^{28}+179074315m^{30}-80929522m^{32}-71522261m^{34}\\
&\quad +96455335m^{36}-29061458m^{38}-15523117m^{40}+14939871m^{42}\\
&\quad -3761442m^{44}-515145m^{46}+562249m^{48}-116636m^{50}\\
&\quad +9683m^{52}+3373m^{54}-176m^{56}+47m^{58}+m^{60}\big),\\
S_8(u) &= \frac{1}{9450\Delta(m)^{21}m^{40}}\big(1+44m^2-686m^4\\
&\quad -25756m^6+25339m^8-2848194m^{10}-28212360m^{12}
\end{aligned}
$$

$$+216407820m^{14} - 1122018175m^{16} - 266877530m^{18}$$

$$+19134044852m^{20} - 76571532502m^{22} + 75899475728m^{24}$$

$$+324454438828m^{26} - 1206206901182m^{28} + 1153211096310m^{30}$$

$$+1903970421177m^{32} - 5957756639958m^{34} + 4180507070492m^{36}$$

$$+4649717451712m^{38} - 10132372721949m^{40} + 4649717451712m^{42}$$

$$+4180507070492m^{44} - 5957756639958m^{46} + 1903970421177m^{48}$$

$$+1153211096310m^{50} - 1206206901182m^{52} + 324454438828m^{54}$$

$$+75899475728m^{56} - 76571532502m^{58} + 19134044852m^{60}$$

$$-266877530m^{62} - 1122018175m^{64} + 216407820m^{66} - 28212360m^{68}$$

$$-2848194m^{70} + 25339m^{72} - 25756m^{74} - 686m^{76} + 44m^{78} + m^{80}\big)\,.$$

Table 6.3: Perturbative invariants $S_n^{(\mathrm{geom})}(u)$ up to eight loops.

According to (5.2.3), the coefficient $S_1^{(\mathrm{geom})}(u)$ in the perturbative Chern-Simons partition function should be related to the Reidemeister-Ray-Singer torsion of M twisted by $\mathcal{A}^{(\mathrm{geom})}$, which has been independently computed. Our function matches[9] that appearing in *e.g.* [98], up to a shift by $-\log\pi$. The constants of integration for the remaining coefficients have been fixed by comparison to the asymptotics of the colored Jones polynomial, using (5.4.5) and the results of Section 5.4. Note that at $u = 0$, the arithmetic invariants of Section 5.4 at the complete hyperbolic structure should be reproduced.

Conjugate branch

For the "conjugate" branch, the solution for $S_0(u)$ is now chosen to be

$$S_0^{(\mathrm{conj})}(u) = -\frac{i}{2}\mathrm{Vol}(\mathbf{4_1}; 0) + \int_0^u du\, v_{\mathrm{conj}}(u) + i\pi u \qquad (\mathrm{mod}\ 2\pi u), \tag{6.6.16}$$

so that $S_0^{(\mathrm{conj})}(u) = -S_0^{(\mathrm{geom})}(u)$. As for the geometric branch, this is then substituted into remainder of the hierarchy of equations. Calculating the subleading coefficients, the

[9] To compare with [98], note that $k_{\mathrm{there}} = k_{\mathrm{here}} = i\pi/\hbar$, and $u_{\mathrm{there}} = 2u_{\mathrm{here}}$. The shift by $-\log(\pi)$ is directly related to a jump in the asymptotics of the colored Jones polynomial at $u = 0$.

constants of integration can all be fixed so that

$$S_n^{(\mathrm{conj})}(u) = (-1)^{n+1} S_{n+1}^{(\mathrm{geom})}(u), \tag{6.6.17}$$

This is precisely what one expects for an amphicheiral knot when a conjugate pair of branches coincides with a "signed" pair, as discussed in Section 6.4.

Abelian branch

For completeness, we can also mention perturbation theory around an abelian flat connection $\mathcal{A}^{(\mathrm{abel})}$ on M, although it has no obvious counterpart in the state integral model.

For an abelian flat connection $\mathcal{A}^{(\mathrm{abel})}$, the classical Chern-Simons action (5.2.1) vanishes. This is exactly what one finds from (6.3.14):

$$S_0^{(\mathrm{abel})}(u) = \int_0^u du\, v_{\mathrm{abel}}(u) + i\pi u = 0 \qquad (\mathrm{mod}\ 2\pi i u)\,, \tag{6.6.18}$$

fixing the constant of integration so that $S_0^{(\mathrm{abel})}(0) = 0$. From the hierarchy of differential equations, the first few subleading coefficients are

$$\begin{aligned}
S_1^{(\mathrm{abel})}(u) &= \log \frac{m(m^2-1)}{1-3m^2+m^4}, \\
S_2^{(\mathrm{abel})}(u) &= 0 \\
S_3^{(\mathrm{abel})}(u) &= \frac{4(m^2-1)^2}{(1-3m^2+m^4)^3}\big(1-7m^2+16m^4-7m^6+m^8\big), \\
S_4^{(\mathrm{abel})}(u) &= 0 \\
S_5^{(\mathrm{abel})}(u) &= \frac{4(m^2-1)^2}{3(1-3m^2+m^4)^6}\big(41-656m^2+4427m^4-16334m^6+35417m^8-46266m^{10} \\
&\qquad +35417m^{12}-16334m^{14}+4427m^{16}-656m^{18}+41m^{20}\big) \\
S_6^{(\mathrm{abel})}(u) &= 0 \ \ldots.
\end{aligned}$$

Table 6.4: Perturbative invariants $S_n^{(\mathrm{abel})}(u)$ up to six loops.

In the language of Section 6.4, the abelian branch must be its own "signed pair," guaranteeing that all even $S_{2k}^{(\mathrm{abel})}(u)$ vanish.

Chapter 7

Wilson loops for complex gauge groups

The goal of this chapter is to explain the relationship between Chern-Simons theory with Wilson loops and Chern-Simons theory on knot complements, and to use this relationship to elucidate the limit taken in "analytic continuation" of Chern-Simons theory with compact gauge group G to Chern-Simons theory with complex gauge group $G_{\mathbb{C}}$.

For compact gauge groups, the relation between Wilson loops and knot complements have been understood for a long time [13, 122]. Part of our discussion here reviews and explains these results in greater detail, as they provide the groundwork for the complex case. The main idea of the approach in (*e.g.*) [122] is to rewrite a Wilson loop as a new path integral for quantum mechanics of particles moving along the loop. This has two advantages: it allows a generalization to complex gauge group (taking the trace of a holonomy in a given representation does *not*); and it most directly connects boundary conditions and representations.

Unfortunately, the generalization to complex gauge group requires a certain number of mathematical preliminaries. Thus, we spend the first part of the chapter reviewing principal series representations of complex groups and their realizations via the orbit method, following [123, 124, 125]. In the second part of the chapter, we incorporate these results into Wilson loops and Chern-Simons theory.

7.1 Some representation theory

Finite and infinite-dimensional representations

The Lie algebra $\mathfrak{sl}(2,\mathbb{C})$ is generated as a complex vector space by the elements E, F, H satisfying

$$[E,F] = H\,, \quad [H,E] = 2E\,, \quad [H,F] = -2F\,. \tag{7.1.1}$$

In the defining representation, these elements correspond to the matrices

$$H = \begin{pmatrix} 1 & 0 \\ 0 & -1 \end{pmatrix}, \quad E = \begin{pmatrix} 0 & 1 \\ 0 & 0 \end{pmatrix}, \quad F = \begin{pmatrix} 0 & 0 \\ 1 & 0 \end{pmatrix}. \tag{7.1.2}$$

One exponentiates (with no i's) to obtain the group $SL(2,\mathbb{C})$. The compact subgroup $SU(2)$ of $SL(2,\mathbb{C})$ has a Lie algebra $\mathfrak{su}(2)$ generated as a real vector space over anti-Hermitian generators (*a.k.a.* Pauli matrices):

$$\mathfrak{su}(2) = \langle iH, E-F, i(E+F)\rangle_{\mathbb{R}}\,. \tag{7.1.3}$$

All representations of $\mathfrak{su}(2)$ can be extended to be *holomorphic* representations of $\mathfrak{sl}(2,\mathbb{C})$. They act most generally as

$$\begin{aligned} \rho_\lambda(E) &= -\lambda z + z^2\partial_z\,, \\ \rho_\lambda(F) &= -\partial_z\,, \\ \rho_\lambda(H) &= -\lambda + 2z\partial_z \end{aligned} \tag{7.1.4}$$

on holomorphic functions $f(z)$ of a single complex variable. Here, ρ is a complex-linear homomorphism on the generators of the Lie algebra. The quadratic Casimir of this representation is

$$C_2(\lambda) = \rho_\lambda\left(\frac{1}{2}H^2 + EF + FE\right) = \frac{1}{2}\lambda(\lambda+2)\,. \tag{7.1.5}$$

While representation (7.1.4) is a perfectly good representation of $\mathfrak{sl}(2,\mathbb{C})$ or its subalgebras for any $\lambda \in \mathbb{C}$, it is not always integrable to representations of $SL(2,\mathbb{C})$ or its subgroups. If ρ_λ *is* integrable, then it integrates generically to

$$\rho_\lambda\begin{pmatrix} a & b \\ c & d \end{pmatrix} \cdot f(z) = (-bz+d)^\lambda f\left(\frac{az-c}{-bz+d}\right)\,. \tag{7.1.6}$$

For $SU(2)$ and $SL(2,\mathbb{C})$, it is sufficient to check that this is well-defined on the maximal tori generated by H, and in particular that $\rho(I) = \rho_\lambda(e^{2\pi i H}) := e^{2\pi i \rho_\lambda(H)} = 1$. This forces λ to be an integer. Indeed, when $\lambda \in \mathbb{Z}_{\geq 0}$, ρ_λ can be restricted to a finite-dimensional representation acting on polynomials in z of degree $\leq \lambda$. The dimension of this representation is $N = \lambda + 1$.

In the case of $SU(2)$, these finite-dimensional representations are unitary. For $SL(2,\mathbb{C})$ however, they are not. In order to find unitary representations of $SL(2,\mathbb{C})$, one must break its complex structure. That is, consider $\mathfrak{sl}(2,\mathbb{C})$ to be a *real* Lie algebra[1] generated over the basis $\{E,\, F,\, H,\, \tilde{E} := iE,\, \tilde{F} := iF,\, \tilde{H} := iH\}$. We seek representations ρ with $\rho(\tilde{T}) \neq i\rho(T)$ for $T = E, F, H$.

It is convenient to complexify the Lie algebra $\mathfrak{sl}(2,\mathbb{C})$ (a second time), and to extend ρ complex-linearly under this second complexification. Working over $\mathbb{C}$, we then redefine generators

$$\begin{aligned} 2E_L &= E - i\tilde{E}, \qquad & 2E_R &= E + i\tilde{E}\,, \\ 2F_L &= F - i\tilde{F}, \qquad & 2F_R &= F + i\tilde{F}\,, \\ 2H_L &= H - i\tilde{H}, \qquad & 2H_R &= H + i\tilde{H}\,. \end{aligned} \tag{7.1.7}$$

Each (E_L, F_L, H_L) and (E_R, F_R, H_R) generate independent (commuting) $\mathfrak{sl}(2,\mathbb{C})$ subalgebras, and we obtain an isomorphism $\mathfrak{sl}(2,\mathbb{C})_{\mathbb{C}} \simeq \mathfrak{sl}(2,\mathbb{C})_L \times \mathfrak{sl}(2,\mathbb{C})_R$. Now, generic non-holomorphic representations of $\mathfrak{sl}(2,\mathbb{C})$ should be given as $\rho_{\lambda_L,\lambda_R} = \rho_{\lambda_L} \times \rho_{\lambda_R}$, using (7.1.4) for each of the two factors $\mathfrak{sl}(2,\mathbb{C})_{L,R}$. The representation space consists of nonholomorphic functions $f(z,\bar{z})$, with ρ_{λ_L} acting on z and ρ_{λ_R} acting on $\bar{z}$. The corresponding quadratic Casimir is

$$C_2(\lambda_L, \lambda_R) = \lambda_L(\lambda_L + 2) + \lambda_R(\lambda_R + 2)\,. \tag{7.1.8}$$

When naively integrating the representation $\rho_{\lambda_L,\lambda_R}$ described above, one obtains

$$\rho_{\lambda_L,\lambda_R}\begin{pmatrix} a & b \\ c & d \end{pmatrix} \cdot f(z,\bar{z}) = (-bz+d)^{\lambda_L}\overline{(-bz+d)}^{\lambda_R} f\left(\frac{az-c}{-bz+d}, \frac{\bar{a}\bar{z}-\bar{c}}{-\bar{b}\bar{z}+\bar{d}}\right). \tag{7.1.9}$$

This expression is well-defined only when $\boxed{\lambda_L - \lambda_R \in \mathbb{Z}}$. This condition can be seen by writing the multiplicative factor above as

$$|-bz+d|^{\lambda_L+\lambda_R}\left(\frac{-bz+d}{|-bz+d|}\right)^{\lambda_L-\lambda_R}.$$

[1] In this description, we have $\mathfrak{sl}(2,\mathbb{C}) = \mathfrak{spin}(3,1)$.

Then, for $\rho_\lambda(e^{2\pi\tilde{H}}) = 1$ the exponent of the phase must be an integer. It is clear from (7.1.9) that when $\lambda_R = 0$ we just obtain the old holomorphic representations, with $\lambda = \lambda_L$.

For a pair $\lambda_L, \lambda_R \in \mathbb{C}$ satisfying $\lambda_L - \lambda_R \in \mathbb{Z}$, the expression (7.1.9) defines a *generalized principal series representation* of $SL(2,\mathbb{C})$. This infinite-dimensional representation is more commonly labelled as $\mathcal{P}^{\mathfrak{k},w}$ (*cf.* [123]), with

$$w = -(\lambda_L + 1) - (\lambda_R + 1) \in \mathbb{C}, \qquad \mathfrak{k} = -(\lambda_L - \lambda_R) \in \mathbb{Z}\,. \tag{7.1.10}$$

For w imaginary and arbitrary $\mathfrak{k}$, the principal series representations are unitary under the standard inner product on $L^2(\mathbb{C})$. For real $0 < w < 2$ and $\mathfrak{k} = 0$, the representations are unitary under a non-standard inner product, and are called the complementary series. In terms of $\mathfrak{k}$ and w, the quadratic Casimir is

$$\frac{1}{4}(w^2 + \mathfrak{k}^2) - 1\,. \tag{7.1.11}$$

Representations related by $(w,\mathfrak{k}) \leftrightarrow (-w,-\mathfrak{k})$ are isomorphic, and this is the only equivalence in the series. The unitary principal series and complementary series are the only unitary representations of $SL(2,\mathbb{C})$. They are irreducible unless $w \in \mathbb{Z}$, $|k| < |w|$, and $k \equiv w \bmod 2$ [123].

Induction

Given a group G, a subgroup $H \subset G$, and a representation σ of H, one can form an *induced representation* $\mathrm{ind}_H^G(\sigma)$. This acts on the space of functions on G valued in the vector space of the representation σ that satisfy

$$f(xh) = \sigma(h^{-1})f(x) \tag{7.1.12}$$

for $h \in H$, $x \in G$. This space, formally $C_c^\infty(H\backslash G;\sigma)$, can equivalently be thought of as sections of a bundle on the coset space G/H. The action of G on $f \in C_c^\infty(H\backslash G;\sigma)$ is by the left-regular representation

$$\mathrm{ind}_H^G(\sigma)(g)\cdot f(x) := f(g^{-1}x)\,. \tag{7.1.13}$$

For a general semi-simple reductive group, *all* so-called admissible representations are generated by the operation of induction from simpler representations of parabolic subgroups,

and then by taking quotients to obtain irreducible representations. In the case of $SL(2,\mathbb{C})$, the story is very simple. The only nontrivial parabolic subgroup is the Borel subgroup B of upper-triangular matrices. It has a decomposition $B = MAN$ corresponding to the decomposition $\mathfrak{b} = \mathfrak{a} \oplus \mathfrak{m} \oplus \mathfrak{n}$ with

$$\begin{aligned} \mathfrak{a} &= \langle H \rangle, & A &= \{\exp tH\} \quad (t \in \mathbb{R}), \\ \mathfrak{m} &= \langle iH \rangle, & M &= \{\exp tiH\} \simeq U(1), \\ \mathfrak{n} &= \langle E, iE \rangle, & N &= \{\exp(tE + t'iE)\}. \end{aligned} \tag{7.1.14}$$

Then, letting $\nu \in (\mathfrak{a}^*)_{\mathbb{C}}$ and $\kappa \in \mathfrak{m}^*$ be (real) linear functionals defined by

$$\nu(H) = -iw, \quad \kappa(iH) = \mathfrak{k}; \qquad \nu(iH) = \kappa(H) = 0, \tag{7.1.15}$$

and letting ρ be the half-sum of positive restricted roots satisfying

$$\rho(H) = 2, \qquad \rho(iH) = 0, \tag{7.1.16}$$

the principal series representation $\mathcal{P}^{\mathfrak{k},w}$ is induced from the representation $\exp(i\nu + \rho) \otimes \exp i\kappa \otimes id$ of $B = MAN$:

$$\mathbb{P}^{\mathfrak{k},w} = \mathrm{ind}_B^{G_{\mathbb{C}}}(e^{i\nu + i\kappa + \rho}). \tag{7.1.17}$$

Observe that the defining data here is a pair of linear functionals κ and ν, corresponding to the parameters $\mathfrak{k}$ and w, that act on the maximal torus $T_{\mathbb{C}} \simeq GL(1)$ of the group $G_{\mathbb{C}}$. The functional acting on the compact part of $T_{\mathbb{C}}$ is quantized. This is true in general for maximal parabolic subgroups: principal series representations are induced from representations of the maximal torus that act trivially on the off-diagonal part of the parabolic subgroup. The representation $T_{\mathbb{C}}$ (here $e^{i\nu + i\kappa + \rho}$) is called the quasi-character of the induced representation.

7.2 Representations as coadjoint orbits

The mathematical machinery that connects representations with conjugacy classes (and for us Wilson loops with boundary conditions) is the Borel-Weil-Bott theorem [126] and generalizations thereof to noncompact groups (developed by Kirillov and others). The basic idea is that irreducible representations a group $G_{(\mathbb{C})}$ can be obtained by the geometric quantization of its coadjoint orbits. Excellent reviews of the topic can be found in [124] or

[125] (see also [127] and [48] in the physics literature). Here, we will give a brief overview of the general procedure, stating necessary results, and then specializing to the example of $SU(2)$ and $SL(2,\mathbb{C})$.

The adjoint action of G on $\mathfrak{g}$ can be written as $g : X \to gXg^{-1}$. Likewise, there is a coadjoint action of G on the dual space $\mathfrak{g}^*$. Since $\mathfrak{g}^*$ and $\mathfrak{g}$ can be identified for reductive groups by a non-degenerate trace form, we can write weights $\lambda \in \mathfrak{g}^*$ as matrices; then the coadjoint action is $g : X \to g\lambda g^{-1}$. The coadjoint *orbit*

$$\Omega_\lambda = \{g\lambda g^{-1}\}_{g\in G} \tag{7.2.1}$$

through a point λ has the geometry of the coset G/H_λ (or sometimes a quotient thereof), where H_λ is the stabilizer of λ:

$$H_\lambda = \{h \in G \mid h\lambda h^{-1} = \lambda\}\,. \tag{7.2.2}$$

In the case of compact or complex G, H_λ is conjugate to the maximal torus of G for generic λ. The left-regular G-action on G/H_λ is equivalent to the coadjoint action on Ω_λ, and is the action used for representations.

The coadjoint orbit $\Omega_\lambda \simeq H_\lambda$ has a natural G-invariant symplectic structure. The symplectic form can be written as

$$\omega = -\mathrm{Tr}(\lambda\, g^{-1}dg \wedge g^{-1}dg) \tag{7.2.3}$$

for $g \in G/H_\lambda$. To geometrically quantize Ω_λ one must form a line bundle $\mathcal{L} \to \Omega_\lambda$ with curvature ω, choose a *polarization* that effectively cuts out half the degrees of freedom (half the coordinates) on Ω_λ, and construct a Hilbert space V as the space of square-integrable polarization-invariant sections of $\mathcal{L}$. Considering λ again to be a linear functional $\lambda \in \mathfrak{g}^*$, the line bundle $\mathcal{L}$ can is obtained as a quotient of $\mathbb{C} \times G$ by the representation $e^{i\lambda}$ of $H_\lambda \in G$ acting on $\mathbb{C}$; in other words, it is essentially the space $C^\infty(G, e^{i\lambda})$ of the induced representation $\mathrm{ind}_{H_\lambda}^G(e^{i\lambda})$ described in Section 7.1. The line bundle exists if and only if the representation $e^{i\lambda}$ is integrable.

In the case of compact group G, where $H_\lambda \simeq \mathbb{T}$ is a maximal torus, one can induce a complex structure on G/H_λ via the equivalence

$$G/H_\lambda \simeq G_{\mathbb{C}}/B\,, \tag{7.2.4}$$

where B is the upper-triangular Borel subgroup of $G_{\mathbb{C}}$ containing H_λ. Then, to obtain the unitary finite-dimensional representations, one must choose a *holomorphic* polarization. Specifically, if $-\lambda$ is the dominant weight of a sought representation R, then the space $H^0_{\bar\partial}(G/H_\lambda; e^{i\lambda})$ of holomorphic sections of the bundle $\mathcal{L}$ is finite dimensional and G acts on it in the left-regular representation to furnish R.

In the case of complex group $G_{\mathbb{C}}$, principal series representations are obtained by considering *real* polarizations on the line bundle over $G_{\mathbb{C}}/H_\lambda$, where λ is now a non-complex-linear element of the dual $\mathfrak{g}^*_{\mathbb{C}}$. The set of all sections of this line bundle is the representation space of a representation induced from H_λ by $e^{i\lambda}$. To get the desired representation induced from the *Borel* subgroup $B = H_\lambda N$ by $e^{i\lambda} \otimes id$, the polarization is chosen precisely such that sections are independent of coordinates in N. (This process can also be extended to describe induction from generic non-maximal parabolic subgroups, *e.g.* by choosing λ such that its isotropy group H_λ is non-minimal.)

In both compact and complex cases, the representations of the group $G_{(\mathbb{C})}$ end up being described by choices of coadjoint orbits. Since a coadjoint orbit is defined by an element $\lambda \in \mathfrak{g}^*_{(\mathbb{C})} \simeq \mathfrak{g}_{(\mathbb{C})}$ *up to conjugacy*, this establishes an equivalence between representations and conjugacy classes of $\mathfrak{g}_{(\mathbb{C})}$.

Example: $SU(2)$

In the simplest case of $SU(2)$, let us write a matrix $g \in SU(2)$ as

$$g = \begin{pmatrix} w & -\bar z \\ z & \bar w \end{pmatrix}, \qquad w,\, z \,\in\, \mathbb{C}. \tag{7.2.5}$$

with $|w|^2 + |z|^2 = 1$. The right action of a diagonal matrix $\mathrm{diag}(e^{i\theta}, e^{-i\theta})$ in the maximal torus $H = \mathbb{T}$ acts by sending $(w, z) \mapsto (e^{i\theta}w, e^{i\theta}z)$. From this, we immediately see that $SU(2)$ has the geometry of S^3, and the H action is just rotation in the S^1 fiber of the Hopf bundle $S^1 \to S^3 \to S^2$. Therefore, a generic coadjoint orbit looks like

$$\Omega \simeq SU(2)/\mathbb{T} = S^2 \simeq \mathbb{P}^1\,. \tag{7.2.6}$$

We already know what all *holomorphic* bundles on $\mathbb{P}^1$ look like: they are tensor powers of the canonical line bundle, $\mathcal{O}(\tilde\lambda)$ for $-\tilde\lambda \in \mathbb{Z}$. These have curvature

$$\omega = -\mathrm{Tr}(\lambda g^{-1}dg \wedge g^{-1}dg)\,, \tag{7.2.7}$$

where λ is the matrix

$$\lambda = \frac{\tilde{\lambda}}{2i}\begin{pmatrix} 1 & 0 \\ 0 & -1 \end{pmatrix}, \tag{7.2.8}$$

or equivalently the corresponding element of $(\mathfrak{g}^*)_{\mathbb{C}}$ acting as $\mathrm{Tr}[\lambda, \cdot\,]$. Moreover, for $\tilde{\lambda} < 0$, the bundle $\mathcal{O}(-\tilde{\lambda})$ has an $(|\tilde{\lambda}| + 1)$-dimensional space of square-integrable holomorphic sections. A basis of this space is given by the polynomials $\{1, z, ..., z^{-\tilde{\lambda}}\}$ in local coordinates on $SU(2)/H$ where $w \neq 0$; this is precisely the $(|\tilde{\lambda}| + 1)$-dimensional representation of $SU(2)$. It is easy to see that the generators of the Lie algebra $\mathfrak{su}(2)$ act on local functions $f(z)$ exactly as in (7.1.4).

By using the symplectic form (7.2.6), and working in projective coordinates $(w : z)$ on $\mathbb{P}^1$, it is also possible to show that the variables $\bar{w}$ and $\bar{z}$ become identified after quantization with the conjugate momenta

$$\tilde{\lambda}\bar{w} \sim -\partial_w, \quad \tilde{\lambda}\bar{z} \sim -\partial_z. \tag{7.2.9}$$

Example: $SL(2, \mathbb{C})$

Let us write an element of $SL(2, \mathbb{C})$ in complex coordinates as

$$g = \begin{pmatrix} w & -x \\ z & y \end{pmatrix}, \quad wy + zx = 1, \qquad z, w, x, y \in \mathbb{C}\,. \tag{7.2.10}$$

We can also put $w = b+ic$, $y = b-ic$, $z = d+ie$, $x = d-ie$ (four new complex coordinates); then $SL(2, \mathbb{C}) = \{b^2 + c^2 + d^2 + e^2 = 1\} \simeq T^*S^3 \simeq T^*(SU(2))$.

There is a single Cartan subgroup (or maximal torus) $H = \mathbb{T}_{\mathbb{C}}$, and almost all of $SL(2, \mathbb{C})$ is conjugate to it. In the coadjoint orbit $SL(2, \mathbb{C})/\mathbb{T}_{\mathbb{C}}$, there is a rescaling symmetry $(w, z, x, y) \mapsto (aw, az, a^{-1}x, a^{-1}y)$ for $a \in \mathbb{C}^*$. A slightly nontrivial argument shows that $SL(2, \mathbb{C})/T_{\mathbb{C}}$ is isomorphic to $\{b^2 + c^2 + f^2 = 1\} \in \mathbb{C}^3$ (we have essentially set $f^2 = zx$ and used the scaling to set $x = 1$ or $z = 1$, or both, except at a point). Therefore, a genetic coadjoint orbit looks like

$$\Omega \simeq SL(2, \mathbb{C})/\mathbb{T}_C \simeq T^*S^2. \tag{7.2.11}$$

Unlike the case of $SU(2)$, this is a noncompact manifold, and will lead to infinite-dimensional Hilbert spaces (representations) upon geometric quantization.

In the case of $SU(2)$, we implicitly extended the isomorphism $\mathfrak{g}^* \simeq \mathfrak{g}$ to an isomorphism $(\mathfrak{g}^*)_{\mathbb{C}} \simeq \mathfrak{g}$ by complex linearity. We need do the same for the Lie algebra $\mathfrak{sl}(2, \mathbb{C})$, viewed as

a *real* Lie algebra in order to access principal series representations. To simplify notation, let $\mathfrak{g} = \mathfrak{sl}(2,\mathbb{C})$ (rather than using $\mathfrak{g}_{\mathbb{C}}$). Then, as in Section 7.1, the complexification of this real Lie algebra satisfies $\mathfrak{g}_{\mathbb{C}} \simeq \mathfrak{g} \times \mathfrak{g}$. An appropriate complexification of the nondegenerate trace form ReTr is given by $\langle\, ,\, \rangle : \mathfrak{g}^{\mathbb{C}} \times \mathfrak{g} \simeq (\mathfrak{g} \times \mathfrak{g}) \times \mathfrak{g} \to \mathbb{C}$, such that

$$\langle (X_L, X_R), Y\rangle = \frac{1}{2}\mathrm{Tr}(X_L\, Y) + \frac{1}{2}\mathrm{Tr}(X_R\, \bar{Y}\,, \tag{7.2.12}$$

where $\bar{Y}$ denotes the usual complex conjugation in the ("broken") complex structure on $\mathfrak{sl}(2,\mathbb{C})$. This leads to an identification of linear functionals and matrices

$$\nu \in (\mathfrak{a}^*)^{\mathbb{C}} \;\leftrightarrow\; \nu = -\frac{iw}{2}\begin{pmatrix} 1 & 0 \\ 0 & -1 \end{pmatrix}, \qquad \kappa \in (\mathfrak{m}^*)^{\mathbb{C}} \;\leftrightarrow\; \kappa = -\frac{i\not{k}}{2}\begin{pmatrix} 1 & 0 \\ 0 & -1 \end{pmatrix}. \tag{7.2.13}$$

The pair $\nu \oplus \kappa \in (\mathfrak{m}^* \oplus \mathfrak{a}^*)^{\mathbb{C}} \subset (\mathfrak{g}^*)^{\mathbb{C}}$ is identified with

$$\nu \oplus \kappa \;\;\leftrightarrow\;\; (X_L, X_R) = (\nu + \kappa, \nu - \kappa) \;\;\in \mathfrak{sl}(2,\mathbb{C})^{\mathbb{C}} \simeq \mathfrak{sl}(2,\mathbb{C}) \times \mathfrak{sl}(2,\mathbb{C})\,. \tag{7.2.14}$$

The natural symplectic form resulting from the above isomorphism is

$$\omega_{\nu,\kappa} = \frac{1}{2}\mathrm{Tr}((\nu+\kappa)g^{-1}dg \wedge g^{-1}dg) + \frac{1}{2}\mathrm{Tr}((\nu-\kappa)\overline{g^{-1}dg \wedge g^{-1}dg}). \tag{7.2.15}$$

Due to the compact cycle S^2 in the coadjoint orbit $\Omega \simeq T^*S^2$, this form can is the curvature of a line bundle $\mathcal{L}$ if and only if $k \in \mathbb{Z}$. Moreover, when the line bundle $\mathcal{L}$ exists, it will be unique (since T^*S^2 is simply-connected). Using a polarization in which sections of $\mathcal{L}$ depend only on a single complex projective coordinate $(w : z)$, we see that the sections induced from $e^{i\nu+i\kappa+\rho}$ will transform as

$$f(aw, az, \bar{a}\bar{w}, \bar{a}\bar{z}) = a^{-\frac{1}{2}(w+\not{k})-1}\bar{a}^{-\frac{1}{2}(w-\not{k})-1} f(w, z, \bar{w}, \bar{z}), \quad a \in \mathbb{C}^*. \tag{7.2.16}$$

This, of course, is precisely the right transformation for the principal series representation $\mathcal{P}^{\not{k},w}$.

The conjugate momenta to the complex projective coordinates $(w : z)$ and $(\bar{w} : \bar{z})$ are

$$x \sim \frac{-2}{w+\not{k}}\partial_z, \quad y \sim \frac{-2}{w+\not{k}}\partial_w, \quad \bar{x} \sim \frac{-2}{w-\not{k}}\bar{\partial}_z, \quad \bar{y} \sim \frac{-2}{w-\not{k}}\bar{\partial}_w\,. \tag{7.2.17}$$

On sections of $\mathcal{L}$, one has that

$$z\partial_z + w\partial_w = -\frac{1}{2}(w+\not{k}) - 1, \qquad \bar{z}\bar{\partial}_z + \bar{w}\bar{\partial}_w = -\frac{1}{2}(w-\not{k}) - 1. \tag{7.2.18}$$

7.3 Quantum mechanics for Wilson loops

For compact gauge groups, Wilson loops in a representation R supported on a curve C are typically written as

$$W_R(C;\mathcal{A}) = \mathrm{Tr}_R \,\mathrm{Hol}_C \mathcal{A} = \mathrm{Tr}_R \left[P \oint_C e^{\mathcal{A}} \right]. \tag{7.3.1}$$

Unfortunately, "Tr_R" does not entirely make sense for infinite-dimensional representations of complex gauge groups. It may be possible to replace this trace with a distributional character from the mathematical theory of reductive Lie groups in order to define infinite-dimensional Wilson loops. However, a better approach was suggested during the early development of Chern-Simons theory with compact gauge group: Wilson loops as in (7.3.1) can alternatively be written as path integrals in a quantum mechanical theory of particles moving along the loop [122, 128, 28]. Specifically, one has

$$W_R(K;\mathcal{A}) = \int_{LG/LH} \mathcal{D}g \, e^{iS[g]}, \qquad S[g] = \int_C \mathrm{Tr}(\lambda g^{-1}(d+\mathcal{A})g)\,, \tag{7.3.2}$$

For compact groups, λ is the highest weight of the finite-dimensional representation R, identified with an element of $\mathfrak{g}$ via Tr. In this section, we will explain why (7.3.2) makes sense for compact groups (a thorough discussion seems absent from the literature). Then we will show that a version of this formula works perfectly for noncompact groups when λ is identified with the quasi-character of an induced representation.

In the path integral (7.3.2), we let $0 \geq t < 2\pi$ be the time coordinate along the loop C. The path integral goes over maps $g : C \to G$, in other words over the loop group LG. There is, however, a gauge symmetry: any right-translation $g \mapsto gh$, with h belonging to the isotropy group H_λ of λ for all t, leaves the integrand e^{iS} invariant. (This holds for compact or noncompact G.) Thus one really integrates over the space LG/LH.

Let $\mathcal{A}_t dt$ be the component of $\mathcal{A}$ along the loop C. The Lagrangian of the action in (7.3.2) is $L = \mathrm{Tr}(\lambda g^{-1}(\partial_t g - A_t g))$. If we somewhat naively take g_{ij} to be our coordinates, we find that canonical momenta are

$$p_{ij} = \frac{\partial L}{\partial(\partial_t g_{ij})} = (\lambda g^{-1})_{ji}.$$

We can then construct a (local) symplectic form for this system as

$$\omega = dp_{ij} \wedge dg_{ij} = \mathrm{Tr}(\lambda dg^{-1} \wedge dg) = \mathrm{Tr}((-\lambda) g^{-1} dg \wedge g^{-1} dg). \tag{7.3.3}$$

Finally, to find the (classical) Hamiltonian, we calculate

$$\mathcal{H} = p_{ij}\partial_t g_{ij} - L = -\mathrm{Tr}(\lambda g^{-1} A_t g). \tag{7.3.4}$$

In order to justify (7.3.2), we will proceed to quantize the path integral in a Hamiltonian formalism, and rewrite the partition function as a trace over an appropriate Hilbert space. To this end, consider the system at some fixed time t. The classical phase space of the system is just G/H_λ, since all elements of presumed canonical momenta λg^{-1} are just algebraic functions of the elements of g. (Put another way, this is a first-order Lagrangian, so both momenta and coordinates are contained in g.) But then the symplectic form (7.3.3) on G/H_λ is nothing but the canonical symplectic form (7.2.3) on the coadjoint orbit of weight $-\lambda \in \mathfrak{g}^*$, at least if G is compact. Therefore, we immediately conclude that the Hilbert space of this quantum mechanical system is the space of the representation with highest weight λ.

Somewhat less trivially, we claim that the quantization of the Hamiltonian $i\mathcal{H} = -i\mathrm{Tr}(\lambda g^{-1}\mathcal{A}_t g)$ is precisely the matrix $\mathcal{A}_t$ acting on the Hilbert space in the representation with highest weight λ. In other words, conjugation by a quantum operator g effectively converts matrices into the right coadjoint orbit representation! Then we can simply "cut" the Wilson loop in the path integral at time $t = 0$ and use to Hamiltonian formalism to see that

$$\int \mathcal{D}g\, e^{iS[g]} = \mathrm{Tr}_{\text{Hilbert space}}\, T\, \exp\Big(\int_0^{2\pi} i\mathcal{H}(t)\, dt\Big), \tag{7.3.5}$$

becomes precisely the holonomy of the gauge connection $\mathcal{A}$ (where T is a time ordering that because the Wilson loop path ordering).

For $G = SU(2)$, the claim that the Hamiltonian is just the matrix $\mathcal{A}$ acting on the Hilbert space can be proven explicitly by writing $\mathcal{A}_t = aH + bE + cF$ and simply expressing $-i\mathrm{Tr}(\lambda g^{-1}\ \cdot\ g)$ in terms of quantum operators for each generator H, E, F. For example, with λ as in (7.2.8) and operators as in (7.2.9) we find

$$\begin{aligned}
-i\mathrm{Tr}(\lambda g^{-1} E g) &= -\frac{\tilde{\lambda}}{2}\mathrm{Tr}\Big[\begin{pmatrix} \bar{w} & \bar{z} \\ z & -w \end{pmatrix}\begin{pmatrix} 0 & 1 \\ 0 & 0 \end{pmatrix}\begin{pmatrix} w & -\bar{z} \\ z & \bar{w} \end{pmatrix}\Big] \\
&= -\tilde{\lambda} z\bar{w} \\
&= -z\partial_w \\
&\simeq -\tilde{\lambda} z + z^2\partial_z\,,
\end{aligned}$$

and similarly $-i\mathrm{Tr}(\lambda g^{-1}Hg) = -\tilde{\lambda} + 2z\partial_z$ and $-i\mathrm{Tr}(\lambda g^{-1}Fg) = -\partial_z$.

Wilson loops for complex groups

In the case of $G_{\mathbb{C}} = SL(2,\mathbb{C})$, we propose that a Wilson loop in representation $\mathcal{P}^{\kappa,w}$ be defined by the path integral (7.3.2), but with an action

$$S = -\frac{1}{2}\int_C \mathrm{Tr}[(\nu+\kappa)g^{-1}(d+\mathcal{A})g + (\nu-\kappa)\overline{g^{-1}(d+\mathcal{A})g}], \tag{7.3.6}$$

This modified action will lead exactly to the symplectic form (7.2.15) relevant for constructing principal series representations from coadjoint orbits.

To show that the resulting Hamiltonian $i\mathcal{H} = \frac{i}{2}\mathrm{Tr}[(\nu+\kappa)g^{-1}\mathcal{A}g + (\nu-\kappa)\bar{g}^{-1}\bar{\mathcal{A}}\bar{g}]$ is again just $\mathcal{A}$ in the $\mathcal{P}^{\kappa,w}$ representation, we can use the operator expressions (7.2.17) and explicitly derive the operators for basis elements $\mathcal{A} = H, \tilde{H}, E, \tilde{E}, F, \tilde{F}$ just as in the $SU(2)$ case.

For other complex gauge groups, this procedure can be easily generalized. The action (7.3.6) will still involve a sum of two terms, but ν and κ need to be replaced by the relevant linear functionals that induce the desired principal series representation.

7.4 Wilson loops *vs.* boundary conditions

As a culmination of the above theory and proposal for defining Wilson loops with infinite-dimensional representations, we can finally derive the relation between a partition function on a knot complement and a partition function with a knot in Chern-Simons theory with complex gauge group. We obtain a map between boundary conditions and representations, and use it to explain the limits used in the "analytic continuation" of Chapter 6.

As a starting point, for arbitrary gauge group G and a Euclidean 3-manifold M, consider the action

$$I_{CS}[\mathcal{A}] = \frac{1}{4\pi}\int_M \mathrm{Tr}\big(\mathcal{A}\wedge d\mathcal{A} + \frac{2}{3}A\wedge\mathcal{A}\wedge\mathcal{A}\big)\,. \tag{7.4.1}$$

If we put the theory on a manifold of topology $\mathbb{R}\times\Sigma$ (or $S^1\times\Sigma$), where Σ is some 2-surface, we can split the gauge field into a component A^t along "time" $\mathbb{R}$, and a "spatial" component

$\mathcal{A}^\perp$. With suitable boundary conditions on $\mathcal{A}^t$ at ∂M, we can integrate by parts and rewrite

$$I_{CS}[\mathcal{A}] = \frac{1}{4\pi}\int_M \mathrm{Tr}(\mathcal{A}^\perp \wedge d\mathcal{A}^\perp) + \frac{1}{2\pi}\int_M F^\perp \wedge \mathcal{A}^t\,, \tag{7.4.2}$$

where $F^\perp = d\mathcal{A}^\perp + \mathcal{A}^\perp \wedge \mathcal{A}^\perp$ is the curvature of $A^\perp$. Then the field A^t becomes nondynamical, and we can integrate it out to obtain a condition

$$F^\perp = 0 \tag{7.4.3}$$

which the new path integral in $\mathcal{A}^\perp$ must obey. This is the origin of the reasoning that we restrict to moduli spaces of flat connections in geometric quantization: the classical phase space of the theory consists of flat connections $\mathcal{A}^\perp$ on Σ (at fixed t), modulo gauge transformations.

We want to specialize the theory to compact and complex gauge groups, and to show how condition (7.4.3) is altered by Wilson loops. The compact case was considered in (*e.g.*) [122], but we review it because it will be relevant for analytic continuation.

Representations and boundary conditions for compact groups

Chern-Simons theory with compact gauge group (say $SU(N)$) has an action $S = kI_{CS}$. Gauge-invariance under large gauge transformations on M force the constant k to be an integer. By fixing orientation on M, one usually takes k to be a positive integer – the level of the theory.

Now put the theory on $S^1 \times \Sigma$ and add a Wilson loop in representation λ parallel to the S^1. Let t be the coordinate on S^1 as before, and let (x_1, x_2) be local coordinates on Σ, so that the Wilson loop goes through $(x_1, x_2) = 0$. From Section 7.3, we know that we can write the path integral of the theory with the Wilson loop insertion as $\int \mathcal{D}\mathcal{A}\,\mathcal{D}g\, e^{iS}$, where the full effective action is

$$\begin{aligned} S &= kI_C S + \int_C \mathrm{Tr}(\lambda g^{-1}(d+\mathcal{A})g) \\ &= kI_{CS} + \int_M \delta(x) dx_1 \wedge dx_2 \wedge \mathrm{Tr}(\lambda g^{-1}(d+\mathcal{A}^t)g)\,. \end{aligned} \tag{7.4.4}$$

Therefore, we can again integrate out $\mathcal{A}^t$. However, instead of complete flatness in the perpendicular directions, we now obtain the constraint[2]

$$\frac{k+h^\vee}{2\pi}F^\perp + g(\lambda+\rho)g^{-1}\delta(x)dx_1 \wedge dx_2 = 0. \tag{7.4.5}$$

[2]When performing this integration in the full quantum theory for compact gauge groups, two

In other words, $\mathcal{A}^\perp$ must be flat everywhere on Σ *except* at the point $x = 0$. At fixed time t_0, we can take a small disc $D \subset \Sigma$ around $x = 0$ and integrate $F^\perp$ on it to find

$$\frac{k+h^\vee}{2\pi}\int_D F^\perp = -g(t_0)(\lambda+\rho)g^{-1}(t_0) = \frac{k}{2\pi}\log \mathrm{Hol}_{\partial D}(\mathcal{A}^\perp).$$

For $SU(2)$ (for example), this argument shows that the holonomy of $\mathcal{A}^\perp$ linking the Wilson loop is always conjugate to

$$\mathrm{Hol}_{\partial D}(\mathcal{A}^\perp) \overset{conj}{\sim} \begin{pmatrix} e^{\frac{i\pi}{k+2}N} & 0 \\ 0 & e^{-\frac{i\pi}{k+2}N} \end{pmatrix}, \tag{7.4.6}$$

where $N = \tilde{\lambda} + 1 \sim \lambda + \rho$ is the dimension of a given representation.

Representations and boundary conditions for complex groups

Let us consider $SL(2,\mathbb{C})$ theory. The Chern-Simons action is (5.1.1) is $\frac{t}{2}I_{CS}[\mathcal{A}] + \frac{\bar{t}}{2}I_{CS}[\bar{\mathcal{A}}]$. The appropriate Wilson loop action is given by (7.3.6). Treating $\mathcal{A}$ and $\bar{\mathcal{A}}$ as independent fields, we can separately integrate out both $\mathcal{A}^t$ and $\bar{\mathcal{A}}^t$, yielding *two* constraints:

$$\frac{t}{4\pi}F^\perp - \frac{1}{2}g(\nu+\kappa)g^{-1}\,\delta(x)dx_1\wedge dx_2 = 0, \tag{7.4.7a}$$

$$\frac{\bar{t}}{4\pi}\bar{F}^\perp - \frac{1}{2}\bar{g}(\nu-\kappa)\bar{g}^{-1}\,\delta(x)dx_1\wedge dx_2 = 0. \tag{7.4.7b}$$

These only makes sense if F and $\bar{F}$ obey conjugate equations.

We can also look at restrictions imposed by unitarity. As explained in Section 5.1, there are two possible unitarity structures for Chern-Simons theory with complex gauge group. In both structures, constraints (7.4.7) become compatible if unitary principal series representations ($w \in i\mathbb{R}$, $k \in \mathbb{Z}$) are used for the Wilson loop. In the Chern-Simons unitarity structure relevant for Euclidean quantum gravity, with $t, \bar{t} \in \mathbb{R}$, representations with $w \in \mathbb{R}$ are also allowed. Therefore, it may be possible to have Wilson loops with complementary series representations as well.[3]

matching shifts of "coupling constants" happen: the Chern-Simons level k is shifted to $k + h^\vee$ (where $h^\vee$ is the dual Coxeter number of G), and the weight λ is shifted to $\lambda + \rho$ (where ρ is half the sum of positive roots). Neither of these happen in the complex case [48].

[3]This may explain a short remark by Witten in [39] that the unitarity structure relevant for Euclidean quantum gravity is related to complementary series representations.

The holonomy of $\mathcal{A}$ is given generically by

$$\mathrm{Hol}_{\partial D}(\mathcal{A}^{\perp}) \overset{conj}{\sim} \begin{pmatrix} e^{-\frac{i\pi}{t}(w+\ell)} & 0 \\ 0 & e^{\frac{i\pi}{t}(w+\ell)} \end{pmatrix}. \tag{7.4.8}$$

Again, for more general complex gauge group this expression will simply be generalized to contain various eigenvalues of the linear functionals or quasi-characters that characterize principal series representations.

TQFT

The above arguments relate representations and conjugacy classes of the holonomy of $\mathcal{A}$. Another way of phrasing the results is that the Chern-Simons path integral on a solid torus $D^2 \times S^1$ with a knot in its center is always an exact delta-function that forces the holonomy of $\mathcal{A}$ around the (contractible) cycle on the boundary of this torus to be determined by the representation on the knot. By cutting solid neighborhoods of knots out of three-manifolds, this then shows that a partition function with a Wilson loop is equivalent to a partition function on the loop's complement with fixed boundary conditions. A somewhat longer discussion of this relation appears in the review [6].

Analytic continuation

Let us finally use these results to motivate the limit used in the analytic continuation of Chern-Simons theory with compact group G to Chern-Simons theory with complex group $G_{\mathbb{C}}$.

In Chapter 6, we considered $SL(2,\mathbb{C})$ (say) Chern-Simons theory on a knot complement, with a boundary condition that the holomony of $\mathcal{A}$ on a small loop linking the knot was

$$\mathrm{Hol}_{bdy}(\mathcal{A}) \overset{conj}{\sim} \begin{pmatrix} e^{u} & 0 \\ 0 & e^{-u} \end{pmatrix}. \tag{7.4.9}$$

Comparing this to the holonomy (7.4.6) of $SU(2)$ theory, we see that

$$u \equiv \frac{i\pi N}{k+2} = N\hbar\,. \tag{7.4.10}$$

Thus, one must "analytically continue" at this fixed value of $N/(k+2)$. For general groups

G and $G_{\mathbb{C}}$, the relation will be

$$u \equiv \frac{i\pi(\lambda+\rho)}{k+h^{\vee}} = (\lambda+\rho)\hbar\,. \tag{7.4.11}$$

From the relation (7.4.8), we also finally see that u is related to a principal series $SL(2,\mathbb{C})$ representation $\mathcal{P}^{\cancel{k},w}$ via

$$u = (-)\frac{i\pi(w+\cancel{k})}{t}\,. \tag{7.4.12}$$

Chapter 8

The state integral model

In this chapter, we introduce a "state integral" model for $Z^{(\rho)}(M;\hbar)$ in the simplest case of $G_{\mathbb{C}} = SL(2,\mathbb{C})$. Our construction will rely heavily on the work of Hikami [52, 53], where a new invariant of hyperbolic 3-manifolds was introduced using ideal triangulations. The resulting invariant is very close to the state integral model we are looking for. However, in order to make it into a useful tool for computing $Z^{(\rho)}(M;\hbar)$ we will need to understand Hikami's construction better and make a number of important modifications. In particular, as we explain below, Hikami's invariant is written as a certain integral along a path in the complex plane (or, more generally, over a hypersurface in complex space) which was ill-defined[1] in the original work [52, 53]. Another issue that we need to address is how to incorporate in Hikami's construction a choice of the homomorphisms (5.1.4) (page 82),

$$\rho : \pi_1(M) \to SL(2,\mathbb{C})\,. \tag{8.0.1}$$

(The original construction assumes very special choices of ρ that we called "geometric" in Section 5.2.) It turns out that these two questions are not unrelated and can be addressed simultaneously, so that Hikami's invariant can be extended to a state sum model for $Z^{(\rho)}(M;\hbar)$ with an arbitrary ρ.

To properly describe the state integral model, we will need a more thorough review of the properties of hyperbolic manifolds and hyperbolic triangulations, presented in Section

[1] The choice mentioned in [52, 53] is to integrate over the real axis (resp. real subspace) of the complex parameter space. While this choice is in some sense natural, it encounters some very bad singularities and a closer look shows that it cannot be correct.

8.1. The state integral model that we give here depends on ideal hyperbolic triangulations.[2] We will also take a small digression in Section 8.3 to define and discuss the main properties of the *quantum dilogarithm*. This function is central to the state integral model, and has also appeared previously in the description of motivic BPS invariants, back in Chapter 4.

Throughout this chapter, we work in the u-space representation for $SL(2,\mathbb{C})$ partition functions. In particular, we use the identification (6.1.16) and denote the perturbative $SL(2,\mathbb{C})$ invariant as $Z^{(\alpha)}(M;\hbar,u)$. The discussion here follows [3].

8.1 Hyperbolic geometry

The construction of a state integral model described in the rest of this chapter applies to orientable hyperbolic 3-manifolds of finite volume (possibly with boundary) and uses ideal triangulations in a crucial way. Therefore, we begin this section by reviewing some relevant facts from hyperbolic geometry (more details can be found in [113, 129, 130]).

Recall that hyperbolic 3-space $\mathbb{H}^3$ can be represented as the upper half-space $\{(x_1,x_2,x_3)|\ x_3>0\}$ with metric (5.2.7) of constant curvature -1. The boundary $\partial\mathbb{H}^3$, topologically an $\mathbf{S}^2$, consists of the plane $x_3=0$ together with the point at infinity. The group of isometries of $\mathbb{H}^3$ is $PSL(2,\mathbb{C})$, which acts on the boundary via the usual Möbius transformations. In this picture, geodesic surfaces are spheres of any radius which intersect $\partial\mathbb{H}^3$ orthogonally.

An ideal tetrahedron Δ in $\mathbb{H}^3$ has by definition all its faces along geodesic surfaces, and all its vertices in $\partial\mathbb{H}^3$ — such vertices are called *ideal points*. After Möbius transformations, one can fix three of the vertices at $(0,0,0)$, $(1,0,0)$, and infinity. The coordinate of the fourth vertex $(x_1,x_2,0)$, with $x_2\geq 0$, defines a complex number $z=x_1+ix_2$ called the *shape parameter* (sometimes also called *edge parameter*). At various edges, the faces of the tetrahedron Δ form dihedral angles $\arg z_j$ $(j=1,2,3)$ as indicated in Figure 8.1, with

$$z_1=z\,,\quad z_2=1-\frac{1}{z}\,,\quad z_3=\frac{1}{1-z}\,. \tag{8.1.1}$$

The ideal tetrahedron is noncompact, but has finite volume given by

$$\mathrm{Vol}(\Delta_z)\ =\ D(z)\,, \tag{8.1.2}$$

[2]It is nevertheless fairly clear that it should work for general three-manifolds, in part because any three-manifold with boundary *has* an ideal topological triangulation even when its hyperbolic volume is zero. A description of the state sum model for torus knots will appear in [5].

where $D(z)$ is the Bloch-Wigner dilogarithm function, related to the usual dilogarithm Li_2 (see Section 8.3) by

$$D(z) = \mathrm{Im}\big(\mathrm{Li}_2(z)\big) + \arg(1-z)\,\log|z|\,. \tag{8.1.3}$$

Note that any of the z_j can be taken to be the shape parameter of Δ, and that $D(z_j) = \mathrm{Vol}(\Delta_z)$ for each j. We will allow shape parameters to be any complex numbers in $\mathbb{C}-\{0,1\}$, noting that for $z \in \mathbb{R}$ an ideal tetrahedron is degenerate and that for $\mathrm{Im}\, z < 0$ it technically has negative volume due to its orientation.

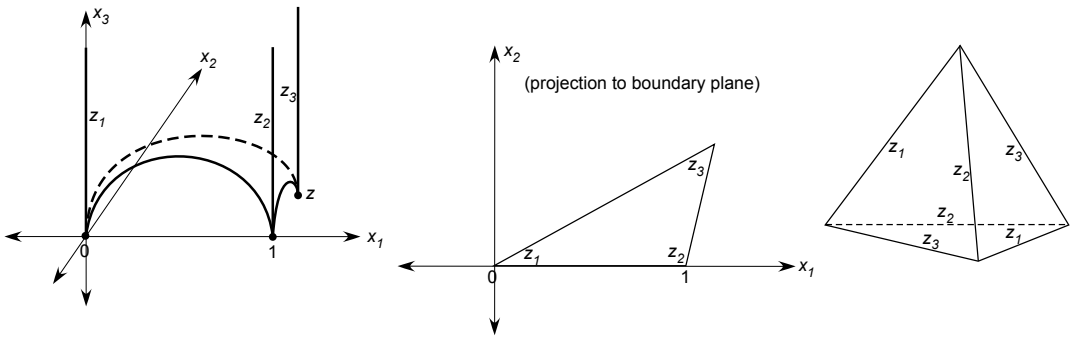

Figure 8.1: An ideal tetrahedron in $\mathbb{H}^3$.

A hyperbolic structure on a 3-manifold is a metric that is locally isometric to $\mathbb{H}^3$. A 3-manifold is called hyperbolic if it admits a hyperbolic structure that is geodesically complete and has finite volume. Most 3-manifolds are hyperbolic, including the vast majority of knot and link complements in $\mathbf{S}^3$. Specifically, a knot complement is hyperbolic as long as the knot is not a torus or satellite knot [131]. Every closed 3-manifold can be obtained via Dehn surgery on a knot in $\mathbf{S}^3$, and for hyperbolic knots all but finitely many such surgeries yield hyperbolic manifolds [113].

By the Mostow rigidity theorem [132, 133], the complete hyperbolic structure on a hyperbolic manifold is unique. Therefore, geometric invariants like the hyperbolic volume are actually topological invariants. For the large class of hyperbolic knot complements in $\mathbf{S}^3$, the unique complete hyperbolic structure has a parabolic holonomy with unit eigenvalues around the knot. In $SL(2,\mathbb{C})$ Chern-Simons theory, this structure corresponds to the "geometric" flat connection $\mathcal{A}^{(\mathrm{geom})}$ with $u = 0$. As discussed in Section 5.2, hyperbolic manifolds with complete hyperbolic structures can also be described as quotients $\mathbb{H}^3/\Gamma$.

Given a hyperbolic knot complement, one can deform the hyperbolic metric in such a way that the holonomy u is not zero. Such deformed metrics are unique in a neighborhood

of $u = 0$, but they are not geodesically complete. For a discrete set of values of u, one can add in the "missing" geodesic, and the deformed metrics coincide with the unique complete hyperbolic structures on closed 3-manifolds obtained via appropriate Dehn surgeries on the knot in $\mathbf{S}^3$. For other values of u, the knot complement can be completed by adding either a circle S^1 or a single point, but the resulting hyperbolic metric will be singular. For example, if $u \in i\mathbb{R}$ one adds a circle and the resulting metric has a conical singularity. These descriptions can easily be extended to link complements (*i.e.* multiple cusps), using multiple parameters u_k, one for each link component.

Any orientable hyperbolic manifold M is homeomorphic to the interior of a compact 3-manifold $\bar{M}$ with boundary consisting of finitely many tori. (The manifold M itself can also be thought of as the union of $\bar{M}$ with neighborhoods of the cusps, each of the latter being homeomorphic to $T^2 \times [0, \infty)$.) All hyperbolic manifolds therefore arise as knot or link complements in closed 3-manifolds. Moreover, every hyperbolic manifold has an ideal triangulation, *i.e* a finite decomposition into (possibly degenerate[3]) ideal tetrahedra; see *e.g.* [113, 134].

To reconstruct a hyperbolic 3-manifold M from its ideal triangulation $\{\Delta_i\}_{i=1}^N$, faces of tetrahedra are glued together in pairs. One must remember, however, that vertices of tetrahedra are not part of M, and that the combined boundaries of their neighborhoods in M are not spheres, but tori. (Thus, some intuition from simplicial triangulations no longer holds.) There always exists a triangulation of M whose edges can all be oriented in such a way that the boundary of every face (shared between two tetrahedra) has two edges oriented in the same direction (clockwise or counterclockwise) and one opposite. Then the vertices of each tetrahedron can be canonically labeled 0, 1, 2, 3 according to the number of edges entering the vertex, so that the tetrahedron can be identified in a unique way with one of the two numbered tetrahedra shown in Figure 8.3 of the next subsection. This at the same time orients the tetrahedron. The orientation of a given tetrahedron Δ_i may not agree with that of M; one defines $\epsilon_i = 1$ if the orientations agree and $\epsilon_i = -1$ otherwise. The edges of each tetrahedron can then be given shape parameters $(z_1^{(i)}, z_2^{(i)}, z_3^{(i)})$, running counterclockwise around each vertex (viewed from outside the tetrahedron) if $\epsilon_i = 1$ and clockwise if $\epsilon_i = -1$.

For a given M with cusps or conical singularities specified by holonomy parameters u_k,

[3]It is conjectured and widely believed that nondegenerate tetrahedra alone are always sufficient.

the shape parameters $z_j^{(i)}$ of the tetrahedra Δ_i in its triangulation are fixed by two sets of conditions. First, the product of the shape parameters $z_j^{(i)}$ at every edge in the triangulation must be equal to 1, in order for the hyperbolic structures of adjacent tetrahedra to match. More precisely, the sum of some chosen branches of $\log z_j^{(i)}$ (equal to the standard branch if one is near the complete structure) should equal $2\pi i$, so that the total dihedral angle at each edge is 2π. Second, one can compute holonomy eigenvalues around each torus boundary in M as a product of $z_j^{(i)}$'s by mapping out the neighborhood of each vertex in the triangulation in a so-called developing map, and following a procedure illustrated in, *e.g.*, [114]. There is one distinct vertex "inside" each boundary torus. One then requires that the eigenvalues of the holonomy around the kth boundary are equal to $e^{\pm u_k}$. These two conditions will be referred to, respectively, as *edge* and *cusp* relations.

Every hyperbolic 3-manifold has a well-defined class in the Bloch group [135]. This is a subgroup[4] of the quotient of the free $\mathbb{Z}$-module $\mathbb{Z}[\mathbb{C} - \{0, 1\}]$ by the relations

$$[x] - [y] + [\frac{y}{x}] - [\frac{1 - x^{-1}}{1 - y^{-1}}] + [\frac{1 - x}{1 - y}] = 0\,. \tag{8.1.4}$$

This five-term or pentagon relation accounts for the fact that a polyhedron with five ideal vertices can be decomposed into ideal tetrahedra in multiple ways. The five ideal tetrahedra in this polyhedron (each obtained by deleting an ideal vertex) can be given the five shape parameters x, y, y/x, ... appearing above. The signs of the different terms correspond to orientations. Geometrically, an instance of the five-term relation can be visualized as the 2-3 Pachner move, illustrated in Figure 8.2.

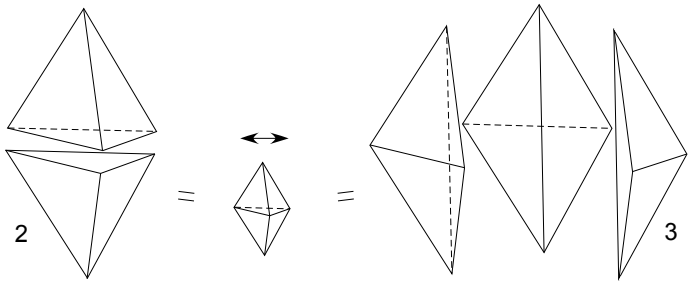

Figure 8.2: The 2-3 Pachner move.

The class $[M]$ of a hyperbolic 3-manifold M in the Bloch group can be computed by summing (with orientation) the shape parameters $[z]$ of any ideal triangulation, but it

[4]Namely, the kernel of the map $[z] \mapsto 2z \wedge (1 - z) \in \mathbb{C}^* \wedge_{\mathbb{Z}} \mathbb{C}^*$ acting on this quotient module.

is *independent* of the triangulation. Thus, hyperbolic invariants of 3-manifolds may be obtained by functions on the Bloch group — *i.e.* functions compatible with (8.1.4). For example, the Bloch-Wigner function (8.1.3) satisfies

$$D(x) - D(y) + D\big(\frac{y}{x}\big) - D\big(\frac{1-x^{-1}}{1-y^{-1}}\big) + D\big(\frac{1-x}{1-y}\big) = 0\,, \tag{8.1.5}$$

and the hyperbolic volume of a manifold M triangulated by ideal tetrahedra $\{\Delta_i\}_{i=1}^N$ can be calculated as

$$\mathrm{Vol}(M) = \sum_{i=1}^{N} \epsilon_i D(z^{(i)})\,. \tag{8.1.6}$$

The symbols ϵ_i here could be removed if shape parameters were assigned to tetrahedra in a manner independent of orientation, noting that reversing the orientation of a tetrahedron corresponds to sending $z \mapsto 1/z$ and that $D(1/z) = -D(z)$. This is sometimes seen in the literature.

The complexified volume $i(\mathrm{Vol}(M) + i\mathrm{CS}(M))$ is trickier to evaluate. For a hyperbolic manifold with a spin structure, corresponding to full $SL(2,\mathbb{C})$ holonomies, this invariant is defined modulo $4\pi^2$. Here, we will outline a computation of the complexified volume modulo π^2, following [136]; for the complete invariant modulo $4\pi^2$, see [137]. To proceed, one must first make sure that the three shape parameters $z^{(i)} = z_1^{(i)}$, $z_2^{(i)}$, and $z_3^{(i)}$ are specifically assigned to edges $[v_1^{(i)}, v_2^{(i)}]$, $[v_1^{(i)}, v_3^{(i)}]$, and $[v_1^{(i)}, v_2^{(i)}]$ (respectively) in each tetrahedron Δ_i of an oriented triangulation of M, where $[v_a^{(i)}, v_b^{(i)}]$ denotes the edge going from numbered vertex $v_a^{(i)}$ to numbered vertex $v_b^{(i)}$. One also chooses logarithms $(w_1^{(i)}, w_2^{(i)}, w_3^{(i)})$ of the shape parameters such that

$$e^{w_1^{(i)}} = \pm z_1^{(i)}\,, \quad e^{w_2^{(i)}} = \pm z_2^{(i)}\,, \quad e^{w_3^{(i)}} = \pm z_3^{(i)}\,, \tag{8.1.7a}$$

$$w_1^{(i)} + w_2^{(i)} + w_3^{(i)} = 0 \quad \forall\, i\,, \tag{8.1.7b}$$

and defines integers $(q^{(i)}, r^{(i)})$ by

$$w_1^{(i)} = \mathrm{Log}(z^{(i)}) + \pi i q^{(i)}\,, \qquad w_2^{(i)} = -\mathrm{Log}(1 - z^{(i)}) + \pi i r^{(i)}\,, \tag{8.1.8}$$

where Log denotes the principal branch of the logarithm, with a cut from 0 to $-\infty$. For a consistent labeling of the triangulation, called a "combinatorial flattening," the sum of log-parameters $w_j^{(i)}$ around every edge must vanish, and the (signed[5]) sum of log-parameters

[5]Signs arise from tetrahedron orientations and the sense in which a path winds around edges; see [136], Def. 4.2.

along the two paths generating $\pi_1(T^2) = \mathbb{Z}^2$ for any boundary (cusp) T^2 must equal twice the logarithm of the $SL(2,\mathbb{C})$ holonomies around these paths.[6] The complexified volume is then given, modulo π^2, as

$$i(\mathrm{Vol}(M) + i\mathrm{CS}(M)) \;=\; \sum_{i=1}^{N} \epsilon_i \mathrm{L}(z^{(i)}; q^{(i)}, r^{(i)}) - \sum_{\text{cusps } k} (v_k \overline{u}_k + i\pi u_k)\,, \tag{8.1.9}$$

with

$$\mathrm{L}(z; q, r) = \mathrm{Li}_2(z) + \frac{1}{2}(\mathrm{Log}(z) + \pi i q)(\mathrm{Log}(1-z) + \pi i r) + \frac{\pi^2 q r}{2} - \frac{\pi^2}{6}\,. \tag{8.1.10}$$

The function $\mathrm{L}(z; q, r)$, a modified version of the Rogers dilogarithm, satisfies a five-term relation in an extended Bloch group that lifts (8.1.4) in a natural way to the space of log-parameters.[7]

8.1.1 Example: figure-eight knot complement

Let K be the figure-eight knot (shown in Figure 6.1) and let M be its complement in the 3-sphere. In order to compute the perturbative invariants $S_n^{(\rho)}$ for an arbitrary $\rho:\ \pi_1(M) \ \to\ SL(2,\mathbb{C})$ we first need to review the classical geometry of M in more detail and, in particular, to describe the moduli space of flat $SL(2,\mathbb{C})$ connections on M. As we already mentioned earlier, the knot group $\pi_1(M)$ is generated by two elements, a and b, such that $a^{-1}bab^{-1}a = ba^{-1}bab^{-1}$. The corresponding representation into $SL(2,\mathbb{C})$ is given by

$$\rho(a) = \begin{pmatrix} 1 & 1 \\ 0 & 1 \end{pmatrix}\,, \qquad \rho(b) = \begin{pmatrix} 1 & 0 \\ \zeta & 1 \end{pmatrix}\,, \tag{8.1.11}$$

where $\zeta = (-1 + \sqrt{-3})/2$ is the cube root of unity, $\zeta^3 = 1$.

The complement of the figure-eight knot can be also represented as a quotient space $\mathbb{H}^3/\Gamma$ (5.2.6), where the holonomy group Γ is generated by the above two matrices. Specifically,

[6] Explicitly, in the notation of Section 6.1 and above, the sum of log-parameters along the two paths in the neighborhood of the kth cusp must equal $2u_k$ and $2v_k + 2\pi i$, respectively.

[7] The branch of Li_2 in (8.1.10) is taken to be the standard one, with a cut from 1 to $+\infty$. Note, however, that we could also take care of ambiguities arising from the choice of dilogarithm branch by rewriting (8.1.10) in terms of the function $\tilde{\mathrm{L}}(w) = \int_{-\infty}^{w} \frac{t\,dt}{1-e^{-t}}$. This is a well-defined holomorphic function $: \mathbb{C} \to \mathbb{C}/4\pi^2\mathbb{Z}$ because all the residues of $t/(1-e^t)$ are integer multiplies of $2\pi i$, and it coincides with a branch of the function $\mathrm{Li}_2(e^w) + w\log(1-e^w)$.

we have

$$\Gamma \cong PSL(2, \mathcal{O}_{\mathbb{K}})\,, \tag{8.1.12}$$

where $\mathcal{O}_{\mathbb{K}}$ is the ring of integers in the imaginary quadratic field $\mathbb{K} = \mathbb{Q}(\sqrt{-3})$. The fundamental domain, $\mathcal{F}$, for Γ is described by a geodesic pyramid in $\mathbb{H}^3$ with one vertex at infinity and the other four vertices at the points:

$$\begin{aligned} v_1 &= j \\ v_2 &= \frac{1}{2} - \frac{\sqrt{3}}{6} i + \sqrt{\frac{2}{3}} j \\ v_3 &= \frac{1}{2} + \frac{\sqrt{3}}{6} i + \sqrt{\frac{2}{3}} j \\ v_4 &= \frac{1}{\sqrt{3}} i + \sqrt{\frac{2}{3}} j\,. \end{aligned} \tag{8.1.13}$$

Explicitly, we have

$$\mathcal{F} = \{ z + x_3 j \in \mathbb{H}^3 \mid z \in \mathcal{F}_z,\ x_3^2 + |z|^2 \geq 1 \}\,, \tag{8.1.14}$$

where $z = x_1 + i x_2$ and

$$\begin{aligned} \mathcal{F}_z = \{ z \in \mathbb{C} \mid 0 \leq \mathrm{Re}(z),\ \frac{1}{\sqrt{3}} \mathrm{Re}(z) \leq \mathrm{Im}(z),\ \mathrm{Im}(z) \leq \frac{1}{\sqrt{3}} (1 - \mathrm{Re}(z)) \} \\ \cup \{ z \in \mathbb{C} \mid 0 \leq \mathrm{Re}(z) \leq \frac{1}{2},\ -\frac{1}{\sqrt{3}} \mathrm{Re}(z) \leq \mathrm{Im}(z) \leq \frac{1}{\sqrt{3}} \mathrm{Re}(z) \} \end{aligned} \tag{8.1.15}$$

is the fundamental domain of a 2-torus with modular parameter $\tau = \zeta$. The region of large values of x_3 in $\mathcal{F}$ corresponds to the region near the cusp of the figure-eight knot complement M.

The standard triangulation of the figure eight knot complement comprises two ideal tetrahedra of opposite simplicial orientations, as in Figure 8.3, glued together in the only nontrivial consistent manner possible,

$$M = \Delta_z \cup \Delta_w\,. \tag{8.1.16}$$

Here, z and w are complex numbers, representing the shapes of the ideal tetrahedra; we take Δ_z to be positively oriented and Δ_w to be negatively oriented. As explained in Section 8.1, the shape parameters z and w must obey edge relations, which in the case of the figure-eight knot reduce to a single algebraic relation (see *e.g.* Chapter 4 of [113] and Section 15 of [136]):

$$(z-1)(w-1) = z^2 w^2\,. \tag{8.1.17}$$

The shape parameters z and w are related to the $SL(2,\mathbb{C})$ holonomy eigenvalue, l, along the longitude[8] of the knot in the following way

$$\frac{z^2}{z-1} = -l\,, \qquad \frac{w^2}{w-1} = -l^{-1}\,, \tag{8.1.18}$$

which automatically solves the edge condition (8.1.17). Similarly, the holonomy eigenvalue $m = e^u$ around the noncontractible meridian of the torus is given by

$$zw = m^2. \tag{8.1.19}$$

By eliminating z and w from (8.1.17), (8.1.18), and (8.1.19), one obtains the non-abelian irreducible component of the A-polynomial for the figure-eight knot from (6.6.9),

$$m^4 - (1 - m^2 - 2m^4 - m^6 + m^8)l + m^4 l^2 = 0\,. \tag{8.1.20}$$

Given the decomposition (8.1.16) of the 3-manifold M into two tetrahedra, we can find its volume by adding the (signed) volumes of Δ_z and Δ_w,

$$\mathrm{Vol}(M;u) = \mathrm{Vol}(\Delta_z) - \mathrm{Vol}(\Delta_w) = D(z) - D(w)\,, \tag{8.1.21}$$

where the volume of an ideal tetrahedron is given by (8.1.2). Similarly, following the prescription in Section 8.1, the complexified volume can be given by[9]

$$i(\mathrm{Vol}(M;u) + i\mathrm{CS}(M;u)) = L(z;0,0) - L(w;0,0) - v\bar{u} - i\pi u\,. \tag{8.1.22}$$

Notice that due to the edge relation (8.1.17) the total volumes (8.1.21), (8.1.22) are functions of one complex parameter, or, equivalently, a point on the zero locus of the A-polynomial, $A(l,m) = A(-e^v, e^u) = 0$.

From the relation (8.1.18) we find that the point $(l,m) = (-1,1)$ corresponding to the complete hyperbolic structure on M is characterized by the values of z and w which solve the equation

$$z^2 - z + 1 = 0\,. \tag{8.1.23}$$

In order to obtain tetrahedra of positive (signed) volume, we must choose z to be the root of this equation with a positive imaginary part, and w its inverse:

$$z = \frac{1 + i\sqrt{3}}{2}\,, \qquad w = \frac{1 - i\sqrt{3}}{2}\,. \tag{8.1.24}$$

[8] A 1-cycle on $\Sigma = T^2$ which is contractible in the knot complement M.

[9] This expression differs slightly from the one given in [136], because we use $2v + 2\pi i$ rather than $2v$ as the logarithm of the "longitudinal" holonomy, as mentioned in Footnote 6 of Section 8.1.

These value correspond to regular ideal tetrahedra, and maximize (respectively, minimize) the Bloch-Wigner dilogarithm function $D(z)$.

8.2 Hikami's invariant

We can now describe Hikami's geometric construction. Roughly speaking, to compute the invariant for a hyperbolic manifold M, one chooses an ideal triangulation of M, assigns an infinite-dimensional vector space V or V^* to each tetrahedron face, and assigns a matrix element in $V \otimes V \otimes V^* \otimes V^*$ to each tetrahedron. These matrix elements depend on a small parameter $\hbar$, and in the classical $\hbar \to 0$ limit they capture the hyperbolic structure of the tetrahedra. The invariant of M is obtained by taking inner products of matrix elements on every pair of identified faces (gluing the tetrahedra back together), subject to the cusp conditions described above in the classical limit.

To describe the process in greater detail, we begin with an orientable hyperbolic manifold that has an oriented ideal triangulation $\{\Delta_i\}_{i=1}^N$, and initially forget about the hyperbolic structures of these tetrahedra. As discussed in Section 8.1 and indicated in Figure 8.3, each tetrahedron comes with one of two possible orientations of its edges, which induces an ordering of its vertices $v_j^{(i)}$ (the subscript j here is not to be confused with the shape parameter subscript in (8.1.1)), an ordering of its faces, and orientations on each face. The latter can be indicated by inward or outward-pointing normal vectors. The faces (or their normal vectors) are labelled by $p_j^{(i)}$, in correspondence with opposing vertices. The normal face-vectors of adjacent tetrahedra match up head-to-tail (and actually define an oriented dual decomposition) when tetrahedra are glued to form M.

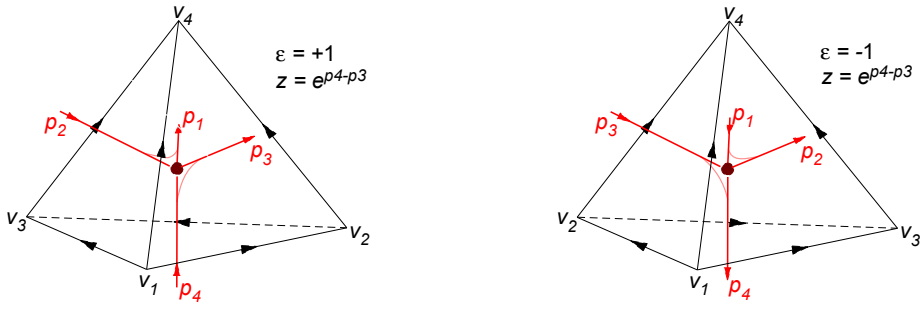

Figure 8.3: Oriented tetrahedra, to which matrix elements $\langle p_1, p_3|\mathbf{S}|p_2, p_4\rangle$ (left) and $\langle p_2, p_4|\mathbf{S}^{-1}|p_1, p_3\rangle$ (right) are assigned.

Given such an oriented triangulation, one associates a vector space V to each inward-oriented face, and the dual space V^* to each outward-oriented face. (Physicists should think of these spaces as "Hilbert" spaces obtained by quantizing the theory on a manifold with boundary.) The elements of V are represented by complex-valued functions in one variable, with adjoints given by conjugation and inner products given by integration. Abusing the notation, but following the very natural set of conventions of [52, 53], we denote these complex variables by $p_j^{(i)}$, which we used earlier to label the corresponding faces of the tetrahedra. As a result, to the boundary of every tetrahedron Δ_i one associates a vector space $V \otimes V \otimes V^* \otimes V^*$, represented by functions of its four face labels, $p_1^{(i)}$, $p_2^{(i)}$, $p_3^{(i)}$, and $p_4^{(i)}$.

To each tetrahedron one assigns a matrix element $\langle p_1, p_3|\mathbf{S}|p_2, p_4\rangle$ or $\langle p_2, p_4|\mathbf{S}^{-1}|p_1, p_3\rangle$, depending on orientation as indicated in Figure 8.3. Here, the matrix $\mathbf{S}$ acts on functions $f(p_1, p_2) \in V \otimes V$ as

$$\mathbf{S} \;=\; e^{\hat{q}_1\hat{p}_2/2\hbar}\,\Phi_\hbar(\hat{p}_1 + \hat{q}_2 - \hat{p}_2)\,, \tag{8.2.1}$$

where $\hat{p}_i f = p_i f$ and $\hat{q}_i f = 2\hbar\frac{\partial}{\partial p_i} f$. The function $\Phi_\hbar$ is the quantum dilogarithm, to be described in the next subsection. Assuming that $\int \frac{idq}{4\pi\hbar}|q\rangle\langle q| = \int dp\,|p\rangle\langle p| = 1$ and $\langle p|q\rangle = e^{\frac{pq}{2i\hbar}}$ (the exact normalizations are not important for the final invariant), one obtains via Fourier transform

$$\langle p_1, p_3|\mathbf{S}|p_2, p_4\rangle = \frac{\delta(p_1 + p_3 - p_2)}{\sqrt{-4\pi i\hbar}}\Phi_\hbar(p_4 - p_3 + i\pi + \hbar)\, e^{\frac{1}{2\hbar}\left(p_1(p_4-p_3)+\frac{i\pi\hbar}{2}-\frac{\pi^2-\hbar^2}{6}\right)}\,, \tag{8.2.2}$$

$$\langle p_2, p_4|\mathbf{S}^{-1}|p_1, p_3\rangle = \frac{\delta(p_1 + p_3 - p_2)}{\sqrt{-4\pi i\hbar}}\frac{1}{\Phi_\hbar(p_4 - p_3 - i\pi - \hbar)} e^{\frac{1}{2\hbar}\left(p_1(p_3-p_4)-\frac{i\pi\hbar}{2}+\frac{\pi^2-\hbar^2}{6}\right)}\,. \tag{8.2.3}$$

In the classical limit $\hbar \to 0$, the quantum dilogarithm has the asymptotic $\Phi_\hbar(p) \sim \frac{1}{2\hbar}\mathrm{Li}_2(-e^p)$. One therefore sees that the classical limits of the above matrix elements look very much like exponentials of $\frac{1}{2\hbar}$ times the complexified hyperbolic volumes of tetrahedra. For example, the asymptotic of (8.2.2) coincides with $\exp(L(z;\cdot,\cdot)/(2\hbar))$ if we identify $e^{p_4-p_3}$ with z and e^{-2p_1} with $1/(1-z)$. For building a quantum invariant, however, only half of the variables p_j really "belong" to a single tetrahedron. Hikami's claim [52, 53] is that if we only identify a shape parameter

$$z^{(i)} = e^{p_4^{(i)} - p_3^{(i)}}\,, \tag{8.2.4}$$

for every tetrahedron Δ_i, the classical limit of the resulting quantum invariant will completely reproduce the hyperbolic structure and complexified hyperbolic volume on M.[10]

[10] Eqn. (8.2.4) is a little different from the relation appearing in [52, 53], because our convention for assigning shape parameters to edges based on orientation differs from that of [52, 53].

To finish calculating the invariant of M, one glues the tetrahedra back together and takes inner products in every pair V and V^* corresponding to identified faces. This amounts to multiplying together all the matrix elements (8.2.2) or (8.2.3), identifying the $p_j^{(i)}$ variables on identified faces (with matching head-to-tail normal vectors), and integrating over the $2N$ remaining p's. To account for possible toral boundaries of M, however, one must revert back to the hyperbolic structure. This allows one to write the holonomy eigenvalues $\{e^{u_k}\}$ as products of shape parameters $(z^{(i)},\, 1-1/z^{(i)},\, 1/(1-z^{(i)}))$, and, using (8.2.4), to turn every cusp condition into a linear relation of the form $\sum p\text{'s} = 2u_k$. These relations are then inserted as delta functions in the inner product integral, enforcing global boundary conditions. In the end, noting that each matrix element (8.2.2)-(8.2.3) also contains a delta function, one is left with $N - b_0(\Sigma)$ nontrivial integrals, where $b_0(\Sigma)$ is the number of connected components of $\Sigma = \partial M$. For example, specializing to hyperbolic 3-manifolds with a single torus boundary $\Sigma = T^2$, the integration variables can be relabeled so that Hikami's invariant takes the form

$$H(M;\hbar,u) = \frac{1}{(4\pi\hbar)^{N/2}} \int \prod_{i=1}^{N} \Phi_\hbar\big(\, g_i(\mathbf{p},2u) + \epsilon_i(i\pi+\hbar)\,\big)^{\epsilon_i}\, e^{f(\mathbf{p},2u,\hbar)/2\hbar}\, dp_1 \dots dp_{N-1}\,. \tag{8.2.5}$$

The g_i are linear combinations of $(p_1,\dots,p_{N-1},2u)$ with integer coefficients, and f is a quadratic polynomial, also with integer coefficients for all terms involving p_k's or u. In the classical limit, this integral can naively be evaluated in a saddle-point approximation, and Hikami's claim is that the saddle-point relations coincide precisely with the edge conditions for the triangulation on M. There is more to this story, however, as we will see in Section 8.4.

8.3 Quantum dilogarithm

Since quantum dilogarithms play a key role here, we take a little time to discuss some of their most important properties.

Somewhat confusingly, there are at least three distinct—though related—functions which have occurred in the literature under the name "quantum dilogarithm":

i) The function $\mathrm{Li}_2(x;q)$ is defined for x, $q \in \mathbb{C}$ with $|x|$, $|q| < 1$ by

$$\mathrm{Li}_2(x;q) \;=\; \sum_{n=1}^{\infty} \frac{x^n}{n\,(1-q^n)}\,; \tag{8.3.1}$$

its relation to the classical dilogarithm function $\mathrm{Li}_2(x) = \sum\limits_{n=1}^{\infty} \dfrac{x^n}{n^2}$ is that

$$\mathrm{Li}_2\big(x;\, e^{2\hbar}\big) \;\sim\; -\frac{1}{2\hbar}\,\mathrm{Li}_2(x) \qquad \text{as } \hbar \to 0\,. \tag{8.3.2}$$

ii) The function $(x;q)_\infty$ is defined for $|q| < 1$ and all $x \in \mathbb{C}$ by

$$(x;q)_\infty \;=\; \prod_{r=0}^{\infty} \big(1 - q^r x\big)\,, \tag{8.3.3}$$

and is related to $\mathrm{Li}_2(x;q)$ for $|x| < 1$ by

$$(x;q)_\infty \;=\; \exp\big(-\mathrm{Li}_2(x;q)\big)\,. \tag{8.3.4}$$

It is also related to the function $\mathbf{E}(x)$ of Chapter 4 as

$$\mathbf{E}(x) = \big(-q^{\frac{1}{2}}x;q\big)^{-1}\,. \tag{8.3.5}$$

Finally,

iii) the function $\Phi(z;\tau)$ is defined for $\mathrm{Re}(\tau) > 0$ and $2|\mathrm{Re}(z)| < 1 + \mathrm{Re}(\tau)$ by

$$\Phi(z;\tau) \;=\; \exp\!\left(\frac{1}{4}\int_{\mathbb{R}^{(+)}} \frac{e^{2xz}}{\sinh x\,\sinh \tau x}\,\frac{dx}{x}\right) \tag{8.3.6}$$

(here $\mathbb{R}^{(+)}$ denotes a path from $-\infty$ to ∞ along the real line but deformed to pass over the singularity at zero). It is related to $(x;q)_\infty$ by

$$\Phi(z;\tau) \;=\; \begin{cases} \dfrac{\big(-\mathbf{e}(z+\tau/2);\,\mathbf{e}(\tau)\big)_\infty}{\big(-\mathbf{e}((z-1/2)/\tau);\,\mathbf{e}(-1/\tau)\big)_\infty} & \text{if } \mathrm{Im}(\tau) > 0\,, \\[2ex] \dfrac{\big(-\mathbf{e}((z+1/2)/\tau);\,\mathbf{e}(1/\tau)\big)_\infty}{\big(-\mathbf{e}(z-\tau/2);\,\mathbf{e}(-\tau)\big)_\infty} & \text{if } \mathrm{Im}(\tau) < 0\,. \end{cases} \tag{8.3.7}$$

(Here and in future we use the abbreviation $\mathbf{e}(x) = e^{2\pi i x}$.)

It is the third of these functions, in the normalization

$$\Phi_\hbar(z) \;=\; \Phi\big(\frac{z}{2\pi i};\,\frac{\hbar}{i\pi}\big)\,, \tag{8.3.8}$$

which occurs in our "state integral" and which we will take as our basic "quantum dilogarithm," but all three functions play a role in the analysis, so we will describe the main

properties of all three here. We give complete proofs, but only sketchily since none of this material is new. For further discussion and proofs, see, *e.g.*, [138, 139, 140, 141, 142], and [143] (subsection II.1.D).

1. The asymptotic formula (8.3.2) can be refined to the asymptotic expansion

$$\mathrm{Li}_2\big(x; e^{2\hbar}\big) \;\sim\; -\frac{1}{2\hbar}\,\mathrm{Li}_2(x) - \frac{1}{2}\log(1-x) - \frac{x}{1-x}\,\frac{\hbar}{6} + 0\hbar^2 + \frac{x+x^2}{(1-x)^3}\frac{\hbar^3}{90} + \cdots \tag{8.3.9}$$

as $\hbar \to 0$ with x fixed, in which the coefficient of $\hbar^{n-1}$ for $n \geq 2$ is the product of $-2^{n-1}B_n/n!$ (here B_n is the nth Bernoulli number) with the negative-index polylogarithm $\mathrm{Li}_{2-n}(x) \in \mathbb{Q}\big[\frac{1}{1-x}\big]$. More generally, one has the asymptotic formula

$$\mathrm{Li}_2\big(xe^{2\lambda\hbar};\, e^{2\hbar}\big) \;\sim\; -\sum_{n=0}^{\infty} \frac{2^{n-1}B_n(\lambda)}{n!}\,\mathrm{Li}_{2-n}(x)\,\hbar^{n-1} \tag{8.3.10}$$

as $\hbar \to 0$ with λ fixed, where $B_n(t)$ denotes the nth Bernoulli polynomial.[11] Both formulas are easy consequences of the Euler-Maclaurin summation formula. By combining (8.3.7), (8.3.4), and (8.3.10), one also obtains an asymptotic expansion

$$\Phi_\hbar(z + 2\lambda\hbar) = \exp\left(\sum_{n=0}^{\infty} \frac{2^{n-1}B_n(1/2+\lambda)}{n!}\hbar^{n-1}\mathrm{Li}_{2-n}(-e^z)\right). \tag{8.3.11}$$

(To derive this, note that in (8.3.7) $(-\mathbf{e}(z \pm 1/2)/\tau; \mathbf{e}(\pm 1/\tau))_\infty \sim 1$ to all orders in $\hbar$ as $\hbar \to 0$.)

2. The function $(x;q)_\infty$ and its reciprocal have the Taylor expansions (*cf.* (4.1.14))

$$(x;q)_\infty \;=\; \sum_{n=0}^{\infty} \frac{(-1)^n}{(q)_n}\, q^{\frac{n(n-1)}{2}}\, x^n\,, \qquad \frac{1}{(x;q)_\infty} \;=\; \sum_{n=0}^{\infty} \frac{1}{(q)_n}\, x^n \tag{8.3.12}$$

around $x = 0$, where

$$(q)_n \;=\; \frac{\big(q;q\big)_\infty}{\big(q^{n+1};q\big)_\infty} \;=\; (1-q)(1-q^2)\cdots(1-q^n) \tag{8.3.13}$$

is the nth q-Pochhammer symbol. These, as well as formula (8.3.4), can be proved easily from the recursion formula $(x;q)_\infty = (1-x)(qx;q)_\infty$, which together with the initial value $(0;q)_\infty = 1$ determines the power series $(x;q)_\infty$ uniquely. (Of course, (8.3.4) can also be proved directly by expanding each term in $\sum_r \log(1-q^r x)$ as a power series in x.) Another

[11] This is the unique polynomial satisfying $\int_x^{x+1} B_n(t)dt = x^n$, and is a monic polynomial of degree n with constant term B_n.

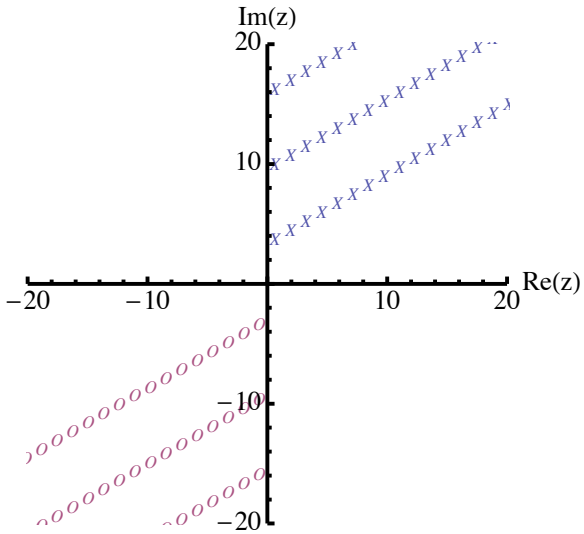

Figure 8.4: The complex z-plane, showing poles (X's) and zeroes (O's) of $\Phi_\hbar(z)$ at $\hbar = \frac{3}{4}e^{i\pi/3}$.

famous result, easily deduced from (8.3.12) using the identity $\sum_{m-n=k} \frac{q^{mn}}{(q)_m(q)_n} = \frac{1}{(q)_\infty}$ for all $k \in \mathbb{Z}$, is the Jacobi triple product formula

$$(q;q)_\infty\,(x;q)_\infty\,(qx^{-1};q)_\infty \;=\; \sum_{k\in\mathbb{Z}} (-1)^k q^{\frac{k(k-1)}{2}}\, x^k\,, \tag{8.3.14}$$

relating the function $(x;q)_\infty$ to the classical Jacobi theta function.

3. The function $\Phi(z;\tau)$ defined (initially for $\mathrm{Re}(\tau) > 0$ and $|\mathrm{Re}(z)| < \frac{1}{2} + \frac{1}{2}\mathrm{Re}(\tau)$) by (8.3.6) has several functional equations. Denote by $I(z;\tau)$ the integral appearing in this formula. Choosing for $\mathbb{R}^{(+)}$ the path $(-\infty,-\varepsilon] \cup \varepsilon\exp([i\pi,0]) \cup [\varepsilon,\infty)$ and letting $\varepsilon \to 0$, we find

$$I(z;\tau) \;=\; \frac{2\pi i}{\tau}\left(\frac{1+\tau^2}{12} - z^2\right) \;+\; 2\int_0^\infty \left(\frac{\sinh 2xz}{\sinh x\,\sinh \tau x} \;-\; \frac{2z}{\tau x}\right)\frac{dx}{x}\,. \tag{8.3.15}$$

Since the second term is an even function of z, this gives

$$\Phi(z;\tau)\,\Phi(-z;\tau) \;=\; \mathbf{e}\Big(\frac{\tau^2 - 12z^2 + 1}{24\tau}\Big)\,. \tag{8.3.16}$$

From (8.3.15) we also get

$$I(z+1/2;\tau) \;-\; I(z-1/2;\tau) \;=\; -\frac{4\pi i z}{\tau} \;+\; 4\int_0^\infty \left(\frac{\cosh 2xz}{\sinh \tau x} \;-\; \frac{1}{\tau x}\right)\frac{dx}{x}\,. \tag{8.3.17}$$

The integral equals $-\log(2\cos(\pi z/\tau))$ (proof left as an exercise). Dividing by 4 and exponentiating we get the first of the two functional equations

$$\frac{\Phi(z-1/2;\tau)}{\Phi(z+1/2;\tau)} \;=\; 1 \;+\; \mathbf{e}\big(z/\tau\big)\,, \qquad \frac{\Phi(z-\tau/2;\tau)}{\Phi(z+\tau/2;\tau)} \;=\; 1 \;+\; \mathbf{e}\big(z\big)\,, \tag{8.3.18}$$

and the second can be proved in the same way or deduced from the first using the obvious symmetry property

$$\Phi(z;\tau) \;=\; \Phi(z/\tau;1/\tau)\,, \tag{8.3.19}$$

of the function Φ. (Replace x by x/τ in (8.3.6).)

4. The functional equations (8.3.18) show that $\Phi(z;\tau)$, which in its initial domain of definition clearly has no zeros or poles, extends (for fixed τ with $\mathrm{Re}(\tau)>0$) to a meromorphic function of z with simple poles at $z\in\Xi(\tau)$ and simple zeros at $z\in-\Xi(\tau)$, where

$$\Xi(\tau) \;=\; \big(\mathbb{Z}_{\geq 0}+\tfrac{1}{2}\big)\,\tau \;+\; \big(\mathbb{Z}_{\geq 0}+\tfrac{1}{2}\big) \;\subset\; \mathbb{C}\,. \tag{8.3.20}$$

In terms of the normalization (8.3.8), this says that $\Phi_\hbar(z)$ has simple poles at $z\in\tilde\Xi(\hbar)$ and simple zeroes at $z\in-\tilde\Xi(\hbar)$, where

$$\tilde\Xi(\hbar) = (2\mathbb{Z}_{\geq 0}+1)i\pi + (2\mathbb{Z}_{\geq 0}+1)\hbar\,. \tag{8.3.21}$$

This is illustrated in Figure 8.4. Equation (8.3.7) expressing Φ in terms of the function $(x;q)_\infty$ also follows, because the quotient of its left- and right-hand sides is a doubly periodic function of z with no zeros or poles and hence constant, and the constant can only be ±1 (and can then be checked to be $+1$ in several ways, e.g., by evaluating numerically at one point) because the right-hand side of (8.3.7) satisfies the same functional equation (8.3.16) as $\Phi(z;\tau)$ by virtue of the Jacobi triple product formula (8.3.14) and the well-known modular transformation properties of the Jacobi theta function.

5. From (8.3.15) we also find the Taylor expansion of $I(z;\tau)$ at $z=0$,

$$I(z;\tau) \;=\; 4\sum_{k=0}^{\infty} C_k(\tau)\,z^k\,,$$

with coefficients $C_k(\tau)=\tau^{-k}C_k(1/\tau)$ given by

$$\begin{aligned}
C_0(\tau) \;&=\; \frac{\pi i}{24}\big(\tau+\tau^{-1}\big)\,, \qquad C_1(\tau) \;=\; \int_0^\infty\!\left(\frac{1}{\sinh x\,\sinh\tau x} \;-\; \frac{1}{\tau x^2}\right)dx\,,\\
C_2(\tau) \;&=\; -\frac{\pi i}{2\tau}\,, \qquad C_k(\tau) \;=\; 0 \quad \text{for } k\geq 4 \text{ even},\\
C_k(\tau) \;&=\; \frac{2^{k-1}}{k!}\int_0^\infty \frac{x^{k-1}\,dx}{\sinh x\,\sinh\tau x} \quad \text{for } k\geq 3 \text{ odd}.
\end{aligned}$$

By expanding $1/\sinh(x)$ and $1/\sinh(\tau x)$ as power series in e^{-x} and $e^{-\tau x}$ we can evaluate the last of these expressions to get

$$C_k(\tau) \;=\; \frac{2^{k+1}}{k!}\sum_{m,n>0,\ \mathrm{odd}}\int_0^\infty e^{-mx-n\tau x}\,x^{k-1}\,dx \;=\; \frac{2}{k}\sum_{s\in\Xi(\tau)} s^{-k} \quad (k\geq 3 \text{ odd})$$

with $\Xi(\tau)$ as in (8.3.20). Dividing by 4 and exponentiating gives the Weierstrass product expansion

$$\Phi(z;\tau) \;=\; \exp\!\Big(\frac{\pi i}{24}\big(\tau+\tau^{-1}\big) \,+\, C_1(\tau)\,z \,-\, \frac{\pi i z^2}{2\tau}\Big) \prod_{s\in\Xi(\tau)} \Big(\frac{s+z}{s-z}\,e^{-2z/s}\Big) \tag{8.3.22}$$

of $\Phi(z;\tau)$. From this expansion, one finds that $\Phi(z;\tau)$ extends meromorphically to $\mathbb{C}\times\big(\mathbb{C}\smallsetminus(-\infty,0]\big)$ with simple poles and simple zeros for $z\in\Xi(\tau)$ and $z\in-\Xi(\tau)$ and no other zeros or poles. (This analytic continuation can also be deduced by rotating the path of integration in (8.3.6), e.g. by replacing $\int_{\mathbb{R}^{(+)}}$ by $\int_{\mathbb{R}^{(+)}/\sqrt{\tau}}$ for z sufficiently small.)

6. The quantum dilogarithm is related via the Jacobi triple product formula to the Jacobi theta function, which is a Jacobi form, i.e., it has transformation properties not only with respect to the lattice translations $z\mapsto z+1$ and $z\mapsto z+\tau$ but also with respect to the modular transformations $\tau\mapsto\tau+1$ and $\tau\mapsto-1/\tau$. The function $\Phi(z;\tau)$ has the lattice transformation properties (8.3.18) and maps to its inverse under $(z,\tau)\mapsto(z/\tau,\,-1/\tau)$, but it does not transform in a simple way with respect to $\tau\mapsto\tau+1$. Nevertheless, it has an interesting modularity property of a different kind (cocycle property) which is worth mentioning here even though no use of it will be made in the remainder of this thesis. Write (8.3.7) as

$$\Phi(z;\tau) \;=\; \frac{S(z;\tau)}{S(z/\tau;-1/\tau)}\,, \qquad S(z;\tau) \;=\; \begin{cases} \prod_{n\,>\,0\ \mathrm{odd}}\big(1+q^{n/2}\mathbf{e}(z)\big) & \text{if } \mathrm{Im}(\tau)>0,\\ \prod_{n\,<\,0\ \mathrm{odd}}\big(1+q^{n/2}\mathbf{e}(z)\big)^{-1} & \text{if } \mathrm{Im}(\tau)<0, \end{cases}$$

where $q=\mathbf{e}(\tau)$. The function $S(z;\tau)$ has the transformation properties

$$S(z;\tau)=S(z+1;\tau)=(1+q^{1/2}\mathbf{e}(z))\,S(z+\tau;\tau)=S(z+\tfrac{1}{2};\tau+1)=S(z;\tau+2)$$

amd from these we deduce by a short calculation the two three-term functional equations

$$\Phi(z;\tau) \;=\; \Phi\big(z\pm\frac{1}{2},\tau+1\big)\,\Phi\big(\frac{z\mp\tau/2}{\tau+1},\,\frac{\tau}{\tau+1}\big) \tag{8.3.23}$$

of Φ. This is highly reminiscent of the fact (cf. [144]) that the holomorphic function

$$\psi(\tau) \;=\; f(\tau)-\tau^{-2s}f(-1/\tau)\,, \qquad f(\tau) \;=\; \begin{cases} \sum_{n>0}a_nq^n & \text{if } \mathrm{Im}(\tau)>0,\\ -\sum_{n<0}a_nq^n & \text{if } \mathrm{Im}(\tau)<0 \end{cases}$$

associated to a Maass cusp form $u(\tau)$ on $SL(2,\mathbb{Z})$ with spectral parameter s, where a_n are the normalized coefficients in the Fourier-Bessel expansion of u, satisfies the Lewis functional

equation $\psi(\tau) = \psi(\tau+1) + (\tau+1)^{-2s}\psi\big(\frac{\tau}{\tau+1}\big)$ and extends holomorphically from its initial domain of definition $\mathbb{C} \smallsetminus \mathbb{R}$ to $\mathbb{C} \smallsetminus (-\infty, 0]$.

7. Finally, the quantum dilogarithm functions satisfy various five-term relations, of which the classical five-term functional equation of $\mathrm{Li}_2(x)$ is a limiting case, when the arguments are non-commuting variables. The simplest and oldest is the identity

$$(Y;q)_\infty\,(X;q)_\infty \;=\; (X;q)_\infty\,(-YX;q)_\infty\,(Y;q)_\infty \tag{8.3.24}$$

for operators X and Y satisfying $XY = qYX$ (*cf.* Eqn. (4.1.21) for $\mathbf{E}(x)$). From this one deduces the "quantum pentagon relation"

$$\Phi_\hbar(\hat{p})\,\Phi_\hbar(\hat{q}) \;=\; \Phi_\hbar(\hat{q})\,\Phi_\hbar(\hat{p}+\hat{q})\,\Phi_\hbar(\hat{p}) \tag{8.3.25}$$

for operators $\hat{p}$ and $\hat{q}$ satisfying $[\hat{q},\hat{p}] = 2\hbar$. Letting $\mathbf{S}_{ij}$ be a copy, acting on the i^{th} and j^{th} factors of $V \otimes V \otimes V$, of the $\mathbf{S}$-matrix introduced in (8.2.1), we deduce from (8.3.25) the operator identity

$$\mathbf{S}_{23}\mathbf{S}_{12} \;=\; \mathbf{S}_{12}\mathbf{S}_{13}\mathbf{S}_{23}\,. \tag{8.3.26}$$

It is this very special property which guarantees that the gluing procedure used in the definition of (8.2.5) is invariant under 2-3 Pachner moves on the underlying triangulations and produces a true hyperbolic invariant [52, 53, 145]. This identity is also related to the interesting fact that the fifth power of the operator which maps a nicely behaved function to the Fourier transform of its product with $\Phi_\hbar(z)$ (suitably normalized) is a multiple of the identity [142].

8.4 A state integral model for $Z^{(\rho)}(M;\hbar)$

Now, let us return to the analysis of the integral (8.2.5) and compare it with the perturbative $SL(2,\mathbb{C})$ invariant $Z^{(\alpha)}(M;\hbar,u)$. Both invariants compute quantum (*i.e.* $\hbar$-deformed) topological invariants of hyperbolic 3-manifolds and, thus, are expected to be closely related. However, in order to establish a precise relation, we need to face two problems mentioned in the beginning of this section:

i) the integration contour is not specified in (8.2.5), and

ii) the integral (8.2.5) does not depend on the choice of the classical solution α.

These two problems are related, and can be addressed by studying the integral (8.2.5) in various saddle-point approximations. Using the leading term in (8.3.11), we can approximate it to leading order as

$$H(M;\hbar,u) \underset{\hbar\to 0}{\sim} \int e^{\frac{1}{\hbar}V(p_1,\ldots,p_{N-1},u)}\, dp_1 \ldots dp_{N-1}\,, \tag{8.4.1}$$

with the "potential"

$$V(\mathbf{p},u) \;=\; \frac{1}{2}\sum_{i=1}^{N} \epsilon_i \mathrm{Li}_2(-\exp(g_i(\mathbf{p},2u)+i\pi\epsilon_i)) + \frac{1}{2} f(\mathbf{p},2u,\hbar=0)\,. \tag{8.4.2}$$

As explained below (8.3.11), the branches of Li_2 must be chosen appropriately to coincide with the half-lines of poles and zeroes of the quantum dilogarithms in (8.2.5). The leading contribution to $H(M;\hbar,u)$ will then come from the highest-lying critical point through which a given contour can be deformed.

It was the observation of [53] that the potential V always has one critical point that reproduces the classical Chern-Simons action on the "geometric" branch, that is a critical point $\mathbf{p}^{(\mathrm{geom})}(u)$ such that

$$l_{\mathrm{geom}}(u) = \exp\left[\tfrac{d}{du} V(\mathbf{p}^{(\mathrm{geom})}(u),u)\right] \tag{8.4.3}$$

and

$$S_0^{(\mathrm{geom})}(u) = V(\mathbf{p}^{(\mathrm{geom})}(u),u)\,. \tag{8.4.4}$$

This identification follows from the fact that both $S_0^{(\mathrm{geom})}(u)$ and matrix elements (8.2.2)-(8.2.3) in the limit $\hbar \to 0$ are related to the complexified volume function $i(\mathrm{Vol}(M;u) + i\mathrm{CS}(M;u))$. We want to argue presently that in fact *every* critical point of V corresponds to a classical solution in Chern-Simons theory (that is, to a branch of $A(l,m)=0$) in this manner, with similar relations

$$l_\alpha(u) = e^{\frac{d}{du}V(\mathbf{p}^{(\alpha)}(u),u)} \tag{8.4.5}$$

and

$$S_0^{(\alpha)}(u) = V(\mathbf{p}^{(\alpha)}(u),u) \tag{8.4.6}$$

for some α. In particular, $l_\alpha(u)$ as given by (8.4.5) and $m = e^u$ obey (6.3.13).

To analyze generic critical points of V, observe that the critical point equations take the form

$$2\frac{\partial}{\partial p_j} V(\mathbf{p},u) = -\sum_{i=1}^{N} \epsilon_i G_{ji} \log(1+\exp(g_i(\mathbf{p},2u)+i\pi\epsilon_i)) + \frac{\partial}{\partial p_j} f(\mathbf{p},2u,0) = 0 \qquad \forall\, j\,, \tag{8.4.7}$$

where $G_{ji} = \frac{\partial}{\partial p_j} g_i(\mathbf{p}, 2u)$ are some constants and the functions $\frac{\partial}{\partial p_j} f(\mathbf{p}, 2u, 0)$ are linear. Again, the cuts of the logarithm must match the singularities of the quantum dilogarithm. Exponentiating (8.4.7), we obtain another set of conditions

$$r_j(\mathbf{x}, m) = 1 \quad \forall\, j\,, \tag{8.4.8}$$

where

$$r_j(\mathbf{x}, m) = \exp\left(2\frac{\partial}{\partial p_j} V(\mathbf{p}, u)\right) = \prod_i (1 - e^{g_i})^{-\epsilon_i G_{ji}} \exp\left(\frac{\partial}{\partial p_j} f\right) \tag{8.4.9}$$

are all *rational* functions of the variables $x_j = e^{p_j}$ and $m = e^u$. Note that an entire family of points $\{\mathbf{p} + 2\pi i \mathbf{n} \,|\, \mathbf{n} \in \mathbb{Z}^{N-1}\}$ maps to a single $\mathbf{x}$, and that all branch cut ambiguities disappear in the simpler equations (8.4.8). Depending on $\arg(\hbar)$ and the precise form of f, solutions to (8.4.8) either "lift" uniquely to critical points of the potential V, or they lift to a family of critical points at which V differs only by integer multiples of $2\pi i u$.

Now, the system (8.4.8) is algebraic, so its set of solutions defines a complex affine variety

$$\mathcal{R} = \{(x_1, \ldots, x_{N-1}, m) \in \mathbb{C}^N \,|\, r_j(x_1, \ldots, x_{N-1}, m) = 0 \quad \forall\, j\}\,, \tag{8.4.10}$$

which is closely related to the representation variety $\mathcal{L}$ given by $A(l, m) = 0$. Both generically have complex dimension one. Noting that $s(x_1, \ldots, x_{N-1}, m) = \exp\left(\frac{\partial}{\partial u} V\right)$ is also a rational function, we can define a rational map $\phi : \mathbb{C}^N \to \mathbb{C}^2$ by

$$\phi(x_1, \ldots, x_{N-1}, m) = (s(x_1, \ldots, x_{N-1}, m), m)\,. \tag{8.4.11}$$

The claim in [53] that one critical point of V always corresponds to the geometric branch of $\mathcal{L}$ means that $\overline{\phi(\mathcal{R})}$ (taking an algebraic closure) always intersects $\mathcal{L}$ nontrivially, along a subvariety of dimension 1. Thus, some irreducible component of $\overline{\phi(\mathcal{R})}$, coming from an irreducible component of $\mathcal{R}$, must coincide with the entire irreducible component of $\mathcal{L}$ containing the geometric branch. Every solution $\mathbf{x} = \mathbf{x}(m)$ in this component of $\mathcal{R}$ corresponds to a branch of the A-polynomial. Moreover, if such a solution $\mathbf{x}^{(\alpha)}$ (corresponding to branch α) can be lifted to a real critical point $\mathbf{p}^{(\alpha)}(u)$ of V, then one must have relations (8.4.5) and (8.4.6).

This simple algebraic analysis shows that *some* solutions of (8.4.8) will cover an entire irreducible component of the curve $\mathcal{L}$ defined by $A(l, m) = 0$. We cannot push the general argument further without knowing more about the reducibility of $\mathcal{R}$. However, we can look

at some actual examples. Computing $V(\mathbf{p}, u)$ for thirteen hyperbolic manifolds with a single torus boundary,[12] we found in every case that solutions of (8.4.8) completely covered all non-abelian branches $\alpha \neq$ abel; in other words, $\overline{\phi(\mathcal{R})} = \mathcal{L}'$, with $\mathcal{L}' = \{A(l,m)/(l-1) = 0\}$. For six of these manifolds, we found unique critical points $\mathbf{p}(u)$ corresponding to every non-abelian branch of $\mathcal{L}$ at $\arg(\hbar) = i\pi$. Motivated by these examples, it is natural to state the following conjecture:

Conjecture 2: *Every critical point of V corresponds to some branch α, and all $\alpha \neq$* abel *are obtained in this way. Moreover, for every critical point $\mathbf{p}^{(\alpha)}(u)$ (corresponding to some branch α) we have* (8.4.5)-(8.4.6) *and to all orders in perturbation theory:*

$$Z^{(\alpha)}(M;\hbar,u) = \sqrt{2}\int_{C_\alpha} \prod_{i=1}^{N} \Phi_\hbar\big(\, g_i(\mathbf{p},2u) + \epsilon_i(i\pi+\hbar)\,\big)^{\epsilon_i}\, e^{\frac{1}{2\hbar}f(\mathbf{p},2u,\hbar)-u} \prod_{j=1}^{N-1} \frac{dp_j}{\sqrt{4\pi\hbar}}\,, \quad (8.4.12)$$

where C_α is an arbitrary contour with fixed endpoints which passes through $\mathbf{p}^{(\alpha)}(u)$ and no other critical point.

A slightly more conservative version of this conjecture might state that only those α that belong to the same irreducible component of $\mathcal{L}$ as the geometric branch, $\alpha =$ geom, are covered by critical points of V. Indeed, the "abelian" branch with $l_{\text{abel}} = 1$ is not covered by the critical points of V and it belongs to the separate component $(l-1)$ of the curve $A(l,m) = 0$. It would be interesting to study the relation between critical points of V and irreducible components of $\mathcal{L}$ further, in particular by looking at examples with reducible A-polynomials aside from the universal $(l-1)$ factor.

The right-hand side of (8.4.12) is the proposed state integral model for the *exact* perturbative partition function of $SL(2,\mathbb{C})$ Chern-Simons theory on a hyperbolic 3-manifold M with a single torus boundary $\Sigma = T^2$. (A generalization to 3-manifolds with an arbitrary number of boundary components is straightforward.) This state integral model is a modified version of Hikami's invariant (8.2.5). Just like its predecessor, eq. (8.4.12) is based on an ideal triangulation $\{\Delta_i\}_{i=1}^N$ of a hyperbolic 3-manifold M and inherits topological

[12]Namely, the complements of hyperbolic knots $\mathbf{4_1}(\mathbf{k2_1})$, $\mathbf{5_2}(\mathbf{k3_2})$, $\mathbf{12n_{242}}$ ($\mathbf{3_1}$, (-2,3,7)-pretzel knot), $\mathbf{6_1}(\mathbf{k4_1})$, $\mathbf{6_3}(\mathbf{k6_{43}})$, $\mathbf{7_2}(\mathbf{k4_2})$, $\mathbf{7_3}(\mathbf{k5_{20}})$, $\mathbf{7_4}(\mathbf{k6_{28}})$, $\mathbf{10_{132}}(\mathbf{K5_9})$, $\mathbf{10_{139}}(\mathbf{K5_{22}})$, and $\mathbf{11n_{38}}(\mathbf{K5_{13}})$, as well as the one-punctured torus bundles L^2R and LR^3 over $\mathbf{S}^1$ (also knot complements, but in a manifold other than $\mathbf{S}^3$).

invariance from the pentagon identity (8.3.25) of the quantum dilogarithm.

However, in writing (8.4.12) we made two important modifications to Hikami's invariant (8.2.5). First, we introduced contours C_α running across the sadle points $\mathbf{p}_\alpha$, which now encode the choice of a classical solution in Chern-Simons theory. Second, in (8.4.12) we introduced an extra factor of $\sqrt{8\pi\hbar}e^{-u}$, which is needed to reproduce the correct asymptotic behavior of $Z^{(\alpha)}(M;\hbar,u)$. To understand this correction factor, we must look at the higher-order terms in the expansion of $Z^{(\alpha)}(M;\hbar,u)$. By using (8.3.11), one can continue the saddle-point approximations described above to arbitrary order in $\hbar$. The result has the expected form (5.1.9),

$$Z^{(\alpha)}(M;\hbar,u) = \exp\left(\frac{1}{\hbar}S_0^{(\alpha)}(u) - \frac{1}{2}\delta^{(\alpha)}\log\hbar + \sum_{n=0}^{\infty} S_{n+1}^{(\alpha)}(u)\hbar^n\right), \tag{8.4.13}$$

with the correct leading term $S_0^{(\alpha)}(u)$ that we already analyzed above, *cf.* eq. (8.4.6).

Let us examine the next-leading logarithmic term. Its coefficient $\delta^{(\alpha)}$ receives contributions from two places: from the prefactor $(4\pi\hbar)^{-(N-1)/2}$ in (8.4.12), and from the standard Gaussian determinant. The former depends on the total number of tetrahedra, N, in the triangulation of M and therefore must be cancelled (at least partially) since the total integral (8.4.12) is a topological invariant and cannot depend on N. This is indeed what happens. For example, in a saddle-point approximation around a nondegenerate critical point $\mathbf{p}^{(\alpha)}(u)$, the contribution of the Gaussian determinant goes like $\sim \hbar^{(N-1)/2}$ and exactly cancels the contribution of the prefactor $\sim \hbar^{-(N-1)/2}$. An example of such critical point is the critical point $\mathbf{p}^{(\mathrm{geom})}(u)$ corresponding to the geometric branch. Therefore, the asymptotic expansion of the integral (8.4.12) around the critical point $\mathbf{p}^{(\mathrm{geom})}(u)$ has the form (8.4.13) with

$$\delta^{(\mathrm{geom})} = 0\,, \tag{8.4.14}$$

which is the expected result.[13] Indeed, as explained *e.g.* in [40, 98], the rigidity of the flat connection $\mathcal{A}^{(\mathrm{geom})}$ associated with a hyperbolic structure on M implies $h^0 = h^1 = 0$, so that (5.2.2) gives $\delta^{(\mathrm{geom})} = 0$.

[13] Recall that throughout this work $Z^{(\rho)}(M;\hbar)$ (resp. $Z^{(\alpha)}(M;\hbar,u)$) stands for the *unnormalized* perturbative $G_{\mathbb{C}}$ invariant. A normalized version, obtained by dividing by $Z(\mathbf{S}^3)$, has an asymptotic expansion of the same form (5.1.9) (resp. (8.4.13)) with the value of $\delta^{(\alpha)}$ shifted by $\dim(G)$ for every α. This is easy to see from (5.3.6).

Using (8.3.11) , one can also calculate the higher-order perturbative coefficients $S_n^{(\alpha)}(u)$, with $n \geq 1$. In the following section, we carry out this analysis to high order for the figure-8 knot complement and find perfect agreement with the results obtained by methods of Section 6.6. (Other interesting examples and further checks will appear elsewhere [5].)

Note that the $S_n^{(\alpha)}(u)$'s do not depend on the details of the contours C_α. The only part of (8.4.12) which actually depends on the details of C_α is exponentially suppressed and is not part of the perturbative series (8.4.13). Finally, we also note that we use only those critical points of the full integrand (8.4.12) which correspond to critical points of V in the limit $\hbar \to 0$. For any fixed $\hbar > 0$, the actual integrand has many other critical points which become trapped in the half-line singularities of quantum dilogarithms as $\hbar \to 0$, so the integrals over them do not have a well-behaved limit.

We conclude this section by observing that Conjecture 2 implies Conjecture 1. From (8.3.11), we can write an asymptotic double series expansion (for very small p):

$$\begin{aligned}\Phi_\hbar(p_0+p) &= \exp\left(\sum_{n=0}^{\infty} B_n\big(\frac{1}{2}+\frac{p}{2\hbar}\big)\,\mathrm{Li}_{2-n}\big(-e^{p_0}\big)\,\frac{(2\hbar)^{n-1}}{n!}\right)\\ &= \exp\left(\sum_{k=-1}^{\infty}\sum_{j=0}^{\infty}\frac{B_{k+1}(1/2)\,2^k}{(k+1)!j!}\mathrm{Li}_{1-j-k}(-e^{p_0})\,\hbar^k p^j\right). \qquad (8.4.15)\end{aligned}$$

Using this formula and taking into account the shifts by $\pm(i\pi+\hbar)$, we expand every quantum dilogarithm appearing in the integrand of (8.4.12) around a critical point $\mathbf{p}^{(\alpha)}$. At each order in $\hbar$, the state integral model then reduces to an integral of a polynomial in $\mathbf{p}$ with a Gaussian weight. Due to the fact that Li_k is a rational function for $k \leq 0$, the coefficients of these polynomials are all rational functions of the variables $\mathbf{x}^{(\alpha)} = \exp(\mathbf{p}^{(\alpha)})$ and m. Therefore, the resulting coefficients $S_n^{(\alpha)}(m)$, for $n > 1$, will also be rational functions of $\mathbf{x}^{(\alpha)}$ and m. At $m = 1$, the solutions $\mathbf{x}^{(\alpha)}(m)$ to the rational equations (8.4.8) all belong to some algebraic number field $\mathbb{K} \subset \overline{\mathbb{Q}}$, leading immediately to Conjecture 1. In particular, for the geometric branch $\alpha = \mathrm{geom}$, the field $\mathbb{K}$ is nothing but the trace field $\mathbb{Q}(\mathrm{tr}\,\Gamma)$.

Chapter 9

Saddle points and new invariants

In this chapter, we begin by performing explicit computations with the state integral model of Chapter 8, using the algorithm outlined very briefly at the end of Section 8.4. We use the hyperbolic figure-eight knot $\mathbf{4_1}$ and the knot $\mathbf{5_2}$ (or rather their complements in the three-sphere) as our main examples. In both cases, we how the equations of geometric quantization $\hat{A} \cdot Z = 0$ can be easily verified directly within the state integral model. Of course, for $\mathbf{4_1}$ our coefficients $S_n(u)$ will agree with those obtained in Section 6.6 directly from geometric quantization. Unlike geometric quantization, however, the state integral model fixes (almost) all potentially undetermined constants in the invariants $S_n(u)$; one can check that for $\mathbf{4_1}$ and $\mathbf{5_2}$, these invariants reduce to the arithmetic invariants found in Section 5.4 at $u = 0$.

The knot $\mathbf{5_2}$ is not amphicheiral, and its perturbative invariants display several novel features. In particular, the $\mathbf{5_2}$ knot complement has three branches of non-abelian flat connections, two of which are conjugate to each other (but are not a signed pair), and one which is a real self-conjugate branch. Unlike the case of self-conjugate abelian branches, the non-abelian real branch here has interesting arithmetic properties. Moreover, the conjugate branches have a non-vanishing Chern-Simons invariant.

In Section 9.3, we will then use functional equations for the quantum dilogarithm to obtain direct (though unrigorous) analytic continuations of the colored Jones polynomials of knots $\mathbf{4_1}$ and $\mathbf{5_2}$, as well as the non-hyperbolic trefoil $\mathbf{3_1}$. The resulting analytic continuations become integrals of products of quantum dilogarithms just like the partition functions of the state integral model. In some cases, the integrals are identical. Saddle-point

approximations can be applied in this case as well, leading to the same perturbative $G_{\mathbb{C}}$ invariants.

The figure-eight example appeared first in our work [3]. The $\mathbf{5_2}$ example, verification of $\hat{A} \cdot Z = 0$, and direct analytic continuation will appear in [5]. The integral for the trefoil obtained by analytic continuation suggests the existence of a non-hyperbolic state integral model.

9.1 Figure-eight knot 4_1

The state integral model (8.4.12) for the figure-eight knot complement gives:

$$Z^{(\alpha)}(M;\hbar,u) = \frac{1}{\sqrt{2\pi\hbar}} \int_{C_\alpha} dp \frac{\Phi_\hbar(p+i\pi+\hbar)}{\Phi_\hbar(-p-2u-i\pi-\hbar)} e^{-\frac{2}{\hbar}u(u+p)-u} \,. \tag{9.1.1}$$

There are two tetrahedra ($N = 2$) in the standard triangulation of M, and so two quantum dilogarithms in the integral. There is a single integration variable p, and we can identify $g_1(p,u) = p,\ g_2(p,u) = -p-2u$, and $f(p,2u,\hbar) = -4u(u+p)$.

It will be convenient here to actually change variables $p \mapsto p-u-i\pi-\hbar$, removing the $(i\pi+\hbar)$ terms in the quantum dilogarithms, and obtaining the somewhat more symmetric expression

$$Z^{(\alpha)}(M;\hbar,u) = \frac{1}{\sqrt{2\pi\hbar}} e^{\frac{2\pi i u}{\hbar}+u} \int_{C_\alpha} dp \frac{\Phi_\hbar(p-u)}{\Phi_\hbar(-p-u)} e^{-\frac{2pu}{\hbar}} \tag{9.1.2}$$

$$= \frac{1}{\sqrt{2\pi\hbar}} e^{\frac{2\pi i u}{\hbar}+u} \int_{C_\alpha} dp\, e^{\Upsilon(\hbar,p,u)} \,. \tag{9.1.3}$$

We define $e^{\Upsilon(\hbar,p,u)} = \frac{\Phi_\hbar(p-u)}{\Phi_\hbar(-p-u)} e^{-\frac{2pu}{\hbar}}$. Figures 9.1 and 9.2 show plots of $|e^{\Upsilon(\hbar,p,u)}|$ and $\log|e^{\Upsilon(\hbar,p,u)}| = \mathrm{Re}\,\Upsilon(\hbar,p,u)$ at $\hbar = i/3$ and two values of u. The half-lines of poles and zeroes of the two quantum dilogarithms combine into similar singularities for $\Upsilon(\hbar,p,u)$, as is depicted in Figure 9.3; note the splitting of these poles and zeroes by an amount $2u$.

After our change of variables, the "potential" function $V(p,u)$ as in (8.4.2) is now seen to be

$$V(p,u) = \frac{1}{2}\left[\mathrm{Li}_2(-e^{p-u}) - \mathrm{Li}_2(-e^{-p-u}) - 4pu + 4\pi i u\right] \,. \tag{9.1.4}$$

Instead of looking directly at $\frac{\partial}{\partial p}V = 0$ to find its critical points, we consider the simpler equation

$$r(x,m) = e^{2\frac{\partial}{\partial p}V} = \frac{x}{m^2(m+x)(1+mx)} = 1\,, \tag{9.1.5}$$

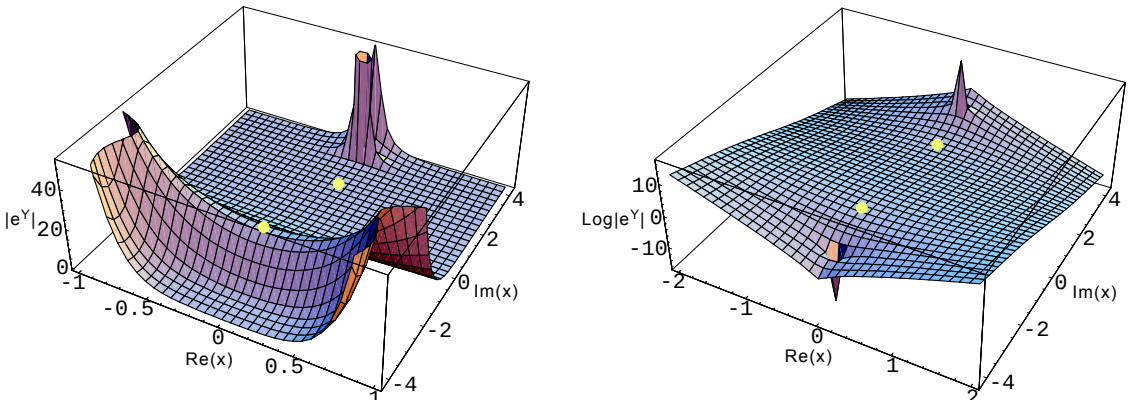

Figure 9.1: Plots of $|e^{\Upsilon(\hbar,p,u)}|$ and its logarithm at $u = 0$ and $\hbar = \frac{i}{3}$.

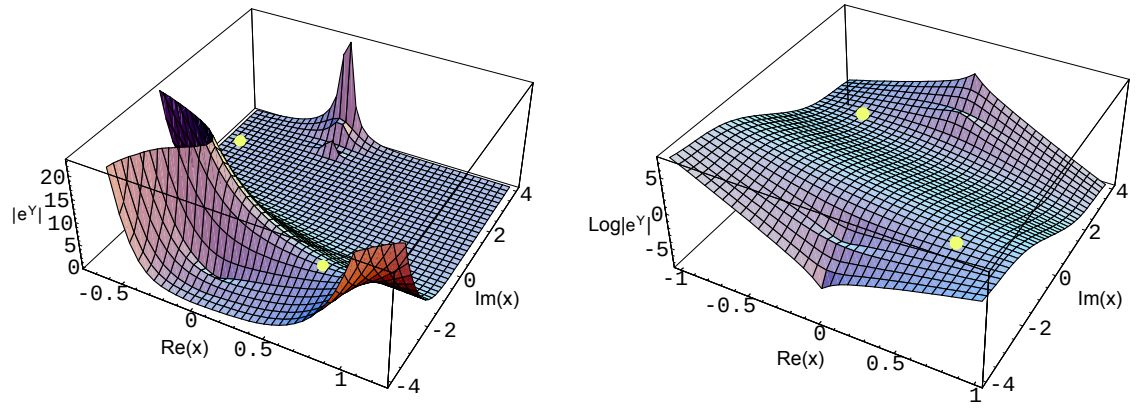

Figure 9.2: Plots of $|e^{\Upsilon(\hbar,p,u)}|$ and its logarithm at $u = \frac{1}{2}i$ and $\hbar = \frac{i}{3}$.

in terms of $x = e^p$ and $m = e^u$. This clearly has two branches of solutions, which both lift to true critical points of V, given by

$$p^{(\text{geom,conj})}(u) = \log\left[\frac{1 - m^2 - m^4 \mp m^2\Delta(m)}{2m^3}\right], \tag{9.1.6}$$

with $\Delta(m)$ defined as in (6.6.12):

$$\Delta(m) = i\sqrt{-m^{-4} + 2m^{-2} + 1 + 2m^2 - m^4}\,. \tag{9.1.7}$$

The lift is unique if (say) $\hbar \in i\,\mathbb{R}_{>0}$. We claim that these correspond to the geometric and conjugate branches of the A-polynomial described in Section 6.6, which can be verified by calculating[1] $s(x,m) = \exp\left(\frac{\partial}{\partial u}V(p,u)\right) = \left[\frac{m+x}{x^3+mx^4}\right]^{1/2}$, and checking indeed that $s(x^{(\text{geom,conj})}(m), m) = l_{\text{geom,conj}}(m)$.

[1]Here $s(x,m)$ is the square root of a rational function rather than a rational function itself due to our redefined variables. Using (9.1.1) directly, we would have gotten a pure rational expression.

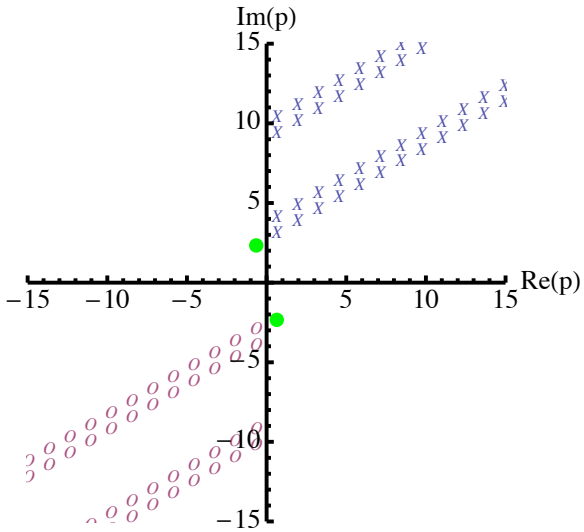

Figure 9.3: Poles, zeroes, and critical points of $e^{\Upsilon(\hbar,p,u)}$ for $u = \frac{1}{2}i$ and $\hbar = \frac{3}{4}e^{i\pi/6}$.

The two critical points of $\Lambda_\hbar$ which correspond to the critical points of V (as $\hbar \to 0$) are indicated in Figures 9.1 and 9.2. As mentioned at the end of Section 8.4, at any fixed $\hbar \neq 0$ there exist many other critical points of $\Lambda_\hbar$ that can be seen between consecutive pairs of poles and zeroes in Figures 9.1 and 9.2; however, these other critical points become trapped in half-line singularities as $\hbar \to 0$, and their saddle-point approximations are not well-defined.

We now calculate the perturbative invariants $S_n^{(\mathrm{geom})}(u)$ and $S_n^{(\mathrm{conj})}(u)$ by doing a full saddle-point approximation of the integral (9.1.2) on (dummy) contours passing through the two critical points. We begin by formally expanding $\Upsilon(\hbar, p, u) = \log \Lambda_\hbar(p, u)$ as a series in both $\hbar$ and p around some fixed point p_0:

$$\Upsilon(\hbar, p_0 + p, u) = \sum_{j=0}^{\infty} \sum_{k=-1}^{\infty} \Upsilon_{j,k}(p_0, u)\, p^j \hbar^k \,. \tag{9.1.8}$$

Our potential $V(p, u)$ is identified with $\Upsilon_{0,-1}(p, u) + 2\pi i u$, and critical points of V are defined by $\Upsilon_{1,-1}(p, u) = \frac{\partial}{\partial p} V(p, u) = 0$. Let us also define

$$b(p, u) := -2\Upsilon_{2,-1}(p, u) = -\frac{\partial^2}{\partial p^2} V(p, u) \,. \tag{9.1.9}$$

Then at a critical point $p_0 = p^{(\alpha)}(u)$, the integral (9.1.2) becomes[2]

$$Z^{(\alpha)}(M;\hbar,u) = \frac{e^{u+\frac{1}{\hbar}V^{(\alpha)}(u)}}{\sqrt{2\pi\hbar}} \int_{C_\alpha} dp\, e^{-\frac{b^{(\alpha)}(u)}{2\hbar}p^2} \exp\left[\frac{1}{\hbar}\sum_{j=3}^{\infty} \Upsilon^{(\alpha)}_{j,-1}(u)\, p^j + \sum_{j=0}^{\infty}\sum_{k=1}^{\infty} \Upsilon^{(\alpha)}_{j,k}(u)\, p^j \hbar^k\right], \tag{9.1.10}$$

where $V^{(\alpha)}(u) = V(p^{(\alpha)}(u), u)$, $b^{(\alpha)}(u) = b(p^{(\alpha)}(u), u)$, and $\Upsilon^{(\alpha)}_{j,k}(u) = \Upsilon_{j,k}(p^{(\alpha)}(u), u)$ are implicitly functions of u alone.

We can expand the exponential in (9.1.10), integrate each term using

$$\int dp\, e^{-\frac{b}{2\hbar}p^2} p^n = \begin{cases} (n-1)!!\left(\frac{\hbar}{b}\right)^{n/2}\sqrt{\frac{2\pi\hbar}{b}} & n \text{ even} \\ 0 & n \text{ odd} \end{cases}, \tag{9.1.11}$$

and re-exponentiate the answer to get a final result. The integrals in (9.1.11) are accurate up to corrections of order $\mathcal{O}(e^{-\text{const}/\hbar})$, which depend on a specific choice of contour and are ignored. Following this process, we obtain

$$Z^{(\alpha)}(M;\hbar,u) = \frac{1}{\sqrt{2\pi\hbar}}\sqrt{\frac{2\pi\hbar}{b^{(\alpha)}}} e^{u+\frac{1}{\hbar}V^{(\alpha)}(u)} e^{S_2^{(\alpha)}\hbar + S_3^{(\alpha)}\hbar^2 + \dots} \tag{9.1.12}$$

$$= \exp\left[\frac{1}{\hbar}V^{(\alpha)}(u) - \frac{1}{2}\log b^{(\alpha)} + u + S_2^{(\alpha)}\hbar + S_3^{(\alpha)}\hbar^2 + \dots\right], \tag{9.1.13}$$

where the coefficients S_n can be straightforwardly computed in terms of b and the Υ's. For example, $S_2^{(\alpha)} = \frac{15}{2(b^{(\alpha)})^3}\Upsilon^{(\alpha)}_{3,-1} + \frac{3}{(b^{(\alpha)})^2}\Upsilon^{(\alpha)}_{4,-1} + \Upsilon^{(\alpha)}_{0,1}$ and $S_3^{(\alpha)} = \frac{3465}{8(b^{(\alpha)})^6}(\Upsilon^{(\alpha)}_{3,-1})^4 +$ (sixteen other terms). In addition, we clearly have

$$S_0^{(\alpha)}(u) = V^{(\alpha)}(u)\,, \tag{9.1.14}$$

$$\delta^{(\alpha)} = 0\,, \tag{9.1.15}$$

$$S_1^{(\alpha)}(u) = -\frac{1}{2}\log\frac{b^{(\alpha)}}{m^2}\,. \tag{9.1.16}$$

To actually evaluate the coefficients $\Upsilon_{i,j}(p,u)$, we refer back to the expansion (8.4.15) of the quantum dilogarithm in Section 8.4. We find

$$\Upsilon_{j,k}(p,u) = \frac{B_{k+1}(1/2)\,2^k}{(k+1)!j!}\left[\mathrm{Li}_{1-j-k}(-e^{p-u}) - (-1)^j \mathrm{Li}_{1-j-k}(-e^{-p-u})\right] \tag{9.1.17}$$

when $j \geq 2$ or $k \geq 0$, and that all $\Upsilon_{j,2k}$ vanish.

Therefore: to calculate the expansion coefficients $S_n^{(\alpha)}(u)$ around a given critical point, we substitute $p^{(\alpha)}(u)$ from (9.1.6) into equations (9.1.4) and (9.1.17) to obtain $V^{(\alpha)}$, $b^{(\alpha)}$,

[2]This expression assumes that $\Upsilon_{j,k} = 0$ when k is even, a fact that shall be explained momentarily.

and $\Upsilon^{(\alpha)}_{j,k}$; then we substitute these functions into expressions for the S_n and simplify. At the geometric critical point $p^{(\mathrm{geom})}(u)$, we obtain

$$V^{(\mathrm{geom})}(u) = \frac{1}{2}\left[\mathrm{Li}_2(-e^{p^{(\mathrm{geom})}(u)-u}) - \mathrm{Li}_2(-e^{-p^{(\mathrm{geom})}(u)-u}) - 4p^{(\mathrm{geom})}(u)\,u + 4\pi i u\right], \tag{9.1.18}$$

$$b^{(\mathrm{geom})}(u) = \frac{im^2}{2}\Delta(m)\,, \tag{9.1.19}$$

and it is easy to check with a little algebra that all the expansion coefficients $S_n^{(\mathrm{geom})}(u)$ reproduce *exactly*[3] what we found in Table 6.3 of Section 6.6 by quantizing the moduli space of flat connections. (This has been verified to eight-loop order.) Moreover, the present state integral model completely fixed all the constants of the $S_n^{(\mathrm{geom})}(u)$, which had to be fixed in Table 6.3 by comparison to analytic continuation of the Jones polynomial.

Similarly, at the conjugate critical point $p^{(\mathrm{conj})}(u)$, we have

$$V^{(\mathrm{conj})}(u) = -V^{(\mathrm{geom})}(u)\,, \qquad b^{(\mathrm{conj})}(u) = -\frac{im^2}{2}\Delta(m)\,, \tag{9.1.20}$$

and more generally $S_n^{(\mathrm{conj})} = (-1)^{n-1}S_n^{(\mathrm{geom})}$. It is not hard to actually prove this relation between the geomtric and conjugate critical points to all orders by inspecting the symmetries of $e^{\Upsilon(\hbar,p,u)}$. Thus, we find complete agreement with the results of Section 6.6.

9.1.1 Checking $\hat{A}\cdot Z = 0$

An alternative and more convenient way to check that the quantum A-polynomial annihilates the perturbative partition functions of the state integral model (more convenient than computing $S_n(u)$'s independently in both approaches) is to apply the operator $\hat{A}(\hat{l},\hat{m})$ directly to the state integral.

Let us write, as usual,

$$\hat{A}(\hat{l},\hat{m}) = \sum_j a_j(\hat{m},q)\hat{l}^j\,. \tag{9.1.21}$$

By virtue of the functional relation

$$\Phi_\hbar(p-\hbar) = (1+e^p)\Phi_\hbar(p+\hbar)\,, \tag{9.1.22}$$

[3]There appears to be a small "correction" of $\frac{1}{2}\log(-1) = \log(\pm i)$ in $S_1^{(\mathrm{geom})}$, comparing (9.1.16) with the value in Table 6.3. This merely multiplies the partition function by i and can be attributed to the orientation of the stationary-phase contour passing through the geometric critical point. We also allow the usual modulo $2\pi i u$ ambiguity in matching S_0.

the operator $\hat{l}$ has a very simple action on quantum dilogarithms. In the case of the figure-eight knot, shifts of u and relabeling of the integration variable p can be combined to show that

$$Z(u+j\hbar) = \frac{1}{\sqrt{2\pi\hbar}}\, e^{\frac{2\pi i u}{\hbar}} \int dp\, e^{\frac{(u+j\hbar)(2ip+(2j-1)\hbar)}{\hbar}} \frac{\Phi_\hbar(p-u)}{\Phi_\hbar(-p-u)} \big(- e^{p-u-(2j-1)\hbar}; q\big)_j\,, \quad (9.1.23)$$

where $(x;q)_j$ denotes the *finite* q-Pochhammer symbol $(x;q)_j = \prod_{r=0}^{j-1}(1-q^r x)$. Then we have

$$\hat{A}\cdot Z(u) = \frac{1}{\sqrt{2\pi\hbar}}\, e^{\frac{2\pi i u}{\hbar}} \int dp\, \frac{\Phi_\hbar(p-u)}{\Phi_\hbar(-p-u)} \sum_{j=0}^{3} a_j(e^u, q) \big(- e^{p-u-(2j-1)\hbar}; q\big)_j e^{\frac{(u+j\hbar)(2ip+(2j-1)\hbar)}{\hbar}}\,. \quad (9.1.24)$$

The classical saddle point of this integral is unchanged from the original case (9.1.2), and the very same saddle point methods used above to find the perturbative coefficients of $Z(u)$ can be applied to the integral here to show that it vanishes perturbatively to all orders. This is actually somewhat easier than computing $Z(u)$ itself, because the terms S_0 and S_1, appearing multiplicatively in front of (9.1.12) can be completely ignored, and there are no branch cut ambiguities to worry about.

It may be possible that the integral (9.1.24) can be shown to vanish identically, without using any perturbative expansions (although, as written, the integrand is certainly not zero). It would be interesting to explore this further.

9.2 Three-twist knot 5_2

The complement knot $\mathbf{5_2}$ can be divided into three hyperbolic tetrahedra. They can be chosen to all have negative orientation; at the complete hyperbolic structure, they all have equal (negative) volumes. See, *e.g.*, [137] for a full description of the hyperbolic structure. The resulting state sum model can be written as a two-dimensional integral

$$Z(u) = \frac{1}{2\sqrt{2}\pi\hbar}\, e^{-u} \int dp_x\, dp_y\, \frac{e^{\frac{1}{2\hbar}\left[(p_x+4u+i\pi+\hbar)(p_y+2u+i\pi+\hbar)-\frac{3}{2}i\pi\hbar+\frac{\pi^2-\hbar^2}{2}\right]}}{\Phi_\hbar(p_y)\Phi_\hbar(p_x+2u)\Phi_\hbar(p_x)}\,. \quad (9.2.1)$$

As in the case of the figure-eight knot, each quantum dilogarithm only involves a single integration variable, making the asymptotic expansions of the quantum dilogarithms very simple.

The A-polynomial for the knot $\mathbf{5_2}$ is

$$A(l,m) = (l-1)(m^{14}l^3+(-m^{14}+2m^{12}+2m^{10}-m^6+m^4)l^2+(m^{10}-m^8+2m^4+2m^2-1)l+1)\,. \tag{9.2.2}$$

There are three non-abelian branches, two conjugate to each other and one real. Since this knot is chiral, there is no symmetry $A(l,m^{-1}) \sim A(l,m)$.

Since the A-polynomial has three non-abelian branches, one expects to find three saddle points in the integrand of (9.2.1). In terms of the "downstairs" variables $x = e^{p_x}$ and $y = e^{p_y}$, the saddle points are given by the equations

$$m^4 x(y+1) = -1\,, \qquad m^2(x+1)y\left(m^2x+1\right) = -1\,. \tag{9.2.3}$$

It is easy to solve for $y = \frac{m^4(-x)-1}{m^4 x}$, but the subsequent equation for x is (as expected) a third-degree irreducible polynomial:

$$m^6x^3 + m^6x^2 + m^4x^2 + m^4x + m^2x^2 + x + 1 = 0\,. \tag{9.2.4}$$

The solutions to this polynomial have the same arithmetic structure as the solutions to the A-polynomial. It is most convenient to leave an algebraic dependence on x in the perturbative invariants $S_n^{(\alpha)}(u)$, reducing them as much as possible with the equation (9.2.4). The resulting general expressions for $S_n^{(\alpha)}(u)$ can then be specialized to various branches α by substituting in the three actual solutions of (9.2.4).

The leading coefficient $S_0^{(\alpha)}(u)$ is given by

$$S_0^{(\alpha)}(u) = \frac{1}{2}\left[-\mathrm{Li}_2(-e^{p_x}) - \mathrm{Li}_2(-e^{p_x+2u}) - \mathrm{Li}_2(-e^{p_y}) + (p_y+2u)(p_x+4u) + i\pi(p_x+p_y+6u) - \frac{\pi^2}{2}\right]\,, \tag{9.2.5}$$

and specializes as expected to $\mathrm{Vol}+i\mathrm{CS}$, its conjugate, and a nonzero real quantity (for real or imaginary u) when an appropriate lift of the solution to is used.

The other coefficients quickly become more complicated, but the present saddle-point methods can still calculate them easily up to about sixth order. For example, one has

$$S_1 = -\frac{1}{2}\log\left[-\frac{3m^6x^2+2m^6x+2m^4x+m^4+2m^2x+1}{2m^2}\right]\,, \tag{9.2.6}$$

and

$$S_2^{(\alpha)}(m) = \frac{1}{12\left(m^{16}-6m^{14}+11m^{12}-12m^{10}-11m^8-12m^6+11m^4-6m^2+1\right)^2} \tag{9.2.7}$$
$$\times \big(-2m^{34}x^2-2m^{34}x+16m^{32}x^2+12m^{32}x-3m^{32}-106m^{30}x^2-68m^{30}x$$
$$+30m^{30}+254m^{28}x^2+112m^{28}x-148m^{28}-182m^{26}x^2-78m^{26}x+384m^{26}$$
$$-370m^{24}x^2-148m^{24}x-641m^{24}+392m^{22}x^2-280m^{22}x+410m^{22}$$
$$-1654m^{20}x^2-336m^{20}x+250m^{20}+392m^{18}x^2-1922m^{18}x-1116m^{18}$$
$$-370m^{16}x^2-336m^{16}x-529m^{16}-182m^{14}x^2-280m^{14}x-1116m^{14}$$
$$+254m^{12}x^2-148m^{12}x+250m^{12}-106m^{10}x^2-78m^{10}x+410m^{10}$$
$$+16m^8x^2+112m^8x-641m^8-2m^6x^2-68m^6x+384m^6+12m^4x-148m^4$$
$$-2m^2x+30m^2-3\big).$$

The same approach of applying the quantum A-polynomial directly to the state integral can be used to show that these expressions are fully compatible with geometric quantization. The quantum A-polynomial for $\mathbf{5_2}$ appears in [118].

9.3 Direct analytic continuation

Let us finally describe the approach of direct analytic continuation from the colored Jones polynomial. This works in a few special cases where the colored Jones polynomial has a closed form expression as a sum of products, or more precisely a sum of finite q-Pochhammer symbols. The trick is to use the functional identity (9.1.22) for the quantum dilogarithm to write each q-Pochhammer symbol as a ratio of quantum dilogarithms, and to approximate the sum by an integral as $\hbar \to 0$ (this was also done in [102]). Then perturbative invariants $S_n^{(\alpha)}(u)$ can then be derived via our now standard methods of saddle-point approximation.

The analytic continuations involved here have *not* been made rigorous, but they certainly seem to work for practical computations. Moreover, unlike the current formulation of the state integral model, they work just as well for non-hyperbolic knots as for hyperbolic ones.

Figure-eight 4_1

Normalized (as explained in Section 5.4) to agree with the Chern-Simons partition function, the $SU(2)$ colored Jones polynomial for the figure-eight knot is [146]

$$J_N(q) = -\sqrt{\frac{2i\hbar}{\pi}}\sinh u \sum_{j=0}^{N-1} q^{Nj} \prod_{k=1}^{j}(1-q^{-N}q^{-k})(1-q^{-N}q^{k}) \tag{9.3.1}$$

$$= -\sqrt{\frac{2\hbar}{\pi}}\sinh u \sum_{j=0}^{N-1} q^{Nj} \frac{\Phi_\hbar(-2u+i\pi+\hbar)}{\Phi_\hbar(-2u-i\pi-\hbar)} \frac{\Phi_\hbar(-2i-i\pi-\hbar-2j\hbar)}{\Phi_\hbar(-2u+i\pi+\hbar+2j\hbar)} \tag{9.3.2}$$

$$= -\sqrt{\frac{2\hbar}{\pi}} e^{u}(1-e^{\frac{-2\pi i u}{\hbar}}) \sum_{j=0}^{N-1} q^{Nj} \frac{\Phi_\hbar(-2i-i\pi-\hbar-2j\hbar)}{\Phi_\hbar(-2u+i\pi+\hbar+2j\hbar)}\,. \tag{9.3.3}$$

As usual, $q = e^{2\hbar}$, and in analytic continuation $u = \hbar N$ (*cf.* (6.2.4)). Equating $-i\pi-\hbar+2j\hbar$ with a new integration variable p, and letting $dp = 2\hbar$, this sum is approximated by an integral in the limit $\hbar \to 0$. Specifically,

$$J_N(q) \to \frac{1}{\sqrt{2\pi i\hbar}}\left(e^{\frac{i\pi u}{\hbar}} - e^{-\frac{i\pi u}{\hbar}}\right) \int_{-i\pi+\hbar-2u}^{i\pi-i\hbar} dp\, e^{-\frac{up}{\hbar}} \frac{\Phi_\hbar(p-2u)}{\Phi_\hbar(-p-2u)}\,. \tag{9.3.4}$$

This expression looks very similar to the state integral model (9.1.2), though it has not been possible yet to prove their equivalence. It has several nice properties, including a more manifest symmetry under $u \to -u$ and a preferred choice of contour. It turns out that (9.3.4) has exactly two saddle points, and doing abstract saddle point expansions around them yields exactly the same perturbative invariants $S_n^{(\text{geom,conj})}(u)$ obtained from the state integral model. The preferred contour indicated here crosses the geometric saddle — perhaps this is not a surprise, since it is the saddle that should govern the leading asymptotics of the colored Jones.

Note that the two nonperturbative terms in the prefactor $\left(e^{\frac{i\pi u}{\hbar}} - e^{-i\frac{\pi u}{\hbar}}\right)$ are related by a difference of $2\pi i u/\hbar$ in the exponent, which has always been an ambiguity in the partition function. Also note that when $u\hbar = N$ is an integer (*i.e.* the dimension of an $SU(2)$ representation), the prefactor $\left(e^{\frac{i\pi u}{\hbar}} - e^{-i\frac{\pi u}{\hbar}}\right)$ vanishes. This is a general feature of the subtle analytic continuation of compact Chern-Simons partition functions, and (partly) explains why exponential growth only appears when $N \notin \mathbb{Z}$ (*cf.* [41]).

Three-twist 5_2

There is a sum-of-products expression for the colored Jones polynomial of the knot $\mathbf{5_2}$ at the complete hyperbolic structure $u = 0$. It is given by [102]

$$J_N(q) = -\sqrt{\frac{2i\hbar}{\pi}} \sum_{0 \le k \le l < N} \frac{(q;q)_l^2}{(q^{-1};q^{-1})_k} q^{-k(l+1)} \,. \tag{9.3.5}$$

In the analytic continuation limit $\hbar \to 0$ (and $u = N\hbar$ fixed), letting the two summation indices be identified with integration variables p_x and p_y, this formally becomes exactly the same expression as the state integral model (9.2.1) at $u = 0$.

Trefoil 3_1

The analogous expression for the trefoil can be evaluated exactly, in accordance with fact that higher-order invariants vanish on the non-abelian branch (*cf.* Section 6.6). The colored Jones polynomial is

$$J_N(q) = -\sqrt{\frac{2i\hbar}{\pi}} \sinh u q^{1-N} \sum_{j=0}^{N-1} q^{-jN} \prod_{k=1}^{j} (1 - q^{k-N}) \tag{9.3.6}$$

$$\to \sqrt{\frac{2i\hbar}{\pi}} (e^u - e^{-u}) \Phi_\hbar(-2u + \hbar - i\pi) \int_0^{2\pi i + 2u} \frac{e^{-\frac{1}{2\hbar}(p(2u+2\pi i) - 2u + 2\hbar)}}{\Phi_\hbar(p - 2u - i\pi + \hbar)} \,. \tag{9.3.7}$$

After a formal shift of countour, this is just a Fourier transform of the quantum dilogarithm. The Fourier transform of $\Phi_\hbar(x)^{\pm 1}$, described in [140], is just another quantum dilogarithm $\Phi_\hbar(x)^{\pm 1}$. In fact, the result of the integral in(9.3.7) is a quantum dilogarithm that almost exactly cancels the prefactor $\Phi_\hbar(-2u + \hbar - i\pi)$, resulting in an expression that involves no quantum dilogarithms at all. We find

$$J_N(q) \sim e^{\frac{3u^2 + i\pi u}{\hbar}} \,, \tag{9.3.8}$$

up to some additional constants, just as in the geometric quantization analysis of Section 6.6.

The form of the expression (9.3.7) suggests that the $SL(2,\mathbb{C})$ Chern-Simons partition function for the trefoil knot complement might have a state integral model despite the fact that the trefoil is not a hyperbolic knot. Indeed, it is known that the trefoil knot complement does have *topological* ideal triangulation consisting of two tetrahedra, the same as the

number of quantum dilogarithms appearing in (9.3.7). A topological ideal triangulation of a three-manifold is similar to a geometric one, with all vertices of the triangulation being located on the manifold's boundary. For a torus knot such as the trefoil, the "problem" with imposing a hyperbolic geometric structure on this triangulation is that gluing conditions require all tetrahedra to be flat when $u = 0$. However, this should be no problem for Chern-Simons theory: an $SL(2, \mathbb{C})$ structure does not care whether tetrahedra are "flat." These ideas are explained further in [5].

Bibliography

[1] T. Dimofte and S. Gukov, *Refined, Motivic, and Quantum*, *Lett. Math. Phys.* **91** (2010), no. 1 1, [arXiv:0904.1420].

[2] T. Dimofte, S. Gukov, and Y. Soibelman, *Quantum Wall Crossing in N=2 Gauge Theories*, arXiv:0912.1346.

[3] T. Dimofte, S. Gukov, J. Lenells, and D. Zagier, *Exact Results for Perturbative Chern-Simons Theory with Complex Gauge Group*, *Comm. Num. Thy. and Phys.* **3** (2009), no. 2 363–443, [arXiv:0903.2472].

[4] T. Dimofte and D. Jafferis, in preparation.

[5] T. Dimofte and J. Lenells, *Triangulating the Trefoil: SL(2,C) Chern-Simons Theory on General Manifolds*, in preparation.

[6] T. Dimofte and S. Gukov, *Quantum Field Theory and the Volume Conjecture*, *to appear* (2010).

[7] T. Dimofte, *Type IIB Flux Vacua at Large Complex Structure*, *JHEP* **0809** (2008) 064. Published in: JHEP0809:064,2008 42 pages.

[8] J. M. Maldacena, *The Large N Limit of Superconformal Field Theories and Supergravity*, *Adv. Theor. Math. Phys.* **2** (1998) 231–225, [hep-th/9711200v3].

[9] D. Maulik, N. Nekrasov, A. Okounkov, and R. Pandharipande, *Gromov-Witten theory and Donaldson-Thomas theory, I*, *Compos. Math.* **142** (2006), no. 5 1263–1285, [math/0312059v3].

[10] D. Maulik, N. Nekrasov, A. Okounkov, and R. Pandharipande, *Gromov-Witten theory and Donaldson-Thomas theory, II*, *Compos. Math.* **142** (2006), no. 5 1286–1304, [math/0406092v2].

[11] R. Gopakumar and C. Vafa, *M-Theory and Topological Strings-I*, hep-th/9809187v1.

[12] R. Gopakumar and C. Vafa, *M-Theory and Topological Strings-II*, hep-th/9812127v1.

[13] E. Witten, *Quantum field theory and the Jones polynomial*, *Commun. Math. Phys.* **121** (1989) 351–399.

[14] J. M. F. Labastida, *Chern-Simons Gauge Theory: Ten Years After*, hep-th/9905057v1.

[15] M. Kontsevich and Y. Soibelman, *Stability structures, motivic Donaldson-Thomas invariants and cluster transformations*, arXiv:0811.2435.

[16] F. Denef, *Supergravity flows and D-brane stability*, *JHEP* **08** (2000) 050, [hep-th/0005049v2].

[17] M. R. Douglas, *D-branes, Categories and N=1 Supersymmetry*, *J. Math. Phys.* **42** (2001) 2818–2843, [hep-th/0011017v4].

[18] T. Bridgeland, *Stability conditions on triangulated categories*, *Ann. of Math.* **166** (2007), no. 2 317–345, [math/0212237v3].

[19] H. Ooguri, A. Strominger, and C. Vafa, *Black Hole Attractors and the Topological String*, *Phys. Rev.* **D70** (2004) [hep-th/0405146v2].

[20] F. Denef and G. W. Moore, *Split States, Entropy Enigmas, Holes and Halos*, hep-th/0702146v2.

[21] S. Katz, D. R. Morrison, and M. R. Plesser, *Enhanced Gauge Symmetry in Type II String Theory*, *Nucl. Phys.* **B477** (1996) [hep-th/9601108v2].

[22] N. A. Nekrasov, *Seiberg-Witten Prepotential From Instanton Counting*, *Adv. Theor. Math. Phys.* **7** (2004) 831–864, [hep-th/0206161v1].

[23] T. J. Hollowood, A. Iqbal, and C. Vafa, *Matrix Models, Geometric Engineering and Elliptic Genera*, *JHEP* **03** (2008) 069, [hep-th/0310272v4].

[24] M. Aganagic, A. Klemm, M. Marino, and C. Vafa, *The Topological Vertex*, *Commun. Math. Phys.* **254** (2005) 425–478, [hep-th/0305132v3].

[25] A. Okounkov, N. Reshetikhin, and C. Vafa, *Quantum Calabi-Yau and Classical Crystals*, hep-th/0309208v2.

[26] A. Iqbal, C. Kozcaz, and C. Vafa, *The Refined Topological Vertex*, hep-th/0701156v2.

[27] R. Gopakumar and C. Vafa, *On the Gauge Theory/Geometry Correspondence*, *Adv. Theor. Math. Phys.* **3** (1999) 1415–1443, [hep-th/9811131v1].

[28] E. Witten, *Topology-Changing Amplitudes in (2+1)-Dimensional Gravity*, *Nucl. Phys.* **B323** (1989) 113.

[29] S. Gukov, A. Iqbal, C. Kozcaz, and C. Vafa, *Link Homologies and the Refined Topological Vertex*, arXiv:0705.1368.

[30] N. M. Dunfield, S. Gukov, and J. Rasmussen, *The Superpolynomial for Knot Homologies*, math/0505662v2.

[31] D. L. Jafferis and G. W. Moore, *Wall crossing in local Calabi Yau manifolds*, arXiv:0810.4909.

[32] P. Sułkowski, *Wall-crossing, free fermions and crystal melting*, arXiv:0910.5485.

[33] K. Nagao and M. Yamazaki, *The Non-commutative Topological Vertex and Wall Crossing Phenomena*, arXiv:0910.5479.

[34] D. Gaiotto, G. W. Moore, and A. Neitzke, *Four-dimensional wall-crossing via three-dimensional field theory*, arXiv:0807.4723.

[35] D. S. Freed, *Remarks on Chern-Simons Theory*, arXiv:0808.2507.

[36] O. Heinonen, *Composite fermions: a unified view of the quantum Hall regime*, *Singapore: World Scientific* (1998).

[37] G. Murthy and R. Shankar, *Hamiltonian Theory of the Fractional Quantum Hall Effect: Effect of Landau Level Mixing*, *Rev. Mod. Phys.* **75** (2003) 1101, [cond-mat/0201082v1].

[38] M. Marino, *Chern-Simons Theory and Topological Strings*, *Rev. Mod. Phys.* **77** (2005) 675, [hep-th/0406005v4].

[39] E. Witten, *Quantization of Chern-Simons gauge theory with complex gauge group*, *Commun. Math. Phys.* **137** (1991) 29.

[40] S. Gukov, *Three-Dimensional Quantum Gravity, Chern-Simons Theory, and the A-Polynomial*, *Commun. Math. Phys.* **255** (2005) 577–627, [hep-th/0306165v1].

[41] E. Witten, *Analytic Continuation of Chern-Simons Theory*, arXiv:1001.2933.

[42] S. Axelrod and I. M. Singer, *Chern-Simons Perturbation Theory*, *Proc. of the XXth International Conference on Differential Geometric Methods in Theoretical Physics* **1, 2** (1991) 3–45, [hep-th/9110056v1].

[43] D. Bar-Natan, *Perturbative aspects of the Chern-Simons topological quantum field theory*, *Thesis (Ph.D.)–Princeton University* (1991).

[44] D. Bar-Natan and E. Witten, *Perturbative expansion of Chern-Simons theory with non-compact gauge group*, *Comm. Math. Phys.* **141** (1991), no. 2 423–440.

[45] N. Woodhouse, *Geometric quantization*, *New York: Oxford Univ. Press* (1992).

[46] F. Bayen, M. Flato, C. Fronsdal, *et al.*, *Deformation theory and quantization. I. Deformations of symplectic structures*, *Annals of Physics* (1978).

[47] M. Kontsevich, *Deformation quantization of algebraic varieties*, *Lett. Math. Phys.* **56** (2006) 271–294, [math/0106006v1].

[48] S. Gukov and E. Witten, *Branes and Quantization*, arXiv:0809.0305.

[49] N. Reshetikhin and V. Turaev, *Invariants of 3-manifolds via link polynomials and quantum groups*, *Invent. Math.* **103** (1991), no. 3 547–597.

[50] V. Turaev and O. Viro, *State sum invariants of 3-manifolds and quantum 6j-symbols*, *Topology* **31** (1992) 865.

[51] S. Baseilhac and R. Benedetti, *Classical and quantum dilogarithmic invariants of flat PSL(2,C)-bundles over 3-manifolds*, *Geom. Topol.* **9** (2005) 493–569, [math/0306283v2].

[52] K. Hikami, *Hyperbolic Structure Arising from a Knot Invariant*, *J. Mod. Phys. A* **16** (2001) 3309–3333, [math-ph/0105039v1].

[53] K. Hikami, *Generalized Volume Conjecture and the A-Polynomials - the Neumann-Zagier Potential Function as a Classical Limit of Quantum Invariant*, *J. Geom. Phys.* **57** (2007) 1895–1940, [math/0604094v1].

[54] S. Cecotti and C. Vafa, *BPS Wall Crossing and Topological Strings*, arXiv:0910.2615.

[55] V. V. Fock and A. B. Goncharov, *The quantum dilogarithm and representations quantum cluster varieties*, *Invent. Math.* **175** (2009), no. 2 223–286, [math/0702397v6].

[56] D. Gaiotto, G. W. Moore, and A. Neitzke, *Wall-crossing, Hitchin Systems, and the WKB Approximation*, arXiv:0907.3987.

[57] F. Denef, *Quantum Quivers and Hall/Hole Halos*, *JHEP* **10** (2002) 023, [hep-th/0206072v3].

[58] B. Pioline, *Lectures on Black Holes, Topological Strings and Quantum Attractors*, *Class. Quant. Grav.* **23** (2006) S981, [hep-th/0607227v5].

[59] M. Becker and J. H. Schwarz, *String theory and M-theory: a modern introduction*, Cambridge, UK: Cambridge Univ. Press (2007) 739 p.

[60] P. Candelas and X. de La Ossa, *Moduli space of Calabi-Yau manifolds*, Prepared for XIII International School of Theoretical Physics: The Standard Model and Beyond, Szczyrk, Poland, 19-26 Sep 1989 (1992).

[61] A. Strominger, *Special geometry*, *Comm. Math. Phys.* **133** (1990) 163.

[62] G. Moore, *Arithmetic and Attractors*, hep-th/9807087v3.

[63] A. Lawrence and N. Nekrasov, *Instanton Sums and Five-Dimensional Gauge Theories*, *Nucl. Phys.* **B513** (1998) [hep-th/9706025v2].

[64] B. Szendroi, *Non-commutative Donaldson-Thomas theory and the conifold*, *Geom. Topol.* **12** (2008) 1171–1202, [arXiv:0705.3419].

[65] R. Dijkgraaf, C. Vafa, and E. Verlinde, *M-theory and a Topological String Duality*, hep-th/0602087v1.

[66] F. Denef, B. Greene, and M. Raugas, *Split attractor flows and the spectrum of BPS D-branes on the Quintic*, *JHEP* **05** (2001) 012, [hep-th/0101135v2].

[67] E. Diaconescu and G. W. Moore, *Crossing the Wall: Branes vs. Bundles*, arXiv:0706.3193.

[68] M. R. Douglas, B. Fiol, and C. Römelsberger, *The spectrum of BPS branes on a noncompact Calabi-Yau*, *JHEP* **09** (2005) 057, [hep-th/0003263v2].

[69] A. King, *Moduli of representations of finite dimensional algebras*, *The Quarterly Journal of Mathematics* (1994).

[70] M. R. Douglas and G. Moore, *D-branes, Quivers, and ALE Instantons*, hep-th/9603167v1.

[71] B. Fiol, *The BPS Spectrum of N=2 SU(N) SYM and Parton Branes*, hep-th/0012079v1.

[72] P. S. Aspinwall, *D-Branes on Calabi-Yau Manifolds*, *TASI lecture notes* (2003) [hep-th/0403166v1].

[73] D. Joyce, *Special Lagrangian submanifolds with isolated conical singularities. V. Survey and applications*, *J. Diff. Geom.* **63** (2003) 279–348, [math/0303272v1].

[74] A. Iqbal, N. Nekrasov, A. Okounkov, and C. Vafa, *Quantum Foam and Topological Strings*, *JHEP* **04** (2008) 011, [hep-th/0312022v2].

[75] W.-Y. Chuang and D. L. Jafferis, *Wall Crossing of BPS States on the Conifold from Seiberg Duality and Pyramid Partitions*, arXiv:0810.5072.

[76] B. Young, *Computing a pyramid partition generating function with dimer shuffling*, arXiv:0709.3079.

[77] Y. Toda, *Curve counting theories via stable objects I. DT/PT correspondence*, arXiv:0902.4371.

[78] T. Graber and R. Pandharipande, *Localization of virtual classes*, *Invent. Math.* **135** (1999), no. 2 487, [alg-geom/9708001v2].

[79] S. Mozgovoy and M. Reineke, *On the noncommutative Donaldson-Thomas invariants arising from brane tilings*, arXiv:0809.0117.

[80] H. Ooguri and M. Yamazaki, *Crystal Melting and Toric Calabi-Yau Manifolds*, arXiv:0811.2801.

[81] N. Elkies, G. Kuperberg, M. Larsen, and J. Propp, *Alternating sign matrices and domino tilings*, *J. Algebraic Combin.* **1** (1992), no. 2 111–132, [math/9201305v1].

[82] S. Katz, A. Klemm, and C. Vafa, *Geometric Engineering of Quantum Field Theories*, *Nucl. Phys.* **B497** (1997) [hep-th/9609239v2].

[83] A. Campillo, F. Delgado, and S. M. Gusein-Zade, *Integrals with respect to the Euler characteristic over spaces of functions and the Alexander polynomial*, *Proc. Steklov Inst. Math.* (2002), no. 3 134–147, [math/0205112v1].

[84] M. Kontsevich and Y. Soibelman, *Cohomological Hall Algebra*, *in preparation* (2009).

[85] N. Seiberg and E. Witten, *Electric-Magnetic Duality, Monopole Condensation, and Confinement In N=2 Supersymmetric Yang-Mills Theory*, *Nucl. Phys.* **B426** (1994) 19–52, [hep-th/9407087v1].

[86] N. Seiberg and E. Witten, *Monopoles, Duality and Chiral Symmetry Breaking in N=2 Supersymmetric QCD*, *Nucl. Phys.* **B431** (1994) 484–550, [hep-th/9408099v1].

[87] S. Kachru, A. Klemm, W. Lerche, P. Mayr, and C. Vafa, *Nonperturbative Results on the Point Particle Limit of N=2 Heterotic String Compactifications*, *Nucl. Phys.* **B459** (1996) [hep-th/9508155v1].

[88] P. S. Aspinwall and R. L. Karp, *Solitons in Seiberg-Witten Theory and D-branes in the Derived Category*, *JHEP* **0304** (2003) 049, [hep-th/0211121v1].

[89] S. Katz and C. Vafa, *Matter From Geometry*, *Nucl. Phys.* **B497** (1997) [hep-th/9606086v1].

[90] S. Katz, P. Mayr, and C. Vafa, *Mirror symmetry and Exact Solution of 4D N=2 Gauge Theories I*, *Adv. Theor. Math. Phys.* **1** (1998) 53–114, [hep-th/9706110v2].

[91] A. Klemm, W. Lerche, P. Mayr, C. Vafa, and N. Warner, *Self-Dual Strings and N=2 Supersymmetric Field Theory*, *Nucl. Phys.* **B477** (1996) [hep-th/9604034v3].

[92] W. Lerche, *Introduction to Seiberg-Witten Theory and its Stringy Origin*, *Nucl. Phys. Proc. Suppl.* **55B** (1996) [hep-th/9611190v1].

[93] A. Bilal and F. Ferrari, *Curves of Marginal Stability and Weak and Strong-Coupling BPS Spectra in $N=2$ Supersymmetric QCD*, *Nucl. Phys.* **B480** (1996) 589–622, [hep-th/9605101v4].

[94] F. Denef, *Attractors at weak gravity*, *Nucl. Phys.* **B547** (1999) 201–220, [hep-th/9812049v2].

[95] A. Schofield, *Birational classification of moduli spaces of representations of quivers*, *Indag. Math. (N.S.)* **12** (2001), no. 3 407–432, [math/9911014v1].

[96] E. Witten, *2+1 dimensional gravity as an exactly soluble system*, *Nucl. Phys.* **B311** (1988) 46.

[97] J. Porti, *Torsion de Reidemesiter poir les variétés hyperboliques*, *Mem. Amer. Math. Soc.* **128** (1997), no. 612.

[98] S. Gukov and H. Murakami, *SL(2,C) Chern-Simons theory and the asymptotic behavior of the colored Jones polynomial*, math/0608324v2.

[99] M. Kontsevich and D. Zagier, *Periods*, *in Mathematics Unlimited – 2001 and Beyond (Springer, Berlin)* (2001) 771–808.

[100] S. Bloch, H. Esnault, and D. Kreimer, *On motives associated to graph polynomials*, *Communications in Mathematical Physics* (2006).

[101] D. Zagier, *Quantum modular forms*, preprint (2009).

[102] R. M. Kashaev, *The hyperbolic volume of knots from quantum dilogarithm*, *Lett. Math. Phys.* **39** (1997) 269–265, [q-alg/9601025v2].

[103] D. Zagier, *Vassiliev invariants and a strange identity related to the Dedekind eta-function*, *Topology* **40** (2001) 945–960.

[104] D. Grünberg and P. Moree, *Sequences of enumerative geometry: congruences and asymptotics*, *Experim. Math.*, to appear.

[105] J. E. Andersen and S. K. Hansen, *Asymptotics of the quantum invariants for surgeries on the figure 8 knot*, *J. Knot Theory and its Remifications* **15** (2006), no. 4 479–548, [math/0506456v1].

[106] O. Costin and S. Garoufalidis, *Resurgence of 1-dimensional sums of Sum-Product type*, in preparation.

[107] S. Garoufalidis and J. Geronimo, *A Riemann-Hilbert approach to the asymptotics of 1-dimensional sums of Sum-Product type*, in preparation.

[108] D. Zagier, *Algebraic and asymptotic properties of quantum invariants of knots*, in preparation (2010).

[109] N. Hitchin, *The self-duality equations on a Riemann surface*, *Proc. London Math. Soc* (1987).

[110] A. Kapustin and E. Witten, *Electric-Magnetic Duality And The Geometric Langlands Program*, hep-th/0604151v3.

[111] D. Cooper, M. Culler, H. Gillet, and D. Long, *Plane curves associated to character varieties of 3-manifolds*, *Invent. Math.* **118** (1994), no. 1 47–84.

[112] S. Garoufalidis, *Difference and differential equations for the colored Jones function*, *J. Knot Theory Ramifications* **17** (2008), no. 4 495–510, [math/0306229v3].

[113] W. Thurston, *The geometry and topology of three-manifolds*, *Lecture notes at Princeton University, Princeton, 1980.*

[114] W. D. Neumann and D. Zagier, *Volumes of hyperbolic three-manifolds*, *Topology* **24** (1985), no. 3 307–332.

[115] T. Yoshida, *The eta-invariant of hyperbolic 3-manifolds*, *Invent. Math.* **81** (1985) 473–514.

[116] D. Cooper and D. Long, *Remarks on the A-polynomial of a knot*, *J. Knot Theory Ram.* **5** (1996), no. 5 609–628.

[117] H. Murakami, *Asymptotic behaviors of the colored Jones polynomials of a torus knot*, *Internat. J. Math.* **15** (2004), no. 6 547–555, [`math/0405126v1`].

[118] S. Garoufalidis and X. Sun, *The non-commutative A-polynomial of twist knots*, `arXiv:0802.4074`.

[119] S. Garoufalidis, *On the characteristic and deformation varieties of a knot*, *Geometry and Topology Monographs* **7** (2004) 291–304, [`math/0306230v4`].

[120] S. Garoufalidis and J. S. Geronimo, *Asymptotics of q-difference equations*, `math/0405331v2`.

[121] K. Hikami and H. Murakami, *Colored Jones polynomials with polynomial growth*, `arXiv:0711.2836`.

[122] S. Elitzur, G. Moore, A. Schwimmer, and N. Seiberg, *Remarks on the canonical quantization of the Chern-Simons-Witten theory*, *Nucl. Phys.* **B326** (1989) 108.

[123] A. W. Knapp, *Representation theory of semisimple groups: an overview based on examples*, *Princeton Univ. Press* (2001) 773.

[124] R. Howe, *A century of Lie theory*, Proceedings of the AMS 1988 centennial symposium (1992).

[125] A. A. Kirillov, *Lectures on the orbit method*, *AMS* (2004) 408.

[126] R. Bott, *Homogeneous vector bundles*, *Annals of Mathematics* (1957).

[127] E. Witten, *Coadjoint orbits of the Virasoro group*, *Commun. Math. Phys.* **114** (1988) 1.

[128] G. Moore and N. Seiberg, *Taming the conformal zoo*, *Phys. Lett.* **B220** (1989) 422.

[129] W. P. Thurston, *Three Dimensional Manifolds, Kleinian Groups, and Hyperbolic Geometry*, *Bull. AMS* **6** (1982), no. 3 357–381.

[130] D. Thurston, *Hyperbolic Volume and the Jones Polynomial*, *Invariants de Neuds et de Varietes de Dimension 3 (Grenoble 1999)*. Institut Fourier, 1999.

[131] W. Thurston, *Hyperbolic structures on 3-manifolds I: Deformation of acylindrical manifolds*, *Ann. Math.* **124** (1986), no. 2 203–246.

[132] G. Mostow, *Strong rigidity of locally symmetric spaces*, *Ann. Math. Studies* **78** (1973).

[133] G. Prasad, *Strong rigidity of Q-rank 1 lattices*, *Invent. Math.* **21** (1973) 255–286.

[134] C. Petronio and J. Weeks, *Partially flat ideal triangulations of cusped hyperbolic 3–manifolds*, *Osaka J. Math* **37** (2000) 453–466.

[135] W. D. Neumann and J. Yang, *Bloch invariants of hyperbolic 3-manifolds*, *Duke Math. J.* **96** (1999) 29–59, [`math/9712224v1`].

[136] W. D. Neumann, *Extended Bloch group and the Cheeger-Chern-Simons class*, *Geom. Topol.* **8** (2004) 413–474, [`math/0307092v2`].

[137] C. K. Zickert, *The Chern-Simons invariant of a representation*, `arXiv:0710.2049`.

[138] L. Faddeev, *Current-like variables in massive and massless integrable models*, *Quantum groups and their applications in physics (Varenna 1994)* (1994) 117–135.

[139] L. Faddeev, *Modular Double of Quantum Group*, *Math. Phys. Stud.* **21** (2000) 149–256, [`math/9912078v1`].

[140] L. D. Faddeev, R. M. Kashaev, and A. Y. Volkov, *Strongly coupled quantum discrete Liouville theory. I: Algebraic approach and duality*, *Commun. Math. Phys.* **219** (2001) 199–219, [`hep-th/0006156v1`].

[141] A. Y. Volkov, *Noncommutative Hypergeometry*, *Commun. Math. Phys.* **258** (2005), no. 2 257–273, [`math/0312084v1`].

[142] A. B. Goncharov, *The pentagon relation for the quantum dilogarithm and quantized M(0,5)*, *Progr. Math.* **256** (2008) [arXiv:0706.4054].

[143] D. Zagier, *The dilogarithm function*, *in Frontiers in Number Theory, Physics, and Geometry II, Springer-Verlag (New York, 2006).*

[144] J. Lewis and D. Zagier, *Period functions for Maass wave forms. I*, *Ann. of Math.* **153** (2001) 191–258, [math/0101270v1].

[145] R. M. Kashaev, *On the spectrum of Dehn twists in quantum Teichmuller theory*, *in Physics and Combinatorics (Nagoya, 2000), World Sci. Publ., River Edge, NJ 2001* **math.QA** (2000) 771–808, [math/0008148v1].

[146] K. Habiro, *On the colored Jones polynomials of some simple links*, *Surikaisekikenkyusho Kokyuroku* **1172** (2000) 34–43.